

Copyright
by
Tianzhi Zhang
2007

**The Dissertation Committee for Tianzhi Zhang Certifies that this is the approved
version of the following dissertation:**

**DESIGN AND SYNTHESIS OF ARTIFICIAL RECEPTORS FOR
SELECTIVE AND DIFFERENTIAL SENSING**

Committee:

Eric V. Anslyn, Supervisor

Brent L. Iverson

John T. McDevitt

Hung-wen (Ben) Liu

C. Grant Willson

**DESIGN AND SYNTHESIS OF ARTIFICIAL RECEPTORS FOR
SELECTIVE AND DIFFERENTIAL SENSING**

by

Tianzhi Zhang, B.S.

Dissertation

Presented to the Faculty of the Graduate School of

The University of Texas at Austin

in Partial Fulfillment

of the Requirements

for the Degree of

DOCTOR OF PHILOSOPHY

The University of Texas at Austin

December, 2007

Dedication

To my Husband, Dayong Sun, my children, Maxwell and Michelle and my family and friends who have encouraged me throughout my education. Their support has been without equal.

Acknowledgements

Getting to this point in my education has been a fantastic journey, and I have received wonderful love and support from my family and friends.

My husband, Dayong, has been a wonderful encourager and supporter throughout my graduate studies. He has tried his best to help me out through the most difficult of times. I have been richly blessed with a loving husband, and I look forward to a lifetime of adventure and learning together.

I am indebted to, and extremely grateful for, my parents and in-laws for their love and encouragement that have helped me from China to the United States to achieve my academic goals. My parents have been excellent role models teaching me hard work and commitment to my goals.

I really believe that I had the kindest, and most supportive, graduate adviser in Eric Anslyn. I have learned so much from him. I am still in awe today at his remarkable knowledge of chemistry, and his capacity to teach it so effectively and patiently. I am so grateful for the start I have received from him, and I hope that I can take the knowledge I learned from him and make him proud during my career. I am also grateful for the encouragement and support I have received from the Anslyn group.

DESIGN AND SYNTHESIS OF ARTIFICIAL RECEPTORS FOR SELECTIVE AND DIFFERENTIAL SENSING

Publication No. _____

Tianzhi Zhang, Ph. D.

The University of Texas at Austin, 2007

Supervisor: Eric V. Anslyn

This dissertation consists of four chapters. The first chapter provides an in-depth background of synthetic receptors for recognitions of phosphorylated molecules. This chapter covers synthetic receptors developed within the last two decades, and it focuses on the diverse functionalities and detection techniques involved in the receptor design.

Chapter 2 discusses the synthesis and employment of a metalated receptor for the selective recognition of organic phosphates and phospho-amino acids, and describes a receptor with a pseudo tetrahedral cavity, which was found to be selective to phosphate, was synthesized utilizing a new and efficient synthetic route. UV-Vis titrations were used to determine binding constants for various organic phosphates and phospho-amino acids. The receptor:Cu(II) complex was found to differentiate the degree and size of phosphate substitutions.

Chapter 3 describes the synthesis and application of a type of differential receptors for the recognition of phosphorylated tri-peptides from regular tri-peptides. The tri-peptide couples described in this chapter were part of sequences in protein

Filamentous R-synuclein, which was discovered to have a close relation to Parkinson's disease. Extensive Ser129 phosphorylation was observed in diseased brains. Both solid phase and solution phase differential receptors were obtained in the investigations of peptide differentiation. A series of screening methods were applied to narrow down the system combinations. Linear discriminant analysis (LDA) statistical analysis generated a large spatial separation among six tripeptides.

Chapter 4 describes the synthesis of a boronic acid based receptor for carboxy and phospho sugars recognition. Due to the large affinity to gluconic acid, which is the only product of enzyme catalyzed glucose oxidation, this receptor was successfully applied in determination of glucose concentration in human serum.

TABLE OF CONTENTS

List of Tables	xii
List of Figures	xiii
List of Schemes	xix
MAJOR SECTIONS	1
Chapter 1 Artificial Receptors for Recognition of Phosphorylated Molecules	1
1.1 Introductions	1
1.2 Sensing Approaches	3
1.2.1 Nuclear Magnetic Resonance	3
1.2.2 Optical Methods	4
1.2.2.1 Colorimetry ("Naked-Eye" Detection)	4
1.2.2.1.1 Covalently Attached Chromophores.....	4
1.2.2.1.2 Indicator Displacement Assay (IDA).....	5
1.2.2.2 Fluorescence	6
1.2.3 Electrochemical Red-ox Activity	7
1.2.3.1 Cyclic Voltammetry (CV).....	7
1.2.3.2 Ion Selective Electrodes (ISEs)	7
1.2.4 Isothermal Titration Calorimetry (ITC)	8
1.3 Major Functionality Applications	9
1.3.1 Hydrogen Bonding Receptors.....	9
1.3.2 Amide Receptors	14
1.3.3 Urea and Thiourea Derivatives	26
1.3.4 Guanidinium Receptors	36
1.3.5 Lewis Acid Receptors	47
1.3.6 Polyammonium and Analogs	49
1.3.7 Macrocyclic Functionalities	71
1.3.8 Transition Metals as Non-Coordination reporters	77
1.3.8.1 Metallocenes as Electrochemical Reporters	78
1.3.8.2 [Ru(bpy) ₃] ²⁺ as Fluorescent Reporter	85

1.3.9 Direct Metal Coordination Receptors	89
1.3.10 Molecularly Imprinted Polymers (MIPs)	96
1.4 Concluding Remarks	98
1.5 References	99

Chapter 2 Molecular Recognition and Indicator-Displacement

Assays for Phosphate	109
2.1 Introduction	109
2.2 Results and Discussions	111
2.2.1 Synthesis	111
2.2.2 Binding Studies	113
2.3 Conclusion	125
2.4 Experimental Section	126
2.4.1 General Considerations	126
2.4.2 Synthesis	126
2.4.2.1 Compound 2.3	126
2.4.2.2 Compound 2.4	127
2.4.2.3 Compound 2.5	128
2.4.3 UV-Vis Titrations	129
2.4.4 Indicator-Displacement Assay	129
2.5 References	130

Chapter 3 The Successful Application of Differential Receptors in the

Recognition of Phosphorylated Peptides	132
3.1 Introduction	132
3.2 Results and Discussions	136
3.2.1 Peptide Synthesis	136
3.2.2 Differential Receptors' Core Ligand Synthesis	138
3.2.3 Differential Receptor Screening	139
3.2.4 Solution based Differential Receptors Synthesis	146
3.2.5 Metal and Indicator Screening	148
3.2.6 Linear discriminant analysis (LDA) studies	157

3.3 Conclusion	167
3.4 Experimental Section	168
3.4.1 General Considerations	168
3.4.2 Peptide Synthesis	169
3.4.3 Phosphopeptide Synthesis	171
3.4.4 Differential Receptor Core Ligand Synthesis	173
3.4.5 Differential Receptor Synthesis	177
3.5 References	179
Chapter 4 A Colorimetric Bornic Acid - Based Sensing Ensemble for Carboxy and	
Phospho Sugars, and Its Application in Monitoring of Glucose Oxidase	
Activity in Blood Serum	183
4.1 Introduction	183
4.2 Results and Discussions	184
4.3 Application: Monitoring Glucose Oxidase Activity in Blood Serum	192
4.4 Conclusion	198
4.5 Experimental Section	199
4.5.1 Synthesis	199
4.5.2 UV-Vis Titration Determination of the Ratio of 4.2 : Cd ²⁺	200
4.5.3 Determinations of Association Constant of a 1:1 Binding	
Isotherm	201
4.5.3.1 Determination of K _{4.2:Cd:PV} and K _{4.2:PV}	202
4.5.3.2 Determination of K _a and K _a '	203
4.5.4 ¹ H NMR and ¹³ C NMR Spectra for 4.2	205
4.5.5 Stock Solution Preparation	207
4.5.6 Concentration Effect of Glucose Oxidase (GOx)	207
4.5.7 Concentration Effect of Catalase	208
4.5.8 pH Effect	209
4.5.9 Glucose Interaction to Receptor System	210
4.5.10 Kinetic Studies Confirmed Enzyme Reactions at Setup	
Conditions	211

4.6 References	212
Vita	215

LIST OF TABLES

Table 2.1:	Design of Host 2.1 , and Previously Reported Affinity Constants in Buffered Water at pH 7.4.....	110
Table 2.2:	Association Constants Obtained by UV-Vis Titration at Room Temperature	115
Table 3.1:	Peptide Sequences Identified by Edman Degradation Mass Spectrometry	143
Table 3.2:	Optimized Differential Receptor Combinations	157
Table 4.1:	Association Constants Determined for the Binding of Anionic Sugars in MeOH/H ₂ O (v/v 3/1)	189

LIST OF FIGURES

Figure 1.1: Covalently Attached Chromophores	5
Figure 1.2: Indicator Displacement Assay (IDA).....	6
Figure 2.1: An example of the titration data used to determine affinity constants: A. Absorbances in UV-Vis titration by increasing the phosphoester concentration; B. The absorbance changed derived from A. Conditions: [2.1] = 1.92 mM, [Tris] = 10 mM, Solvent: water, pH = 7.4, 25 °C.	116
Figure 2.2: UV-Vis titration data of o-phospho-l-serine and l-serine. Conditions: [2.1] = 1.92 mM, [Tris] = 10 mM, Solvent: water, pH = 7.4, 25 °C.	119
Figure 2.3: (A) Binding affinity changes with host 2.1 concentrations. [2.1] = 3.84, 2.69, 1.92, 1.54, 0.96, 0.61 mM (B) Calculated activity coefficients dependence on the host concentrations in the presence of 10 mM Tris buffer, Solvent: water, pH = 7.4, 25 °C.	122
Figure 2.4: (A) Reproducible changes in the UV-Vis spectra of host-indicator solution upon addition of phosphoesters. (B) Example of the titration data used to determine the competing affinity constant. (C) Competition displacement algorithm. ⁹ Conditions: [2.1] = [5(6)-carboxyfluorescein] = 25.0 μM, [Tris] = 10 mM, Solvent: 50:50 methanol/water (v:v), pH = 7.4, 25 °C.	125
Figure 3.1: Metalloligand Core	136
Figure 3.2: Selectively Synthesized Tri-Peptides.....	138
Figure 3.3: Mass Spectrometry Characterized Tripeptides	145
Figure 3.4: Model Core Ligand	148
Figure 3.5: Indicators Structures	150

Figure 3.6: Metal and indicator screening preparation. Conditions: Total volume in each well is 300µl: Plate #1: $[M^{n+}] = [In] = [LG] = 0.03mM$, $[Ser(P)] = 0.3mM$; Plate #2: $[M^{n+}] = [In] = [LG] = 0.03mM$. $[Tris] = 50 mM$, $pH = 7.4$, $25\text{ }^{\circ}C$151

Figure 3.7: UV-Vis absorbances captured by 96-well plate reader in metals and pyrocatechol violet screening using Ser(P) vs. Blank. A. Cr^{3+} ; B. Mn^{2+} ; C. Fe^{2+} ; D. Fe^{3+} ; E. Co^{2+} ; F. Ni^{2+} ; G. Cu^{2+} . Conditions: Total volume in each well is 300µl: Plate #1 (blue): $[M^{n+}] = [pyrocatechol\ violet] = [3.19] = 0.03mM$, $[Ser(P)] = 0.3mM$; Plate #2 (pink): $[M^{n+}] = [pyrocatechol\ violet] = [3.19] = 0.03mM$. $[Tris] = 50 mM$, Solvent: water, $pH = 7.4$, $25\text{ }^{\circ}C$153

Figure 3.8: UV-Vis absorbances captured by 96-well plate reader in metals and celestine blue screening using Ser(P) vs. Blank. A. Cr^{3+} ; B. Mn^{2+} ; C. Fe^{2+} ; D. Fe^{3+} ; E. Co^{2+} ; F. Ni^{2+} ; G. Cu^{2+} . Conditions: Total volume in each well is 300µl: Plate #1 (blue): $[M^{n+}] = [Celestine\ blue] = [3.19] = 0.03mM$, $[Ser(P)] = 0.3mM$; Plate #2 (pink): $[M^{n+}] = [Celestine\ blue] = [3.19] = 0.03mM$. $[Tris] = 50 mM$, Solvent: water, $pH = 7.4$, $25\text{ }^{\circ}C$ 154

Figure 3.9: UV-Vis absorbances captured by 96-well plate reader in metals and gallocyanine screening using Ser(P) vs. Blank. A. Cr^{3+} ; B. Mn^{2+} ; C. Fe^{2+} ; D. Fe^{3+} ; E. Co^{2+} ; F. Ni^{2+} ; G. Cu^{2+} . Conditions: Total volume in each well is 300µl: Plate #1 (blue): $[M^{n+}] = [gallocyanine] = [3.19] = 0.03mM$, $[Ser(P)] = 0.3mM$; Plate #2 (pink): $[M^{n+}] = [gallocyanine] = [3.19] = 0.03mM$. $[Tris] = 50 mM$, Solvent: water, $pH = 7.4$, $25\text{ }^{\circ}C$. 156

Figure 3.10: UV-Vis absorbance changes (Ser(P) vs. Blank) bar plots in metal and indicator screening. Conditions: Total volume in each well is 300µl: Plate #1 (Ser(P)): $[M^{n+}] = [In] = [3.19] = 0.03mM$, $[Ser(P)] = 0.3mM$; Plate #2 (Blank): $[M^{n+}] = [In] = [3.19] = 0.03mM$. $[Tris] = 50 mM$, Solvent: water, pH = 7.4, 25 °C.	156
Figure 3.11: A typical simulated colorimetric observation in 96-well plate. Conditions: Total volume in each well is 300µl: $[M^{n+}] = [In] = [LG_n] = 0.03mM$, $[peptides] = 0.3mM$, $[Tris] = 50 mM$, Solvent: water, pH = 7.4, 25 °C.....	158
Figure 3.12: Example: UV-Vis spectra of S(P)EE/SEE couple with different metallated receptors: A. Receptor TEV (LG 1); B. Receptor RLL (LG 2); C. Receptor YRE (LG 3); D. Receptor YDP (LG 4); E. Receptor KDK (LG 5). Conditions: Total volume in each well is 300µl: $[M^{n+}] = [In] = [LG_n] = 0.03mM$, $[peptides] = 0.3mM$, $[Tris] = 50 mM$, Solvent: water, pH = 7.4, 25 °C.....	162
Figure 3.13: Example: UV-Vis absorbance changes of S(P)EE vs. SEE couple with different metallated receptors (totally 9 trials, the mean values and standard deviations are shown): A. Pyrocatechol Violet (In 4); B. celestine blue (In 5); C. gallocyanine (In 9). Conditions: Total volume in each well is 300µl: $[M^{n+}] = [In] = [LG_n] = 0.03mM$, $[peptides] = 0.3mM$, $[Tris] = 50 mM$, Solvent: water, pH = 7.4, 25 °C.....	164
Figure 3.14: LDA analysis of six peptides. A. F1:F2; B. F1:F3; C. F2:F3	166
Figure 4.1: Anionic Sugars	187

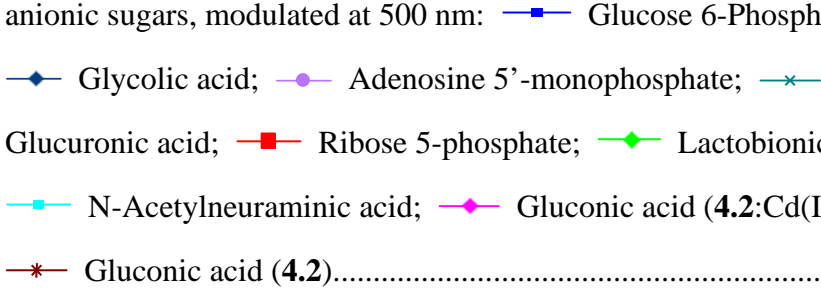
- Figure 4.2: Sugar screening. Conditions: Total volume: 300 μ l; [**4.2**:Cd(II)] = [PV] = 0.1 mM; [Sugars] = 0.5 mM; [HEPES] = 10 mM; Solent: MeOH: Water = 3:1 (v:v); pH = 7.4; 25 $^{\circ}$ C.188
- Figure 4.3: Typical UV-Vis binding curves obtained upon titration of anionic sugars into **4.2**:Cd(II)-indicator solution. Titration conditions: 3/1 Methanol/Water; HEPES buffer 50 mM, pH = 7.4; Indicator: Pyrocatechol Violet; [**4.2**:Cd(II)] = [PV] = 0.1 mM; 25 $^{\circ}$ C.190
- Figure 4.4: Relative absorbance of **4.2**:Cd(II)-indicator system upon addition of anionic sugars, modulated at 500 nm:  Glucose 6-Phosphate; Glycolic acid; Adenosine 5'-monophosphate; Glucuronic acid; Ribose 5-phosphate; Lactobionic acid; N-Acetylneuraminic acid; Gluconic acid (**4.2**:Cd(II)); Gluconic acid (**4.2**).....191
- Figure 4.5: (A) UV-Vis titration results, where [**4.2**:Cd(II)] = 0.13 mM and [PV] = 0.13 mM in MeOH-H₂O 3:1 (v/v). (B) Example pictures: Addition of gluconic acid to receptor **4.2**:Cd(II) causes a displacement of PV from **4.2**:Cd(II), resulting in a large color change. [**4.2**:Cd(II)] = 0.13 mM, [PV] = 0.13 mM, and [G] = 0.13 mM, all in MeOH-H₂O 3:1 (v/v).195
- Figure 4.6: Glucose calibration curves. Titration conditions: 3/1 Methanol/Water; HEPES buffer 50 mM, pH = 7.4; Indicator: Pyrocatechol Violet; [**4.2**:Cd(II)] = [PV] = 0.1 mM; [Glucose] = 50.34 mM, 25 $^{\circ}$ C.197
- Figure 4.7: Glucose concentration determinations in human serum (110 ± 8 mg/dL). All samples were glucose (110 mg/dL), and several tests were performed for different volumes of the serum. Each test was within 7% of the correct glucose value.....198

Figure 4.8: UV-Vis titration determination on Cd^{2+} association. Conditions: [4.2] = 0.040 mM, 750 μl ; $[\text{Cd}(\text{NO}_3)_2]$ = 0.81 mM; 3:1 MeOH:H ₂ O; HEPES (~10mM) at pH = 7.4; 25 °C.	201
Figure 4.9: UV-Vis titration on association constant determination of 4.2 :Cd(II) to PV. Conditions: [PV] = 0.1 mM; [4.2 :Cd(II)] = 2.00 mM, 5 μL aliquots; 3:1 MeOH:H ₂ O; HEPES (~10mM) at pH = 7.4; 25 °C..	203
Figure 4.10: UV-Vis titration determination of 4.2 :Cd(II): PV to Sugar. UV-Vis titration on association constant determination of 4.2 :Cd(II) to PV. Conditions: [PV] = [4.2 :Cd(II)] = 0.1 mM; [Sugar] = 2.00 mM, 5 μL aliquots; 3:1 MeOH:H ₂ O; HEPES (~10mM) at pH = 7.4; 25 °C.	204
Figure 4.11: ^1H NMR and ^{13}C NMR Spectra for 4.2	204
Figure 4.12: Effect of glucose oxidase concentration. Conditions: Glucose 200 μl , Catalase 200 μl , Total volume: 5ml; 250 μl aliquot was used to observe UV absorbance modulations. [PV] = [4.2 :Cd(II)] = 0.13 mM; [Sugar] = 50.00 mM; [catalase] = 10 mg/ml; [GO_x] = 10 mg/ml; 3:1 MeOH:H ₂ O; TRIS (~50mM) at pH = 7.4; 25 °C.	208
Figure 4.13: Effect of catalase concentration. Condition: GO_x 30 μl , Glucose 200 μl , Total volume: 5ml; 250 μl aliquot was used to observe UV modulation. [PV] = [4.2 :Cd(II)] = 0.13 mM; [Sugar] = 50.00 mM; [catalase] = 10 mg/ml; [GO_x] = 10 mg/ml; 3:1 MeOH:H ₂ O; TRIS (~50mM) at pH = 7.4; 25 °C.	209

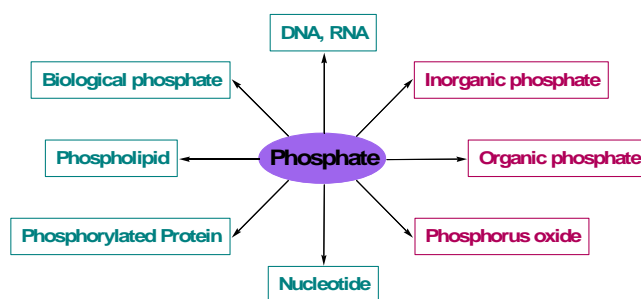
Figure 4.14: Effect of pH (2 trials at the same conditions). Condition: GOx 30 μ l, Glucose 200 μ l, Total volume: 5ml; 250 μ l aliquot was used to observe UV modulation. [P \mathbf{V}] = [4.2:Cd(II)] = 0.13 mM; [glucose] = 50.00 mM; [catalase] = 10 mg/ml; [GO $_x$] = 10 mg/ml; 3:1 MeOH:H $_2$ O; TRIS (~50mM) at pH = 7.4; 25 $^{\circ}$ C.	210
Figure 4.15: Effect of glucose concentration. Conditions: [P \mathbf{V}] = [4.2:Cd(II)] = 0.13 mM; [glucose] = 100 mM, 5 μ l aliquots; 3:1 MeOH:H $_2$ O; TRIS (~50mM) at pH = 7.4; 25 $^{\circ}$ C.	211
Figure 4.16: Kinetic studies showed enzyme catalized ability of glucose oxidation by GO $_x$. Condition: GOx 30 μ l, Catalase 200 μ l, Total volume: 5ml; 250 μ l glucose aliquot was used to observe spectral modulation. A) UV-Vis titations at different glucose concentrations. B) Michaelis-Menten curve. [P \mathbf{V}] = [4.2:Cd(II)] = 0.13 mM; [glucose] = 50.00 mM; [catalase] = 10 mg/ml; [GO $_x$] = 10 mg/ml; 3:1 MeOH:H $_2$ O; TRIS (~50mM) at pH = 7.4; 25 $^{\circ}$ C.	212

LIST OF SCHEMES

Scheme 1.1:	Phosphorylated Molecules	1
Scheme 2.1:	New Synthetic Route to 2.1	112
Scheme 3.1:	Sequences in Protein Filamentous R-Synuclein	135
Scheme 3.2:	Core Ligand Synthesis	139
Scheme 3.3:	Screening Methods.....	141
Scheme 3.4:	Differential Receptor Synthesis	147
Scheme 4.1:	Synthesis of Boronic Acid Receptors 4.2 :Cd(II)	187
Scheme 4.2:	IDA Application in Gluconic Acid Association	194
Scheme 4.3:	Enzyme Catalyzed Glucose Oxidation	195
Scheme 4.4:	Equations in Determinations of Association Constants.....	201

Chapter 1: Artificial receptors for recognition of phosphorylated molecules

1.1 Introductions



Scheme 1.1 Phosphorylated molecules

Phosphate anions (**Scheme 1.1**) are one of the most important constituents of living systems. Together with heterocyclic bases and sugars, phosphates make up DNA, the hereditary element of living systems. In addition, phosphate ions and their derivatives play pivotal roles in signal transduction and energy storage in biological systems.¹

Biological recognition elements, such as antibodies, are typically used in ligand-binding assays of phosphorylated molecules, but they often require special handling and may suffer from poor stability and a complicated, costly production procedure.² To assay inorganic phosphate, a spectrophotometric method detects a molybdenum (IV) phosphate complex using color. This method requires sodium molybdate and a strong

reducing agent, which is time consuming, generates heavy metal waste, and suffers from interference.³

The development of artificial phosphate receptors could afford improved methodologies for detection, separation, or transport of biologically important phosphates. Hence, sensitive and selective detection of phosphorylated molecules is a challenging research area in supramolecular chemistry. However, the large size of the phosphate anion and its high hydrophilicity places it at the bottom of the Hofmeister selectivity (hydration energy) series: $\text{ClO}_4^- > \text{IO}_4^- > \text{CN}^- > \text{F}^- > \text{I}^- > \text{Cl}^- \sim \text{Br}^- \sim \text{OAc}^- > \text{NO}_3^- > \text{HCO}_3^{2-} > \text{SO}_4^{2-} > \text{H}_2\text{PO}_4^-$. As a result, phosphate binding is not particularly efficient through a simple, single recognition event. Therefore, multiple interactions such as hydrogen bonding, electrostatic interactions, van der Waals forces, π - π stacking, shape complementarity, and metal coordination have been employed in sensor design in order to enhance binding affinities.⁴

The balance between rigidity and flexibility is of particular importance for the dynamic properties of receptors and guests. Although high affinity may be achieved with rigidly organized receptors, processes of exchange, regulation, cooperativity and allostery require a built-in flexibility so that the receptor may adapt and respond to changes. Flexibility is of great importance in biological receptor-substrate interactions, where adaptation is often required for regulation to occur. Such designed dynamics are more difficult to control than mere rigidity, and recent developments in computer-assisted molecular design methods, allowing the exploration of both structural and dynamic

features, may greatly help. Receptor design thus considers both static and dynamic features of macropolycyclic structures.⁵

1.2 Sensing approaches

1.2.1 Nuclear magnetic resonance

The detection of an interaction between a host and guest from NMR measurements follows guest-induced ^1H NMR shifts (and/or ^{31}P NMR shifts specific for phosphorylated molecule detections). Thus, hydrogen bonding in complexes of anions such as phosphate with amide protons can be conveniently followed. However, many phosphate moieties, particularly those of biological interest, contain structural elements that modify the phosphate anion. Therefore, extra moieties are sometimes attached to the receptor in order to aid in the selective detection of specific host-guest complexes. Most popular in this respect are aromatic moieties, because they induce changes in NMR chemical shifts that are indicative and characteristically dependent on the complex structure. The association constants of the complexes are often elucidated using EQNMR software.⁶ However, the utility of these guest-induced ^1H NMR shifts to quantitatively determine complexation constants is limited when high association constants between the host and guest species are achieved due to the relatively high concentrations (usually 10^{-2} - 10^{-3} M) required to obtain the NMR signals. This leads to rapid saturation of the NMR signal in a titration and little curvature in the resulting isotherm.

1.2.2 Optical methods

Many sensing systems generally contain some combination of substrate-recognition functionality (receptor) and optical signaling capacity (chromophore), either directly linked or appropriately associated in a noncovalent manner. Such systems are designed to permit the detection of substrates by binding-induced changes in absorption or emission properties of the chromophore or fluorophore and termed colorimetric and fluorescent sensors, respectively. Recently, the utility of these approaches has become increasingly appreciated in terms of both qualitative and quantitative analysis.

1.2.2.1 Colorimetry (“Naked-eye” detection):

1.2.2.1.1 Covalently attached chromophores

Some reporter groups are incorporated into the covalent framework of the host molecule (**Figure 1.1**). Upon complex formation with an anion, the excited state is more strongly stabilized, resulting in a bathochromic shift in λ_{max} , giving rise to a pronounced color change.

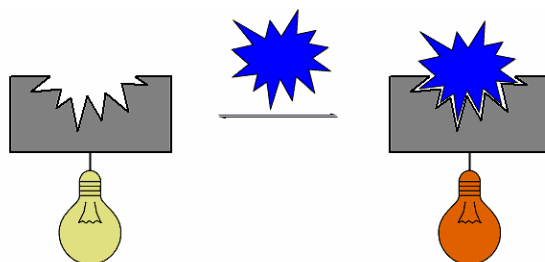


Figure 1.1 Covalently attached chromophores

1.2.2.1.2 Indicator displacement assay (IDA)

Indicator displacement assay (IDA) is a competition method for the sensing of anions (**Figure 1.2**). The molecular ensembles employed consist of a recognition unit designed for selective interaction with a desired analyte along with an external indicator that associates with the recognition unit in the absence of the analyte. When the analyte is added, the indicator is displaced from the binding cavity, producing a measurable change in the indicator's optical properties. Several features of this method make it useful: it can be applied to a variety of receptors without need for covalent attachment of a reporter group; the use of noncovalent indicators makes each system amenable to both fluorescence and UV/Vis spectrophotometry with selection of appropriate indicators; indicators may be chosen based upon relative association ability compared with the analyte to allow tuning of the system to even weakly binding analytes; and several indicators may be used in the same study to verify results.

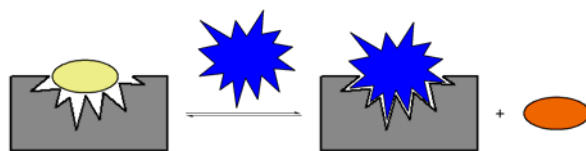


Figure 1.2 Indicator displacement assay (IDA)

1.2.2.2 Fluorescence

Fluorescence is an attractive detection method for sensors for several reasons: high sensitivity of detection, “on-off” switchability, feasible human-molecule communication, subnanometer spatial resolution with submicron visualization and submillisecond temporal resolution.⁷ Many fluorescence anion sensors utilize competitive binding,⁸ photo-induced electron transfer (PET),⁹ metal-to-ligand charge transfer (MLCT),¹⁰ excimer/exiplex formation mechanisms,¹¹ internal charge transfer (ICT)¹², and, rarely, excited-state intra-/intermolecular proton transfer (ESPT). Furthermore, many of the structural features which modulate fluorescence efficiency have been delineated and include: double-bond torsion, low energy $n\delta^*$ levels, “heavy” atoms, weak bonds, and opportunities for photoinduced electron transfer (PET) or electronic energy transfer (EET). Therefore, many opportunities exist for modulating structural features via chemical or physical means at the molecular level.

1.2.3 Electrochemical red-ox activity

1.2.3.1 Cyclic voltammetry (CV)

These is a category of artificial receptors that can signal the presence of substrates due to the attachment of redox-active groups (cobaltocenium, ruthenium (II) bipyridyl groups, ferrocenyl moieties, *etc.*) near their coordination sites. For example, in the presence of the anion, the voltammetric behavior of the metallocenium moiety is shifted toward that of the corresponding metallocene. Among the investigated anions, phosphate traditionally produces the largest cathodic perturbation, which is rationalized by postulating that phosphate stabilizes the positively charged metallocenium moiety more in comparison to metallocene. However, the electroactive character and binding ability of this class of receptors are not necessarily closely related to each other; i.e. the largest cathodic perturbation does not imply the strongest association.

1.2.3.2 Ion selective electrodes (ISEs)

A series of new anion-selective electrodes were introduced recently as a result of the growing interest in the host-guest chemistry of anions. It is especially challenging to achieve a useful selectivity for the strongly hydrophilic phosphate species because the unfavorable standard free enthalpies of transfer from samples to ISE membranes must be

overcompensated by selective complexation. Adequate phosphate selectivities in membranes can be achieved by homogenously distributing ionophores such as organotin, organovanadyl compounds, polyamines, and guanidiniums in the polymer membrane, but these systems often suffer from insufficient stabilities and low detection limits.¹³

1.2.4 Isothermal titration calorimetry (ITC)

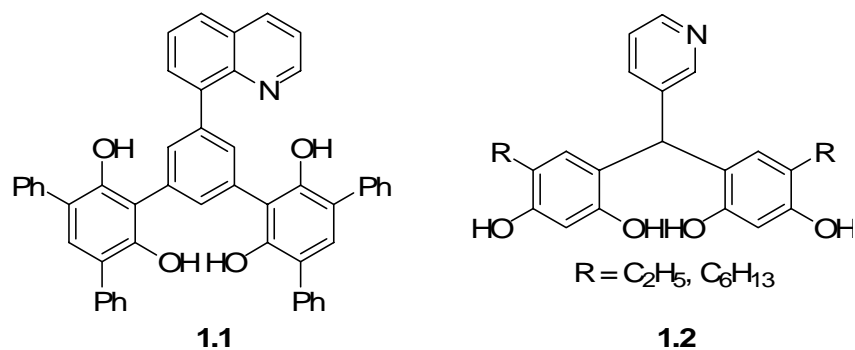
Although NMR is an indispensable tool in the assessment of supramolecular associations and can provide clues to the structural mode of host-guest relationships, the elucidation of the thermodynamic parameters ΔG , ΔH , and ΔS by this instrumental method is laborious, and error-prone. A more direct access to these parameters is offered by modern isothermal titration calorimetry (ITC), which allows the ready dissection of association free energies into their enthalpic and entropic components. Since both are mutually compensating in weak supramolecular interactions, knowledge of the individual enthalpy and entropy contributions, rather than their composite (the free energy ΔG), is informative for deciphering complexation driving forces. Because calorimetric measurements are truly integral reflections of all processes occurring in solution, it is of utmost importance to design very simple host-guest interactions to arrive at interpretable results that can be extended to more complex systems.

1.3 Major functionality applications

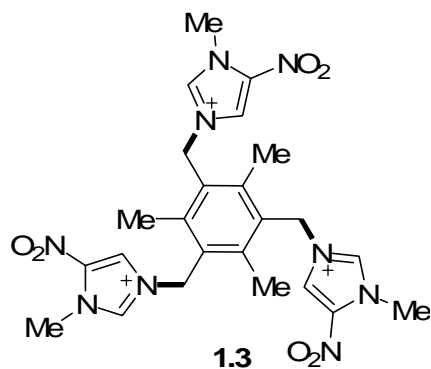
In this section, some typical functionalities utilized in the designation of phosphate selective artificial receptors are introduced with the aim of providing general guidelines in this area of research.

1.3.1 Hydrogen bonding receptors

Hydrogen bonding is an attractive interaction that exists between an electronegative atom and a hydrogen atom bound to another electronegative atom. This type of bonding always involves hydrogen atom(s) and is directional. Hydrogen bonding is largely determined by electrostatic attraction (dipole-dipole, charge-dipole), although significant contributions are also furnished by charge-transfer, dispersive, and covalent forces. Therefore, the typical hydrogen bond is stronger than van der Waals forces, but weaker than covalent or ionic bonds.

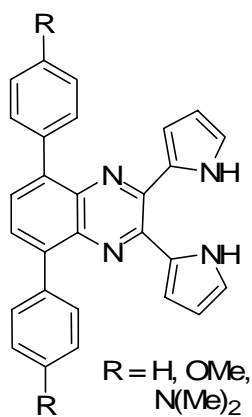


Multipoint hydrogen bonding is a general guiding principle for the molecular recognition of complicated biorelevant molecules. The hydrogen bonding interactions of phosphates often involve salt formation in apolar solvents. Preorganized compounds such as **1.1** and **1.2** can form multiple hydrogen bonds to phosphate anions without intramolecular interference due to steric restraints.¹⁴ The association strength determined by ^1H NMR reflects the number of hydrogen bonds formed.

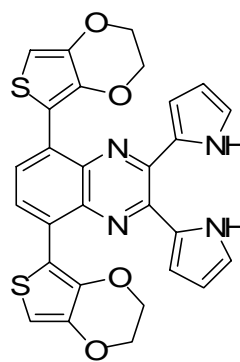


Compound **1.3**, prepared by the Kim group¹⁵, was designed to investigate $(\text{C-H})^+ \cdots \text{X}^-$ hydrogen bonds between the imidazolium rings. In this charge-charge electrostatic

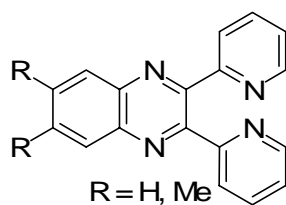
interaction, the anion binding strength can be successfully tuned by increasing the positive charge and steric bulk on the imidazolium ring, which was accomplished by attaching nitro and/or a *t*-butyl groups.



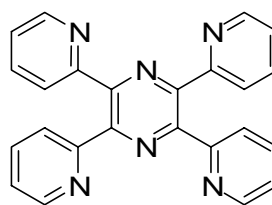
1.4



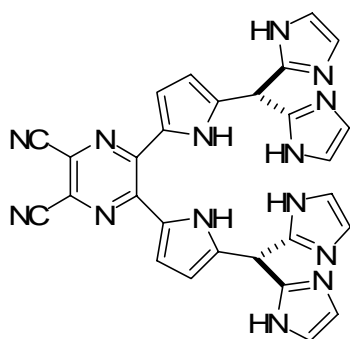
1.5



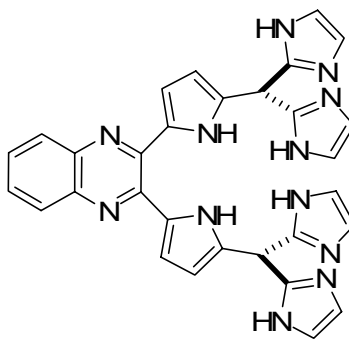
1.6



1.7

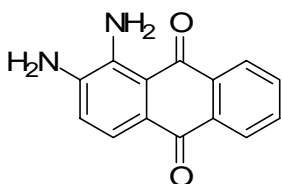


1.8

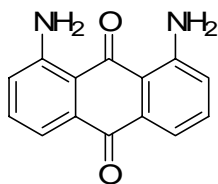


1.9

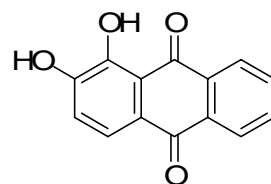
Pyrrolyl- and pyridinyl- quinoxaline receptors (compounds **1.4-1.9**) were synthesized and studied independently by several research groups.¹⁶ All the compounds demonstrated selectivity for phosphate molecules, which was solely ascribed to efficient hydrogen bonding interactions.



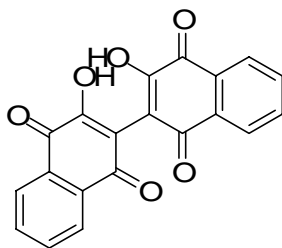
1.10



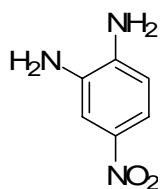
1.11



1.12

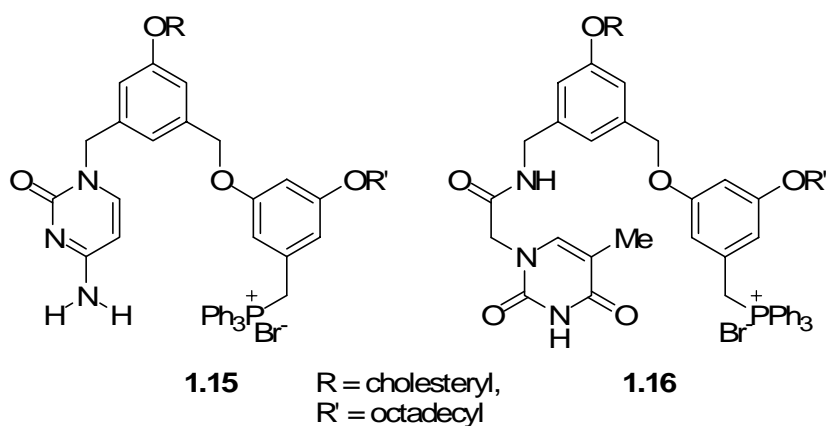


1.13

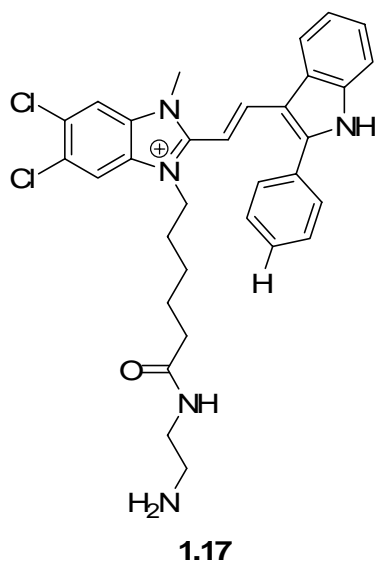


1.14

Off-the-shelf, naked-eye detectable colorimetric indicators (compounds **1.10-1.14**) were applied to anion screening.¹⁷ The resulting bathochromic shifts of these colorimetric sensors relied on their hydrogen bond donating abilities. The most dramatic color changes were observed with indicators that provide two or more -NH₂, -C(O)NHR, or OH-derived binding sites. Although the desired specificity could not be achieved by a single readily available compound, a multi-sensor array was suggested as a possible approach to anion sensing at neutral pH.



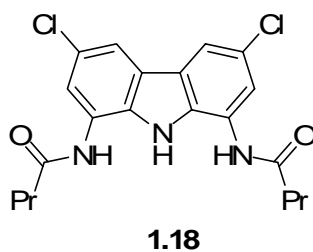
Lipophilic complementary nucleobases **1.15** and **1.16** were found to effectively extract and transport GMP and AMP respectively by forming 1:1 host-to-guest complexes at pH 5.0 and 2:1 host-to-guest complexes at pH 7.0.¹⁸ The slightly more efficient extraction percentage and transportation rate at pH 5.0 is explained by a more entropically favorable bimolecular complex present at lower pH.



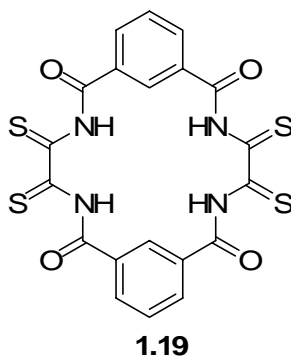
The introduction of two Cl groups into a benzimidazolium ring was found to give a green-red range emission in the presence of phosphate rather than the UV-blue range emission of an unsubstituted benzimidazolium ring. Derivatized receptor **1.17** exhibits unprecedented high selectivity toward GTP and was the first turn-on GTP fluorescent sensor resulting from a designed sensor approach.¹⁹

1.3.2 Amide receptors

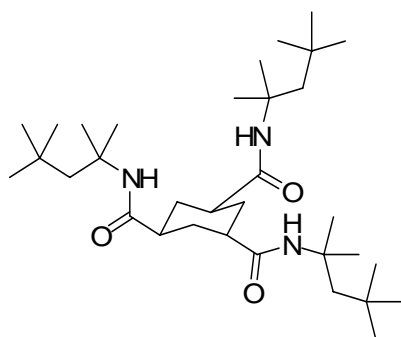
The amide (CO-NH) group is of great importance in anion recognition due to its effective hydrogen bonding donating ability.



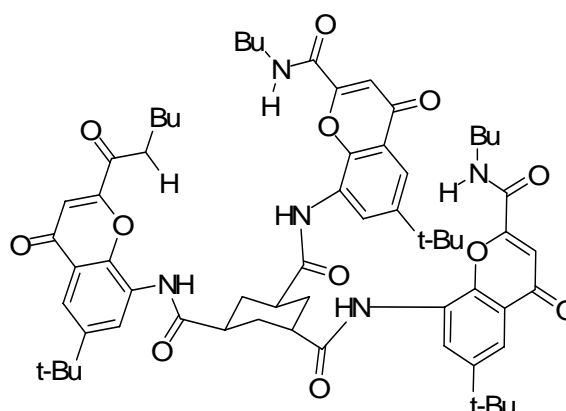
A rigid carbazole skeleton was used in a phosphate receptor (compound **1.18**), which forms a strong 1:1 complex in DMSO- d_6 .²⁰ It is interesting that the aliphatic amide (R=iPr) bound anions more strongly than its aromatic analogue (R=Ph). However, the reason is still not clear.



Electroactive bis-dithioamide receptor **1.19** performed well in the development of a phosphate-selective sensor because it showed less interference from thiocyanate, perchlorate, and iodide than previously designed sensors.²¹

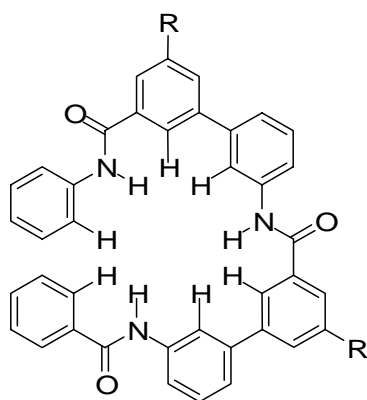


1.20



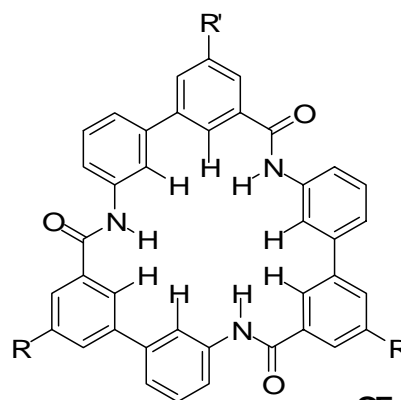
1.21

Phosphate binding receptors with amide moieties (compounds **1.20** and **1.21**) were also reported by Raposo and coworkers.²² The binding properties were studied by ¹H NMR spectra in non-competitive solvents (CDCl₃ or DMSO-D₆), depending upon the solubility of the receptor molecules. Multiple hydrogen bonding interactions were considered as the major driving force for forming stronger complexes with phosphates.



R = CO₂Me

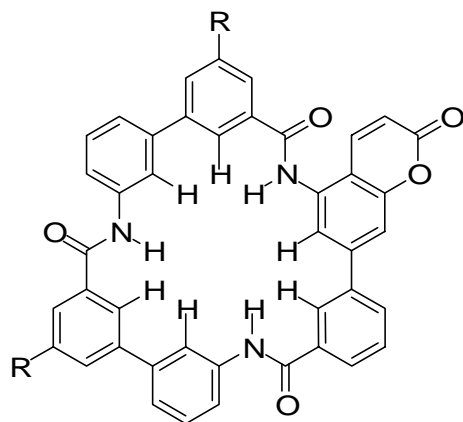
1.22



R = R' = NHBoc

R = NHBoc, R' =

1.23

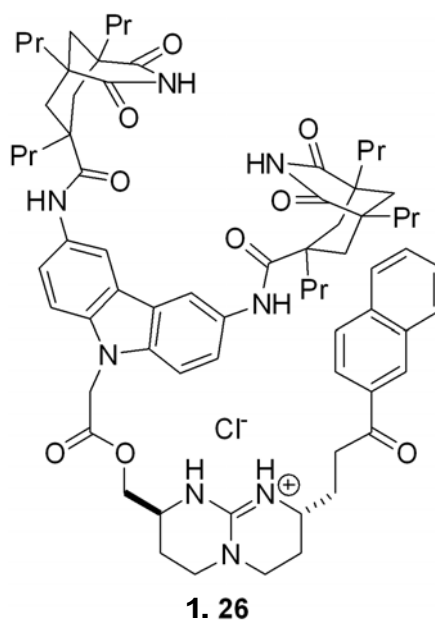
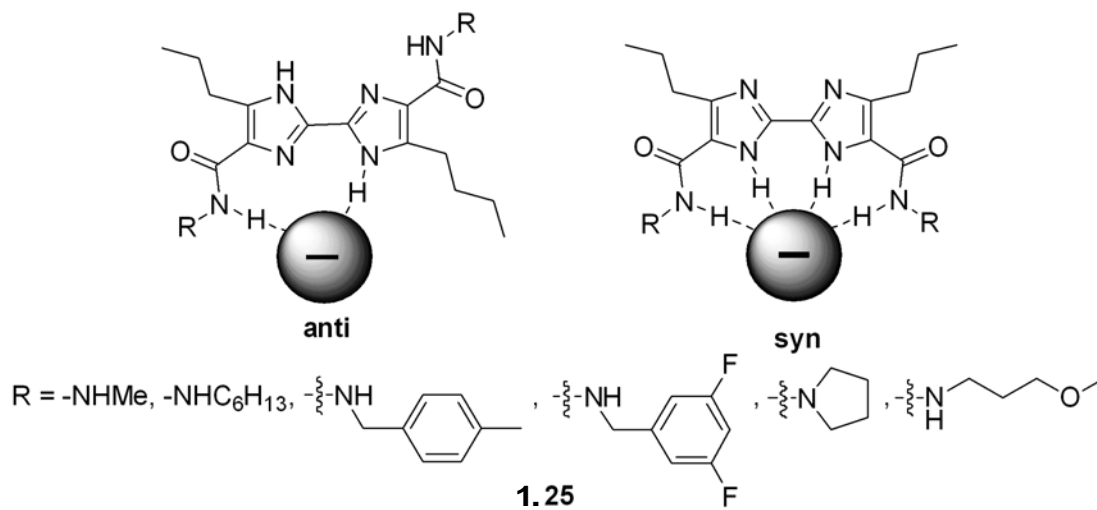


R = NHBoc

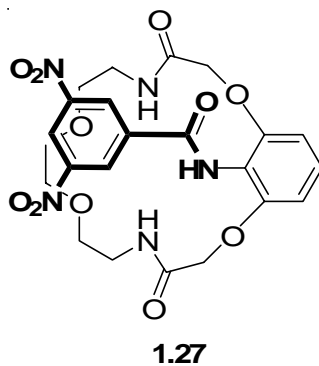
1.24

Convergent macrocyclic receptors (compounds **1.22**, **1.23** and **1.24**) with amide moieties were studied by the Hamilton group.²³ These rigid structures provide convergent multiple hydrogen bonding sites in the interior of the macrocyclic scaffold, and hence, enable the macrocycles to bind anions with size and shape selectivity. Tetrahedral anions such as $p\text{-TsO}^-$, HSO_4^- , and H_2PO_4^- were observed to bind strongly even in competitive solvents such as 100% DMSO, while the binding of halides and nitrate anions decreased dramatically even in 50%DMSO/ CDCl_3 . When a fluorophore was attached to the macrocycles and positioned close to the anion binding sites, the positive charges developed in the fluorophore excited states were stabilized, thus allowing for another fluorescence emission channel through intermolecular excited state proton transfer (ESPT) in addition to the charge transfer (CT) channel. Emissions from the two

channels showed different anion dependencies and, as a result, more selective and sensitive sensing was achieved.

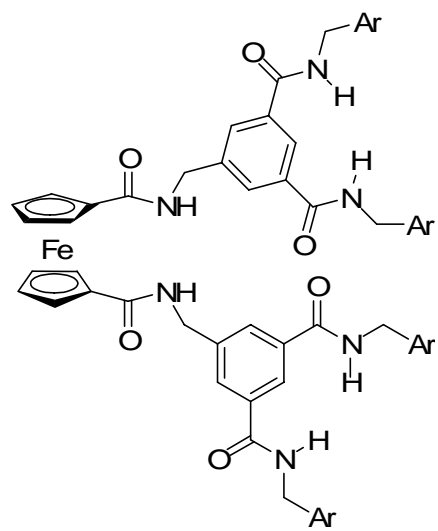
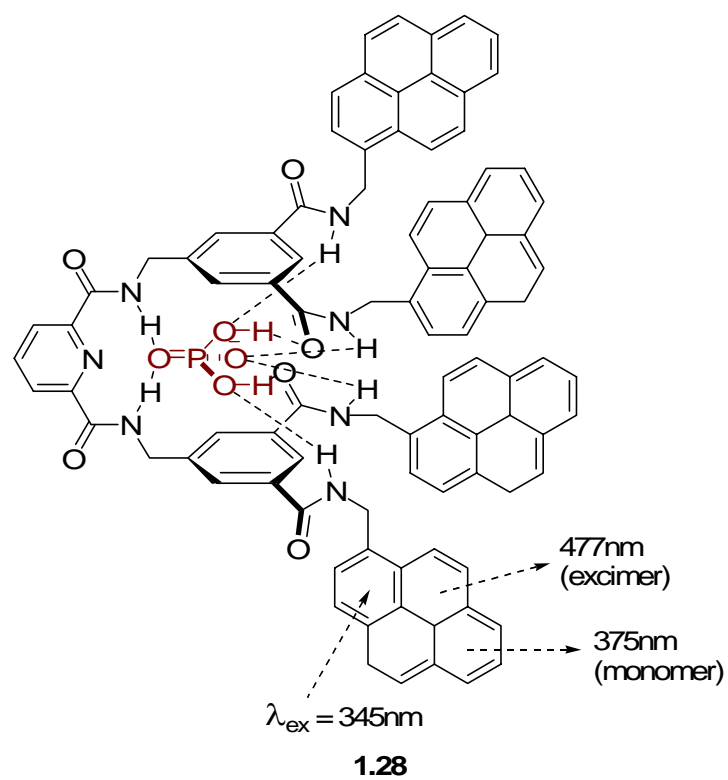


2,2-Biimidazoles (compound **1.25**) with various amide groups at the 4- and 4'-positions were studied by the Allen group.²⁴ Both *syn* and *anti* complexation with anions were proposed. The intrinsic fluorescence of the biimidazole unit was quenched upon addition of dihydrogen phosphate and chloride without an emission shift. 1:1 complexes were formed with association constants on the order of 10^4 M^{-1} for H_2PO_4^- and Cl^- . Incorporation of the biimidazole units into a macrocycle (compound **1.25**) constrained the biimidazoles to adopt only a *syn* conformation, a conformation expected to improve the anion affinities and selectivities. The cleft-shaped receptor **1.26** displayed high affinity for cAMP over cGMP, a selectivity attributed to the loss of a single hydrogen bond in cGMP binding.²⁵



An amide-based macrocyclic sensor (compound **1.27**) studied by the Jurczak group gave a colorimetric detection of F^- , AcO^- and H_2PO_4^- ions in both DMSO and CH_3CN solutions. This optical indicator showed different selectivities in DMSO and CH_3CN for those anions with similar basicities.²⁶ This is because polar aprotic solvents

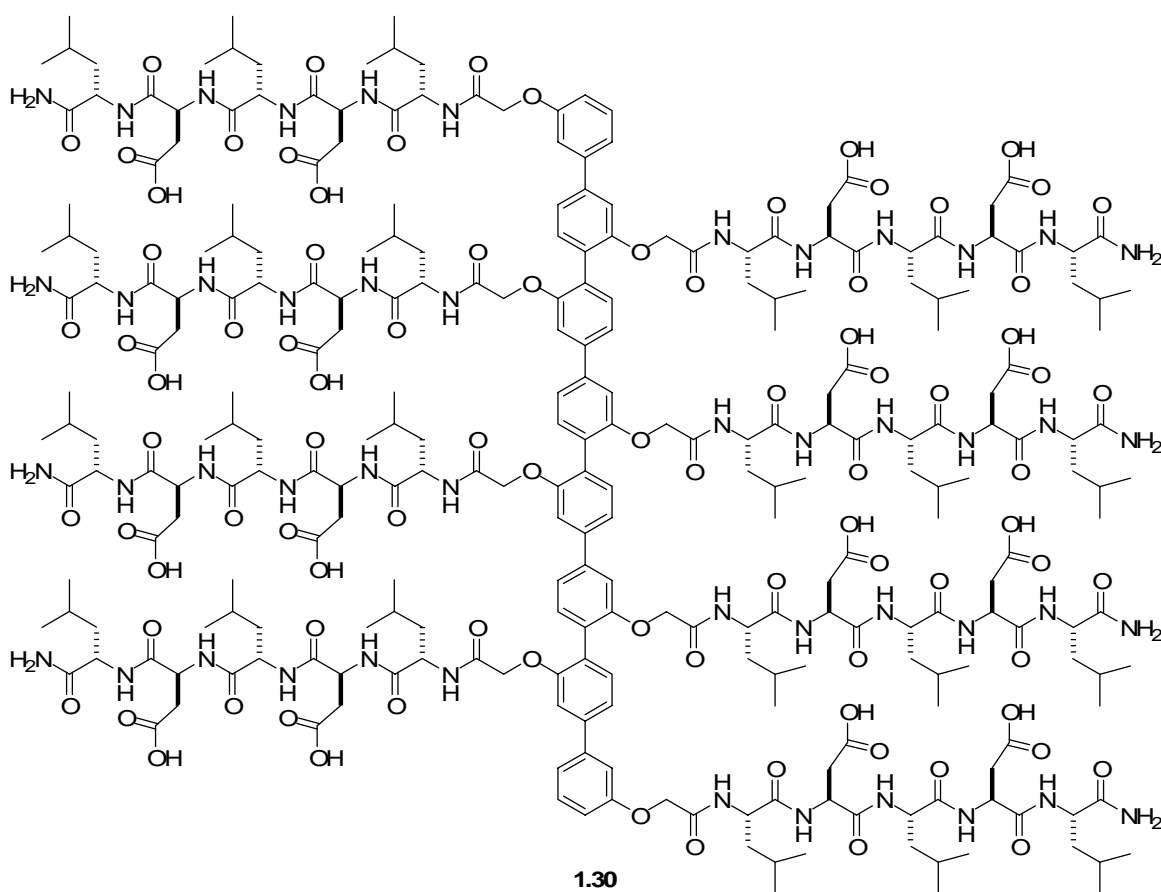
such as DMSO are capable of electron-pair donation (Lewis basic) but are not very effective Lewis acids. Thus, for acetate, dihydrogenphosphate, and sulfate anions, the solvation of DMSO stabilizes the positively polarized atoms of the anions (*i.e.* carbon, phosphorus, and sulfur) rather than the negatively charged oxygen atoms. However, because the positively polarized phosphorus atom of H_2PO_4^- is surrounded by the four negative oxygen atoms, it is not effectively solvated by DMSO. On the contrary, the corresponding carbon atom of the acetate anion must be more susceptible to the solvation of DMSO. Accordingly, the lower binding constants observed for CH_3COO^- than those for H_2PO_4^- can be attributed to the stronger interaction of the former with the solvent than that of the latter.²⁷



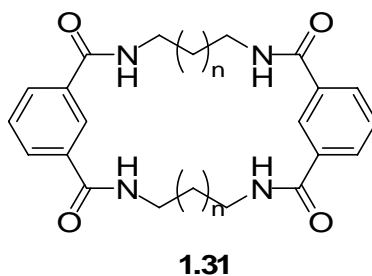
Ar = Ph, 4-nitrophenyl, 1-pyrenyl

1.29

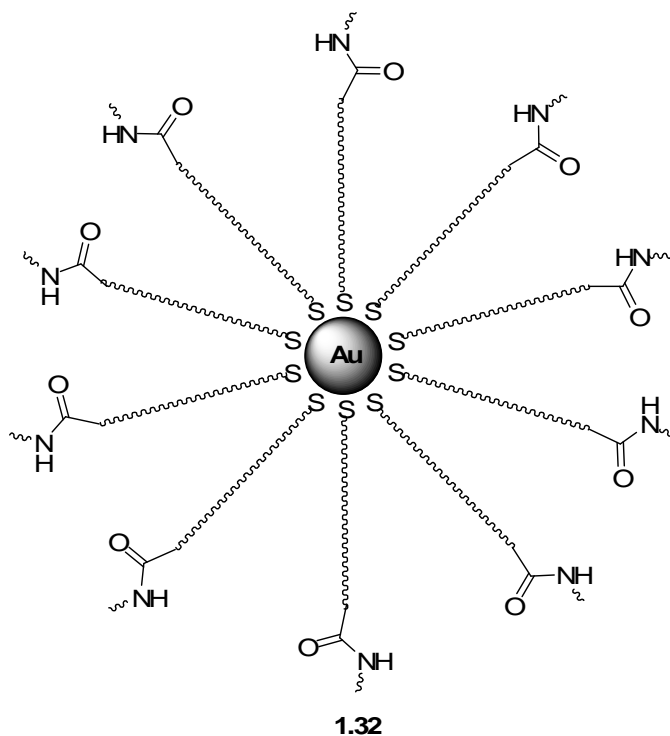
Two-arm amide receptors (compounds **1.28** and **1.29**) were studied by the Fang group.²⁸ These receptors provided pseudo-tetrahedral geometry and multiple hydrogen bonding sites that form strong complexes with the phosphate ion. As for the ferrocene-based receptor, a 1:2 host-to-guest complex was formed. With fluorescence reporting groups, the complexation to phosphate caused both monomer and excimer emissions, which could be utilized as diagnostic devices for the measurement of phosphate concentrations, even in the presence of 50 equivalents of other anions (F^- or AcO^-).



The Matile group reported that cation-selective transmembrane pores formed by synthetic *p*-octiphenyl β barrels with internal aspartate residues could be transformed into anion-permeable metallopores with internal Mg^{2+} -aspartate complexes (compound **1.30**).²⁹ These metallopores were shown to be useful for the fluorimetric sensing of a broad variety of organic anions of biological relevance such as phytate, heparin, thiamine phosphates, and adenosine triphosphate.



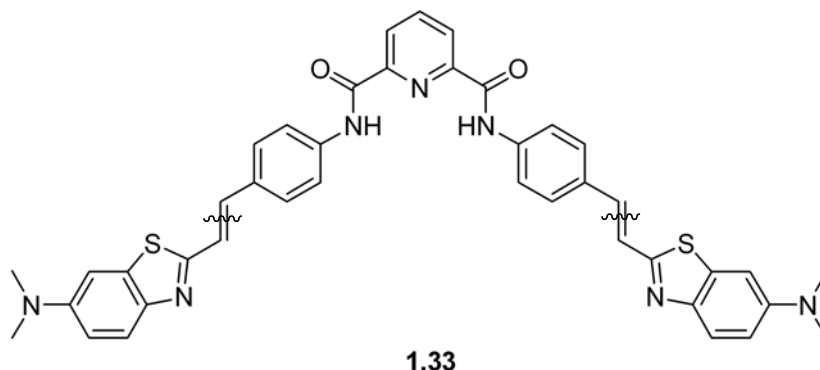
The anion binding of uncharged amido-macrocyclic receptors (compound **1.31**) was tuned by the correct choice of the size of the macrocycles. The effect was quite pronounced, despite the relatively high conformational flexibility of these receptors and competing basicity of the anions.³⁰ For instance, the 20-membered macrocyclic tetraamide ($n = 2$) was found to be selective to H_2PO_4^- in DMSO.



A gold nanoparticle surface modified with amide ligands (compound **1.32**) showed enhanced optical sensing of anions.³¹ The recognition event was due to anion-induced aggregation of **1.32** through hydrogen-bond formation between the anions and the interparticle amide ligands. Coupled dipole approximations showed that a dramatic red shift occurs in the plasmon band when the interparticle distances in the aggregates decrease to less than the average particle radius. Nanoparticles **1.32** within the anion-induced aggregates might not be close enough to cause the color change. Further addition of anions to a solution of **1.32** caused an increase in the extinction coefficient, reflecting the disaggregation of the suprananoparticles composed of **1.32** and anions.

Compound **1.32** was capable of optically sensing changes in anion concentrations of 10^{-6} M, an increase of about three orders of magnitude over that originally expected

from the anion binding ability of neutral amide ligands. This effectiveness cannot be understood only by the cooperative action of the amide ligands assembled on the particle surface. Interparticle van der Waals attractions, which are quite strong, might play a key role, in particular between metal nanoparticles because of the large polarizability of the gold cores. The preference for HSO_4^{2-} and $\text{H}_2\text{PO}_4^{2-}$ over other anions indicates that the hydrogen-bond interaction of $\text{NHCO}\dots\text{HOX}$ ($\text{X} = \text{S}$ or P) significantly contributes to the anion recognition, leading to nanoparticle aggregation.

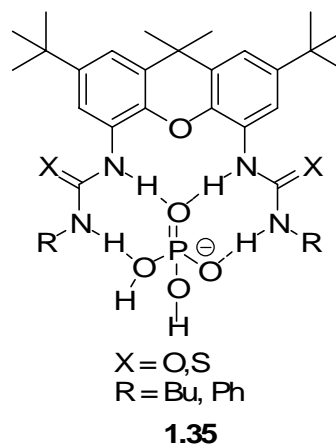
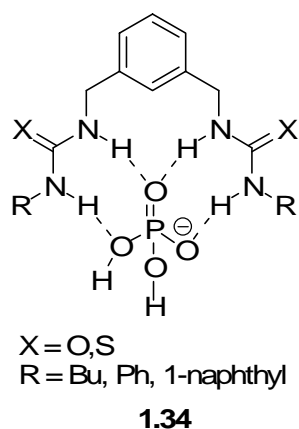


A charge-transfer type fluorescent molecular sensor (compound **1.33**) consisting of a bisamidopyridine receptor and two styryl base chromophores showed H_2PO_4^- and acetate-enhanced fluorescence due to the conversion of weak intramolecular hydrogen bonds into strong ones in the host-guest ensemble.³² In comparison to regular D-A sensors, these tandem-type D1-A2-A3 ICT chromophores employ a bisamidopyridine moiety (A3) for signal generation. A two-fold increase in molar absorptivity for the single-arm sensor dye suggests that the two chromophoric “arms” are not conjugated and do not interact in the ground state. Moreover, A3 acted only as a considerably weak

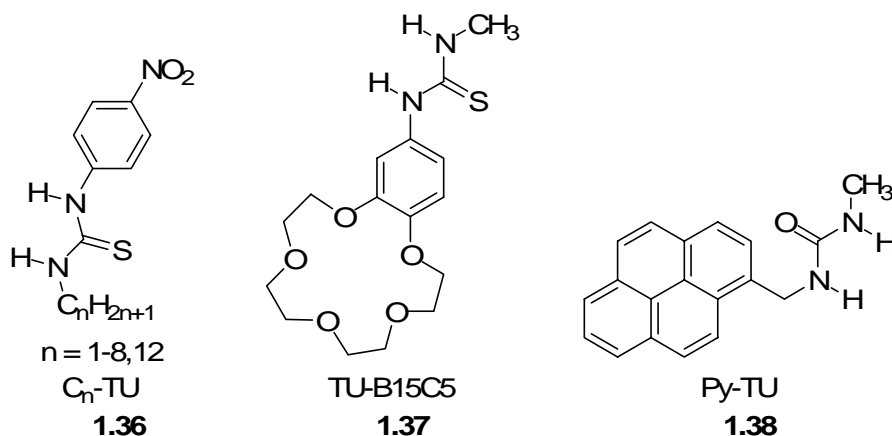
tandem acceptor. Fluorescence studies revealed that the emitting state is largely unchanged, but an efficiently competing, radiationless deactivation channel is activated, which is attributed to a fast hydrogen bond shift in the excited state involving the amino group hydrogen(s) and either a solvent molecule or the pyridino nitrogen atom.

1.3.3 Urea and thiourea derivatives

Urea and thiourea groups are widely used in the design of artificial receptors as a means of providing two hydrogen bonds with a single group. The much stronger binding of H_2PO_4^- by thiourea functionalized receptors is rationalized by the pK_a of the H-bond donating thiourea group, which is roughly 6-9 units smaller than the pK_a of the urea group, making the former a much stronger hydrogen bond donor. The use of thiourea groups also offers further advantages such as solubility in solvents of low polarity and lack of self-association.

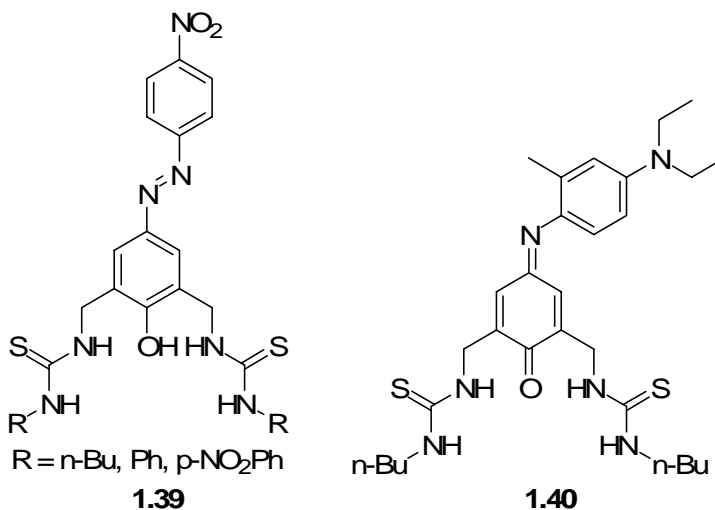


Bis-urea and thiourea receptors (compounds **1.34** and **1.35**) were studied by the Umezawa group.³³ Both 1:1 and 2:2 host-guest complexes were observed at high concentrations by ¹H NMR studies. Multitopic hydrogen bonds were considered to be the driving force of complexation. The selectivity of these hosts for dihydrogen phosphate was explained in terms of the complex geometry and basicity of the guest anions. It was found that the complex stabilities could be significantly increased by using thiourea groups with acidity-enhancing substituents and by preorganizing the receptors with a rigid spacer linking the two thiourea groups. The ion-selective electrodes (ISE) designed based on these receptors were also studied. The influences of the analyte anions on the cyclic voltammograms were largest for dibasic phosphate.

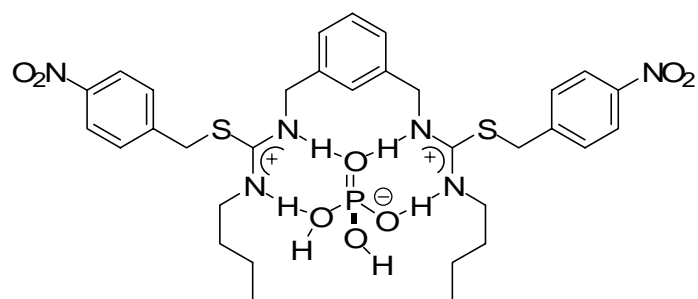


Thiourea-based receptors (compounds **1.36**, **1.37** and **1.38**) with alkyl, crown ether, and 1-methylpyrene moieties were studied by the Thramae group.³⁴ The observed selectivity of compound **1.36** was dependent upon the length of the alkyl chains. The electron-withdrawing p-nitrophenyl group attached to the thiourea moiety provided an effective intramolecular charge transfer conjugated with anion binding, which resulted in a color change and enhanced hydrogen bonding upon anion association. Compound **1.37** was found to bind dihydrogen phosphate selectively over hydrophobic anions at dichloroethane-water interfaces. Compound **1.38** bound CH₃CO₂⁻ monoanion better than H₂PO₄⁻. This observation was explained by the fact that the thiourea moiety acted as an electron donor to quench the excited pyrene. And thus, binding of thiourea with CH₃CO₂⁻ lowered its oxidation potential strongly, so that the complexed thiourea quenched the excited pyrene more effectively than the free thiourea. Also, the fluorescence maximum of the long-wavelength emission was red-shifted with increasing solvent polarity, while the absorption spectra showed little dependence on the solvent polarity. This observation

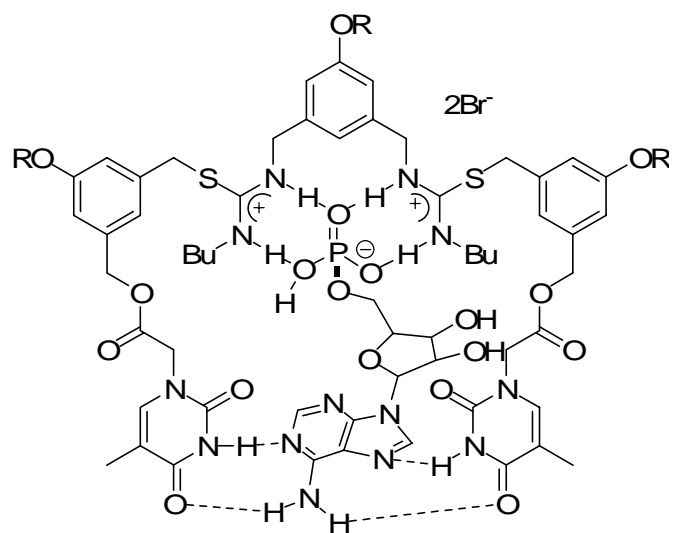
was evidence for the charge-transfer nature of the emission, which resulted from formation of an intramolecular exciplex formed between pyrene and thiourea.



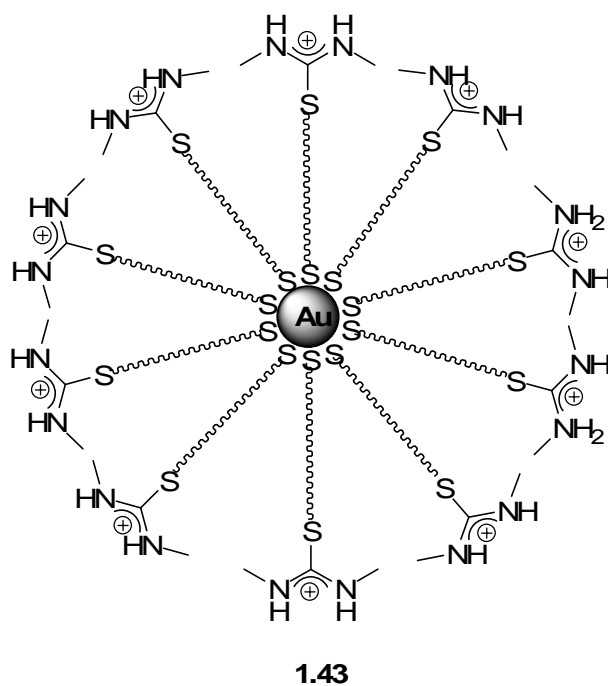
Chromogenic azophenol-thiourea based anion sensor (compounds **1.39** and **1.40**) were developed by the Hong group.³⁵ This system allows for the selective colorimetric detection of H_2PO_4^- , F^- , and AcO^- . Selectivity trends turned out to be dependent upon guest basicity and conformational complementarity between the host and the guest. The introduction of *p*-nitrophenyl groups as an anion-binding site increased the electronic interaction between the host and the anion and resulted in naked eye discrimination of H_2PO_4^- , F^- and AcO^- .



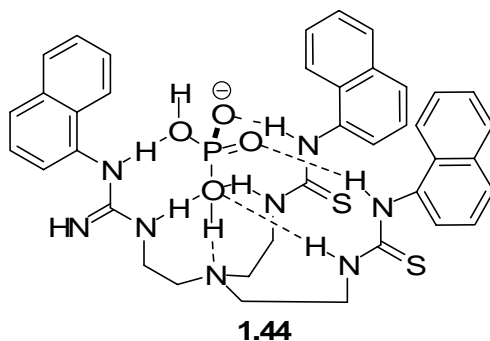
1.41



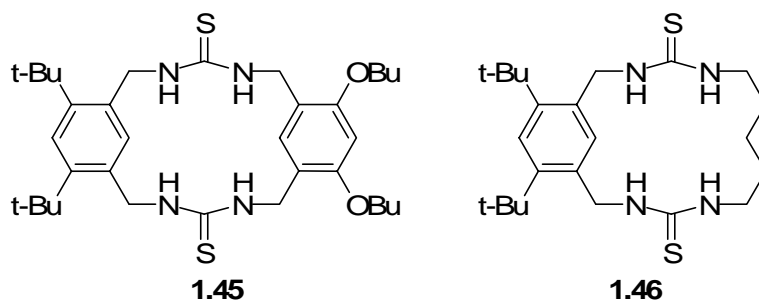
1.42

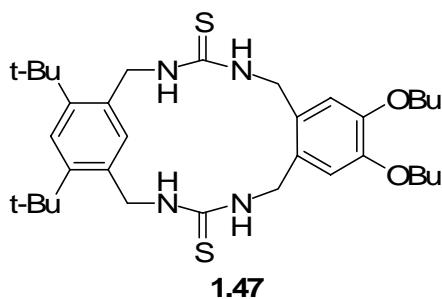


Thiouronium groups (compounds **1.41** and **1.42**) were postulated to be better phosphate recognition elements compared to thiourea groups because of the enhanced acidity of the NH residues and the generation of strong host molecular dipoles. In addition, supramolecular complexes between thiouronium-based receptors and phosphate anions lead to charge balanced and do not need an accompanying cation for transport.³⁶ An appropriately designed lipophilic nucleobase (thymine)-substituted thiouronium carrier (compound **1.42**) was found to show improved extraction and transportation ability for 5'-AMP with both Watson-Crick and Hoogsteen recognition patterns of hydrogen bonding. The isothiouronium-assembled surface on gold nanoparticles (compound **1.43**) lead to a new nanoparticle-based colorimetric sensor of anions based on selective anion-induced aggregation, and it exhibited real-time sensing for oxoanions in aqueous media.³⁷

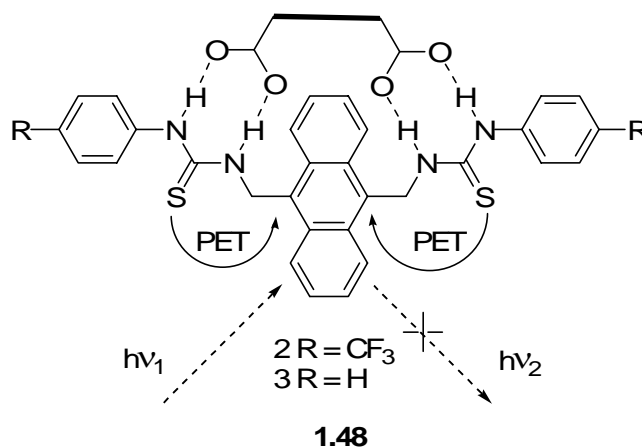


A C_3 symmetrical optically-active receptor (compound **1.44**) was prepared by the Wu group.³⁸ ^1H -NMR spectra revealed that the dihydrogen phosphate was bound tightly into the cavity of the receptor. It was concluded that the size, shape, and the number of interaction sites for both the receptor and the anion guests played an important role in the binding selectivity.



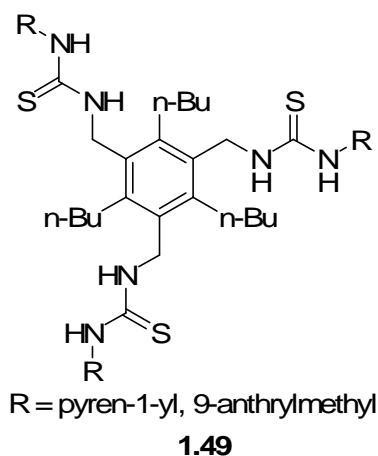


A series of metacyclophane-based cyclic thiourea anion receptors (compounds **1.45**, **1.46** and **1.47**) have been synthesized by Tobe and co-workers.³⁹ ^1H -NMR titration studies showed that the cyclic receptors have higher stability constants with anions than acyclic analogues, and these receptors selectively bound H_2PO_4^- over other anionic guest species due to the lower solvation potential of H_2PO_4^- in DMSO.



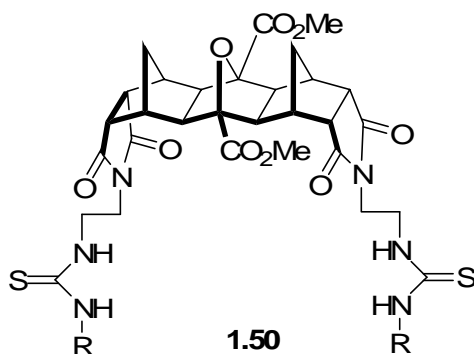
Photoinduced electron transfer (PET) based fluorescent and colorimetric chemosensors (compound **1.48**) were designed by the Gunnlaugsson group for the

recognition of anions such as dicarboxylates and pyrophosphates possessing bidentate binding abilities.⁴⁰ The anion recognition in DMSO took place by bridging the two charge-neutral thiourea receptor sites with concomitant PET quenching of the anthracene moiety. The mechanism of quenching was attributed to an enhancement in the rate of electron transfer from the HOMO of the thiourea–anion complex to the anthracene excited state upon anion recognition (*i.e.* the reduction potential of the thiourea is increased, causing PET to become competitively more viable, which causes the fluorescence emission to be quenched or ‘switched off’).



Tripodal anionic receptors (compound **1.49**) were designed by the Suzuki group.⁴¹ The tripodal fluororeceptor with pyrene moieties adjacent to the thiourea binding sites showed long-wavelength emission upon addition of guest anions in acetonitrile. On the other hand, the structure with methyl-anthracene units showed a decrease in fluorescence intensity upon addition of anions. In both cases, the degree of the change in emission

intensity was in the order of $\text{H}_2\text{PO}_4^- > \text{CH}_3\text{COO}^- > \text{Cl}^- \sim \text{ClO}_4^-$, which was clearly different from that of reference compounds having only one binding site. This trend revealed that geometry matching between host and guest was also important in anion binding selectivity and sensitivity.

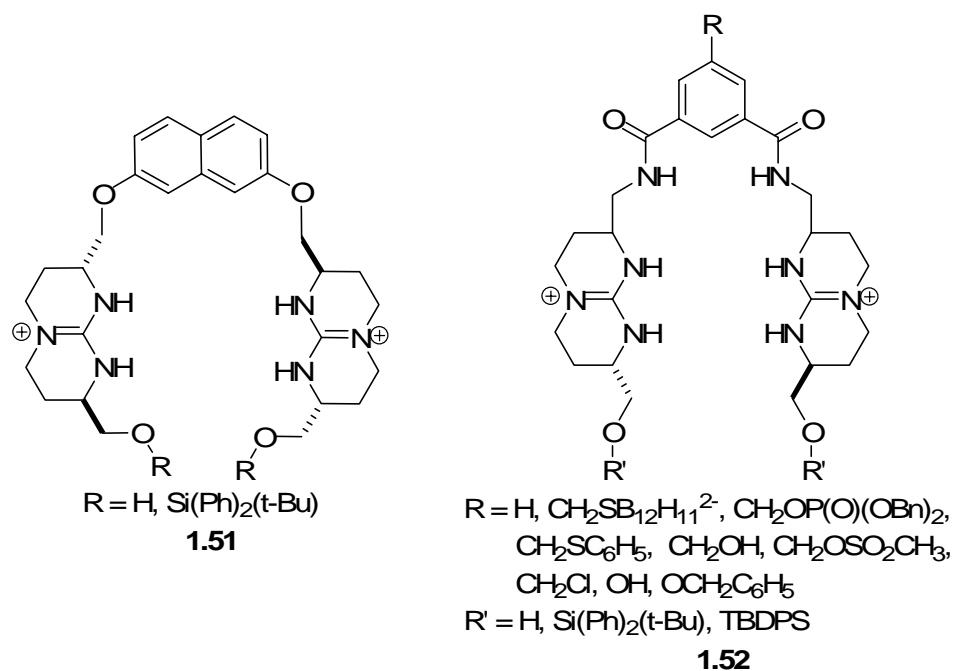


A new family of [3]polynorbornane frameworks exhibiting conformationally preorganized aromatic thiourea (cleft-like) receptors (compound **1.50**) have been designed and synthesized for anion recognition.⁴² These receptors showed excellent affinity for the biologically relevant dihydrogenphosphate (H_2PO_4^-) and dihydrogenpyrophosphate ($\text{H}_2\text{P}_2\text{O}_7^{2-}$) anions (among others), which are bound in 1:1 and 2:1 (host:anion) ratios, respectively. Moreover, visually striking color changes accompanied guest binding, enabling this family to act as colorimetric anion sensors.

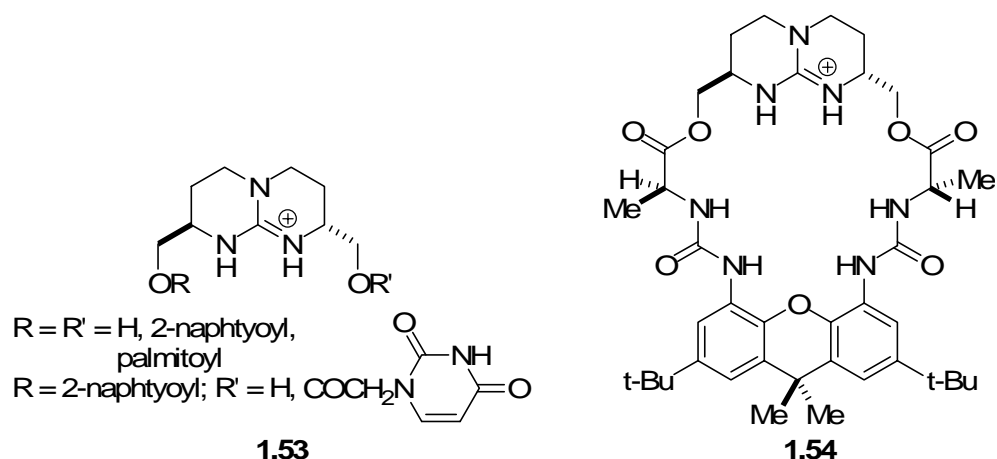
1.3.4 Guanidinium receptors

Guanidine is readily protonated to form the guanidinium ion, which is stabilized by charge delocalization. With a pK_a of 13.6, the guanidinium cation is approximately three orders of magnitude more stable than a protonated secondary amine ($pK_a = 10.5$). Guanidinium therefore remains protonated at high pH values and is ideal for extending the pH range over which anion receptors operate. The reason for the strong interaction with oxoanions lies in the unique binding pattern featuring two parallel hydrogen bonds in addition to the electrostatic attraction. However, the exploitation of this group in host-guest chemistry is hampered by the very effective solvation of the guanidinium function in water along with the lower charge density as compared to that of ammonium-based receptors, leading to weaker electrostatic interactions. In spite of these disadvantages, the attractive features of the guanidinium group have led to the development of an appreciable number of artificial guanidinium-based receptors for anions.

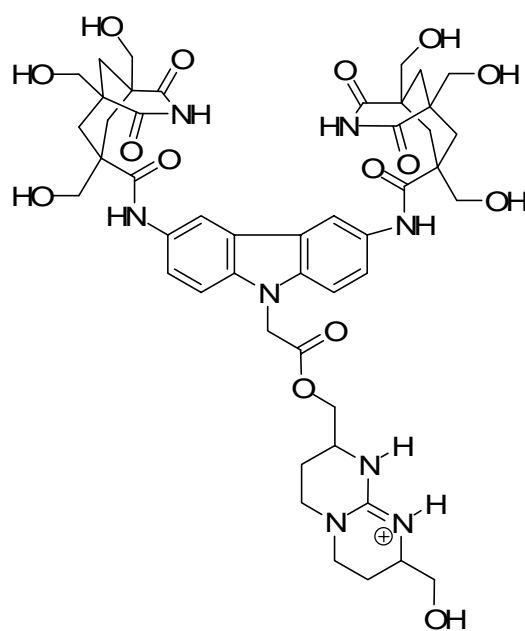
Since the binding is primarily electrostatic, polyammonium salts form more stable complexes (at a given charge) than do polyguanidinium salts. However, whereas the complexation properties of the latter are independent of pH, the complexes of the former are observed only in the limited ranges of pH where both the protonated polyamine and the anion of interest can coexist.



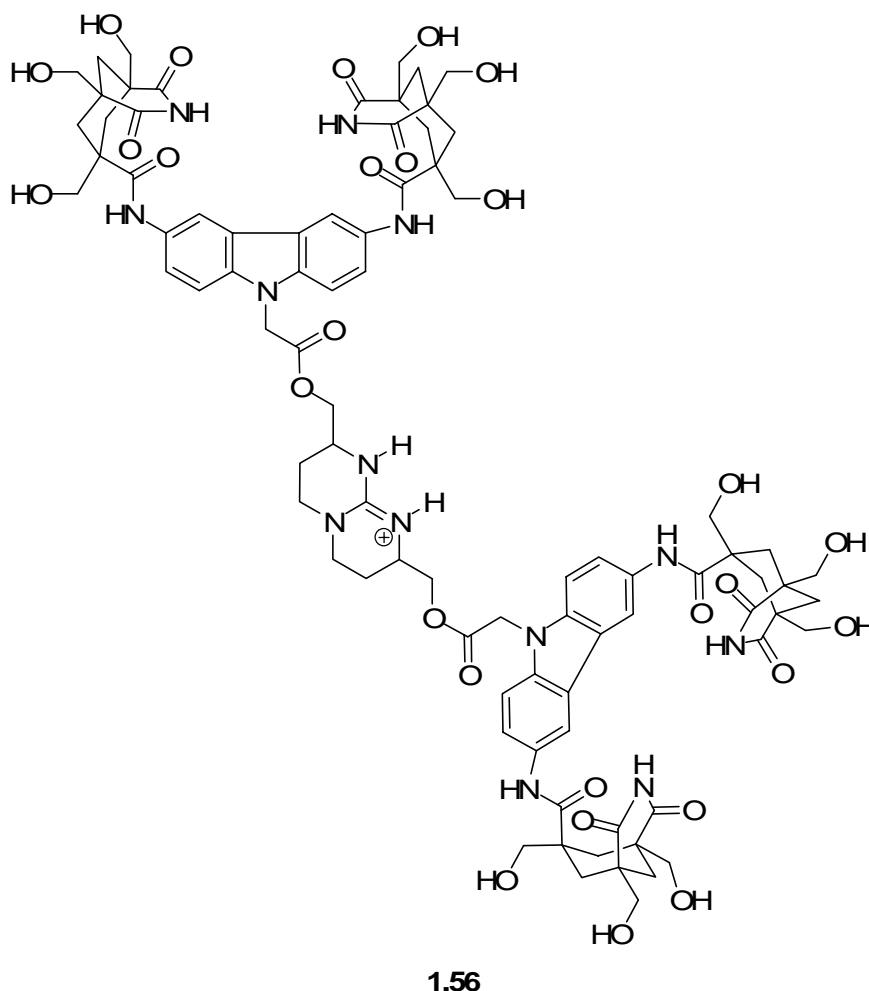
Bis(guanidinium) acyclic receptors (compounds **1.51** and **1.52**) were studied by the Schmidtchen group.⁴³ 1H NMR titration experiments of phosphate with the dicationic chiral host clearly showed 1:1 complexation in dilute solutions. Solvent competition was also observed. The complex stability of compound **1.51** in DMSO was observed to be only one third of that in MeOH. This lower stability was attributed to the higher dielectric constant ($\epsilon(DMSO) = 46.7$; $\epsilon(MeOH) = 32.6$) and stronger donor strength ($DS(DMSO) = 27$; $DS(MeOH) = 16$), which make DMSO a more effective competitor for the hydrogen bonding sites of the host. The ionophores designed based on bis(guanidinium) units (compound **1.52**) were shown to selectively extract oxoanions such as phosphates and sulfate with low detection limits ($10^{-6}M$ for HPO_4^{2-} in the presence of $10^{-3} M Cl^-$.)



The complexation of bicyclic chiral guanidinium receptors (compounds **1.53** and **1.54**) with adenosine monophosphate nucleotides was studied by the de Mendoza group.⁴⁴ However, no chiral recognition was observed even with chiral functionalities. Besides, π - π stacking contributed to better complexation of phosphate to the adenine moiety. As for the macrocyclic receptor **1.54**, molecular mechanics calculations predicted the diphenylphosphate counterion to be located inside the cavity, surrounded by hydrogen bonds with the phosphate oxygens, with the two phenyl rings protruding at each side. At room temperature, ¹H NMR (CDCl₃) spectra showed a pattern consistent with a complex with C₂ symmetry. However, splitting of most signals was observed at 213 K, indicating that the counterion was outside the cavity and rapidly exchanging between both sides of the macrocycle at room temperature. It remains to be established whether this exchange takes place through the annulus or whether the anion was simply jumping from one side to the other without crossing the ring. Such a study would not only clarify the exchange mechanism but also provide understanding of the mode of binding and the potential role of the counterion as a templating agent during the synthesis.



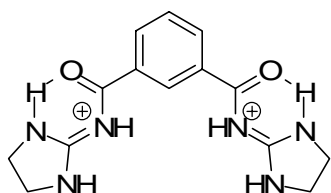
1.55



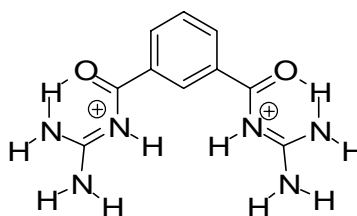
1.56

The Rebek group⁴⁵ prepared highly organized synthetic receptors that selectively bind nucleotide 2',3'-cAMP over 3',5'-cAMP. A combination of hydrophobic, electrostatic, and hydrogen bonding interactions were considered as the reason for this high selectivity. Molecular modeling studies indicated that the lowest energy conformation of the complex of **1.55** and 2', 3'-cAMP featured a hydrogen bond between the hydroxyl proton (exocyclic to the guanidinium) and phosphate and a coplanar arrangement of the two delocalized charges at the phosphate and guanidinium. Thus,

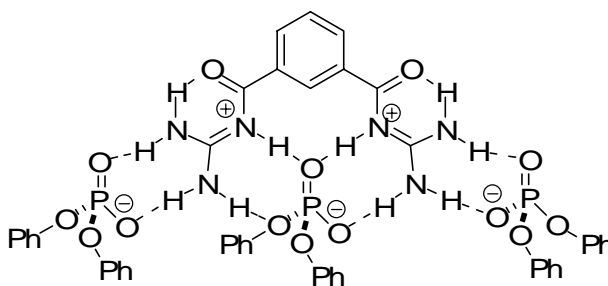
hydrogen bonding occurred between the guanidinium protons and phosphate oxygens in addition to the electrostatic interaction. Conversely, models of the corresponding complex of **1.55** and 3', 5'-cAMP suggest a perpendicular geometry between the two planes of delocalized charge, enabling electrostatic interactions but precluding a salt bridge type of hydrogen-bonding interaction. The phosphate-guanidinium interaction in this system was calculated to be 0.6 kcal/mol (ionic strength, $I_{[\text{NaCl}]} = 51\text{mM}$) and 0.3 kcal/mol ($I_{[\text{NaCl}]} = 501\text{mM}$). The maximum enthalpy of such an electrostatic interaction in water alone was estimated to be 2.4 kcal/mol.



1.57

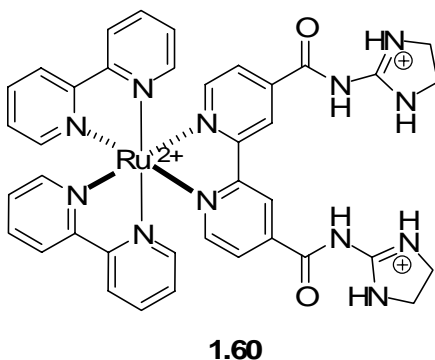


1.58



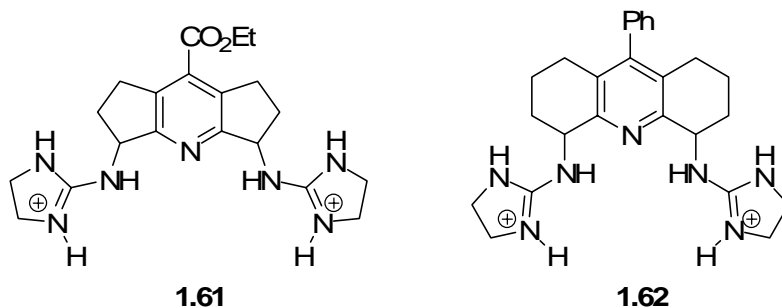
1.59

Receptors **1.57** and **1.58** were studied by the Hamilton group.⁴⁶ Acylguanidinium moieties applied in these receptors not only reduced basicity of the guanidinium moiety but also introduced intramolecular hydrogen bonding that further enhanced the rigidity of this type of receptor. ¹H NMR studies of compound **1.58** showed 1:3 complexation (compound **1.59**) with stronger complexation of the first substrate ($4.6 \pm 1.7 \times 10^4 \text{ M}^{-1}$) in the middle, and weaker complexation of the second and third substrates that were not observed for compound **1.57**.

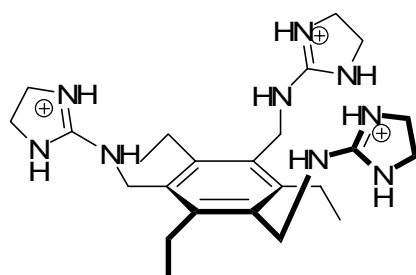


The Watanabe group⁴⁷ studied the complexation between a metalloreceptor (compound **1.60**) and tetraethylammonium diphenyl phosphate (TDPP) or dibenzyl hydrogen phosphate (DBHP). UV-visible responses of complexed **1.60** were attributed to a specific association rather than counter anion exchanges or solvent polarity changes due to a control experiment using $\text{Ru}(\text{bpy})_3^{2+}$ that showed no UV-Vis spectral changes. Fluorescence experiments indicated that the slight blue shift and the increase of the MLCT band in the visible region upon anionic TDPP association was due to the rigidified receptor, inhibiting nonradiative decay from vibrational and rotational relaxation modes.

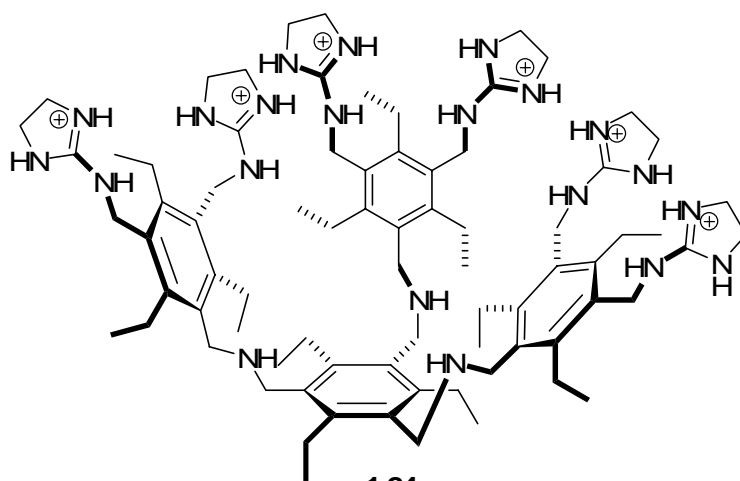
A red shift and a decrease of the MLCT band upon neutral DBHP association were probably caused by intramolecular proton transfer. From these UV-visible absorption changes, K_a 's of 33000 M^{-1} and 4800 M^{-1} were calculated for TDPP and DBHP, respectively. The lower preference of **1.60** for DBHP might be due to electrostatic repulsion between the cationic metal center and the positive charge produced on the neutral binding site of **1.60** upon complexation.



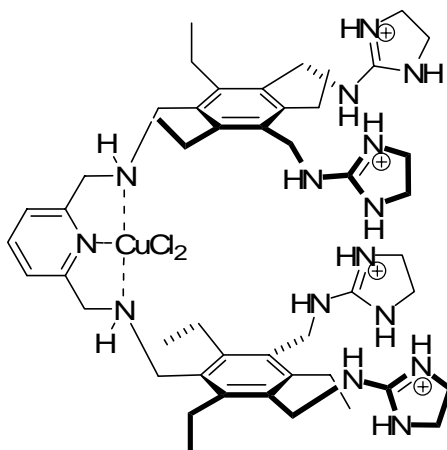
Bis(guanidinium) receptors (compounds **1.61** and **1.62**) were investigated by the Anslyn Group.⁴⁸ The binding affinity and selectivity were tuned by adjusting the receptor's cavity size and conformation flexibility, which was achieved by diastereomeric (*meso*- and *d,l*-) linking of the guanidinium moiety to cyclopenteno (compound **1.61**) and cyclohexeno (compound **1.62**) rings. Stronger binding was found in the *meso*-forms due to the constraint of the two guanidinium groups on the same side thus rigidifying the receptor molecules. Better catalytic ability toward phosphodiester hydrolysis was also achieved from an additional ion pair formation in the transition-state-receptor complex.



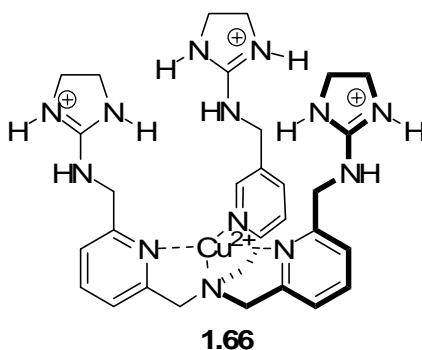
1.63



1.64



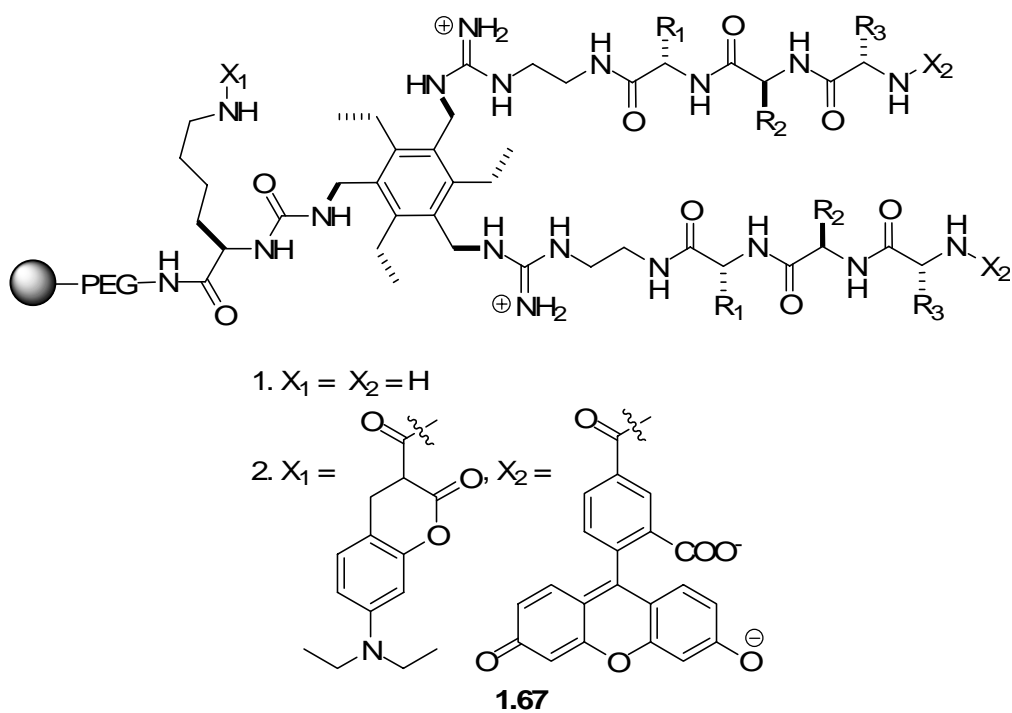
1.65



The hydrogen-bond-mediated complexation of different kinds of phosphate anions with preorganized C_{3v} symmetric synthetic receptors (compounds **1.63**, **1.64**, and **1.66**) was studied by the Anslyn group in order to achieve geometric complementary to the guest in addition to incorporating hydrogen bonding, electrostatic interaction and metal coordination.⁴⁹ Indeed, the phosphate binding affinity did benefit from this proper cavity design. Receptor **1.66** was used to selectively detect inositol trisphosphate (IP_3) at nanomolar concentrations with an association constant $4.7 \times 10^5 \text{ M}^{-1}$ in water ($1.0 \times 10^8 \text{ M}^{-1}$) in methanol without significant ionic strength interference.

2,3-Bisphosphoglycerate (2,3-BPG) is a highly anionic molecule that is strongly hydrated in water. Hence, multiple molecular-recognition contacts are required in a receptor to successfully compete with the solvation of this target. Nature competes with solvation by forming several salt bridges between 2,3-BPG and the cationic side chains of lysine and histidine in deoxyhemoglobin. Based upon this precedent, receptor **1.65** was designed, and an extremely strong binding was observed for 2,3-BPG ($8 \times 10^8 \text{ M}^{-1}$ in 50:50 water/methanol at pH 7.4, $4 \times 10^7 \text{ M}^{-1}$ in pure water at pH 6.8).⁵⁰ The high affinity of this receptor made it possible to deprive hemoglobin of available 2,3-BPG and thus

control the active level of 2,3-BPG and the related oxygenation level of hemoglobin. This use of a small organic receptor to bind and regulate the levels of a biological effector, and thereby control a physiological function, represented a rarely explored means towards the development of a pharmaceutical agent.

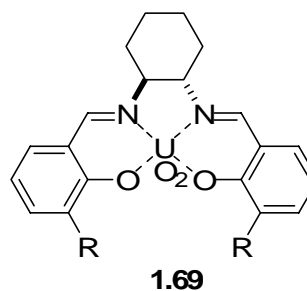
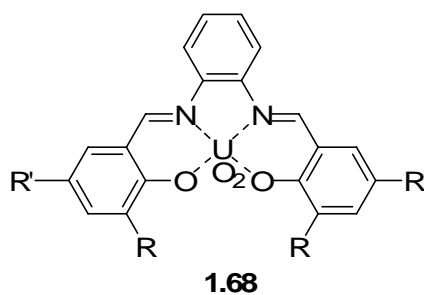


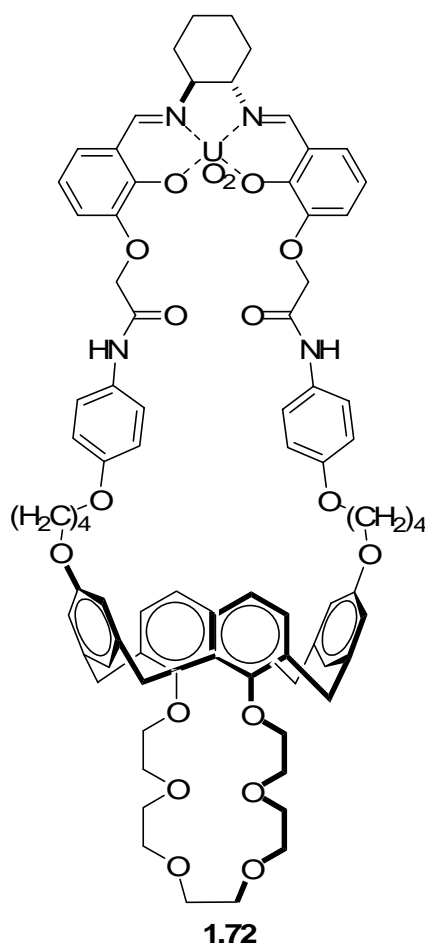
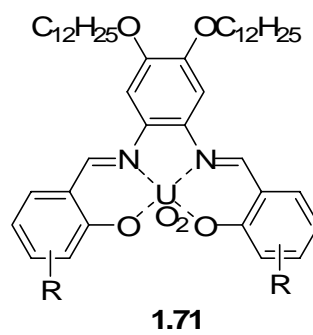
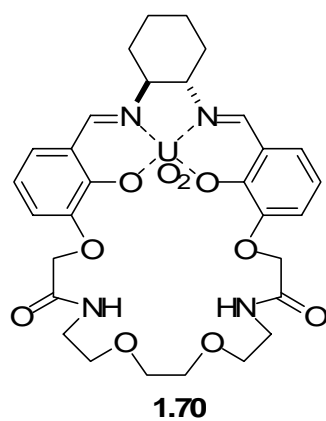
Differential anion chemosensors (compound **1.67**) have been developed using the pinwheel scaffold, which places adjacent groups alternating up and down with respect to the plane formed by the benzene ring, creating a preorganized cavity for binding interactions.⁵¹ The differentiating ability was generated from combinatorially synthesized peptide arms, where peptide Ser-Tyr-Ser exhibited very high detection selectivity for ATP over structurally similar competing analytes. The lack of response to AMP

suggested the necessity for triphosphates to bind strongly to the guanidinium entities of **1.67**, while the lack of response to GTP indicated the specificity for nucleotide bases imparted by the tripeptide arms. The combination of serine and tyrosine suggested π -stacking between the phenol of tyrosine and adenine, and hydrogen bonding interactions between the serine hydroxyl and/or the ribose or adenine.

1.3.5 Lewis Acid Receptors

The concept in designing Lewis acidic receptors is based on the formation of coordinative bonds between Lewis acidic centers such as boron, silicon, tin, mercury, vanadyl and uranyl-containing compounds.⁵² These Lewis acidic centers contain empty orbitals in proper orientations to accept a lone pair electrons from anions to form strong dative bonds, which result in enhanced binding affinity.





The uranyl cation is a chelating center with extensive applications (compounds **1.68-1.72**).⁵³ It prefers pentagonal bipyramidal coordination, with the two oxygen atoms at the apical positions and four of the equatorial positions occupied by the preorganized ligand. The fifth equatorial position can coordinate to nucleophilic guest species.

Uranyl salenes were studied by the Reinhoudt group. This type of neutral anion receptor containing an immobilized Lewis acidic binding site (UO_2^{2+}) led to high thermodynamic stabilities combined with high selectivities and were very important for applications in sensors and membrane transport experiments. Functionalized uranyl salenes bind anion guests through coordination with the uranyl center and multiple hydrogen bonds. Uranyl salenes had such a strong affinity towards phosphate (10^{2-3} over Cl^- and NO_3^-) that the association could be detected by X-ray, NMR, and even FAB spectrometry. Lipophilic uranylsalophene derivatives were also applied as ionophores in membranes and found to be very successful in the transportation of very hydrophilic dihydrogen phosphate even in the presence of an excess amount of lipophilic ions such as nitrate and perchlorate.

1.3.6 Polyammoniums and analogs

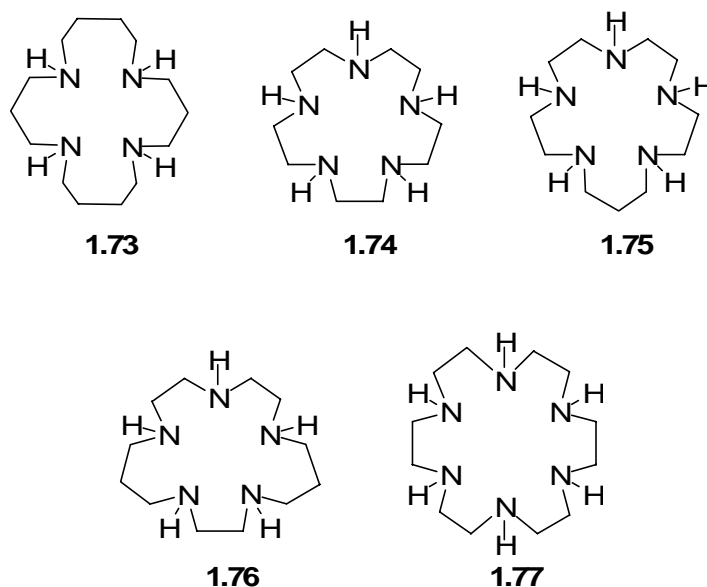
The extensive interest in studying polyammoniums and their analogs arrives from their capability of hydrolyzing bio- and organic phosphate diesters, which imparts potential applicability as antiviral or anticancer therapeutic agents.⁵⁴ Multiply charged polyamines have greater charge density within the molecular skeletons which generate

strong electrostatic interactions in addition to acting as hydrogen bonding donors. In order to be successfully applied in biological systems near neutral pH, amine nitrogens are often separated by 3 or 4 methylene groups yields pKa's in the range of 7 and above. Thus, a larger number of nitrogens can be protonated to give a higher positive charge density.

Moreover, stability and selectivity also results from structural effects, such as the size of macrocycles and the mode of metal coordination. It has been found that size effects can alter the trends of complexation. For example, triprotonated hexaazacyclooctadecane was found to form more stable complexes with ADP^{3-} than those of the equally protonated forms of the pentaaza macrocycles. Dinuclear Cu(II) polyammoniums show an increase of binding strength with increasing charge of both hosts and guests, indicating that the strength of the coordinate bonds, electrostatic attractive forces, and hydrogen bonds all contribute to the stabilities of the ternary Cu(II) complexes. Furthermore, the finite size of bridging group due to a favored Cu-Cu distance, the dinuclear macrocyclic complex can contort to bind less than optimally sized bridging groups, albeit with greater steric strain. Therefore the distance between the coordination sites enabled the Cu(II) complex to be somewhat preorganized to selectively bind certain sizes of anions as bridging groups.

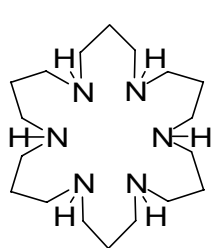
Quaternarized ligands resulted from nitrogen methylation in polyazamacrocycles were also investigated. Nitrogen methylation altered the electronic properties of the amino groups and the ligand conformations. Methyl groups oriented protonation on secondary nitrogens giving rise to the formation of preferential conformations of the

protonated species, increasing selectivity in anion binding. However, the complexes were of reduced stability with respect to the analogous polyazacycloalkanes. The disposition of ammonium binding sites, the low charge density of the receptor as well as the inhibition (by N-quaternarization) of hydrogen bonding can be invoked to explain this behavior.

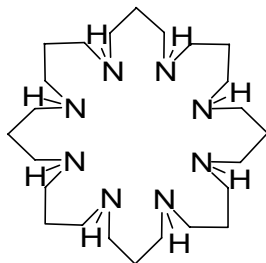


Kimura and coworkers first reported macromonocyclic polyamines that interacted with with biologically important polyanions, such as phosphate, AMP, ADP, and ATP, at neutral pH. (compound **1.73-1.77**).⁵⁵ 1: 1 ion pairings were established between the polycationic forms of the macrocycles and the polyanionic forms of the phosphates by polarographic methods and ¹H NMR shift measurement. Phosphate complex formation was governed mainly by electrostatic forces. Thus, the more negative nucleotides were more strongly attracted to the protonated polyamine macrocycles: the stability sequence

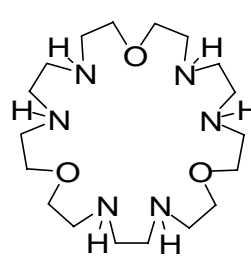
was on the order of $\text{ATP}^{4-} > \text{ADP}^{3-} > \text{AMP}^{2-}$ for each compound. Despite the same charge as HPO_4^{2-} , AMP^{2-} formed 10^{1-2} times more stable complexes with **1.75** and **1.77** than inorganic phosphate. The extra stability for the AMP^{2-} complexes came from an additional interaction of the adenine base with the receptor.



1.78

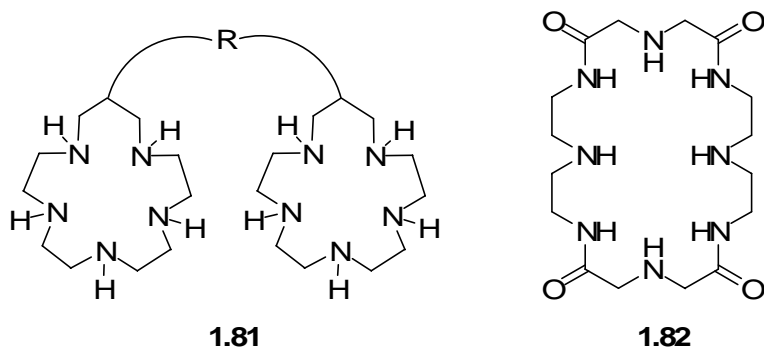


1.79

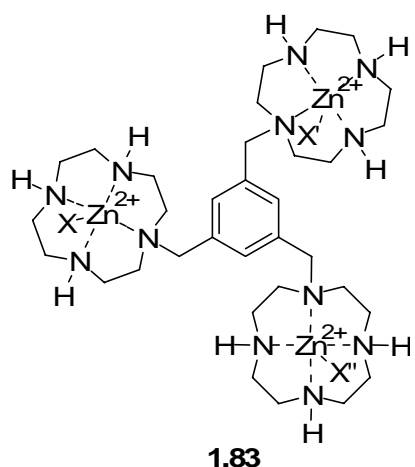


1.80

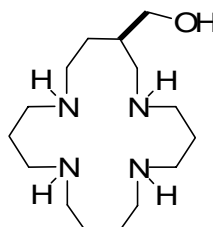
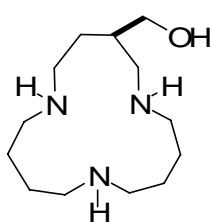
pH-metric measurements showed that the fully protonated compounds **1.78-1.80** formed stable complexes with the nucleotides anions AMP^{2-} , ADP^{3-} , and ATP^{4-} .⁵⁶ Both 1:1 and 1:2 complexes formed depending upon the size of the rings and substrates. Polarographic methods showed that the stability of the complex of a given ligand increased with the charge of the anion (AMP^{2-} , ADP^{3-} , ATP^{4-}). Moreover, for a given anion, the stability increased with the charge (degree of protonation) of the given ligand. Structural effects were also observed; threefold symmetric **1.78** and **1.80** responded more to the substrates of planar or tetrahedral geometries, while fourfold symmetric **1.79** responded more to those of square planar and octahedral geometries. Compound **1.80** was found to bind more strongly than compound **1.78**, and this observation was attributed to the higher local charge density and larger size of compound **1.80**.



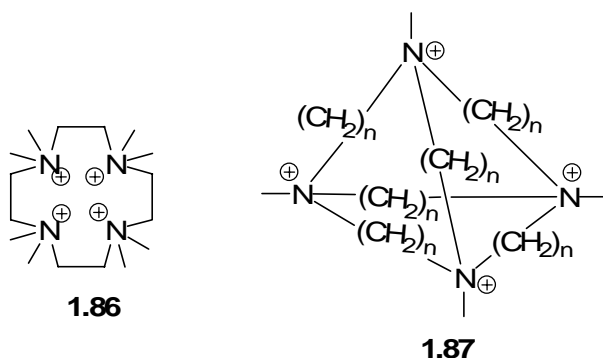
Bis(macrocyclic polyamine) ligands (compound **1.81** and **1.82**) formed stable 1:1 complexes with citrate³⁻, AMP²⁻, ATP⁴⁻, HPO₄²⁻, [Fe(CN)₆]⁴⁻, and [Fe(CN)₆]³⁻ anions.⁵⁷ Comparison of the association constants (K_a) calculated for the bis(macrocyclic polyamine) ligands with those of the parent monomeric polyamines revealed that the attachment of the second polyamine moiety always enhances anion encapsulating abilities. The greater complex stabilities exhibited in the bismacrocycles was understood by invoking a ditopic interaction between the two macrocycles. As indicated by the lowered protonation constants of **1.81** and **1.82** with respect to those of the parent monomacrocyclic, an increase in the number of protons attached to the bismacrocycles would increase electrostatic repulsions between the two protonated moieties in the same molecules. Anion complexation serves to reduce these electrostatic repulsions. This effect is best achieved by invoking a sandwich complex structure, where the donor anion is located between the two protonated macrocycles.



The Kimura group⁵⁸ reported that Tris(ZnII-cyclen) (compound **1.83**) was an effective receptor for C₃-symmetric organic phosphates (and phosphonate) with high 1:1 affinity constants in slightly acidic aqueous solutions. ³¹P NMR titrations revealed that the interaction between phosphate and the polyammonium rings was negligible, and the association exclusively resulted from the cooperative recognition of three zinc(II) ions. The loss of anionic association at neutral pH was attributed to the formation of a strong intramolecular hydrogen-bonding network (closed-form) at pH range 6-8.

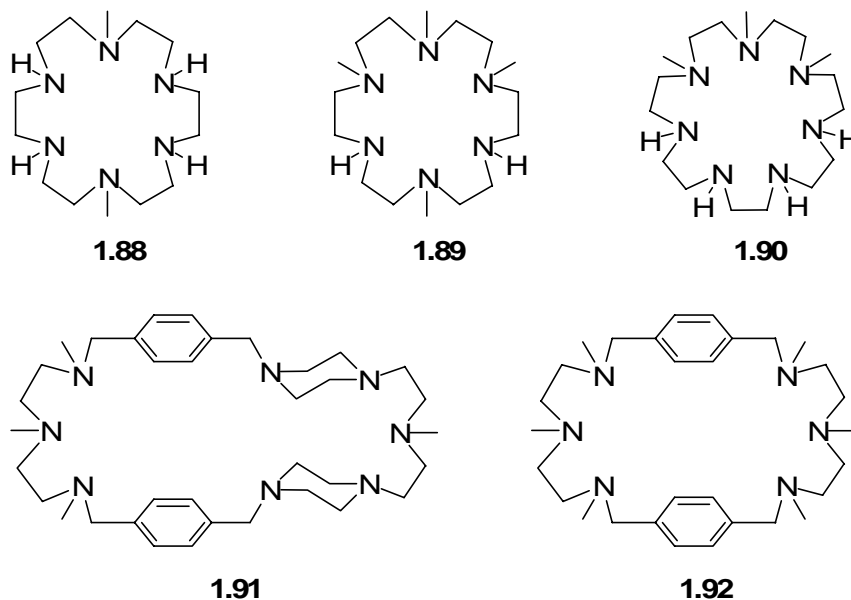


Chiral polyamines (compound **1.84** and **1.85**) were prepared by the Marecek group,⁵⁹ and their binding to ATP was studied. Triammonium macrocycle **1.84** was prepared to test if hydrogen-bonding to the terminal phosphate group of ATP in correct symmetry contributes highly to the stability of the complex. However, receptor **1.85** was found to bind more strongly than **1.84**. It was concluded that the major contribution to the stability of anion complexation in H₂O is the sum of the charge-charge interactions. Tetraprotonation of receptor **1.85** in the presence of the tetraanion ATP⁴⁻ leads to a stronger interaction than with that of **1.84**.

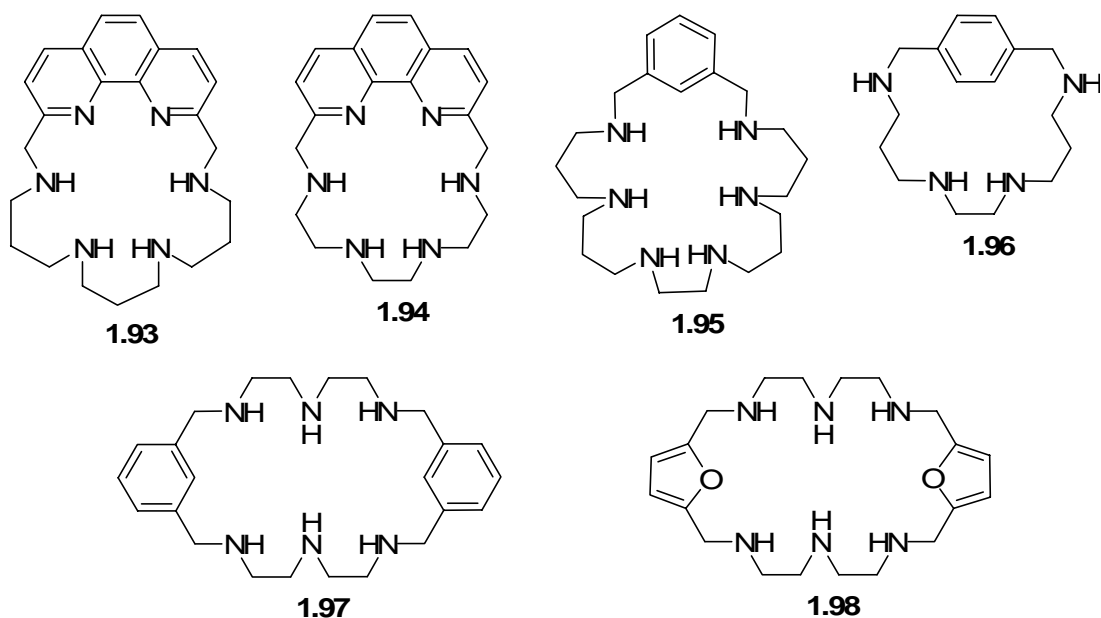


The interactions of phosphate with tetraammonium macrocyclic receptors (compound **1.86** and **1.87**) were studied by the Paoletti group in comparison to their protonated ammonium modes.⁶⁰ Due to the fact that the quaternarization of the nitrogen atoms prevented the formation of hydrogen bonds, no detectable interactions arise with ATP in compound **1.86**. The result was consistent with the hypothesis that the formation of hydrogen bonds played a role of major importance in the interaction between ATP and

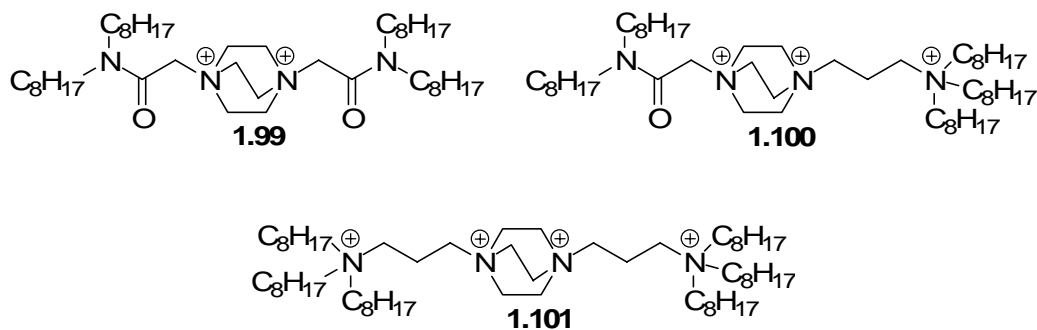
protonated ammonium receptors. However, strong 1:1 inclusive complexes with HPO_4^{2-} was formed by compound **1.87** ($n = 6, 8$), where the coordinating ability of electrostatic interactions and hydrophobicity were believed to dominate in the association.

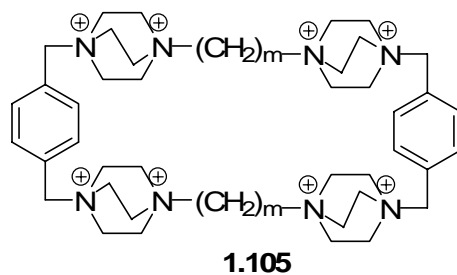
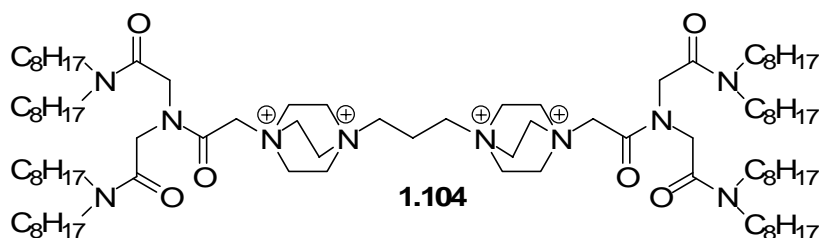
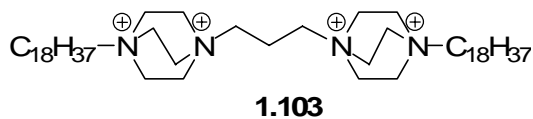
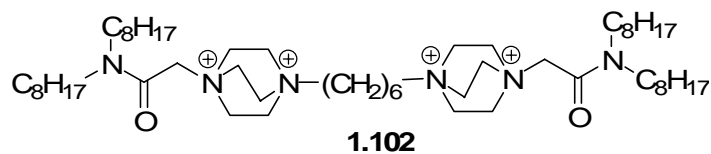


The Paoletti group reported a charge localization effect on partially methylated polyammonium receptors (compound **1.88-1.92**).⁶¹ The investigations revealed that the different basicity between tertiary and secondary amines opposed the redistribution of the positive charges on the macrocycle expected when the anion is approaching the polyammonium receptor. Moreover, the multimethylated derivatives of the polyammonium ligands introduced further topological factors and charge localization, increasing selectivity in anion recognition on a basis besides size criteria.



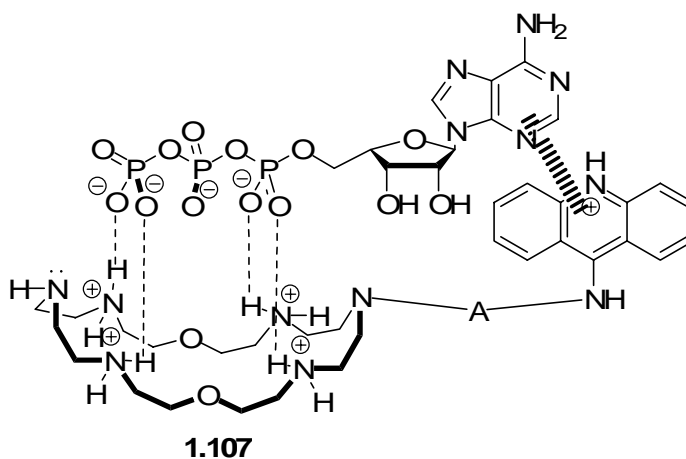
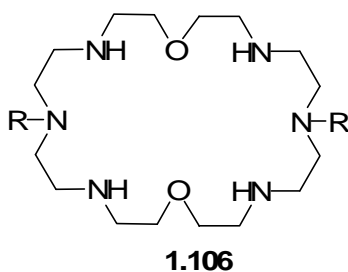
The introduction of aromatic moieties into polyammonium macrocycles (compound **1.93-1.98**) not only rigidified the structure and hence changed the topology of the recognition skeleton, but also provided charge-dipole as well as π - π stacking and hydrophobic interactions, which are particularly important for nucleotide recognition.⁶²





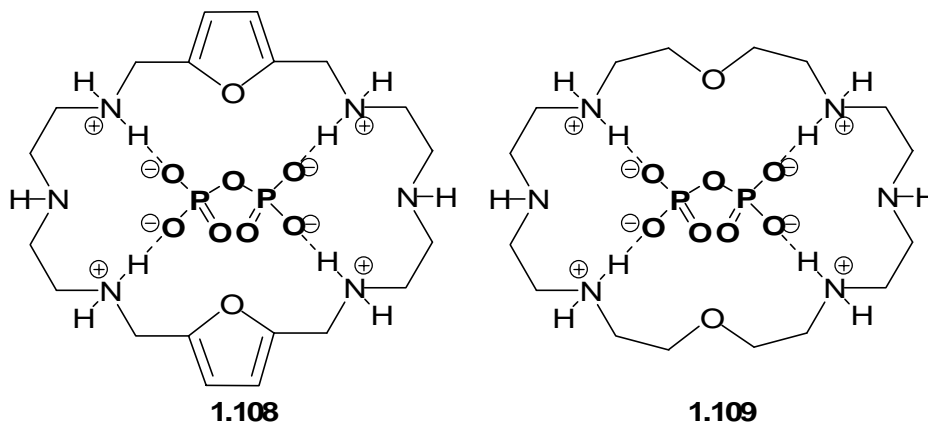
Tetraquaternary 1,4-diaza[2.2.2]-bicyclooctane (DABCO) derivatives (compound **1.99-1.105**) were designed to be selective for nucleotide 5'- triphosphates based on its high local charge density.⁶³ Attachment of lipophilic alkyl chains (compound **1.99-1.104**) made this type of receptor successful carriers in effective transport of ATP from aqueous phase to organic phase without any leakage. However, *in vitro* studies were not successful. In biological systems, the carriers act as detergents that break the liposomal structure and lead to nonspecific leakage from the liposomal interior rather than

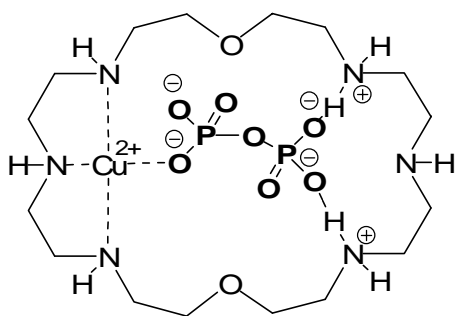
mediating the transport of ATP across liposomes. DABCO-based cyclophanes (compound **1.105**) were synthesized to investigate the intracavity encapsulation ability of guest molecules. A 1:1 binding stoichiometry was established for ATP with the following K_a 's: 13300 M^{-1} ($m=3$), 15900 M^{-1} ($m=5$), 12100 M^{-1} ($m=7$). The guest was suggested to bind externally with the host through π - π stacking and/or electrostatic interactions, where the cavity size is not critical.



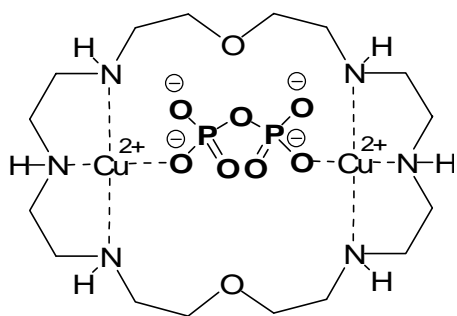
The Lehn research group studied the catalytic activity of the polyammonium macrocycle derivatives **1.106** in the hydrolysis of ATP with an HPLC procedure to

follow the reaction course.⁶⁴ It was found the acridine derivatives stabilized the ATP adenine group by stacking interactions in addition to dominant electrostatic and hydrogen bonding interactions (compound **1.107**). It was also suggested that the catalysis involved: (1) recognition and selectivity in the initial substrate binding by the synthetic receptor-bearing reactive groups, (2) transformation of the bound species, and (3) release of the products, to regenerate the catalyst for a new cycle. Moreover, the hydrolytic reaction could be accelerated in the presence calcium (II) and manganese (II), which suggested that metal cations organize ATP into a more reactive structure, and hence, assist in the displacement of the leaving group.

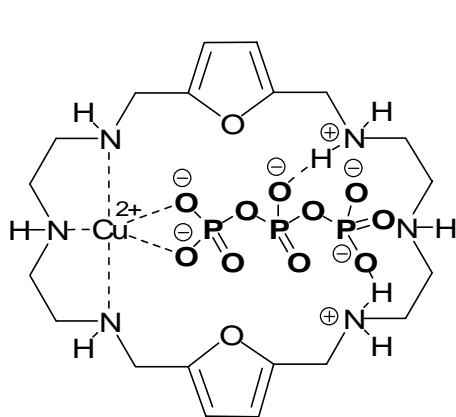




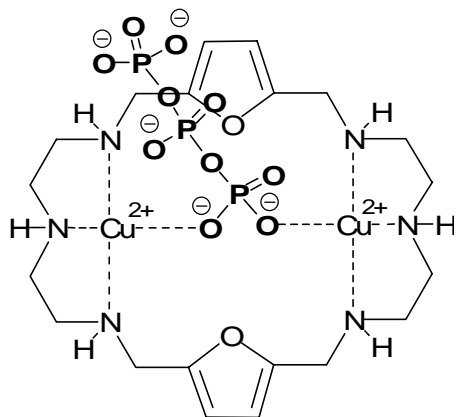
1.110



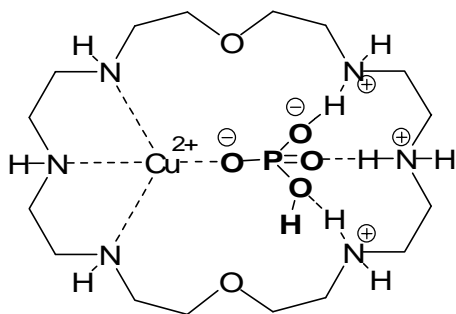
1.111



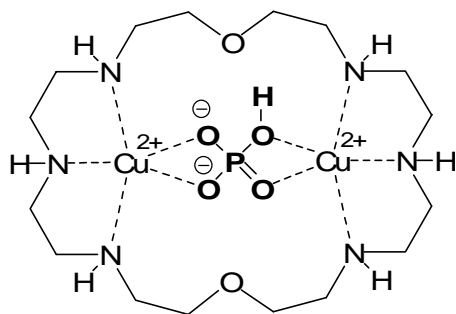
1.112



1.113



1.114



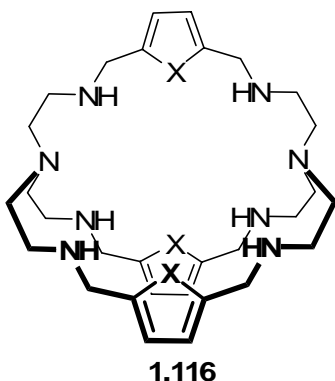
1.115

The interactions between monophosphate, pyrophosphate and triphosphate and 1,4,7,13,16,19-hexaaza-10,22-dioxacyclotetracosane (OBISDIEN), its analog

3,6,9,16,19,22-hexaaza-27,28-dioxatricyclo[22.2.1.1]octacos-1(26),11,13,24-tetraene (BFBD) as well as their metal coordinated scaffolds were investigated by the Martell group (compound **1.108-1.115**).⁶⁵ The information obtained from both solution phase and solid phase (crystal structures) revealed that all scaffolds exhibited affinity in the order: monophosphate < pyrophosphate < triphosphate. This was an effect of not only the increase in negative charge of the anionic substrate and hence an increase in Coulombic attraction for the protonated macrocycle, but also the increase in number of oxygen atoms in the substrate that are able to engage in hydrogen bonding interactions. The effect, however, was not unlimited in the sense that the further increase in the number of condensed phosphates is not expected to lead to more stable complexes since the macrocycle is only of finite size. Geometrical compatibility of substrate and ligand was therefore important.

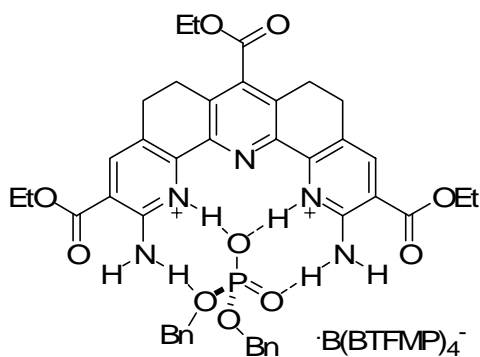
From the structural information on the binary cation BFBD-Tp, an interpretation about the solution structure of BFBD-ATP and the mechanism of catalytic hydrolysis of ATP can be made. The terminal phosphate P(γ) group and the mid phosphate P(β) group on ATP interact with the protonated macrocycle strongly through the multiple hydrogen bonds. The bulky adenosine group attached to the P(α) group prevents this group from effective interaction with the macrocycle. Thus the P-O bond between P(γ) and P(β) is greatly weakened and the ATP-cleavage occurs between P(γ) and P(β) via the attack on P(γ) by nucleophiles present in the solution. At pH \sim 4 and above the central nitrogen atoms on the macrocycle BFBD act as nucleophiles to attack P(γ), provided that they are located in close vicinity of the P(γ) group.

The binding properties of copper (II)-macrocycle-phosphate/polyphosphate systems showed that the phosphates not only possessed high charge but also had structural properties (tetrahedral symmetry) naturally fitting into the space between the protonated diethylenetriamine moiety and the metal ion to which it could coordinate. Even when the nitrogens were not protonated, the phosphate ions could coordinate to the Cu^{2+} ion as well as it could hydrogen-bond to the neutral nitrogens. Thus, the basicity of the anionic substrate, electrostatic attractive forces, hydrogen bonding and the geometrical match between host and guest acted in concert in the formation of ternary complexes.

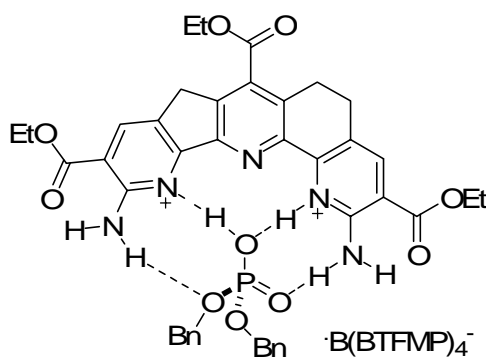


Multidentate cryptand ligand (compound **1.116**) formed high-affinity 1:1 complexes with phosphate, characterized by association constants of almost 10^7 M^{-1} .⁶⁶ The binding affinities and the anion selectivities were mainly caused by the charges of ligands and anion inclusion, which was asserted on the basis of simple calculations of the electrostatic contribution to the anion/receptor interactions. The binding of all

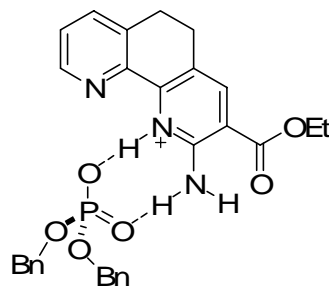
investigated anions was exothermic at 298.2 K. The contribution of the large negative ΔH values to the free energy of anion binding to the pyrrole type ligand was partially compensated by marked negative ΔS values. These unfavorable entropic contributions were attributed to the additional inclusion of water molecules in the anion/receptor complexes.



1.117

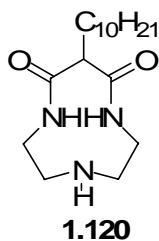


1.118



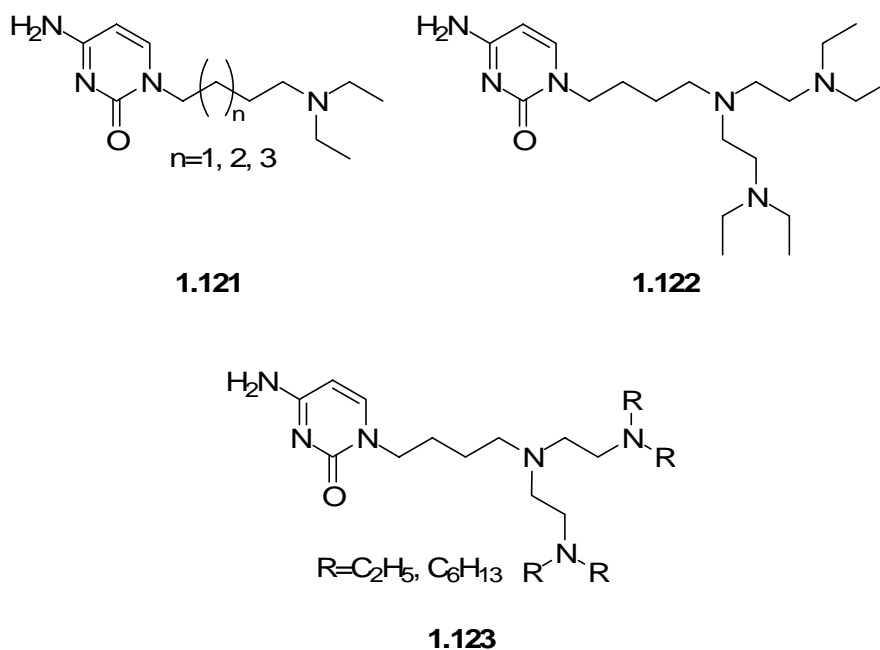
1.119

The Anslyn group designed polyaza-receptors (compound **1.117-1.119**) to investigate the optimum binding cavity size for phosphoric acid diesters in chloroform and to measure the strength of interactions formed by individual host hydrogen bond donors and acceptors.⁶⁷ The binding properties were monitored by isothermic ³¹P or ¹H NMR. The NMR data indicated equilibria involving both 1:1 and 1:2 host-guest complexes. Formation of 2:1 guest-to-host complexes is a result of the large dimerization constants for phosphoric acid diesters ($6.5 \times 10^4 \text{ M}^{-1}$). Fluorescence and UV/vis spectroscopy showed that the 1:1 binding constants measured in chloroform for dibenzyl hydrogen phosphate or dinaphthyl hydrogen phosphate with receptors 1-3 were $7.8 \times 10^3 \text{ M}^{-1}$, $8.9 \times 10^4 \text{ M}^{-1}$, and $1.3 \times 10^3 \text{ M}^{-1}$, respectively. The strength of complexation of phosphoric acid diesters to the polyaza-clefts was dependent upon the number of hydrogen bonds formed and the receptor cavity size.



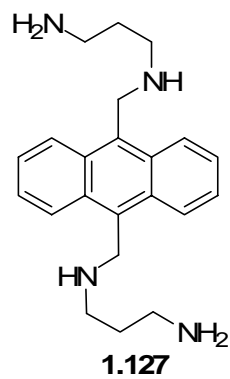
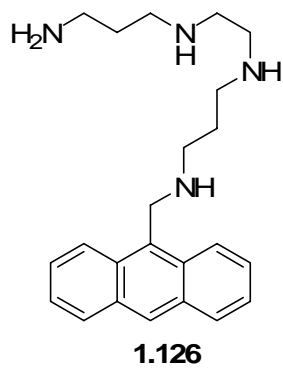
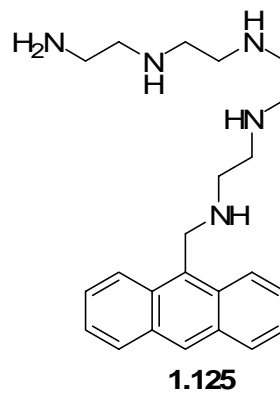
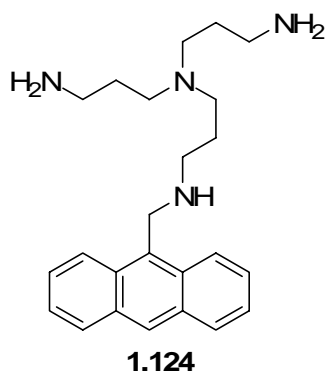
3-decyl-1, 5, 8 triazacyclodecane-2, 4-dione (N₃-cyclic amine) (compound **1.120**) was found to be the best ionophore for a dibasic phosphate-selective electrode compared to other cyclic amine derivatives (N₄, N₅ and N₆).⁶⁸ This electrode exhibited a linear response between 1.0×10^{-7} and 0.1 mol/L with a near-Nernstian slope of $\sim -29 \text{ mV}$ per

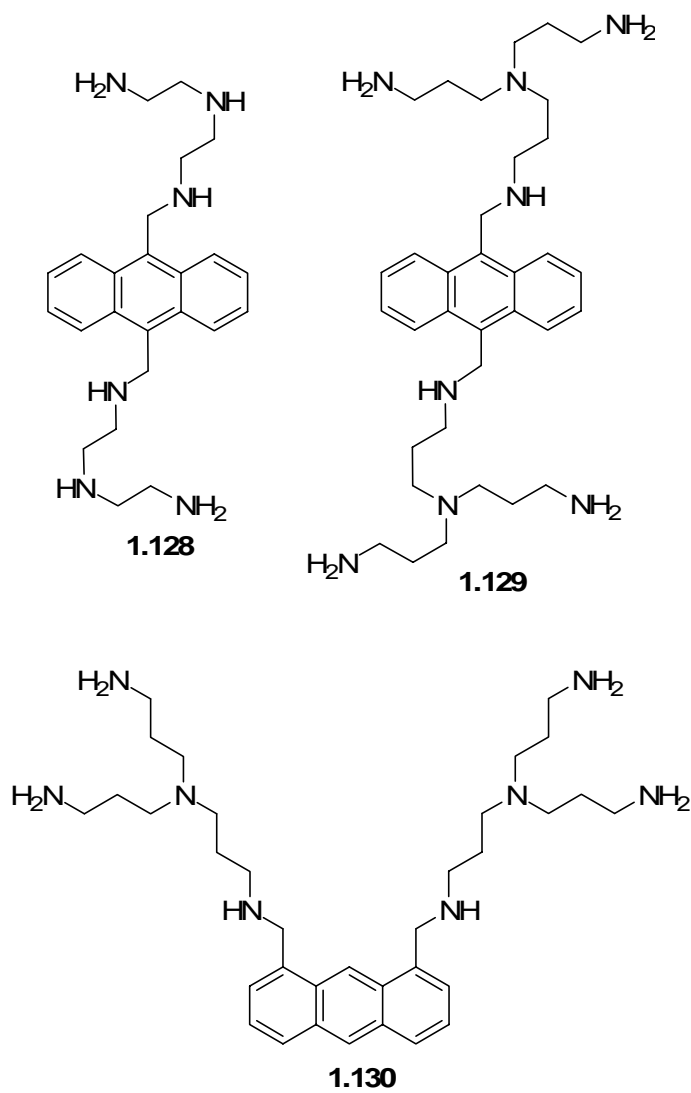
activity decade at pH=6-8, and a selectivity order: $\text{HPO}_4^{2-} \gg \text{SCN}^- = \text{Cl}^- > \text{NO}_3^- > \text{SO}_4^{2-}$ = lactate ion \gg acetate ion. The electrode selectivity for dibasic phosphate over other commonly occurring anions was attributed to size and charge matching between the N_3 -cyclic amine ionophore and HPO_4^{2-} ions.



Cytosine-pendant triamine ditopic receptors were studied by the Sessler group (compound **1.121** and **1.122**).⁶⁹ The greater affinity for GMP in organic solvents arises from the multihydrogen bonding capacity of the cytosine moiety. Also, binding strength could be tuned by the alkyl chain length and the number of nitrogens included. An ion-selective electrode (ISE) (compound **1.123**) based on these receptors displayed a

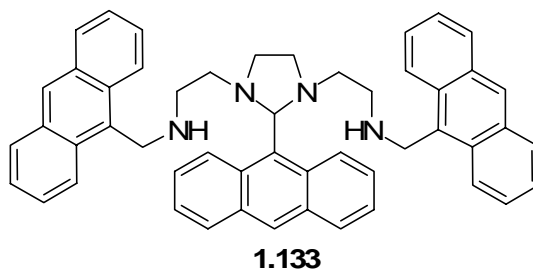
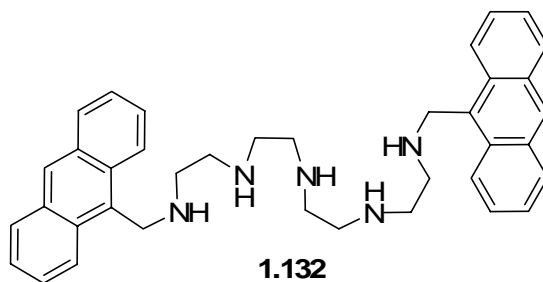
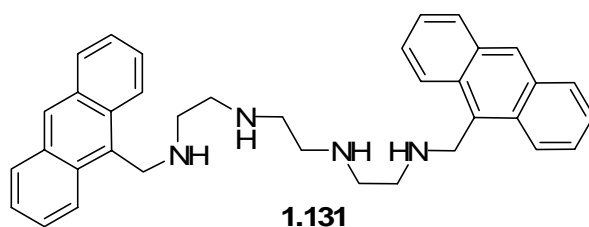
potentiometric response order of $\text{salicylate}^- \gg \text{ClO}_4^- > 5'\text{-GMP} > \text{HPO}_4^{2-} > \text{SCN}^- > \text{SO}_4^{2-}$
 $\geq \text{Br}^- \geq \text{NO}_3^- \geq \text{Cl}^-$.





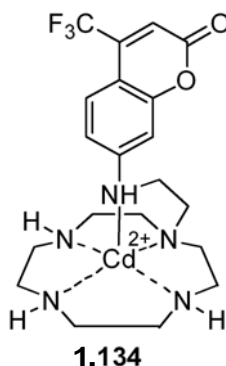
The Czarnik group reported anthrylpolyamine compounds (compound **1.124-1.130**) that exhibited chelation-enhanced fluorescence (CHEF).⁷⁰ It was concluded that a change in protonation or chelation state of a benzylic nitrogen led to large fluorescence enhancements. Chemosensor **1.130** was found to bind pyrophosphate over 2000 times more tightly than monophosphate, and hence, permitted the real-time monitoring of

pyrophosphate hydrolysis. Also, the binding of an anion to an incompletely protonated azamacrocycle changed the effective pKa's of the free amine groups, in most cases raising them.



The anthryl-functionalized open-chain polyaza-alkanes (compound **1.131-1.133**) were reported by the Martinez-Manez group.⁷¹ The emission intensity of **1.131** and **1.132** could be selectively quenched in the presence of ATP at acidic pH in MeCN/H₂O 70:30. However, in H₂O, the emission intensity was enhanced at neutral pH in the presence of

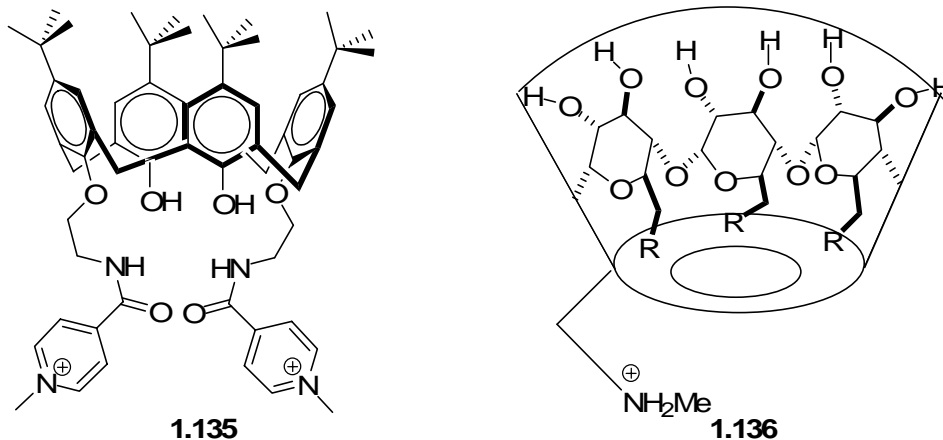
ADP and ATP. This interesting solvent modulation behavior was attributed to the solvent solvation ability. In a less solvated system, i.e. a MeCN/H₂O mixture that has a lower dielectric constant, the electrostatic interactions between receptor and guest anion was more significant, which favored a photoinduced electron transfer (PET) process, and hence, quenched the luminescence. This sensing behavior was not seen in compound **1.133** due to its inherent strains.



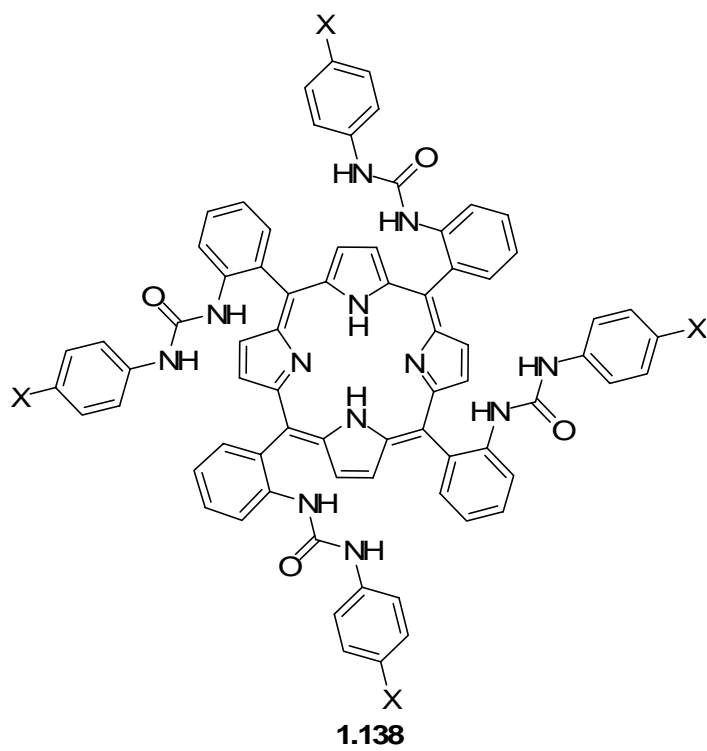
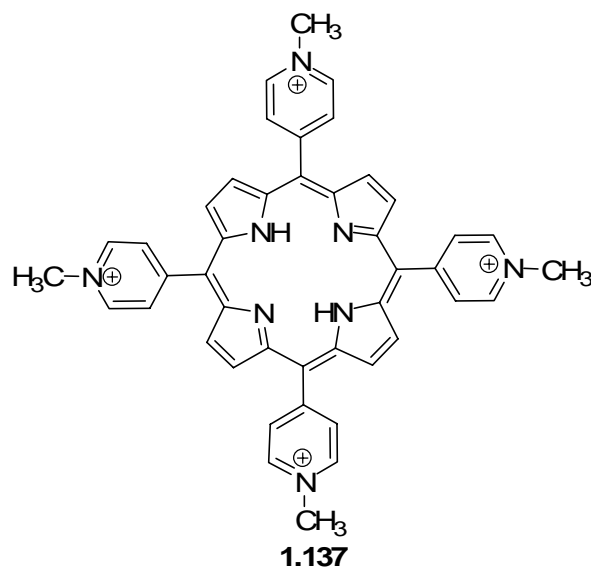
Kikuchi group reported Cd(II) 7-amino-4-trifluoromethylcoumarin (compound **1.134**) as a fluorescent reporter and Cd(II)-cyclen (1,4,7,10-tetraazacyclododecane) as an anion host.⁷² In neutral aqueous solution, Cd(II) was coordinated by the four nitrogen atoms of cyclen and the aromatic amino group of coumarin. When various anions were added, the aromatic amino group of coumarin was displaced from Cd(II) center, causing a change of the excitation spectrum. Among organic anions tested, ATP and ADP gave strong signals, while cAMP showed little signal.

1.3.7 Macrocyclic functionalities

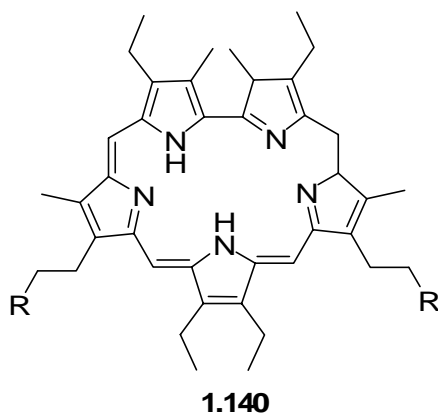
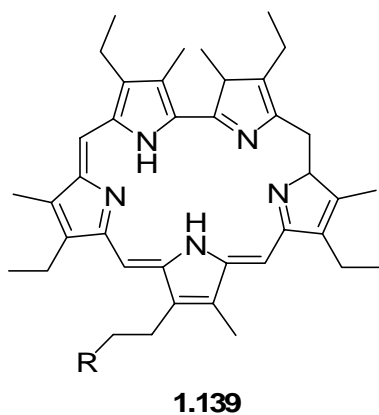
Many macrocyclic ligands were applied in anion detection due to their unique structures and potential in recognition events.⁷³ Calixarene, calixpyrrole, porphyrin and polypyrrole type receptors fall in this catalog. However, effective recognition only can be achieved in combination with other oxoanion selective functionalities.



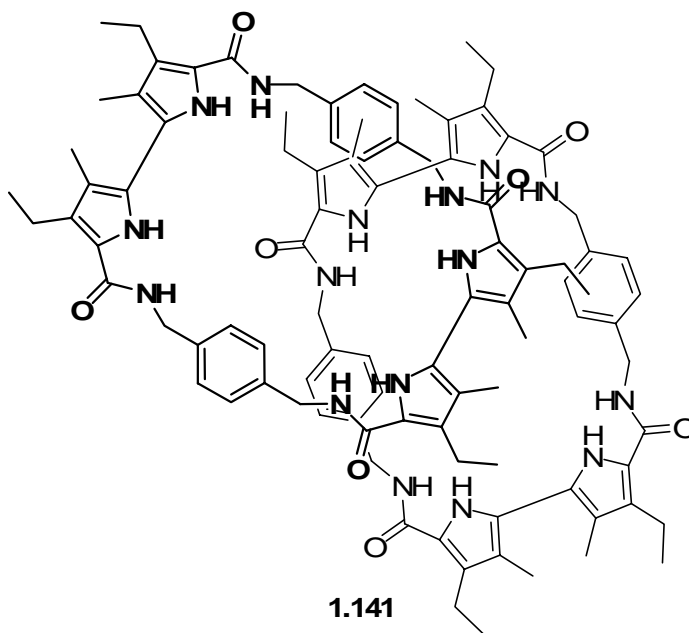
The functionalizations on calix[*n*]arene's (compound **1.135**) (aminocyclodextrin (compound **1.136**)) upper rim and/or lower rim not only changed the topology of macrocyclic ring itself, but also modulated phosphate position inside its cavity.⁷⁴ For example, with bulky and hydrophobic *t*-butyl groups on upper rim, the inclusion of phosphate molecules by calix[*n*]arene moiety forces the phosphate group to point out to the lower rim. Therefore, an introduction of cationic moieties to the lower rims significantly modifies the binding affinity towards dihydrogen phosphate and nucleotides.



A porphyrin receptor, with a pocket shaped cavity, usually allowed selective inclusion of anionic guests depending upon the appended groups on the macrocycle. . Tetrakis(4-N-methylpyridyl)-metaloporphyrin (compound **1.137**) was first found by the Pasternack group to bind GMP, AMP, CMP, TMP at $pK_a=1-2$.⁷⁵ A urea -appended porphyrin (compound **1.138**) studied by Scheidt group was observed to give larger binding affinities with attached electron-withdrawing groups on para position.⁷⁶ The selectivity trends were found to be $Cl^- > Br^- > H_2PO_4^- > HSO_4^-, NO_3^-$. However, the corresponding metalloporphyrins exhibited a loss both in selectivity and binding strength. This decrease in selectivity and binding strength for the metal complexes was explained to result from an increase in rigidity of the metalloporphyrin over that of the free-base receptor. This rigidity, in turn, affects the flexibility and positioning of the urea groups required for optimal hydrogen bonding, as exemplified by the free-base urea analogues. On the other hand, metalloporphyrins can be pentacoordinate, and thus, coordination to the metal on the side of the porphyrin opposite to the urea pocket (bottom-bound) might occur.

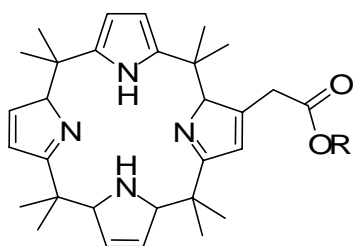


Sapphyrins (compound **1.139-1.140**), unlike porphyrins, have a large and basic inner cavity, which gives the opportunity of stronger binding with phosphates.⁷⁷ Sapphyrin derivatives are protonated and positively charged at neutral pH and bind anions rather than cations both in solution and in the solid-state. For example, sapphyrin had a very strong interaction with DNA double strands via phosphate chelation, π - π stacking, and hydrogen bonding. UV-vis spectroscopic studies showed an 11 nm bathochromic shift when an excess of calf thymus dsDNA was added to the sapphyrin solution.

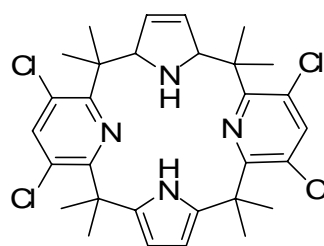


A catenane (compound **1.141**) synthesized by the Sessler group⁷⁸ was found to have a very high association constant with anions (up to 10^7 M^{-1} with H_2PO_4^-),

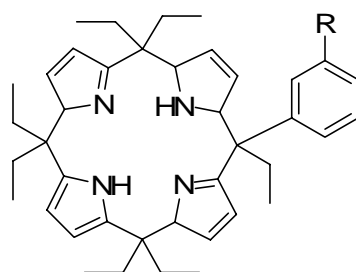
which was attributed to the tetrahedral cavity between the rings that provided an ideal coordination geometry for anion recognition.



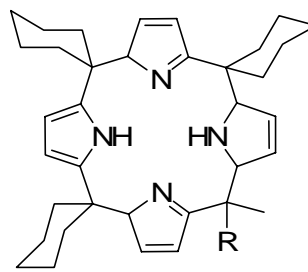
1.142



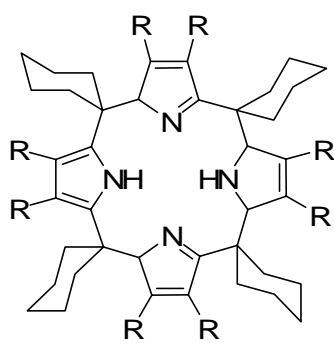
1.143



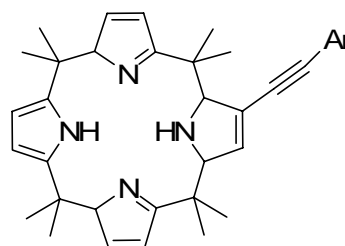
1.144



1.145

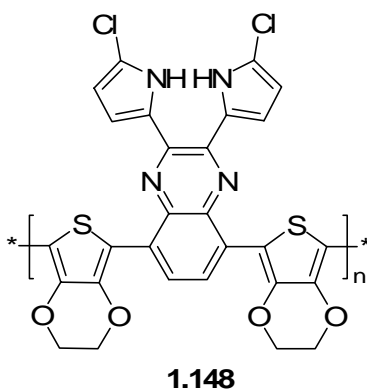


1.146



1.147

Calix[4]pyrroles (compound **1.142-1.147**) were studied by the Sessler group.⁷⁹ These kind of molecules usually have strong affinities toward halide anions. However, functionalized calix[4]pyrroles show enhanced binding towards phosphate anions by forming multiple hydrogen bonds ($>2 \times 10^6 \text{ M}^{-1}$ for pyrophosphate in acetonitrile, pH 7.0). Calix[4]pyrroles attached to aminopropyl silica gel produced new stationary phases for chromatography and were found to be successful in separating mixtures of AMP, ADP and ATP, oligonucleotides, phenyl anions and Cbz-protected amino acids.



A conductive polymer film (compound **1.148**) was built involving multiple hydrogen bonding sites.⁸⁰ Vis-NIR spectra revealed that the addition of fluoride, pyrophosphate, and phosphate anions into the cell containing the sensor films resulted in gradual changes in the absorption spectra. An electrochemical quartz crystal microbalance method (EQCM) was applied to confirm that the changes in the vis-NIR spectra were due to the anion binding to polymer which results in a rapid increase in the mass of the deposited polymer. The role of water in the anion sensing studies utilizing

hydrogen bonding is generally considered to be a disruptive factor as it competes for coordination to anionic analytes. However, the control experiments showed that the addition of water does not change the mass of the deposited polymer or its vis-NIR spectrum. Conversely, the addition of aqueous anion solutions led to significant increases in sensor mass as well as anion-induced changes in vis-NIR spectra. Also, the anion-sensor affinity could be adjusted by external voltage, and the high anion-sensor affinity was a direct result of synergy between low-level p-doping in a polythiophene polymer and receptor–anion hydrogen bonding.

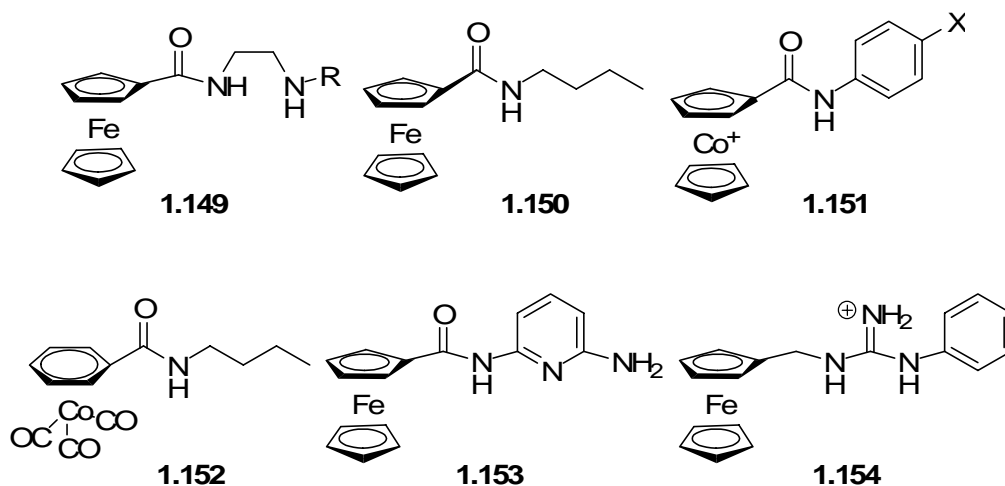
1.3.8 Transition metals as non-coordinating reporters

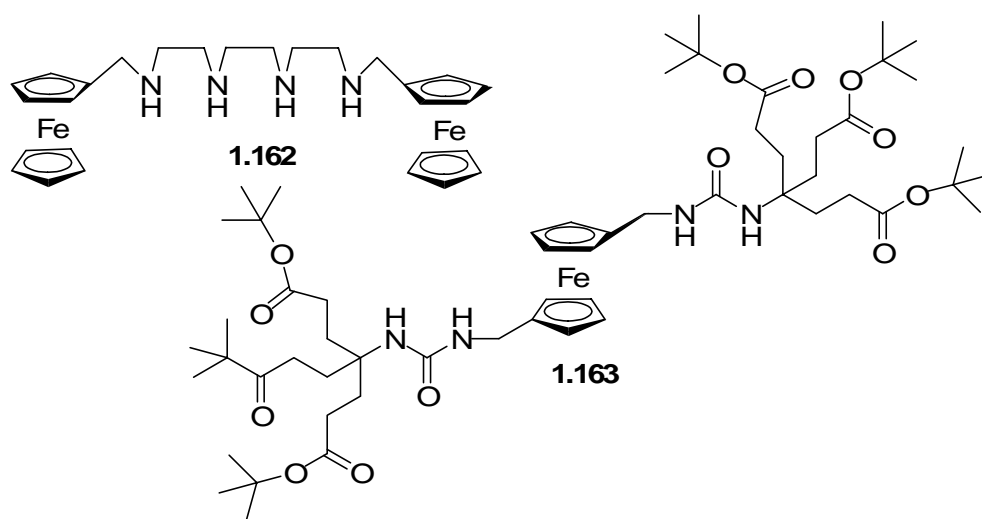
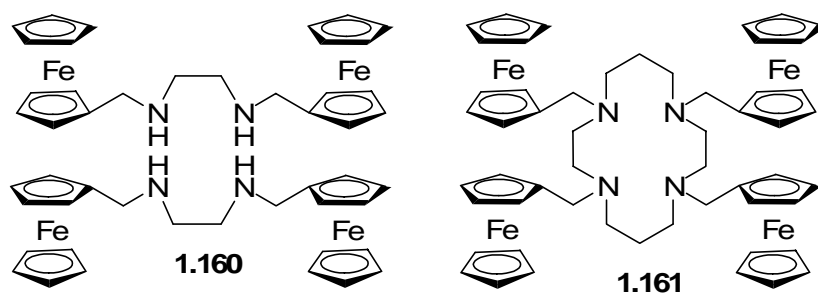
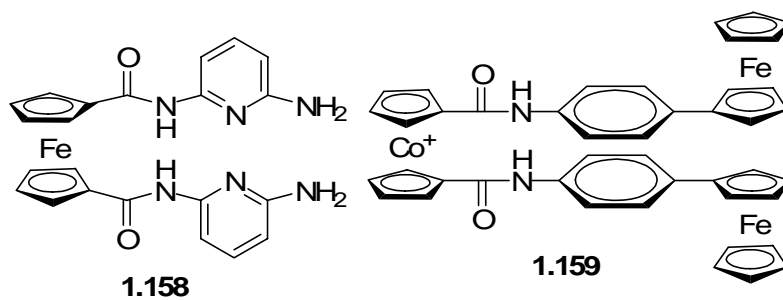
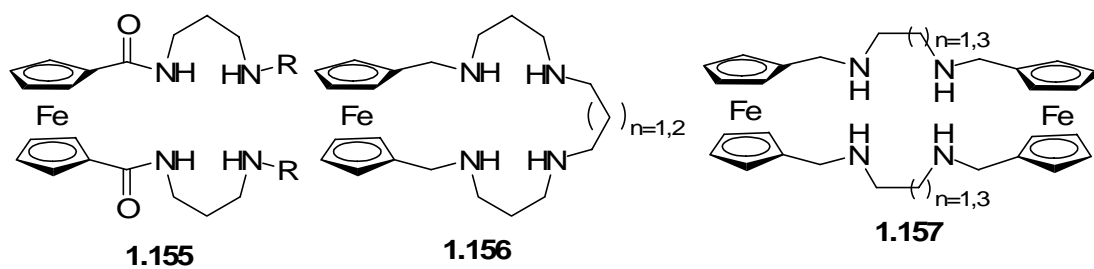
Metal ions are largely involved in anion sensing in various roles serving as: 1. a coordination site for the anion; 2. a non-coordinating reporter group that signals the presence of the anion by a perturbation of its physical properties (i.e. by changes in redox or spectroscopic properties); 3. an element in the receptor designed to withdraw electron density from a p electron system and thus increase the affinity of a hydrophobic receptor for anions; 4. an element of a self-assembled array that binds an anionic guest (whether by an interaction with the metal or another part of the array).

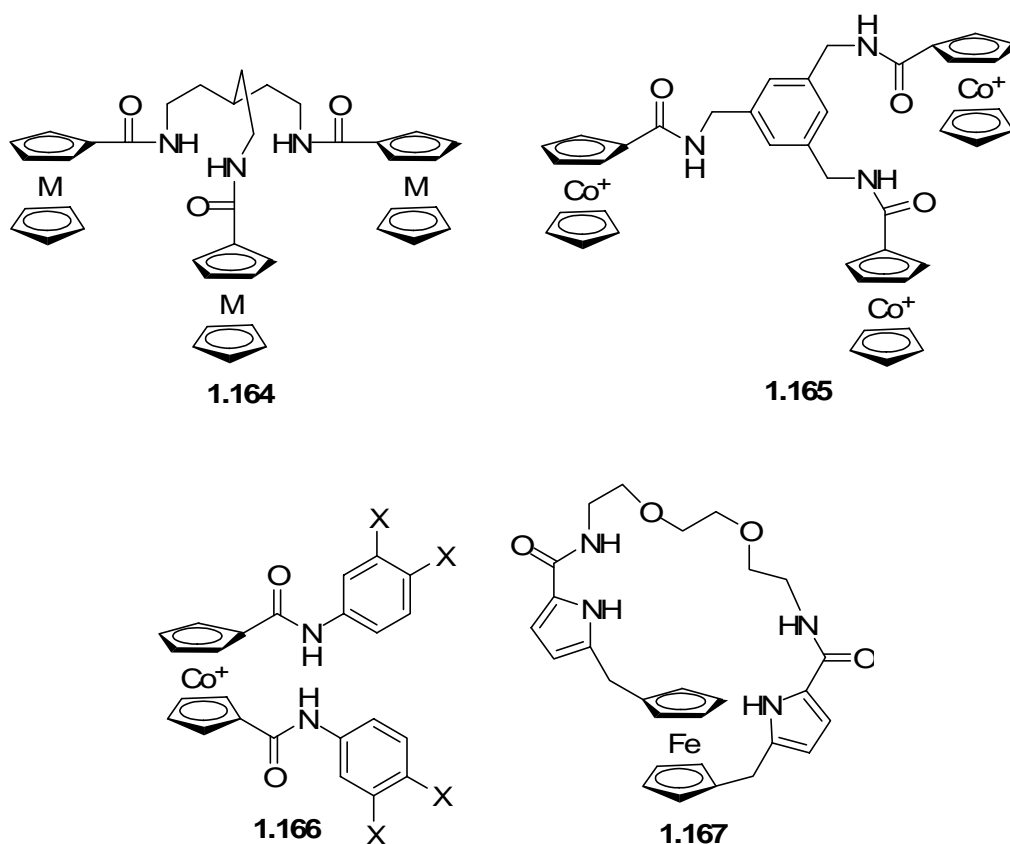
In this section, metal ions acting as non-coordinating reporters will be reviewed with emphasis on metallocene (Mc) as an electrochemical receptor and $[\text{Ru}(\text{bpy})_3]^{2+}$ as a fluorescence reporter.

1.3.8.1 Metallocenes as electrochemical reporters

Both cathodic and anodic peaks of the reversible Mc/Mc^+ redox reaction can be affected by the presence of anions. Anions usually cause both the oxidation and reduction peaks of the metallocene to be cathodically shifted. The electrochemical shift of the oxidation peak of the metallocenyl group to more negative potentials is attributed to the interaction of the receptor with the corresponding anion. An additional effect that was observed is the cathodic shift of the reduction wave of the metallocenyl groups upon addition of anionic guests. This shift is generally attributed to the additional strong interaction between the anionic guest and the Mc^+ cations produced upon oxidation. Other factors such as the metallocene-anion distances and the adsorption processes that control the position of the reduction peak must also influence the value of ΔE_{pc} .

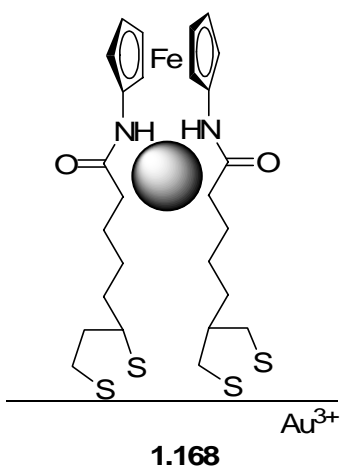




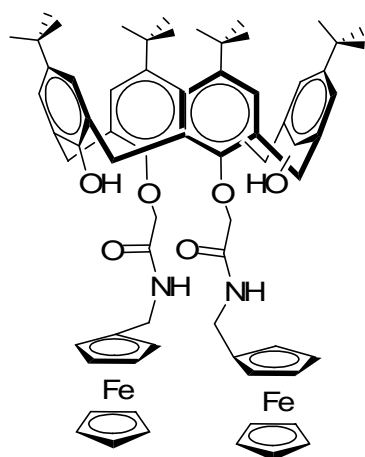


The Beer group built a large group of receptors using metallocenes as the main sensing moieties (compounds **1.149-1.167**).⁸¹ These receptors were redox-active and consistently gave the largest electrical response to phosphate anions in DMSO. Phosphate bound primarily at the particular units such as the amide, amine and guanidinium groups in close proximity to the metallocene unit, which caused a large electrochemical cathodic perturbation (as large as 240 mV). The high preference for phosphate ion was attributed to the special stabilizing ability of phosphate anions on metalloceniums at higher oxidation states irrespective to thermally detected affinity constant values. The redox response usually could not be perturbed much even in the presence of large excess of

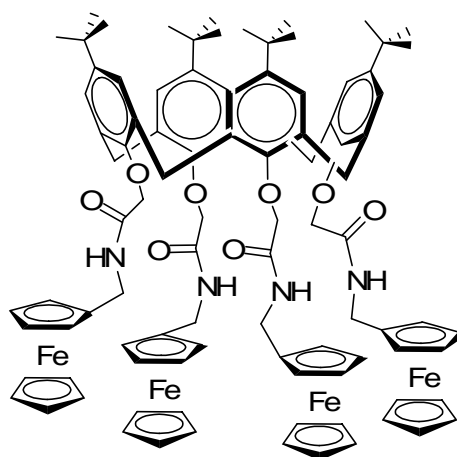
other anions. However, in polyamine functionalized receptors, the presence of the more acidic HSO_4^- protonated the end amine groups and sterically and electronically hindered phosphate binding and hence diminished its response.



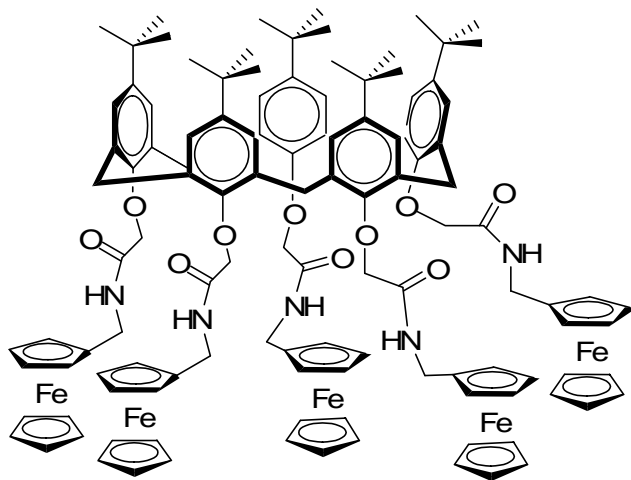
Surface preorganized bis(alkyl-namido) ferrocene (compound **1.168**) was studied.⁸² By introducing disulfide or thiol anchoring moieties into the structure, a well-behaved, robust anion-sensing monolayer was achieved. Such surface preorganization significantly amplified the redox responses observed upon addition of phosphate, halides and perrhennate.



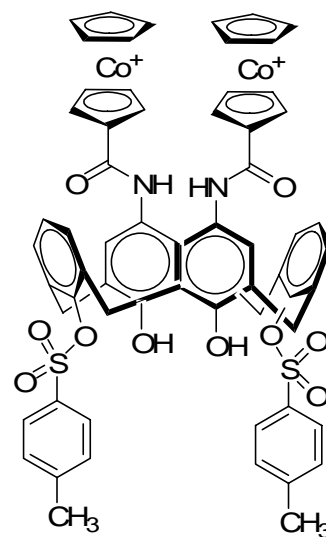
1.169



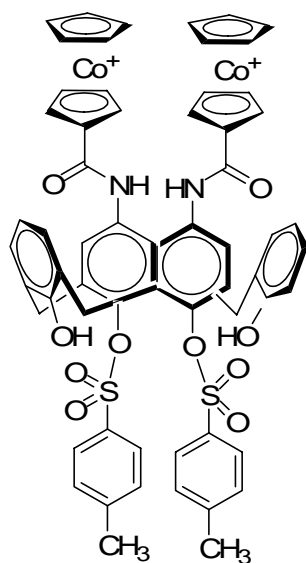
1.170



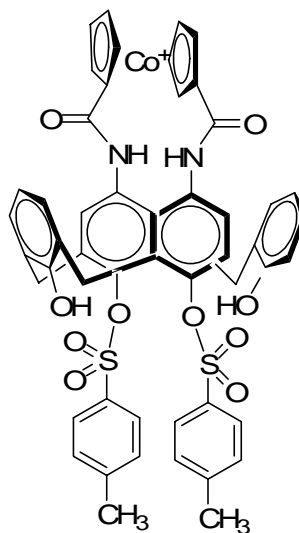
1.171



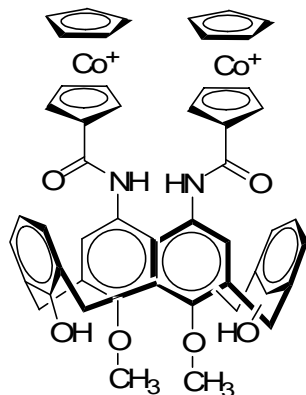
1.172



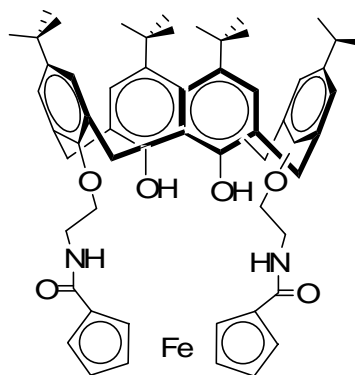
1.173



1.174

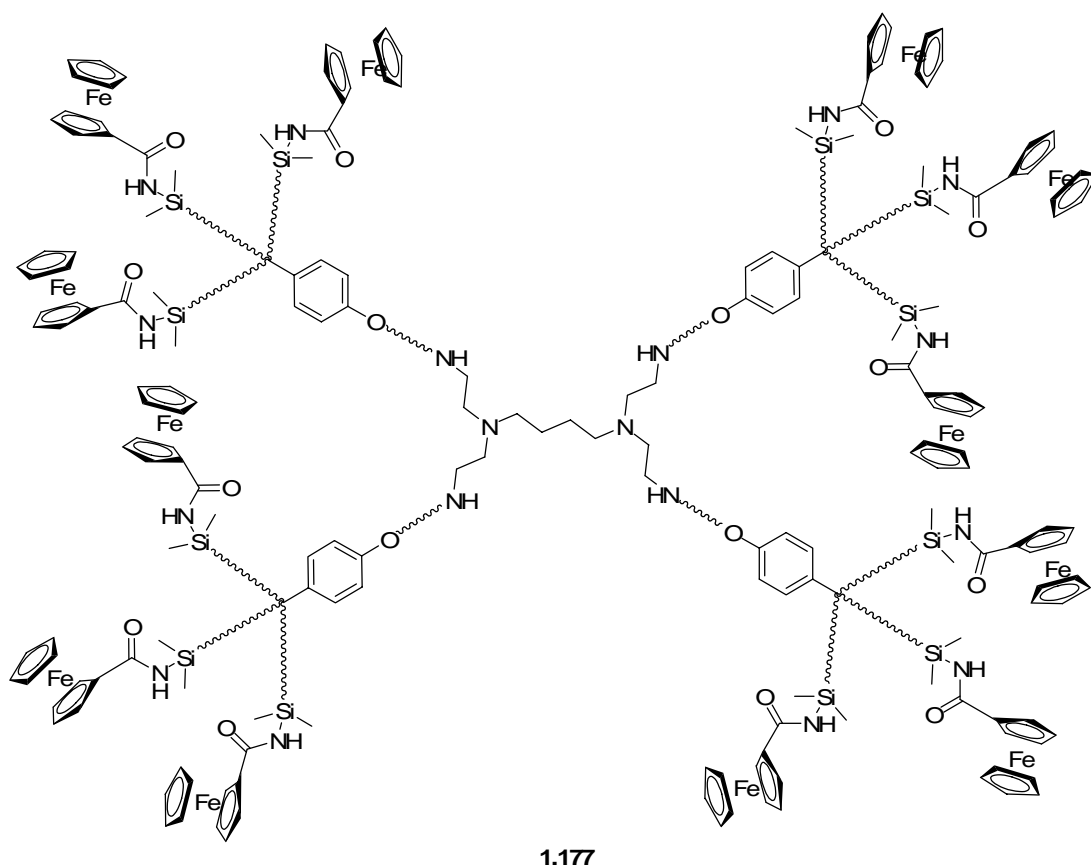


1.175



1.176

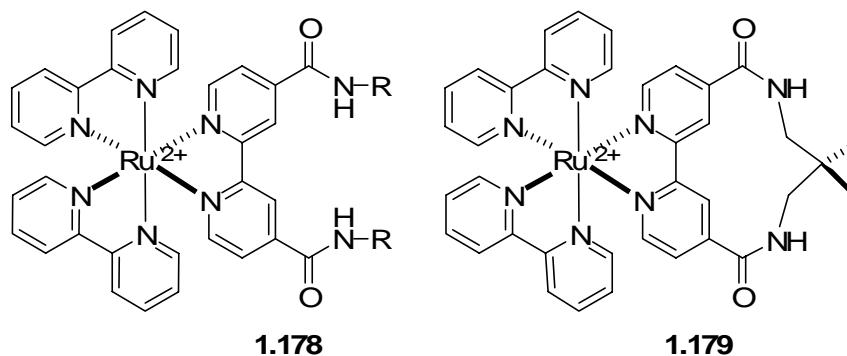
The flexibilities of calix[4]arene- based receptors (compounds **1.169-1.176**) were studied by adjusting the upper and lower-rim functionalities.⁸³ The subtle changes of the size, nature and position of lower-rim (or upper-rim) substituents alters the topology of the other anion recognition site, and hence, alter the selectivity for anions.

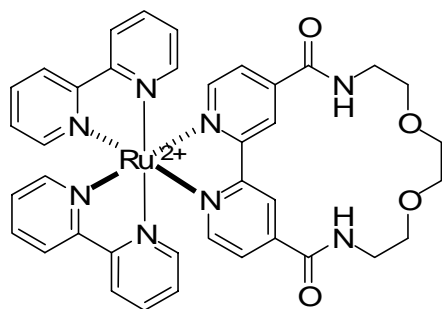


Amidoferrocenyl dendrimers (compound **1.177**) exhibited unusual trends (half-stoichiometry, sudden wave change, dramatic intensity decrease) during electrochemical monitoring of the titrations. These behaviors were rationalized in terms of the formation of a dendritic assembly in which each H_2PO_4^- unit links more than one amidoferrocenyl group at the dendrimer periphery.⁸⁴ The higher generations (G_3 and G_4) showed saturation effects, indicating that the above trend was less efficient for these higher generations because of steric congestion and/or competition of H_2PO_4^- binding between the amido groups.

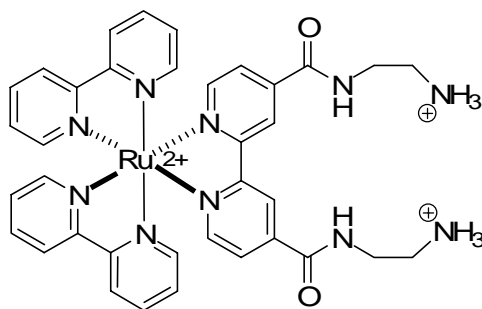
1.3.8.2 $[\text{Ru}(\text{bpy})_3]^{2+}$ as fluorescence reporter

$[\text{Ru}(\text{bpy})_3]^{2+}$ has been applied as a fluorescence reporter in artificial receptors because of its effective metal-ligand charge transfer (MLCT) process in presence of anions. The receptor often exhibits significant blue shift in the emission band and large increase in emission intensity (higher quantum yield) on addition of anionic guest. These modulations were not observed with unfunctionalized $[\text{Ru}(\text{bipy})_3]^{2+}$. It was proposed that this could be a consequence of the bound anion rigidifying the receptor and inhibiting vibrational and rotational relaxation modes of nonradiative decay. The strength of binding can be tuned by the choice of the spacer/bridging moiety to quite a dramatic effect.

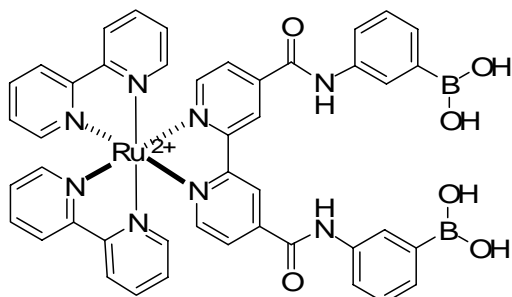




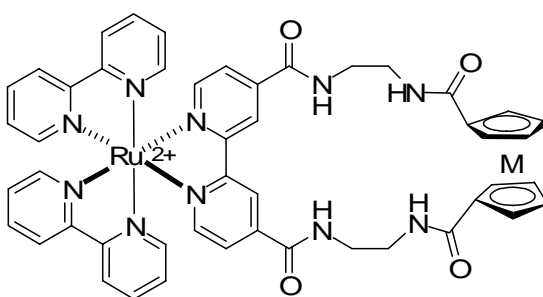
1.180



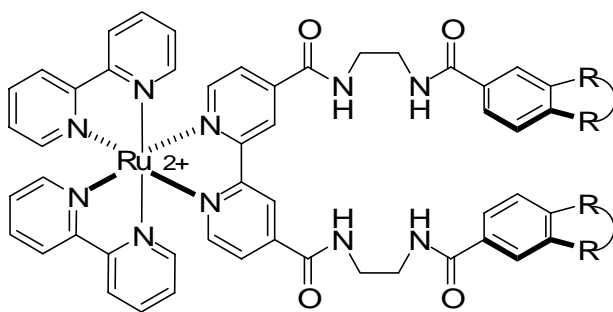
1.181



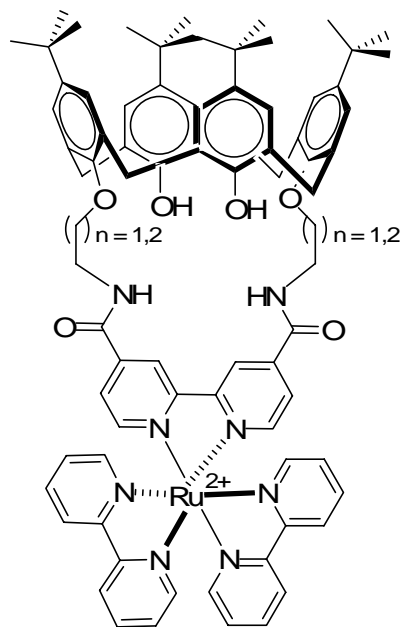
1.182



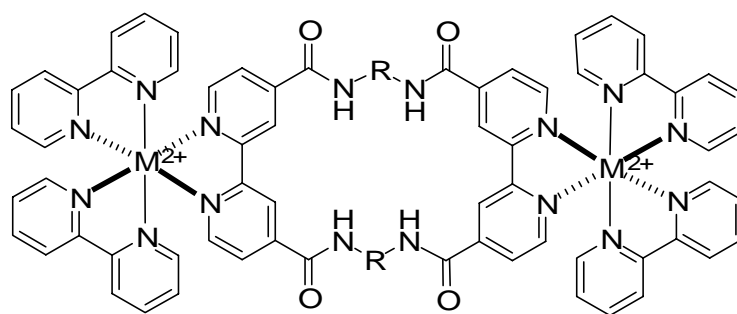
1.183



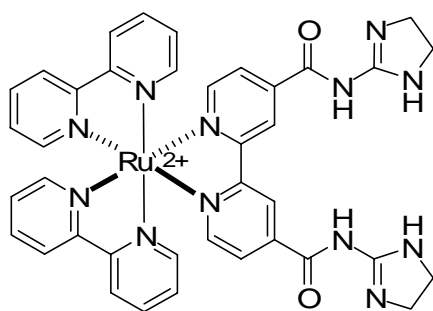
1.184



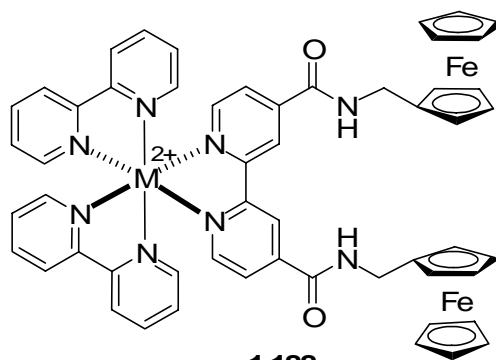
1.185



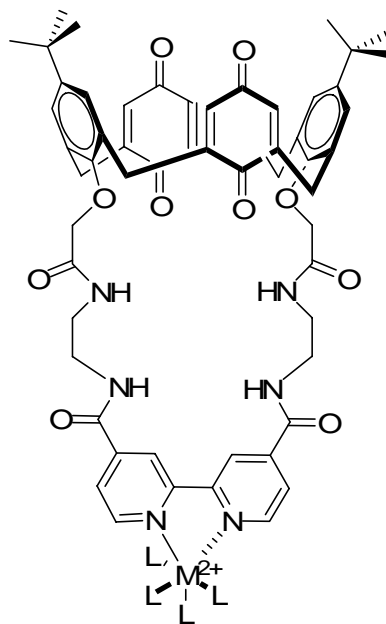
186



1.187



1.188



1.189

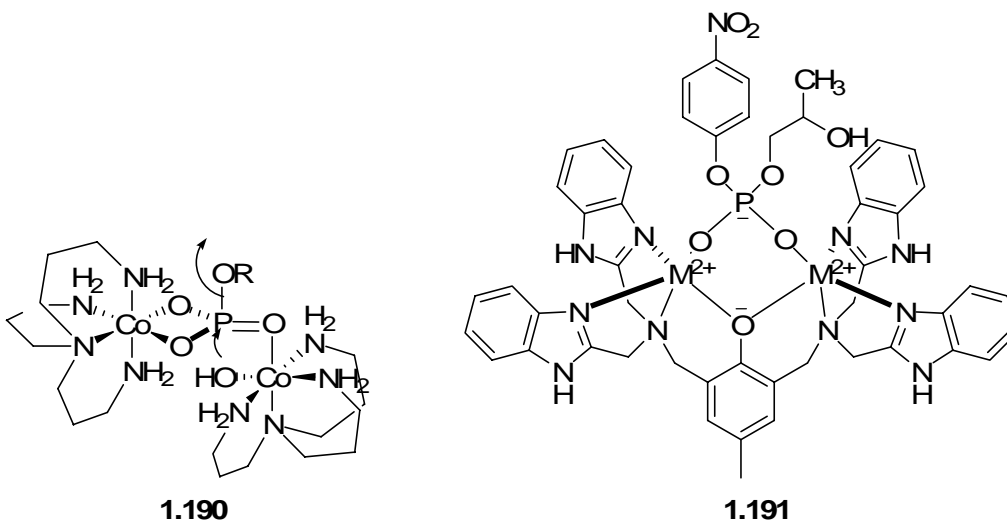
Ruthenium(II) polypyridyl complexes (compounds **1.178-1.189**) exhibited metal-centered (MC), intraligand (π - π^*), and low-energy metal-to-ligand charge-transfer (MLCT) absorption bands.⁸⁵ Significant increases in the extinction coefficient ϵ of the MLCT band was observed with increasing amount of H_2PO_4^- . Selectivity studies suggested the comparative size, degree of preorganization, and topological nature of the macrocyclic receptor cavity influences the anion recognition selection process.

The emission of ruthenium(II) polypyridyl moiety (compounds **1.183** and **1.188**) was almost completely quenched by the appended ferrocene moieties via an intramolecular mechanism. However, the addition of dihydrogenphosphate induced a twenty-fold increase of emission intensity at 690nm and a smaller increase at the usual emission region, 640nm, while addition of chloride or hydrogensulfate did not perturb the emission spectrum to any extent.

Bis-crown ether containing receptors (compound **1.184**) increased the binding stability of Cl^- in presence of K^+ , while significantly decreasing the binding of dihydrogen phosphate.⁸⁶ This observation was explained by suggesting the formation of a sandwich complex between the crown ether and the potassium cation, which decreased the binding of H_2PO_4^- due to steric effects.

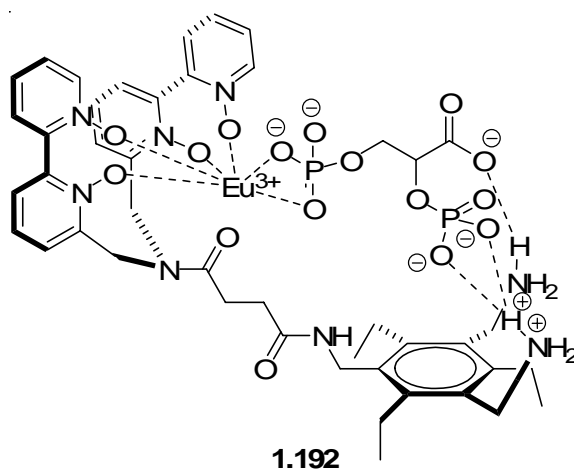
1.3.9 Direct metal coordination receptors

The receptors described in this section mainly rely on the formation of dative coordinative bonds between a receptor and a guest of interest, an interaction which occurs more often in inorganic compounds. Even though other functionalities are applied in order to achieve the desired geometry and/or additional enhancement in binding, metal coordination contributes the most in guest recognition.



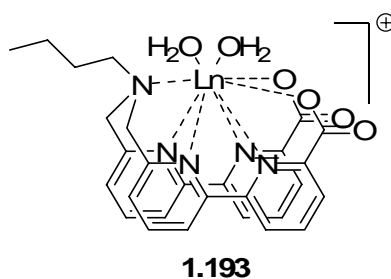
Hydrolysis of unactivated phosphate monoesters in the presence of cobalt(III) and copper(II) complexes $[(\text{trpn})\text{M}(\text{OH}_2)(\text{OH})]^{2+}$ (compound **1.190**) was found to be unprecedentedly efficient by the Chin group.⁸⁷ The mechanism of the hydrolysis involves a 2:1 metal to substrate complex leading to the formation of a binuclear cobalt(III)

complex with a novel doubly bidentate phosphato bridge. The stability of the binuclear complex and the reactivity of $[(\text{trpn})\text{M}(\text{OH}_2)(\text{OH})]^{2+}$ are highly sensitive to the tetraamine ligand structure. The Kim group later reported zinc complex of compound **1.191** using colorimetric methods. Displacement of pyrocatechol violet from $(\text{Zn}^{2+})_2\text{-H-2,6-bis(bis(2-pyridylmethyl)aminomethyl)-4-methyl-phenol [bpmp]}$ (compound **191**) gives a clear color change (blue→yellow). This receptor showed strong binding of phosphate anions.⁸⁸



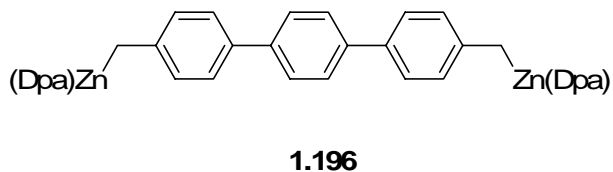
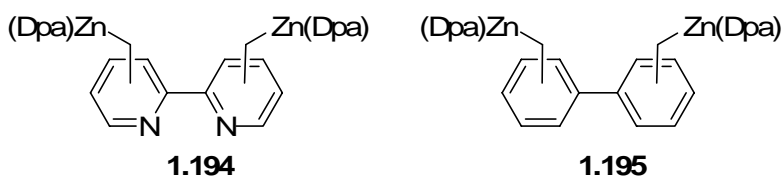
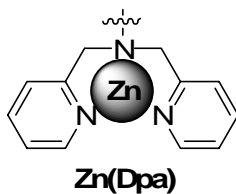
Host **1.192** formed a 1:1 complex with 2,3-bisphosphoglycerate in 50 % methanol/acetonitrile, while the removal of the ammonium pinwheel moiety leads to 2:1 host to guest binding.⁸⁹ This observation showed that the ammonium groups of **1.192** play an important role in the binding of BPG in a 1:1 stoichiometry. Related glycolytic intermediates which lacked the second phosphate undergo 2:1 host to guest binding, most likely because they are not able to interact with the ammonium groups of **1.192**.

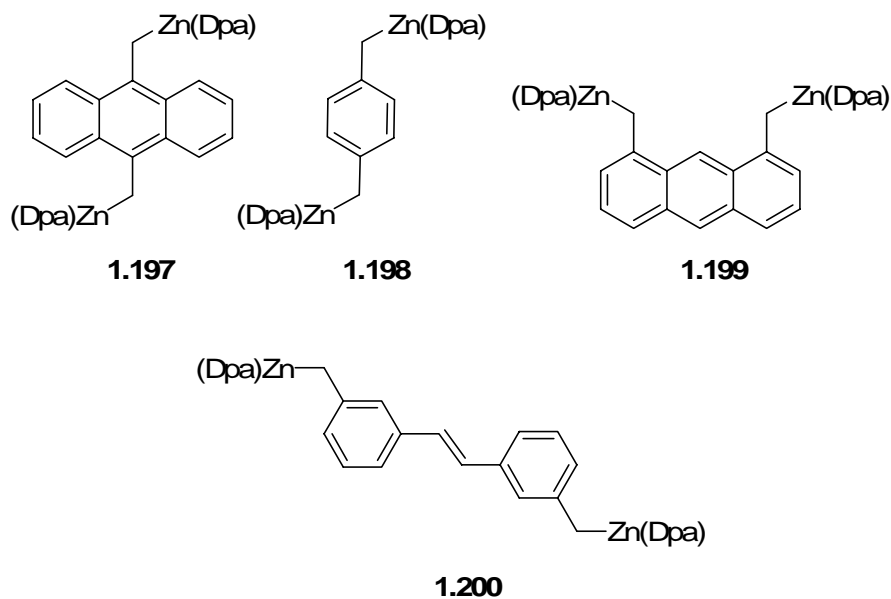
Phenylphosphate, with only one phosphate binding site, exhibited decreased affinity to the host, again probably due to the lack of interaction with the ammoniums of **1.192**. Thus, BPG showed the highest affinity towards **1.192** and was the only guest of the glycolytic intermediates to undergo 1:1 binding. However, problems with the host include its inability to detect binding in $> 5\%$ aqueous solutions due to quenching, and an inability to dramatically increase the affinity for BPG by changing the binding site functional groups.



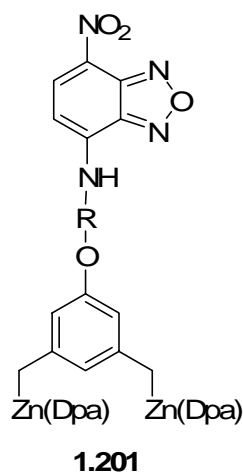
Bipyridyl lanthanide receptor (compound **1.193**) was investigated as an effective ATP sensor for its high negative charge.⁹⁰ Fluorescence studies revealed that upon ATP complexation, the luminescence intensity of the Ln cations decreased, while the excited-state lifetime of the Ln complex increased. This behavior indicated less efficient energy transfer processes, but suggested a substantial decrease of the detrimental nonradiative deactivation pathways in the ternary species. In turn, this result was interpreted in terms of the displacement of water molecules from the first coordination sphere of the cation caused by complexation of ATP. This situation would lead to a better shielding of Eu from the solvent, an effect less pronounced with Tb. Although the coordination of HPO_4^{2-}

and ATP^{4-} resulted in similar photophysical perturbations, their coordination behavior was not the same. While coordination of ATP could occur through the formation of one or two six-membered chelate rings implicating the oxygen atoms of the phosphorylated chain, coordination of the hydrogenophosphate might happen through a monodentate binding mode or potentially as a bidentate ligand, especially if the remaining hydrogen atom of the hydroxyl function is implicated in an intramolecular hydrogen bond with either the nitrogen atom or the carboxylate functions of the ligand.

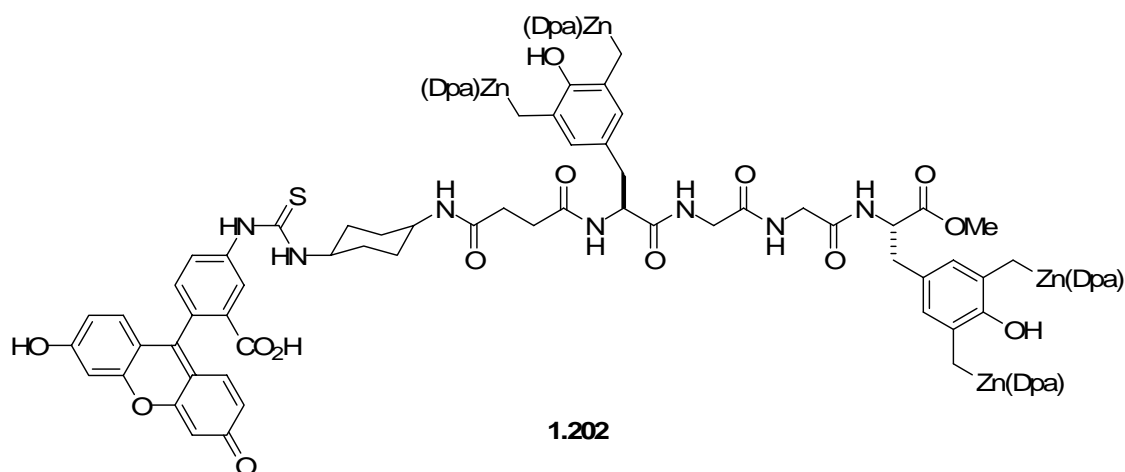




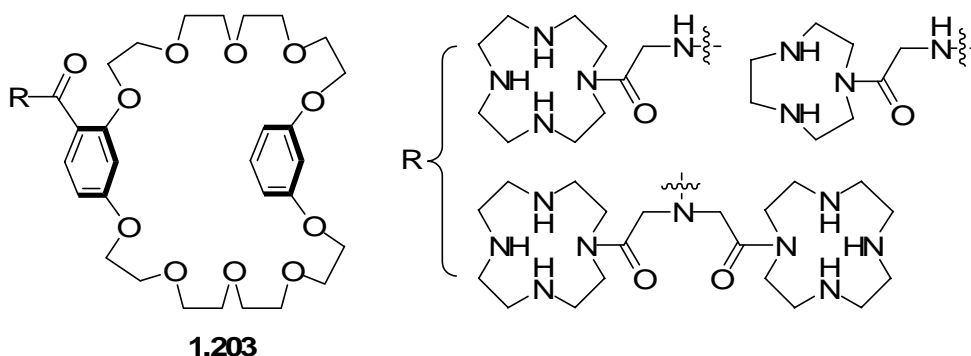
Zn(Dpa) is a useful molecular recognition and fluorescence sensing motif based on metal-ligand coordination chemistry for phosphorylated protein/peptide.⁹¹ It can be constructed as either mononuclear or binuclear Zn(Dpa) complexes (compounds **1.194-1.200**) toward one or two phosphate group(s) on a protein/peptide surface under neutral aqueous conditions. These chemosensors exhibited strong binding affinities for the highly negatively charged peptide. It has been discovered that when the distance between the two Zn(II) centers appropriately fits that of the two phosphate groups of the doubly phosphorylated peptide, a cross-linking was achieved via the artificial receptors bearing the two Zn(II)-Dpa sites. Further functionalization provides a more sophisticated chemosensor for phosphate species of biological importance.



Phospholipid sensor **1.201** was built using Zn(Dpa) and 7-nitrobenz-2-oxa-1,3-diaza-4-yl (NBD) as a fluorophore linked by butyl (relatively hydrophobic) or tris(ethyleneoxy) (TEO, relatively hydrophilic).⁹² The NBD fluorophore is known to exhibit an enhancement in fluorescence intensity upon transfer from a polar environment to an apolar environment. Thus, the fluorescence emission from the sensors was expected to increase upon binding to the surface of a bilayer membrane. It was demonstrated that the sensor responded to membrane-bound phospholipids but not anionic phospholipids that were monodispersed in aqueous solution. Furthermore, this sensor does not disrupt or penetrate the membranes. Use of the more hydrophilic TEO linker produced a sensor with a significantly enhanced emission response to anionic membranes compared to zwitterionic membranes.



D4 tag/Zn(II)-Dpa-Tyr pair (compound **1.202**) was developed as a new molecular tool for protein labeling orthogonal to the His tag system.⁹³ The tag-probe interaction, achieved by multiple coordinative interactions as well as a multivalent effect, was strong enough for the system to be successfully applied to the fluorescence labeling and imaging of receptor proteins on living cell surfaces. The rapid protein labeling, complete within 10 min by simple incubation, was a practical advantage of this labeling system. The tunable cell permeability of the Zn(II)-Dpa-Tyr probes offers the possibility of multiple labeling of distinct proteins in living cells using a combination of enzyme-based or other tag/probe pair labeling methods. However, a complication might conceivably arise due to the relatively large size of the dimeric Zn(II)-Dpa-Tyr probes (ca. 2 kDa), which might interfere with the function of the labeled protein in some cases. Further structural modification is needed to downsize the labeling probe and improve the utility of the present D4 tag system in bio-imaging studies.

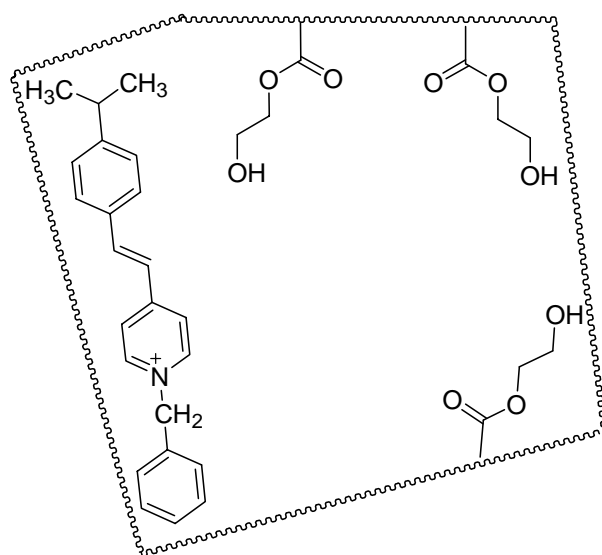


Azamacrocyclic-cyclophane hybrid receptors (compound **1.203**) has been synthesized to incorporate either 1, 4, 7, 10-tetraazacyclododecane (cyclen) or 1, 4, 7-triazacyclononane (tacn) unit(s) tethered via a short amide spacer to an electron donor and a H-bonding crown ether polycycle.⁹⁴ The crown ether is designed to act as a host toward biologically relevant guests, whereas the macrocycle can coordinate a zinc(II) or a copper(II) ion. NMR titrations revealed that addition of M^{2+} ions shift the signals associated with the azamacrocyclic and promotes only minor changes to the signals associated with the crown ether. Isothermal calorimetry experiments carried out on the zinc(II) ligands in buffered water (pH 7.4) at 25 °C showed that the host strongly bound a series of phosphate derivatives, whereas the copper(II) ligand was a poor receptor toward phosphate substrates.

1.3.10 Molecularly Imprinted Polymers (MIPs)

Molecularly imprinted polymers (MIPs) are synthetic polymers with substrate-selective recognition properties and they combine the advantages of facile design with

physical and chemical stability and durability.⁹⁵ MIPs are prepared by molecular imprinting, which entails copolymerization of functional monomers in the presence of a template (print molecule). Imprinting is achieved by interactions, either noncovalent or covalent, which occur between complementary functionalities in the template molecule and the functional monomer units. Noncovalent interactions are formed simply by mixing the template molecule with a suitable mixture of monomers prior to polymerization. Following polymerization, removal of the template by extraction reported leaves microcavities with a three-dimensional structure complementary to the template in both shape and chemical functionality this process enables subsequent recognition of the template. Such MIPs have been used as tailormade separation materials, antibody and receptor mimics in assay systems, biomimetic recognition elements in biological sensors, and artificial enzyme systems for catalytic applications.



1.204

In attempting to obtain MIPs for phosphate molecules, a polymer (compound **1.204**) was prepared with a template (cAMP) and a fluorescent functional monomer (*trans*-4-[*p*-(*N*, *N*-dimethylamino)styryl]-*N*-vinylbenzylpyridinium chloride).⁹⁶ After the copolymerization, cAMP was washed out leaving a preorganized cavity. This three-dimensional network was found to have high affinity towards cAMP ($K_a = 3.5 \pm 1.7 \times 10^5 \text{ M}^{-1}$) over cGMP. The ability of the cAMP-imprinted polymer to distinguish between cAMP and the structurally similar cGMP suggests that cAMP is interacting with specific cAMP-imprinted sites in the polymer.

1.4 Concluding remarks

In this chapter, artificial receptors designed for phosphorylated molecules are reviewed. It is obvious that phosphorylated molecules play crucial roles in a wide range of chemical and biological processes and scientists are eager to design simpler receptors without losing high selectivity and affinity. In the future, the design of coreceptors that contain more subunits (i.e. a combination of chelating, multi-podal, macrocyclic, etc.) might be the direction for phosphate sensing. However, synthetic difficulties will need to be overcome.

1.5 References

- ¹ a) *The Biochemistry of Nucleic Acids, 10th ed.* (Eds.: R. L. P. Adams, J. T. Knower, D. P. Leader), Chapman and Hall, New York, **1986**; b) W. Saenger, *Principles of Nucleic Acid Structure*, Springer, New York, 1998
- ² a) Guilbault, G. G.; Nanjo, M. *Anal. Chim. Acta* **1975**, 78, 69. b) Gajovic, N.; Habermuller, K.; Warsinke, A.; Schuhmann, W.; Scheller, F. W. *Electroanalysis* **1999**, 11, 1377. c) Kubo, I.; Inagawa, M.; Sugawara, T.; Arikawa, Y.; Karube, I. *Anal. Lett.* **1991**, 24, 1711
- ³ a) Gee, A.; Deitz, V. R. *Anal. Chem.* **1953**, 9, 1320-1321. b) Kolmogorova, I. V.; Marek, E. M. *Pharm. Chem.* **1977**, 11, 1568-1570. c) Martin, J. B.; Doty, D. M. *Anal. Chem.* **1949**, 8, 965-967
- ⁴ a) Antonisse, M. M. G.; Reinhoudt, D. N. *Chem. Commun.*, **1998**, 4, 443-448 b) Snowden, T. S.; and Anslyn, E. V. *Curr. Opin. Chem. Biol.* **1999**, 3, 6, 740-746 c) Beer, P. D.; Gale, P. A. *Angew. Chem. Int. Ed.* **2001**, 40, 486-516 d) Aoki, S.; Kimura, E. *Rev. Mol. Biotech.* **2002**, 90, 129-155 e) Lehn, J. M. *Angew. Chem. Int. Ed.* **1988**, 27, 89-112. e) Hartley, J. H. James, T. D. Ward, C. J. *J. Chem. Soc., Perkin Trans. I*, **2000**, 3155-3184
- ⁵ Schmidtchen, F. P.; Berger, M. *Chem. Rev.* **1997**, 97, 1609-1646
- ⁶ Hynes, M. J. *J. Chem. Soc., Dalton Trans.*, **1993**, 311
- ⁷ a) de Silva, A. P.; Gunaratne, H. Q. N.; Gunnlaugsson, T.; Huxley, A. J. M.; McCoy, C.P.; Rademacher, J. T.; Rice, T. E. *Chem. Rev.* **1997**, 97, 1515-1566. b) Czarnik, A. W., Ed.; *ACS Symposium Series 538, American Chemical Society: Washington, DC*, **1993**. c) Martinez-manez, R.; Sancenon, F. *Chem. Rev.* **2003**, 103, 4419-4476. d) Suksai, C.; Tuntulani, T. *Chem. Soc. Rev.* **2003**, 32, 192-202
- ⁸ Ginsberg, A. P.; Lindsell, W. E. *J. Am. Chem. Soc.* **1971**, 93, 2082
- ⁹ Scherer, O. J.; Swarowsky, M.; Swarowsky, H.; Wolmershuser, G. *Organometallics* **1989**, 8, 841
- ¹⁰ a) Cecconi, F.; Ghilardi, C. A.; Midollini, S.; Orlandini, A. *Inorg. Chem.* **1986**, 25, 1766. b) Bryant, G. M.; Fergusson, J. E.; Powell, H. J. K. *Aust. J. Chem.* **1971**, 24, 257
- ¹¹ Di Vaira, M.; Ehses, M.; Peruzzini, M.; Stoppioni, P. *Eur. J. Inorg. Chem.* **2000**, 2193
- ¹² Choi, K.; Hamilton, A. D. *Angew. Chem. Int. Ed.* **2001**, 40, 3192-3195

- ¹³ a) Bakker, E.; Buhlmann, P.; Pretsch, E. *Electroanalysis* **1999**, *11*, 915-933. b) Bakker, E.; Meyerhoff, M. M. *Anal. Chim. Acta* **2000**, *416*, 121-137. c) Bakker, E.; Pretsch, E. *Trends Anal. Chem.* **2001**, *20*, 11-19. d) Buhlmann, P.; Pretsch, E.; Bakker, E. *Chem. Rev.* **1998**, *98*, 1593-1687. e) Sokalski, T.; Ceresa, A.; Zwickl, T.; Pretsch, E. *J. Am. Chem. Soc.* **1997**, *119*, 11347-11348. f) Mathison, S.; Bakker, E. *Anal. Chem.* **1998**, *70*, 303-309. g) Buhlmann, P. *Chem. Sens.* **1998**, *14*, 93-109
- ¹⁴ a) Manabe, K.; Okamura, K.; Date, T.; Koga, K. *J. Am. Chem. Soc.* **1992**, *114*, 6940-6941. b) Motomura T.; Aoyama, Y. *J. Org. Chem.* **1991**, *56*, 7224-7228
- ¹⁵ Ihm, H.; Yun, S.; Kim, H. G.; Kim, J. K.; Kim, K. S. *Org. Lett.*, **2002**, *4*, 2897-2900
- ¹⁶ a) Aldakov, D.; Anzenbacher, P. Jr. *J. Chem. Soc., Chem. Commun.*, **2003**, *12*, 1394-1395. b) Sessler, J. L.; Maeda, H.; Mizuno, T.; Lynch, V. M.; Furuta, H. *J. Chem. Soc., Chem. Commun.* **2002**, 862. c) Sessler, J. L.; Pantos, G. D.; Katayev, E.; Lynch, V. M. *Org. Lett.* **2003**, *5*, 4141-4144. d) Kruger, P. E.; Mackie, P. R.; Nieuwenhuyzen, M. *J. Chem. Soc., Perkin Trans. 2*, **2001**, *7*, 1079-1083
- ¹⁷ a) Miyaji, H.; Sessler, J. L. *Angew. Chem. Int. Ed.*, **2001**, *40*, 154-157. b) Sessler, J. L.; Mody, T. D.; Ford, D. A.; Lynch, V. *Angew. Chem. Int. Ed. Engl.* **1992**, *31*, 452-455
- ¹⁸ Jung, Y.; Yeo, W.; Lee, S. B.; Hong, J. *Chem. Commun.*, **1997**, *11*, 1061-1062
- ¹⁹ Wang, S.; Chang, Y. *J. Am. Chem. Soc.* **2006**, *128*, 10380-10381
- ²⁰ Chmielewski, M. J.; Charon, M.; Jurczak, J. *Org. Lett.* **2004**, *6*, 3501-3504
- ²¹ Jain, A. K.; Gupta, V. K.; Raison, J. R. *Talanta* **2006**, *69*, 1007-1012
- ²² a) Gale, P. A. *Coord. Chem. Rev.* **2000**, *199*, 181-233. b) Raposo, C.; Pérez, N.; Almaraz, M.; Mussons, M. L.; Caballero, M. C.; Morán, J. R. *Tetrahedron Lett.* **1995**, *36*, 3255-3258
- ²³ a) Choi, K.; Hamilton, A. D. *J. Am. Chem. Soc.* **2001**, *123*, 2456-2457. b) Choi, K.; Hamilton, A. D. *Angew. Chem. Int. Ed.* **2001**, *40*, 3912
- ²⁴ Causey, C. P.; Allen, W. E. *J. Org. Chem.* **2002**, *67*, 5963-5968
- ²⁵ Deslongchamps, G.; Galan, A.; Mendoza, H.; Rebek, J. *Angew. Chem. Int. Ed. Engl.* **1992**, *31*, 61-63
- ²⁶ Piatek P.; Jurczak, J. *J. Chem. Soc., Chem. Commun.* **2002**, *20*, 2450-2451

- ²⁷ Bühlmann, P.; Nishizawa, S.; Xiao, K. P.; Umezawa, Y. *Tetrahedron* **1997**, *53*, 1647-1654
- ²⁸ a) Kuo, L.; Liao, J.; Chen, C.; Huang, C.; Chen, C.; Fang, J. *Org. Lett.* **2003**, *5*, 1821-1824. b) Liao, J.; Chen, C.; Fang, J. *Org. Lett.* **2002**, *4*, 561-564
- ²⁹ Das, G.; Onouchi, H.; Yashima, E.; Sakai, N.; Matile, S. *ChemBioChem*, **2002**, *3*, 1089-1096
- ³⁰ Chmielewski, M.; Jurczak, J. *Tetrahedron Lett.* **2004**, *45*, 6007-6010
- ³¹ Watanabe, S.; Sonobe, M.; Arai, M.; Tazume, Y.; Matsuo, T.; Nakamura, T.; Yoshida K. *J. Chem. Soc., Chem. Comm.* **2002**, *23*, 2866-2867
- ³² Kovalchuk, A.; Bricks, J. L.; Reck, G.; Rurack, K.; Schulz, B.; Szumna, A.; Weibhoff, H. *J. Chem. Soc., Chem. Comm.* **2004**, 1946-1947
- ³³ a) Nishizawa, S.; Bühlmann, P.; Iwao, M.; Umezawa, Y. *Tetrahedron Lett.* **1995**, *36*, 6483-6486. b) Snowden, T. S.; Anslyn, E.V. *Curr. Opin. Chem. Biol.* **1999**, *3*, 740-746. c) Bühlmann, P.; Nishizawa, S.; Xiao, K.P.; Umezawa, Y. *Tetrahedron*. **1997**, *53*, 1647-1654. d) Xiao, K. P.; Bühlmann, P.; Nishizawa, S.; Amemiya, S.; Umezawa, Y. *Anal. Chem.*, **1997**, *69*, 1038-1044. e) Xiao, K. P.; Bühlmann, P.; Umezawa, Y. *Anal. Chem.*, **1999**, *71*, 1183-1187
- ³⁴ a) Nishizawa, S.; Kato, R.; Hayashita, T.; Teramae, N. *Anal. Sci.*, **1998**, *14*, 595-597. b) Nishizawa, S.; Kaneda, H.; Uchida, T.; Teramae, N. *J. Chem. Soc., Perkin Trans. 2*, **1998**, *11*, 2325-2328. c) Hayashita, T.; Onodera, T.; Kato, R.; Nishizawa, S.; Teramae, N.; *Chem. Commun.*, **2000**, *9*, 755-756. d) Nishizawa, S.; Yokobori, T.; Shioya, T.; Teramae, N. *Chem. Lett.* **2001**, 1058 e) Shigemori, K.; Nishizawa, S.; Yokobori, T.; Shioya, T.; Teramae, N. *New J. Chem.*, **2002**, *26*, 1102-1104
- ³⁵ a) Yeo, W.; Hong, J. *Tetrahedron Lett.* **1998**, *39*, 3769-3772. b) Lee, D. H.; Lee, K. H.; Hong, J. *Org. Lett.*, **2001**, *3*, 5-8. c) Lee, D. H.; Lee, H. Y.; Hong, J. *Tetrahedron Lett.* **2002**, *43*, 7273-7276
- ³⁶ a) Yeo, W.; Hong, J. *Tetrahedron Lett.* **1998**, *39*, 8137-8140. b) Lee, D. H.; Lee, H. Y.; Lee, K. H.; Hong, J. *Chem. Commun.*, **2001**, *13*, 1188-1189. c) Misawa, Y.; Kubo, Y.; Tokita, S.; Ohkuma, H.; Nakahara, H. *Chem. Lett.* **2004**, *33*, 1118-1119
- ³⁷ Kubo, Y.; Uchida, S.; Kemmochi, Y.; Okubo, T. *Tetrahedron Lett.* **2005**, *46*, 4369-4372
- ³⁸ a) Xie, H.; Yi, S.; Wu, S. *J. Chem. Soc., Perkin Trans. 2*, **1999**, *12*, 2751-2754. b) Xie, H.; Yi, S.; Yang, X.; Wu S. *New J. Chem.* **1999**, *23*, 1105-1110

- ³⁹ Sasaki, S.; Mizuno, M.; Naemura, K.; Tobe, Y. *J. Org. Chem.*, **2000**, *65*, 275-283
- ⁴⁰ a) Gunnlaugsson, T.; Davis, A. P.; O'Brien, J. E.; Glynn, M. *Org. Lett.*, **2002**, *4*, 2449-2452. b) Gunnlaugsson, T.; Ali, H. D. P.; Glynn, M.; Kruger, P. E.; Hussey, G. M.; Pfeffer, F. M.; dos Santos, C. M. G.; Tierney, J. *J. Fluores.* **2005**, *15*, 287-299. c) Gunnlaugsson, T.; Davis, A. P.; O'Brien, J. E.; Glynn, M. *Org. Biomol. Chem.*, **2005**, *3*, 48-56
- ⁴¹ Sasaki, S.; Citterio, D.; Ozawa, S.; Suzuki, K. *J. Chem. Soc., Perkin Trans. 2*, **2001**, 2309-2313
- ⁴² Pfeffer, F. M.; Gunnlaugsson, T.; Jensen, P.; Kruger, P. E. *Org. Lett.* **2005**, *7*, 5357-5360
- ⁴³ a) Schmidtchen, F. P. *Tetrahedron Lett.* **1989**, *30*, 4493-4496. b) Schiessl, P.; Schmidtchen, F. P. *J. Org. Chem.* **1994**, *59*, 509-511. c) Berger, M.; Schmidtchen, F. P. *J. Am. Chem. Soc.*, **1996**, *118*, 8947-8948. d) Berger, M.; Schmidtchen, F. P. *J. Am. Chem. Soc.*, **1999**, *121*, 9986-9993. e) Fibbioli, M.; Berger, M.; Schmidtchen, F. P.; Pretsch, E. *Anal. Chem.* **2000**, *72*, 156-160
- ⁴⁴ a) Alcázar, V.; Segura, M.; Prados, P.; de Mendoza, J. *Tetrahedron Lett.*, **1998**, *39*, 1033-1036. b) Galán, A.; Pueyo, E.; Salmerón, A.; de Mendoza, J. *Tetrahedron Lett.* **1991**, *32*, 1827-1830. c) Gale, P. A. *Coord. Chem. Rev.* **2000**, *199*, 181-233
- ⁴⁵ a) Galan, A.; Mendoza, J. D.; Toiron, C.; Bruix, M.; Deslongchamps, G.; Rebek, J. *J. Am. Chem. Soc.*, **1991**, *113*, 9424-9425. b) Kato, Y. Conn, M. M.; Rebek, J. Jr. *J. Am. Chem. Soc.*, **1994**, *116*, 3279-3284
- ⁴⁶ a) Dixon, R. P.; Geib, S. J.; Hamilton, A. D. *J. Am. Chem. Soc.* **1992**, *114*, 365-366. b) Jubian, V.; Dixon, R. P.; Hamilton, A. D. *J. Am. Chem. Soc.*, **1992**, *114*, 1120-1121. c) Jubian, V.; Veronese, A.; Dixon, R. P.; Hamilton, A. D. *Angew. Chem. Int. Ed. Engl.* **1995**, *34*, 1237-1239
- ⁴⁷ Watanabe, S.; Onogawa, O.; Komatsu, Y.; Yoshida, K. *J. Am. Chem. Soc.*, **1998**, *120*, 229-230
- ⁴⁸ Kneeland, D. M.; Ariga, K.; Lynch, V. M.; Huang, C.; Anslyn, E. V. *J. Am. Chem. Soc.*, **1993**, *115*, 10042-10055
- ⁴⁹ a) Niikura, K.; Metzger, A.; Anslyn, E. V. *J. Am. Chem. Soc.*, **1998**, *120*, 8533-8534. b) Snowden, T. S.; Anslyn, E. V. *Curr. Opin. Chem. Biol.* **1999**, *3*, 740-746. c) Tobey, S. L.; Jones, B. D.; Anslyn, E. V. *J. Am. Chem. Soc.*, **2003**, *125*, 4026-4027. d) Tobey, S. L.; Anslyn, E. V. *Org. Lett.*, **2003**, *5*, 2029-2031. e) Schmuck, C.; Schwegmann, M. *Org. Lett.*, **2005**, *7*, 3517-3520
- ⁵⁰ Zhong, Z.; Anslyn, E. V. *Angew. Chim. Int. Ed.* **2003**, *42*, 3005-3008

- ⁵¹ a) Schneider, S. E.; O'Neil, S. N.; Anslyn, E. V. *J. Am. Chem. Soc.*, **2000**, *122*, 542-543. b) McCleskey, S. C.; Griffin, M. J.; Schneider, S. E.; McDevitt, J. T.; Anslyn, E. V. *J. Am. Chem. Soc.*, **2003**, *125*, 1114-1115. c) Wright, A. T.; Anslyn, E. V. *Chem. Soc. Rev.*, **2006**, *35*, 14-28
- ⁵² a) Liu, D.; Chen, W.; Yang, R.; Shen, G.; Yu, R. *Anal. Chim. Acta.* **1997**, *338*, 209-214. b) Chaniotakis, N. A. *Anal. Chim. Acta.*, **1993**, *282*, 345-352. c) Tsagatakis, J. K.; Chaniotakis, N. A. *Helv. Chim. Acta.*, **1994**, *77*, 2191-2196. d) Ganjali, M. R.; Mizani, F.; Salavati-Niasari, M. *Anal. Chim. Acta.* **2003**, *481*, *1*, 85-90. e) Beer, P. D.; Dickson, C. A. P.; Fletcher, N. C.; Goulden, A. J.; Grieve, A.; Hodacova, J.; Wear, T. *J. Chem. Soc., Chem. Commun.* **1993**, 828. f) Beer, P. D. In *Transition Metals in Supramolecular Chemistry*; Fabrizzi, L., Poggi, A., Eds. *NATO ASI Series C*, No 448; Kluwer Academic Publishers: Dordrecht, The Netherlands, **1994**, p 33
- ⁵³ a) Beer, P. D.; Gale, P. A. *Angew. Chem. Int. Ed. Engl.* **2001**, 486-516. b) Rudkevich, D. M.; Stauthamer, W. P. R. V.; Verboom, W.; Engbersen, J. F. J. Harkema, S.; Reinhoudt, D. N. *J. Am. Chem. Soc.*, **1992**, *112*, 9671-9673. c) Visser, H. C.; Rudkevich, D. M.; Verboom, W.; de Jong, F.; Reinhoudt, D. N. *J. Am. Chem. Soc.*, **1994**, *116*, 11554-11555. d) Rudkevich, D. M.; Verboom, W.; Reinhoudt, D. N. *J. Org. Chem.* **1994**, *59*, 3683-3686. e) Rudkevich, D. M.; Verboom, W.; Brzozka, Z.; Palys, M. J.; Stauthamer, W. P. R. V.; van Hummel, G. J.; Franken, S. M.; Harkema, S.; Engbersen, J. F. J.; Reinhoudt, D. N. *J. Am. Chem. Soc.*, **1994**, *116*, 4341-4351. e) Rudkevich, D. M.; Brzozka, Z.; Palys, M.; Visser, H. C.; Verboom, W.; Reinhoudt, D. N. *Angew. Chem. Int. Ed. Engl.* **1994**, *33*, 467-468. f) Antonisse, M. M. G.; Snellink-Ruël, B. H. M.; Yigit, I.; Engbersen, J. F. J.; Reinhoudt, D. N. *J. Org. Chem.*, **1997**, *62*, 9034-9038. g) Antonisse, M. M. G.; Reinhoudt, D. N. *J. Chem. Soc., Chem. Commun.*, **1998**, *4*, 443-448. h) Wróblewski, W.; Wojciechowski, K.; Dybko, A.; Brzózka, Z.; Egberink, R. J. M.; Snellink-Ruël, B. H. M.; Reinhoudt, D. N. *Sensors and Actuators B: Chemical* **2001**, *78*, 315-319
- ⁵⁴ a) Dietrich, B.; Fyles, D. L.; Fyles, T. M.; Lehn, J. *Helv. Chim. Acta*, **1979**, *62*, 2763-2787. b) Jurek, P. E.; Martell, A. E.; Motekaitis, R. J.; Hancock, R. D. *Inorg. Chem.* **1995**, *34*, 1823-1829. c) Verboom, W.; Rudkevich, D. M.; Reinhoudt, D. N. *Pure & Appl. Chem.*, **1994**, *66*, 679-686. d) Aoki, S.; Kimura, E. *Mol. Biotech.* **2002**, *90*, 129-155
- ⁵⁵ a) Kimura, E.; Kodama, M.; Yatsunami, T. *J. Am. Chem. Soc.* **1982**, *104*, 3182-3187. b) Martell, A. E.; Motekaitis, R. J.; Lu, Q.; Nation, D. A. *Polyhedron*. **1999**, *18*, 3203-3218. c) Umezawa, Y.; Kataoka, M.; Takami, W.; Kimura, E.; Koike, T.; Nada, H. *Anal. Chem.* **1988**, *60*, 2392-2396
- ⁵⁶ Dietrich, B.; Hosseini, M. W.; Lehn, J. M.; Sessions, R. B. *J. Am. Chem. Soc.* **1981**, *103*, 1282-1283

- ⁵⁷ a) Kimura, E.; Kuramoto, Y.; Koike, T.; Fujioka, H. Kodama, M. *J. Org. Chem.* **1990**, *55*, 42-46. b) Kimura, E.; Koike, T. *Chem. Commun.*, **1998**, *15*, 1495-1599
- ⁵⁸ Kimura, E.; Aoki, S.; Koike, T.; Shiro, M. *J. Am. Chem. Soc.* **1997**, *119*, 3068-3076
- ⁵⁹ a) Marecek, J. F.; Burrows, C. J. *Tetrahedron Lett.* **1986**, *27*, 5943-5946. b) Marecek, J. F.; Fischer, P. A.; Burrows, C. J. *Tetrahedron Lett.* **1988**, *29*, 6231-6234
- ⁶⁰ a) Bianchi, A.; Micheloni, M.; Paoletti, P. *Inorg. Chim. Acta*, **1988**, *151*, 269-272. b) Bianchi, A.; Micheloni, M.; Paoletti, P. *Coord. Chem. Rev.* **1991**, *110*, 17-113
- ⁶¹ a) Bencini, A.; Bianchi, A.; Giorgi, C.; Paoletti, P.; Valtancoli, B.; Fusi, V.; García-España, E.; Llinares, J. M.; Ramírez, J. A. *Inorg. Chem.* **1996**, *35*, 1114-1120. b) Andres, A.; Bazzicalupi, C.; Bencini, A.; Bianchi, A. F.; Garcia-Espana, E.; Giorgi, C.; Nardi, N.; Paoletti, P.; Ramirez, J. A.; Baltancoli, B. *J. Chem. Soc., Perkin Trans.2* **1994**, 2367-2373. c) Bazzicalupi, C.; Bencini, A.; Bianchi, A.; Cecchi, M.; Escuder, B.; Fusi, V.; Garcia-Espan, E.; Giorgi, C.; Luis, S. V.; Maccagni, G.; Marcelino, V.; Paoletti, P.; Valtancoli, B. *J. Am. Chem. Soc.* **1999**, *121*, 6807-6815. d) Bazzicalupi, C.; Bencini, A.; Bianchi, A.; Fusi, V.; Giorgi, C.; Granchi, A.; Paoletti, P.; Valtancoli, B. *J. Chem. Soc., Perkin Trans. 2*, **1997**, 775-781
- ⁶² a) Andres, A.; Burguete, M. I.; Garcia-Espana, E.; Luis, S. V.; Miravet, J. F.; Soriano, C. *J. Chem. Soc., Perkin Trans.2* **1993**, 749-755. b) Aguilar, J. A.; Garcia-Espana, E.; Guerrero, J. A.; Luis, S. V.; Llinares, J. M.; Miraver, J. F.; Ramirez, J. A.; Soriano, C. *J. Chem. Soc., Chem. Commun.* **1995**, 2237-2239. c) Bazzicalupi, C.; Beconcini, A.; Bencini, A.; Fusi, V.; Giorgi, C.; Masotti, A.; Valtancoli, B. *J. Chem. Soc., Perkin Trans. 2*, **1999**, *8*, 1675-1682. d) Hartley, J. H.; James, T. D.; Ward, C. J. *J. Chem. Soc., Perkin Trans. 1*, **2000**, 3155-3184
- ⁶³ a) Li, T.; Krasne, S. J.; Persson, B.; Kaback, H. R.; Diederich, F. *J. Org. Chem.* **1993**, *58*, 380-384. b) Li, T.; Diederich, F. *J. Org. Chem.*, **1992**, *57*, 3449-3454. c) Menger, F. M.; Catlin, K. K. *Angew. Chem. Int. Ed. Engl.* **1995**, *34*, 2147-2150
- ⁶⁴ a) Hosseini, M. W.; Lehn, J. M.; Jones, K. C.; Plute, K. E.; Mertes, K. B.; Mertes, M. P. *J. Am. Chem. Soc.* **1989**, *111*, 6330-6335. b) Hosseini, M. W.; Blacker, A. J.; Lehn, J. M. *J. Am. Chem. Soc.* **1990**, *112*, 3896-3904. c) Fenniri, H.; Hosseini, M. W.; Lehn, J. *Helv. Chim. Acta*, **1997**, *80*, 786-803. d) Powell, D.; Bowman-James, K. *Coord. Chem. Rev.* **2003**, *240*, 57-75
- ⁶⁵ a) Motekaitis, R. J.; Martell, A. E. *Inorg. Chem.* **1994**, *33*, 1032-1037. b) Motekaitis, R. J.; Martell, A. E. *Inorg. Chem.* **1992**, *31*, 5534-5542. c) Jurek, P. E.; Martell, A. E.; Motekaitis, R. J.; Hancock, R. D. *Inorg. Chem.* **1995**, *34*, 1823-1829. d) Lu, Q.; Motekaitis, R. J.; Reibenspies, J. J.; Martell, A. E. *Inorg. Chem.* **1995**, *34*, 4958-4964. e) Lu, Q.; Reibenspies, J. J.; Martell, A. E.; Motekaitis, R. J. *Inorg. Chem.* **1996**, *35*, 2630-2636. f) Nation, D. A.; Reibenspies, J.; Martell, A. E.

- Inorg. Chem.* **1996**, *35*, 4597-4603. g) English, J. B.; Martell, A. E.; Motekaitis, R. J.; Murase, I. *Inorg. Chim. Acta*, **1997**, *258*, 183-192. h) Qin, L.; Reibenspies, J. H.; Carroll, R. I.; Martell, A. E.; Clearfield, A. *Inorg. Chim. Acta*, **1998**, *270*, 207-215
- ⁶⁶ Grell, D.; Grell, E.; Bugnon, P.; Dietrich, B.; Lehn, J. M. *J. Thermal Anal. Calorimetry*, **2004**, *77*, 483-495
- ⁶⁷ Chu, F.; Flatt, L. S.; Anslyn, E. V. *J. Am. Chem. Soc.* **1994**, *116*, 4194-4204
- ⁶⁸ Carey, C. M.; Riggan, W. B. Jr. *Anal. Chem.* **1994**, *66*, 3587-3591
- ⁶⁹ a) Tohda, K.; Tange, M.; Odashima, K.; Umezawa, Y.; Furuta, H.; Sessler, J. L. *Anal. Chem.* **1992**, *64*, 960-964. b) Furuta, H.; Magda, D.; Sessler, J. L. *J. Am. Chem. Soc.* **1991**, *113*, 978-985
- ⁷⁰ a) Vance, D. H.; Czarnik, A. W. *J. Am. Chem. Soc.* **1994**, *116*, 9397-9398. b) Czarnik, A. W. *Acc. Chem. Res.* **1994**, *27*, 302-308. c) Huston, M. E.; Akkaya, E. U.; Czarnik, A. W. *J. Am. Chem. Soc.* **1989**, *111*, 8735-8737. d) Powell, D.; Bowman-James, K.; *Coord. Chem. Rev.* **2003**, *240*, 57-75
- ⁷¹ Sancenon, F.; Benito, A.; Lloris, J. M.; Martinez-Manez, R.; Pardo, T.; Soto, J. *Helv. Chim. Acta*. **2002**, *85*, 1505-1516
- ⁷² Mizukami, S.; Nagano, T.; Urano, Y.; Odani, A.; Kikuchi, K. *J. Am. Chem. Soc.* **2002**, *124*, 3920-3925
- ⁷³ a) Hamdi, A.; Nam, K. C.; Ryu, B. J.; Kim, J. S.; Vicens, J. *Tetrahedron Lett.* **2004**, *45*, 4689-4692. b) Lhotak, P.; Svoboda, J.; Stibor, I. *Tetrahedron* **2006**, *62*, 1253-1257
- ⁷⁴ a) Hartley, J. H.; James, T. D.; Ward, C. J. *J. Chem. Soc., Perkin Trans. 1*, **2000**, 3155-3184. b) Beer, P. D.; Drew, M. G. B.; Gradwell, K. *J. Chem. Soc., Perkin Trans. 2*, **2000**, *3*, 511-519. c) Morzherin, Y.; Rudkevich, D. M.; Verboom, W.; Reinhoudt, D. N. *J. Org. Chem.* **1993**, *58*, 7602-7605. d) Tabushi, I.; Kuroda, Y.; Mizutani, T. *Tetrahedron*. **1984**, *40*, 545-552. e) Eliseev, A. V.; Schneider, H. *Angew. Chem. Int. Ed. Engl.* **1993**, *32*, 1331-1333
- ⁷⁵ Pasternack, R. F.; Gibbs, E. J.; Antebi, A.; Bassner, S.; De Poy, L.; Turner, D. H.; Williams, A.; Laplace, F.; Lansard, M. H. *J. Am. Chem. Soc.*, **1985**, *107*, 8179-8186
- ⁷⁶ Jagessar, R. C.; Shang, M.; Scheidt, W. R.; Burns, D. H. *J. Am. Chem. Soc.*, **1998**, *120*, 11684-11692

- ⁷⁷ a) Iverson, B. L.; Shreder, K.; Kral, V.; Sessler, J. L. *J. Am. Chem. Soc.*, **1993**, *115*, 11022-11023. b) Sessler, J. L.; Cyr, M.; Ruruta, H.; Kral, V.; Mody, T.; Morishima, T.; Shionoya, M.; Weghorn, S. *Pure & Appl. Chem.*, **1993**, *65*, 393-398. c) Král, V.; Sessler, J. L. *Tetrahedron*. **1995**, *51*, 539-554. d) Iverson, B. L.; Shreder, K.; Král, V.; Sansom, P.; Lynch, V.; Sessler, J. L. *J. Am. Chem. Soc.*, **1996**, *118*, 1608-1616. e) Král, V.; Furuta, H.; Shreder, K.; Lynch, V.; Sessler, J. L. *J. Am. Chem. Soc.* **1996**, *118*, 1595-1607. f) Sessler, J. L.; Davis, J. M. *Acc. Chem. Res.* **2001**, *34*, 989-997. g) Shevchuk, S. V.; Lynch, V. M.; Sessler, J. L. *Tetrahedron*. **2004**, *60*, 11283-11291
- ⁷⁸ a) Andrievsky, A.; Ahuis, F.; Sessler, J. L.; Vögtle, F.; Gudat, D.; Moini, M. *J. Am. Chem. Soc.*, **1998**, *120*, 9712-9713. b) Gale, P. A. *Coordi. Chem. Rev.* **2000**, *199*, 181-233. c) Beer, P. D.; Gale, P. A. *Angew. Chem. Int. Ed.* **2001**, *40*, 486-516
- ⁷⁹ a) Gale, P. A.; Sessler, J. L.; Král, V.; Lynch, V. *J. Am. Chem. Soc.*, **1996**, *118*, 5140-5141. b) Gale, P. A.; Sessler, J. L.; Král, V. *Chem. Commun.*, **1998**, *1*, 1-8. c) Král, V.; Sessler, J. L.; Shishkanova, T. V.; Gale, P. A.; Volf, R. *J. Am. Chem. Soc.*, **1999**, *121*, 8771-8775. d) Miyaji, H.; Sato, W.; Sessler, J. L. *Angew. Chem. Int. Ed.* **2000**, *39*, 1777-1780. e) Gale, P. A. *Coordi. Chem. Rev.* **2000**, *199*, 181-233. f) Anzenbacher, P.; Jr., Jursíková, K.; Sessler, J. L. *J. Am. Chem. Soc.*, **2000**, *122*, 9350-9351. g) Gale, P. A.; Hursthouse, M. B.; Light, M. E.; Sessler, J. L.; Warrinera, C. N.; Zimmermanb, R. S. *Tetrahedron Lett.* **2001**, *42*, 6759-6762. h) Sessler, J. L.; Kral, V.; Shishkanova, T. V.; Gale, P. A. *PNAS* **2002**, *99*, 4848-4853. i) Shao, S.; Guo, Y.; He, L.; Jiang, S.; Yu X. *Tetrahedron Lett.* **2003**, *44*, 2175-2178. j) Nishiyabu, R.; Anzenbacher, P. Jr. *Org. Lett.* **2006**, *8*, 359-362
- ⁸⁰ Anzenbacher, P. Jr.; Jursikova, K.; Aldakov, D.; Marquez, M.; Pohl, R. *Tetrahedron* **2004**, *60*, 11163-11168
- ⁸¹ a) Chen, Z.; Graydon, A. R.; Beer, P. D. *J. Chem. Soc., Faraday Trans.* **1993**, *92*, 97-102. b) Beer, P. D.; Chen, Z.; Goulden, A. J.; Graydon, A.; Stokes, A. E.; Wear, T. *J. Chem. Soc., Chem. Commun.* **1993**, 1834-1836. c) Delavaux-Nicot, B.; Guari, Y.; Douziech, B.; Mathieu, R. *J. Chem. Soc., Chem. Commun.* **1995**, 585-587. d) Beer, P. D.; Drew, M. G. B.; Graydon, A. R.; Smith, D. K.; Stokes, S. E. *J. Chem. Soc., Dalton Trans.* **1995**, 403-408. e) Beer, P. D.; Graydon, A. R.; Johnson, A. O. M.; Smith, D. K. *Inorg. Chem.* **1997**, *36*, 2112-2118. f) Beer, P. D. *Acc. Chem. Res.* **1998**, *31*, 71-80. g) Beer, P. D.; Chen, Z.; Drew, M. G. B.; Kingston, J.; Ogden, M.; Spencer, P. *J. Chem. Soc., Chem. Commun.* **1993**, 1046-1048. h) Beer, P. D.; Chen, Z.; Drew, M. G. B.; Johnson, A. O. M.; Smith, D. K.; Spencer, P. *Inorg. Chim. Acta*, **1996**, *246*, 143-150. i) Beer, P. D.; Cadman, J.; Lloris, J. M.; Martínez-Mañez, R.; Padilla, M. E.; Pardo, T.; Smith, D. K.; Soto, J. *J. Chem. Soc., Dalton Trans.*, **1999**, *2*, 127-134. j) Beer, P. D.; Gale, P. A. *Angew. Chem. Int. Ed.* **2001**, *40*, 3, 486-516. k) Pratt, M. D.; Beer, P. D. *Polyhedron*. **2003**, *22*, 649-653. l) Lloris, J. M.; Martinez-Manez, R.; Soto, J.; Pardo, T. *J. Organomet. Chem.* **2001**, 637-639, 151-158. m) Lloris, J. M.; Martínez-Mañez, R.;

- Padilla-Tosta, M.; Pardo, T.; María, J. S.; Tendero, J. L. *J. Chem.Soc., Dalton Trans.*, **1998**, 21, 3657-3662. n) Snowden, T. S.; Anslyn, E. V. *Curr. Opin. Chem. Biol.* **1999**, 3, 740-746. o) Coles, S. J.; Denuault, G.; Gale, P. A.; Horton, P. N.; Hursthouse, M. B.; Light, M. E.; Warriner, C. N. *Polyhedron*. **2003**, 22, 699-709. p) Reynes, O.; Moutet, J.; Pecaut, J.; Royala, G.; Saint-Aman, E. *New J. Chem.*, **2002**, 26, 9-12. q) Reynes, O.; Maillard, F.; Moutet, J.; Royal, G.; Saint-Aman, E.; Stanciu, G.; Dutasta, J.; Gosse, I.; Mulatier, J. *J. Organomet. Chem.* **2001**, 637-639, 356-363. r) Markus Scherer. Sessler, J. L.; Gebauer, A.; Lynch, V. *J. Chem. Soc., Chem. Commun.*, **1998**, 1, 85-86. s) Oton, F.; Tarraga, A.; Velasco, M. D.; Molina, P. *Dalton Trans.* **2005**, 1159-1161. t) Oton, F.; Tarraga, A.; Espinosa, A.; Velasco, M. D.; Bautista, D.; Molina, P. *J. Org. Chem.* **2005**, 70, 6603-6608
- ⁸² Beer, P. D.; Davis, J. J.; Drillsma-Milgrom, D. A.; Szemes, F. *J. Chem. Soc., Chem. Commun.* **2002**, 1716-1717
- ⁸³ a) Beer, P. D.; Heseck, D.; Kingston, J. E.; Smith, D. K.; Stokes, S. E.; Drew, M. G. B. *Organometallics* **1995**, 14, 3288-3295. b) Gale, P.A.; Chen, Z.; Drew, M. G. B.; Heath, J. A.; Beer, P. D. *Polyhedron*. **1998**, 17, 405-412. c) Beer, P. D.; Heseck, D.; Nam, K. C.; Drew, M. G. B. *Organometallics* **1999**, 18, 3933-3943. d) Beer, P. D., Gale, P. A. *Angew. Chem. Int. Ed.* **2001**, 40, 486-516. e) Beer, P. D.; Drew, M. G. B.; Heseck, D.; Shade, M.; Szemes, F. *J. Chem. Soc., Chem. Commun.* **1996**, 2161-2162
- ⁸⁴ a) Beer, P. D., Gale, P. A. *Angew. Chem. Int. Ed.* **2001**, 40, 486-516. b) Labande, A.; Ruiz, J.; Astruc, D. *J. Am. Chem. Soc.*, **2002**, 124, 1782-1789. c) Daniel, M.; Ruiz, J.; Astruc, D. *J. Am. Chem. Soc.* **2003**, 125, 1150-1151
- ⁸⁵ a) Beer, P. D.; Chen, Z.; Goulden, A. J.; Grieve, A.; Heseck, D.; Szemes, F.; Wear, T. *J. Chem. Soc., Chem. Commun.* **1994**, 1269-1271. b) Beer, P. D. *J. Chem. Soc., Chem. Commun.* **1996**, 689-696. c) Szemes, F.; Heseck, D.; Chen, Z.; Dent, S. W.; Drew, M. G. B.; Goulden, A. J.; Graydon, A. R.; Grieve, A.; Mortimer, R. J.; Wear, T.; Weightman, J. S.; Beer, P. D. *Inorg. Chem.* **1996**, 35, 5868-5879. d) Beer, P. D.; Graydon, A. R.; Sutton, L. R. *Polyhedron*. **1996**, 15, 2457-2461. e) Beer, P. D.; Szemes, F.; Balzani, V.; Salà, C. M.; Drew, M. G. B.; Dent, S. W.; Maestri, M. *J. Am. Chem. Soc.* **1997**, 119, 11864-11875. f) Beer, P. D.; Dent, S. W. *J. Chem. Soc., Chem. Commun.*, **1998**, 7, 825-826. g) Beer, P. D. *Acc. Chem. Res.* **1998**, 31, 71-80. h) Beer, P. D.; Timoshenko, V.; Maestri, M.; Passaniti, P.; Balzani, V. *J. Chem. Soc., Chem. Commun.*, **1999**, 17, 1755-1756. i) Gale, P. A. *Coord. Chem. Rev.* **2000**, 199, 181-233. j) Cooper, J. B.; Drew, M. G. B.; Beer, P. D. *J. Chem. Soc., Dalton Trans.*, **2000**, 2721-2728. k) Beer, P. D., Gale, P. A. *Angew. Chem. Int. Ed.* **2001**, 40, 486-516. l) Beer, P. D., Cadman, J. *New J. Chem.* **1999**, 23, 347-349. m) Deetz, M. J.; Smith, B. D. *Tetrahedron Lett.* **1998**, 39, 6841-6844. n) Sun, S.; Lees, A. J.; Zavalij, P. Y. *Inorg. Chem.* **2003**, 42, 3445-3453. o) Sun, S.; Lees, A. J. *J. Chem. Soc., Chem. Commun.*, **2000**, 1687-

1688. p) Vickers, M. S.; Martindale, K. S.; Beer, P. D. *J. Mater. Chem.* **2005**, *15*, 2784-2790
- ⁸⁶ Duff, T.; Grüßing, A.; Thomas, J.; Duati, M.; Vos, J.G. *Polyhedron*. **2003**, *22*, 775-780
- ⁸⁷ a) Chin, J.; Banaszczyk, M. *J. Am. Chem. Soc.* **1989**, *111*, 4103-4105. b) Wall, M.; Hynes, R. C.; Chin, J. *Angew. Chem. Int. ed. Engl.* **1993**, *32*, 1633-1635. c) Seo, J. S.; Sung, N.; Hynes, R. C.; Chin, J. *Inorg. Chem.*, **1996**, *35*, 7472-7473
- ⁸⁸ Han, M. S.; Kim, D. H. *Angew. Chem. Int. Ed. Engl.* **2001**, *41*, 3809-3811
- ⁸⁹ Best, M. D.; Anslyn, E.V. *Eur. J. Chem.* **2003**, *9*, 51-57
- ⁹⁰ Mameri, S.; Charbonniere, L. J.; Ziessel, R. F. *Inorg. Chem.* **2004**, *43*, 1819-1821
- ⁹¹ a) Ojida, A.; Park, S.; Mito-oka, Y.; Hamachia, I. *Tetrahedron Lett.* **2002**, *43*, 6193-6195. b) Ojida, A.; Inoue, M.; Mito-oka, Y.; Tsutsumi, H.; Sada, K.; Hamachi, I. *J. Am. Chem. Soc.* **2006**, *128*, 2052-2058. c) Ojida, A.; Miyahara, Y.; Kohira, T.; Hamachi, I. *Biopolymers (Pept. Sci.)* **2004**, *76*, 177-184. d) Ojida, A.; Hamachi, I. *Bull. Chem. Soc. Jpn.* **2006**, *79*, 1. e) Ojida, A.; Kohira, T.; Hamachi, I. *Chem. Lett.* **2004**, *33*, 8. f) Ojida, A.; Mito-oka, Y.; Inoue, M.; Sada, K.; Hamachi, I. *J. Am. Chem. Soc.* **2002**, *124*, 6256-6258. g) Ojida, A.; Inoue, M.; Mito-oka, Y.; Hamachi, I. *J. Am. Chem. Soc.* **2003**, *125*, 10184-10185. h) Ojida, A.; Mito-oka, Y.; Sada, K.; Hamachi, I. *J. Am. Chem. Soc.* **2004**, *126*, 2454-2463
- ⁹² Lakshmi, C.; Hanshaw, R. G.; Smith, B. D. *Tetrahedron* **2004**, *60*, 11307-11315
- ⁹³ Ojida, A.; Honda, K.; Shinmi, D. Kiyonaka, S.; Mori, Y.; Hamachi, I. *J. Am. Chem. Soc.* **2006**, *128*, 10452-10459
- ⁹⁴ a) Benniston, A. C.; Gunning, P.; Peacock, R. D. *J. Org. Chem.* **2005**, *70*, 115-123. b) Peacock, R. D.; Gunning, P.; Benniston, A. C. *J. Chem. Soc., Chem. Comm.*, **2004**, 2226-2227
- ⁹⁵ a) Steinke, J. H. G.; Dunkin, I. R.; Sherrington, D. C. *Macromolecules* **1996**, *29*, 407-415. b) Mosbach, K.; Ramstrom, O. *Biotechnology* **1996**, *14*, 163-170. c) Wulff, G. *EXS* **1997**, *80*, 13-26 (*Frontiers in Biosensorics I. Fundamental Aspects*). d) Wulff, G. *Angew. Chem., Int. Ed. Engl.* **1995**, *34*, 1812-1832. e) Kriz, D.; Ramstrom, O.; Mosbach, K. *Anal. Chem.* **1997**, *69*, 345A-349A. f) Muldoon, M. T.; Stanker, L. H. *Chem. Ind.* **1996**, *6*, 204-207. g) Steinke, J.; Sherrington, D. C.; Dunkin, I. R. *Adv. Polym. Sci.* **1995**, *123*, 81-125. h) Ansell, R. J.; Ramstro"m, O.; Mosbach, K. *Clin. Chem.* **1996**, *42*, 1506-1512. i) Vlatakis, G.; Andersson, L. I.; Muller, R.; Mosbach, K. *Nature* **1993**, *361*, 645-647

Chapter 2: Molecular recognition and indicator-displacement assays for phosphoesters

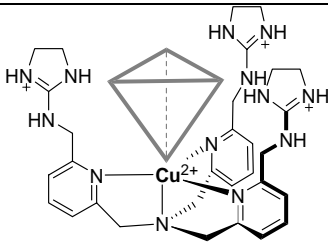
2.1 Introduction

Phosphate esters play a dominant role in the physiology of cells, and hence are essential to many organisms. They are structural and functional elements in DNA, RNA, and their monomeric building blocks. Further, they participate in post-translational signaling in proteins, and serve as a head group in phospholipids.¹ Therefore, the design and synthesis of receptors that have high selectivities and affinities for phosphate esters in aqueous media is a current goal of molecular recognition studies. Receptors functionalized with guanidinium groups,² polyaza groups,³ amides,⁴ and ureas (including thiourea)⁵ have demonstrated high affinities towards phosphate esters through multiple hydrogen bonding and ion-pairing interactions. However, most of the previously reported receptors either lack high affinities or have low selectivities towards these phosphate guest molecules in aqueous media at neutral pH. The impetus for the work described herein is the dearth of effective receptors for phosphate esters that demonstrate both high on selectivity and affinity under physiological conditions. As a secondary goal, an indicator-displacement assay makes for a simple optical technique for detecting phosphoesters.

The Anslyn group previously reported the design and synthesis of the C_{3v} metallo-host molecule **2.1**.⁶ Via a combination of electrostatic interactions, hydrogen bonding

interactions, coordination bonds, and geometrical complementarity in the receptor design, the host showed both high affinities and selectivities towards tetrahedral inorganic anions in aqueous solutions at neutral pH (**Table 2.1**). Specifically, phosphate and arsenate were the most high affinity guests.

Table 2.1 Design of host **2.1** and previously reported affinity constants in buffered water at pH 7.4

 2.1	Guests	Binding constants (K_a) (M^{-1})
	HPO_4^{2-}	1.5×10^4
	$HAsO_4^{2-}$	1.7×10^4
	ReO_4^{2-} , AcO^- , NO_3^- , HCO_3^- , Cl^-	<100

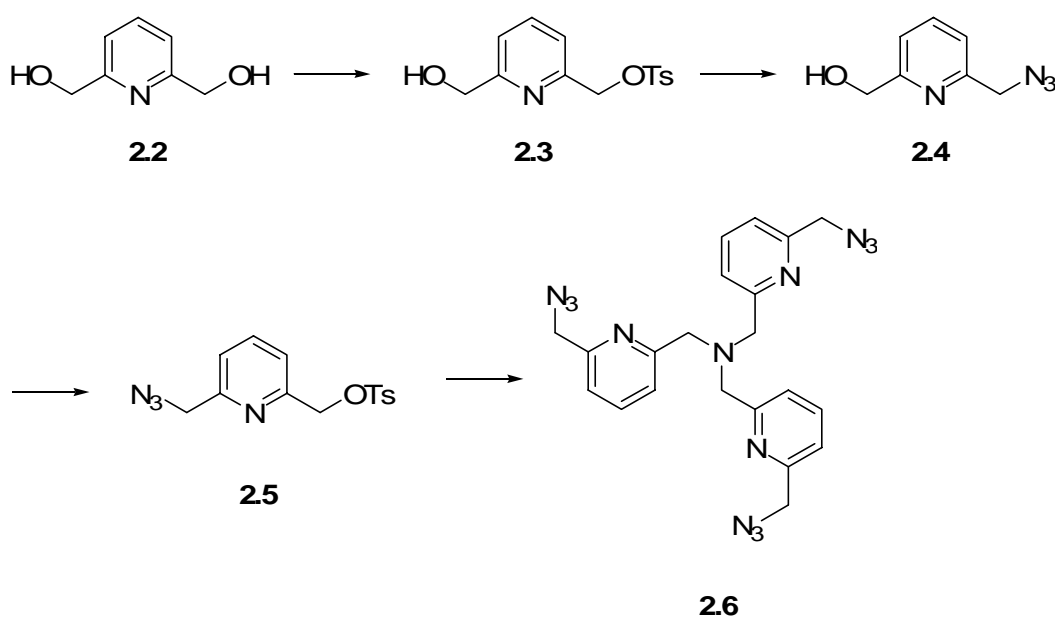
All data were measured at $[2.1] = 1.17 \text{ mM}$.

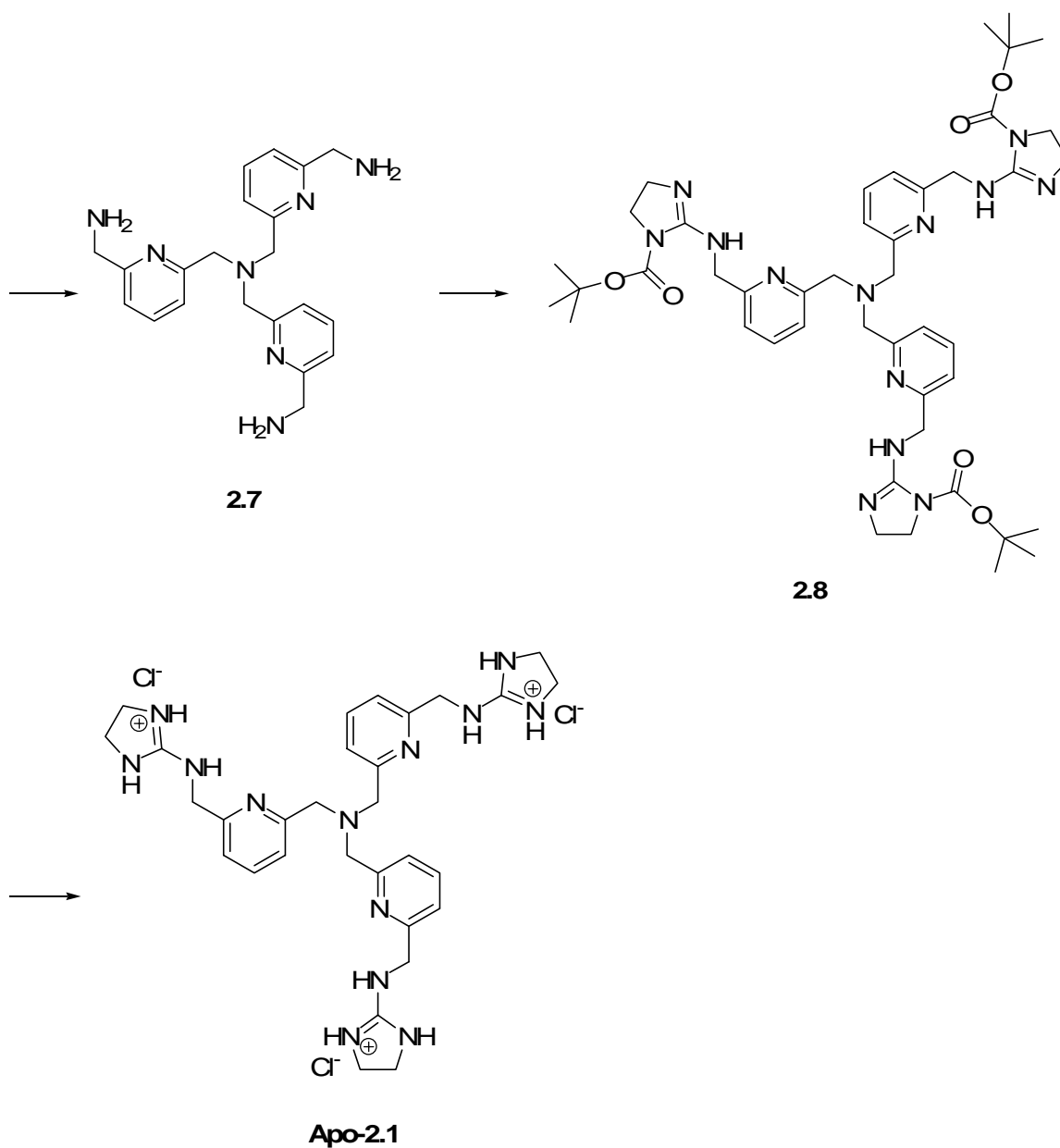
Indicator-displacement assays (IDA) offered a more sensitive analysis technique than direct UV-vis spectral changes of **2.1** upon phosphoester binding. The IDA also provides a more sensitive detection limit for determining phosphoester binding constants. The goal with these studies was to explore the possible targets for **2.1**, and to determine the extent phosphoesters enhance or diminish binding relative to phosphates. A long term goal is the creation of specific receptors that signal mono-phosphorylation events by kinases in biological systems.

2.2 Results and discussions

2.2.1 Synthesis

A synthesis of **2.1** has been previously reported.⁶ However, in the previous route several low yielding steps and difficult chromatographic separations were involved. Due to the interest in expanding the capabilities of **2.1** and future analogous designs a higher yielding and more facile synthetic route was desired (**Scheme 2.1**).





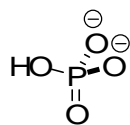
Scheme 2.1 New synthetic route to **2.1**.

The synthesis of receptor **2.1** started with commercially available 2,6-dihydroxymethyl pyridine **2.2**. A CH_2Cl_2 suspension of **2.2**, silver oxide, and potassium

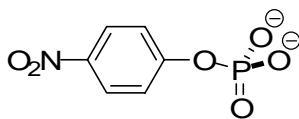
iodide was brought to -20 °C, followed by addition of tosyl chloride as a solid. The reaction system was slowly warmed to room temperature and stirred for 3 h. The mixture was filtered through a pad of silica gel, and the filtrate was washed with EtOAc.⁷ A flash column, first with CH₂Cl₂, then EtOAc, gave monosubstituted **2.3** in a 75% yield as a pink solid. To compound **2.3** was then added NaN₃ in DMF, and the solution was heated at 80 °C for 5 h. A greenish yellow solid of **2.4** was obtained. The second tosylation was carried out using NaOH as a base.⁸ Compound **2.5** was obtained as a yellow oil in 93% yield (using the reagents in step (i) gave near a 100% yield). Na₂CO₃ was found to be a better reagent than K₂CO₃ in the amine alkylation step to obtain the pale yellow oil **2.6**, in a 72% yield. The rest of the steps were the same as previously reported to afford **apo-2.1**.⁶ The complexation of cupric ion occurred upon addition of 1 equiv of cupric chloride into a water solution of **apo-2.1**. Compound **2.1** was then obtained *in situ*.

2.2.2 Binding studies

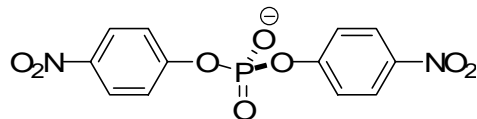
Eleven different phosphate esters were studied in pure water solution. Their binding affinities to **2.1** were monitored by UV-vis absorbance changes (**Table 2.2**). UV-vis titration studies were based on the modulations of the cupric ion absorptions at 775 nm. Small but reproducible changes in the molar absorptivities of the host were observed for all the phosphate esters due to modulations of the d-d forbidden transitions. All phosphate esters showed distinct 1:1 binding curves (see **Figure 2.1** for one example).



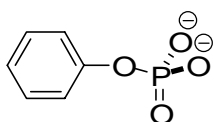
1



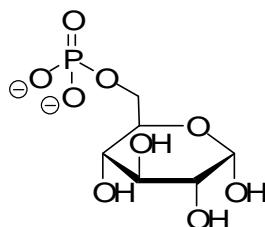
2



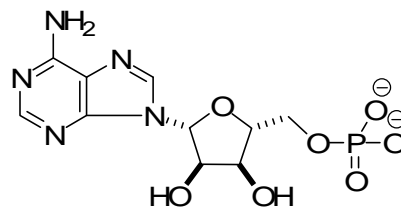
3



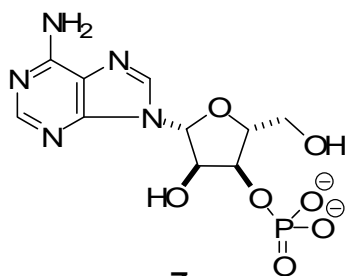
4



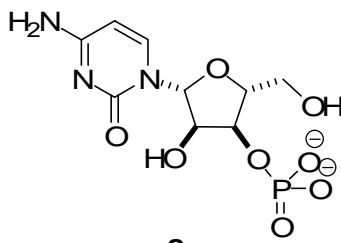
5



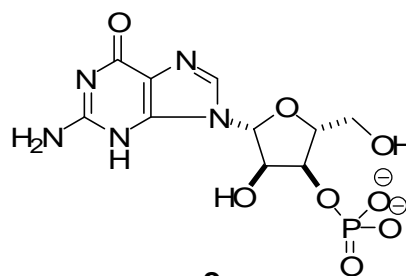
6



7



8



9

1. Dibasic phosphate
2. 4-Nitrophenyl phosphate
3. Bis(4-nitrophenyl) phosphate
4. phenyl phosphate
5. Glucose 6-phosphate
6. (-)-Adenosine 5'-monophosphate
7. Adenosine 3'-monophosphate
8. Cytidine 3'-monophosphate
9. Guanosine 3'-monophosphate

Table 2.2 Association constants obtained by UV-Vis titrations at room temperature

Guest	K_a ($1 \times 10^3 \text{ M}^{-1}$) 25 °C	Guest	K_a ($1 \times 10^3 \text{ M}^{-1}$) 25 °C
1	5.7±0.4	7	2.3±0.2
2	1.0±0.1	8	2.1±0.3
3	-	9	1.3±0.2
4	2.5±0.3	10	4.6±0.6
5	4.5±0.8	11	3.9±0.5
6	6.3±0.8	12	11.4±2.9

All data were measured at **[2.1]** = 1.92 mM.

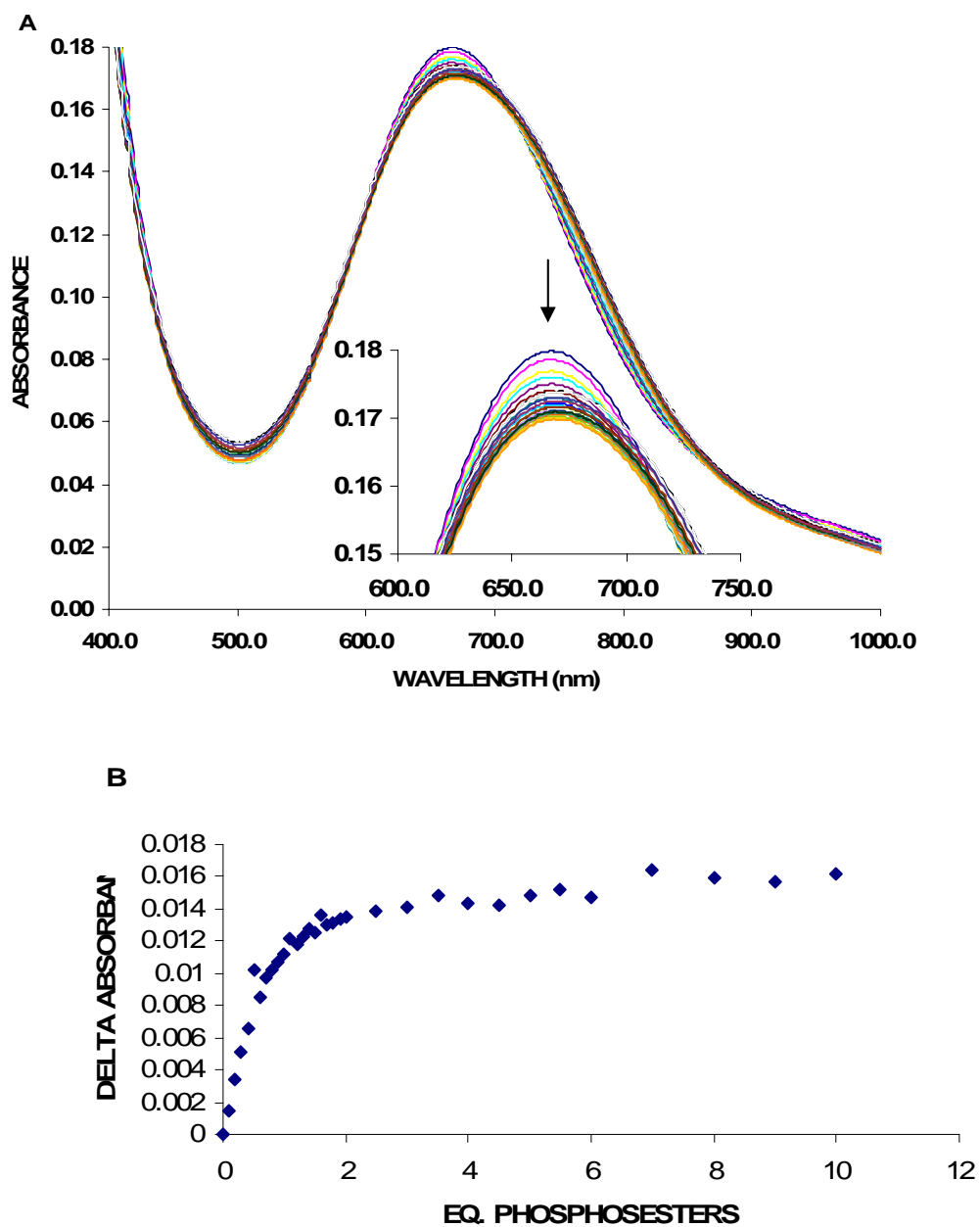


Figure 2.1 An example of the titration data used to determine affinity constants: A. Absorbances in UV-Vis titration by increasing the phosphoester concentration; B. The absorbance changed derived from A. Conditions: [2.1] = 1.92 mM, [Tris] = 10 mM, Solvent: water, pH = 7.4, 25 °C

Clear trends are evident in **Table 2.2** indicating the differences in the ability of **2.1** to bind various phosphoesters. 4-nitrophenyl phosphate esters were the first to be examined. Unsubstituted inorganic phosphate **1** binds the strongest, whereas 4-nitrophenyl phosphate **2** shows reduced binding. Phosphodiester such as bis(4-nitrophenyl) phosphate **3** displayed no binding.

These differences are ascribed to three possible effects. One is the decreased charge on a phosphomonoester relative to phosphate, and even a further decrease in charge with a diester. A second effect derives from the electron withdrawing nature of nitrophenyl ring, which further reduces the charge density on the phosphate group itself. A third possible effect derives from sterics between the host and the guest. The phenyl rings on the 4-nitrophenyl esters might not fit into the cavity of the host, and hence lower the association constant. These various issues were probed by examining parent phenyl groups, alkyl phosphoesters, and primary and secondary alkyl groups.

Monosubstituted phenyl phosphate **4** showed stronger binding than monosubstituted 4-nitrophenyl phosphate **2**. Therefore, the strong electron withdrawing nitro group on the *para* position of **2** did indeed lower the electron density on the phosphate oxygen, thus weakening the ion-pairing driven association with **2.1**.

To examine alkyl phosphoesters, a selection of biologically relevant phosphate monoesters was studied. The binding affinities of glucose 6-phosphate and adenosine 5'-monophosphate were particularly interesting. Importantly, these primary phosphate esters showed almost as strong binding as inorganic phosphate. Apparently, the sterics introduced by a single primary alkyl group do not influence the binding. This observation

is consistent with previous evidence that indicated inorganic phosphate binds to **2.1** in primary its dianionic monoprotic form,⁶ and hence HPO_4^{2-} is analogous to a phosphomonoester (RPO_4^{2-}).

The branching of the alkyl groups also affected the binding strengths. Primary phosphate esters had showed stronger binding than those with secondary alkyl groups (**7**, **8**, **9**). This trend must be a steric effect, indicating that the host does not accommodate branching in the alkyl groups when burying the phosphate group in the cavity. This discovery prompted us to examine the binding differences among phosphoserine **10**, phosphothreonine **11**, and phosphotyrosine **12**.

First, the binding site of these three compounds was determined, because all three have terminal amino groups and carboxyl groups that could also coordinate to the cupric center. Serine was chosen as a control was chosen for UV-vis titration to investigate the binding to the host molecule (**Figure 2.2**). It is clear from the data that serine was not bound to the host **2.1**. Thus, the phosphate group is the binding site to **2.1**, even though it is known that cupric ion has a strong affinity to ligands with lone pair nitrogen atoms.

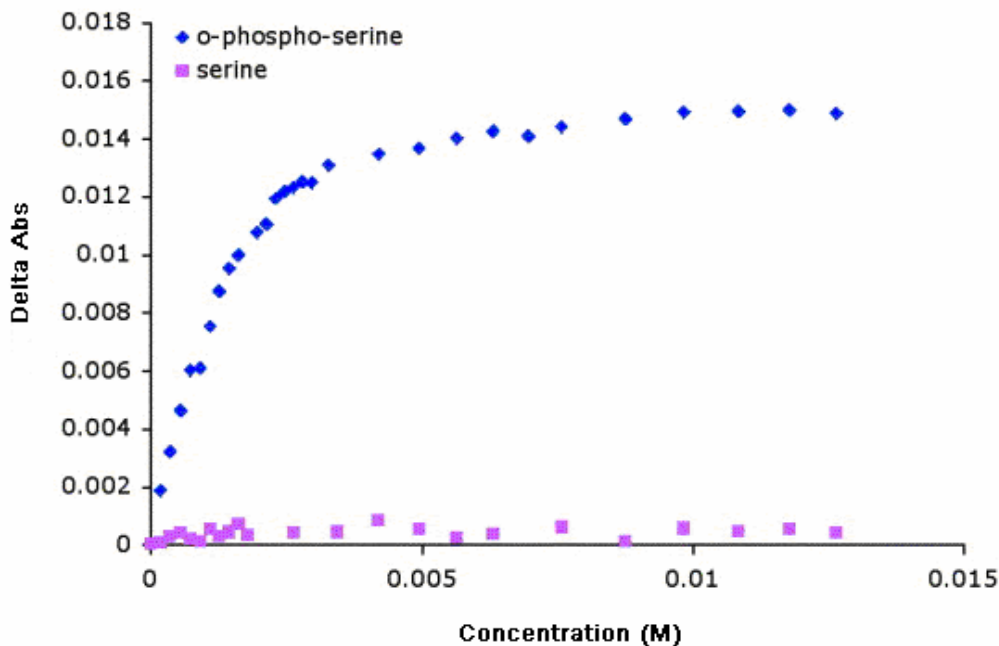


Figure 2.2 UV-Vis titration data of o-phospho-l-serine and l-serine. Conditions: [**2.1**] = 1.92 mM, [Tris] = 10 mM, Solvent: water, pH = 7.4, 25 °C

The affinities of these three amino acid phosphates for **2.1** were similar but not identical. *o*-Phospho-L-threonine binds less effectively than *o*-phospho-L-serine, again reflecting a steric influence. However, *o*-phospho-L-tyrosine **12** showed the strongest binding compared to the other two amino acid phosphates (**10** and **11**).

The concentration dependence of the K_a values was also studied. The binding constants at different concentrations of host molecule (3.84, 2.69, 1.92, 1.54, 0.96, 0.61 mM) towards inorganic phosphate anion were measured at room temperature. It was clear that the lower the host concentration, the larger the binding constants. Because the accuracy of UV-vis studies is dependent upon the detection limit of the UV-vis

spectrometer, there is a larger error at the lower host concentrations. Yet, this fact is not the source of the concentration trend.

The trend was unexpected at first, but can be readily explained by an effect of ionic strength. The Debye-Huckel **Equation 1** for determining ionic strength has a large dependence on multiply charged species. The host is formally positive five, with five negative chloride counterions. The activity coefficient (γ) for a specific ion can be calculated by **Eq. 2**. The size of each ion (α) is not known in this case. However, with concentrations in millimolar range or less, the denominator of **Eq. 2** would be near 1. Therefore, **Eq. 2** can be simplified as shown in **Eq. 3**. The host-guest binding **Eq. 4** and its dependence upon concentrations and activity coefficients **Eq. 5** are shown. The observed binding constant (K_{obs}), which was calculated in this study, is proportional to the activity coefficients of those three species in **Eq. 4** since the theoretical binding constant (K) does not change with concentrations (**Eq. 6**). Therefore, the activity coefficient dependence upon host concentration should have the same trend as the K_{obs} dependence upon host concentration. Similar trends were obtained from K_{obs} versus [2.1] (**Figure 2.3A**) and $\gamma_{\text{H}}\gamma_{\text{G}}/\gamma_{\text{HG}}$ versus [2.1] (**Figure 2.3B**). This analysis supports the notion that as host concentration decreases, a smaller binding constant should be observed.

$$\mu = 1/2 \sum C z^2 \quad (1)$$

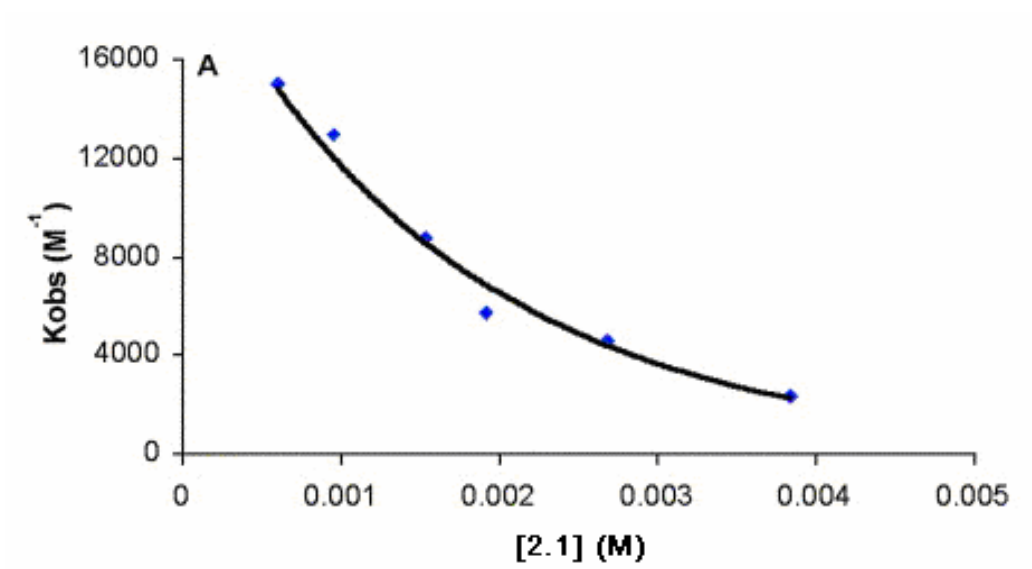
$$\log \gamma = \frac{-0.51 z^2 \mu^{1/2}}{1 + (\alpha \mu / 305)} \quad (2)$$

$$\log \gamma = -0.51 z^2 \mu^{1/2} \quad (3)$$



$$K = \frac{[HG]^{3+} \gamma_{HG}}{[H]^{5+} \gamma_H [G]^{2-} \gamma_G} = \frac{[HG]^{3+}}{[H]^{5+} [G]^{2-}} \cdot \frac{\gamma_{HG}}{\gamma_H \gamma_G} = K_{obs} \cdot \frac{\gamma_{HG}}{\gamma_H \gamma_G} \quad (5)$$

$$K_{abs} = K \cdot \frac{\gamma_H \gamma_G}{\gamma_{HG}} \quad (6)$$



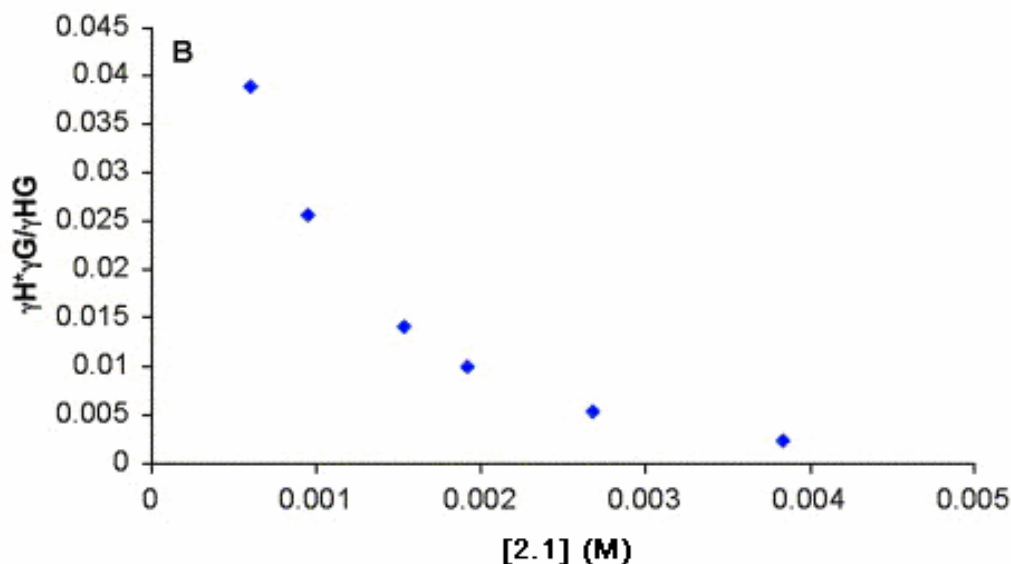
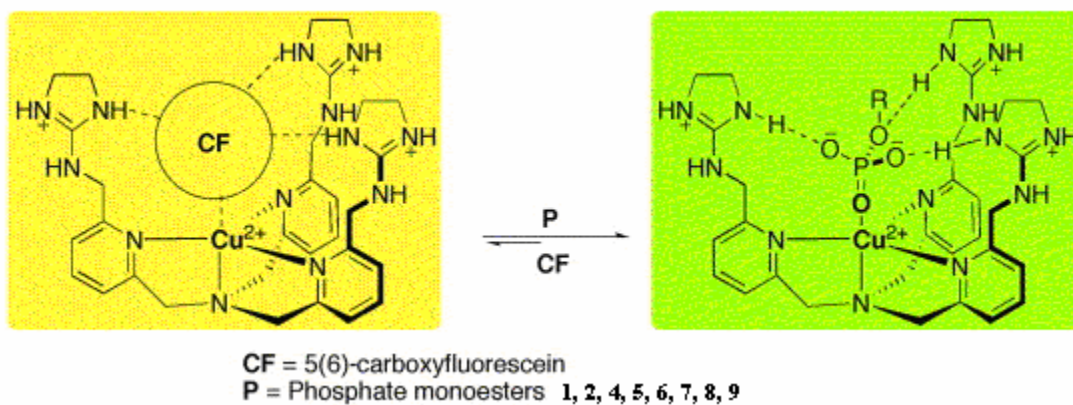
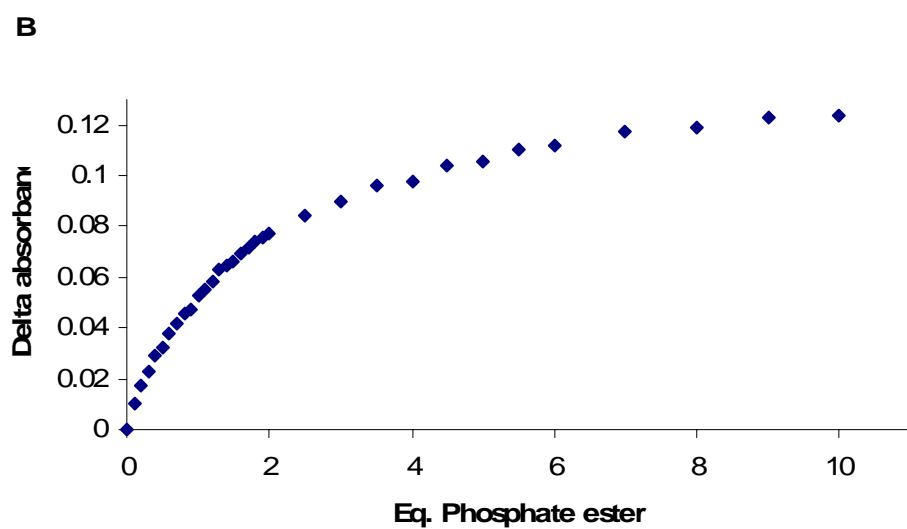
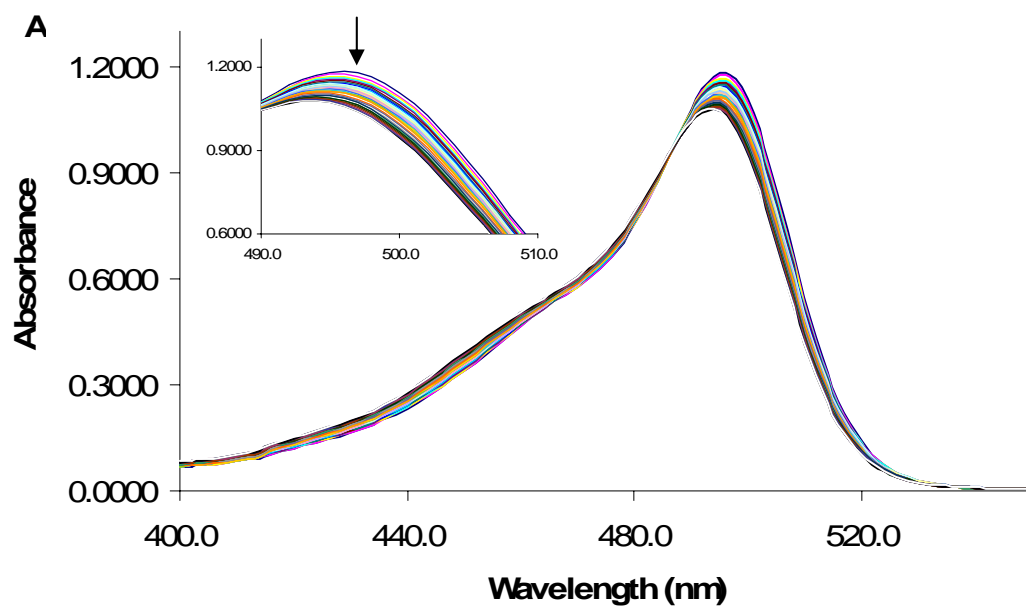


Figure 2.3 (A) Binding affinity changes with host **2.1** concentrations. $[2.1] = 3.84, 2.69, 1.92, 1.54, 0.96, 0.61$ mM (B) Calculated activity coefficients dependence on the host concentrations in the presence of 10 mM Tris buffer, Solvent: water, pH = 7.4, 25 °C.

To create optical sensing methods for the detection of phosphoesters indicator-displacement assays were employed. In the previously research, 5(6)-carboxyfluorescein was employed as an indicator in a 50:50 methanol/water (v:v) solution to quantitate inorganic phosphate in serum and saliva using **2.1** as the host.⁶ In a similar manner to this previous report, clear color changes of light orange to bright yellow were observed upon addition of the phosphate esters **1**, **2**, **4**, **5**, **6**, **7**, **8**, **9** into a solution of a host-indicator complex (**Figure 2.4**). Compounds **5** and **6** were chosen for quantitative indicator-displacement UV-titrations because they showed strong binding in the other UV-vis titrations. In each case, the indicator-displacement by phosphoesters proceeded with a 1:1 stoichiometry. The binding constants calculated from the fitting results were

1.2×10^5 for compound **5** and $1.1 \times 10^5 \text{ M}^{-1}$ for compound **6**, respectively, at **[2.1]** = 25.0 μM . These results are comparable to those obtained from host only titrations (3.6×10^4 and $1.5 \times 10^4 \text{ M}^{-1}$), respectively, at **[2.1]** = 1.92 mM, but a much larger absorbance change was observed. These results confirmed that the binding strength between host and guest is dependent upon both the host concentrations and the solvent. Also, the indicator-displacement assay allowed an opportunity to detect the guests at lower concentrations and with a higher optical response.





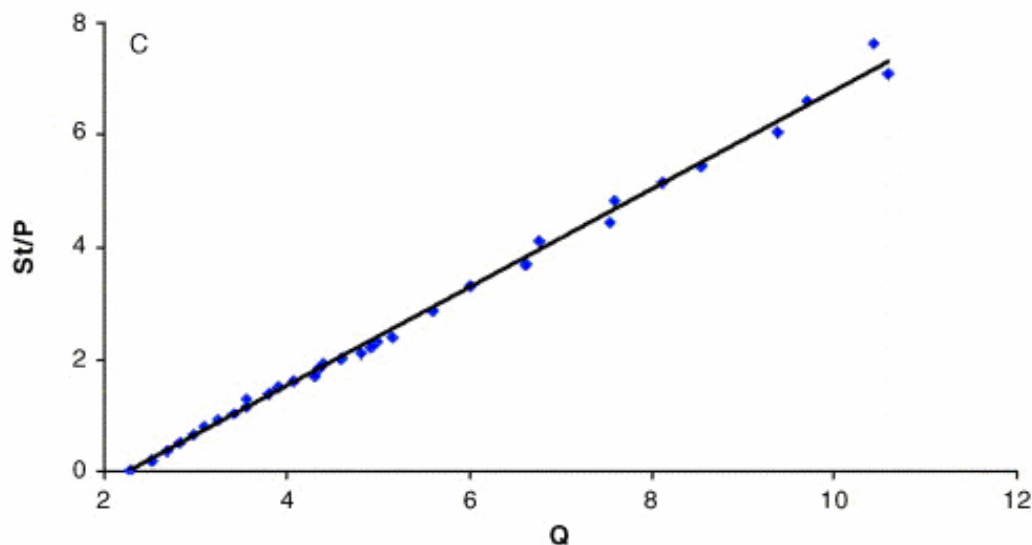


Figure 2.4 (A) Reproducible changes in the UV-Vis spectra of host-indicator solution upon addition of phosphoesters. (B) Example of the titration data used to determine the competing affinity constant. (C) Competition displacement algorithm.⁹ Conditions: [2.1] = [5(6)-carboxyfluorescein] = 25.0 μ M, [Tris] = 10 mM, Solvent: 50:50 methanol/water (v:v), pH = 7.4, 25 $^{\circ}$ C.

2.3 Conclusion

In summary, the binding affinity of host **2.1** towards different phosphoesters was studied. An indicator-displacement assay was also performed, which was able to detect the host-guest interactions with small visual color changes. The degree of substitution of the phosphate, the functionality of the substituents, and the size of the substituents all affected their interactions with the host molecule. The success of using this C_{3v} host to bind phosphomonoesters has offered the opportunity to further exploit this host to monitor phosphorylated organic molecules *in vivo*.

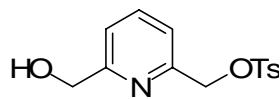
2.4 Experimental section

2.4.1 General considerations

All chemicals used were obtained from Aldrich or Acros and were used without purifications unless noted. Flash chromatography was performed on Whatman 60 Å 230-400 mesh silica gel. ^1H (400 MHz) and ^{13}C (75 MHz) spectra were measured by Varian Unity Plus spectrometer. Mass spectra were recorded on a Finnigan VG analytical ZAB2-E spectrometer. UV-vis spectra were collected on a Beckman DU-640 at various temperatures.

2.4.2 Synthesis

2.4.2.1 Compound 2.3

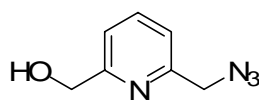


2.3

A CH_2Cl_2 (50 mL) suspension of 2,6-dihydroxymethyl pyridine **2.2** (1.00 g, 7.19 mmol), silver oxide (2.84 g, 10.78 mmol), potassium iodide (0.24 g, 1.44 mmol) was

brought to -20 °C, tosyl chloride (1.51 g, 7.91 mmol) was then added as a solid. The reaction system was slowly warmed up to room temperature and stirred for 3 h. The reaction mixture was filtered through a pad of silica gel, and washed with ethyl acetate. A flash column, first with CH₂Cl₂, then ethyl acetate, gave monosubstituted pink solid **2.3** (1.58 g, 75%). m.p. 56-57.5 °C. ¹H NMR (CDCl₃, 300 Hz) δ 2.44 (3H, s), δ 4.68 (2H, s), δ 5.13 (2H, s), δ 7.21 (1H, d), δ 7.32 (3H, m), δ 7.69 (1H, t), δ 7.83 (2H, d). ¹³C NMR (CDCl₃, 75 Hz) δ 21.54, δ 63.69, δ 71.30, δ 120.15, δ 120.49, δ 127.93, δ 129.84, δ 132.60, δ 137.70, δ 145.08, δ 152.41, δ 158.89. HRCI C₁₄H₁₆NO₄S (M+1) 294.0792 (calcd 294.0792).

2.4.2.2 Compound 2.4

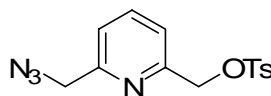


2.4

To compound **2.3** (1.58 g, 5.38 mmol) was added NaN₃ (1.05 g, 16.16 mmol) in a DMF (40 mL) solution, and the solution was heated at 80 °C for 5 h. The DMF was removed by high vac. The residue was redissolved in ethyl acetate. The precipitate was removed via filtration through a pad of celite. Evaporation of the solvent gave a pure greenish yellow solid **2.4** (0.88 g, 100%). ¹H NMR (CDCl₃, 300 Hz) δ 4.35 (2H, s), δ

4.66 (2H, s), δ 7.15 (1H, d), δ 7.20 (1H, d), δ 7.62 (1H, t). ^{13}C NMR (CDCl_3 , 75 Hz) δ 54.92, δ 63.89, δ 119.63, δ 120.25, δ 137.57, δ 154.50, δ 159.54. HRCI $\text{C}_7\text{H}_9\text{N}_4\text{O}$ (M+1) 165.0783 (calcd 165.0783).

2.4.2.3 Compound 2.5



2.5

Compound **2.4** (0.54 g, 3.29 mmol) was dissolved in THF (1.6 mL) and H_2O (1.6 mL), and brought to 0 °C. NaOH (0.39 g, 9.87 mmol) was added. A THF (2.7 mL) solution of tosyl chloride (0.69 g, 3.62 mmol) was added to the previous suspension dropwise while stirring. The system was kept at 0 °C and stirred for 4 h, and then extracted with CH_2Cl_2 . The combined organic layer was washed with brine and dried with Na_2SO_4 . Evaporation of the solvent gave compound **2.5** as a yellow oil (0.97 g, 93%). ^1H NMR (CDCl_3 , 300 Hz) δ 2.37 (3H, s), δ 4.33 (2H, s), δ 5.07 (2H, s), δ 7.21 (1H, d), δ 7.33 (3H, m), δ 7.65 (1H, t), δ 7.77 (2H, d). ^{13}C NMR (CDCl_3 , 75 Hz) δ 21.39, δ 54.94, δ 71.35, δ 120.77, δ 121.37, δ 127.81, δ 129.74, δ 132.44, δ 137.77, δ 144.96, δ 153.56, δ 155.28. HRCI $\text{C}_{14}\text{H}_{15}\text{N}_4\text{O}_3\text{S}$ (M+1) 319.8541 (calcd 319.8541).

2.4.3 UV-Vis titrations

A typical titration is described below, though concentrations varied from experiment to experiment. A stock solution of receptor (15.37 mM) was prepared, and buffered with Tris (10.04 mM) at pH=7.4. A similar solution of the guest (~50 mM) was also prepared and buffered with Tris (10.04 mM). To a quartz cuvette was added 875 μ L of a Tris (10.04 mM) solution and scanned as the blank reading. 125 μ L of the stock solution was introduced to the same cuvette (receptor concentration after dilution 1.92 mM), and the absorbance was recorded. Aliquots of a solution containing the receptor (1.92 mM) and each guest (~38 mM) in Tris buffer were then added to the cuvette and the absorbance was recorded after each addition. At a chosen wavelength of cupric d-d transition, the change in absorbance was calculated relative to the first absorbance reading. These values were then plotted versus the concentration of the added guest for each aliquot. The binding isotherm from this raw data was curve fit using a 1:1 binding algorithm in Origin.

2.4.4 Indicator-displacement assay

All titration solutions contained 10.90 mM Tris buffer in 50/50 (v:v) methanol/water. A stock solution of receptor (99.8 μ M), and 5(6)-carboxyfluorescein (99.8 μ M) was prepared in Tris (10.90 mM) buffered at pH=7.4. A similar solution of the guest (~2.5 mM) was also prepared and buffered with Tris (10.90 mM). To a quartz

cuvette was added 750 μL of a Tris (10.90 mM) solution and scanned as the blank reading. 250 μL of the stock solution was introduced to the same cuvette (receptor and 5(6)-carboxyfluorescein concentrations after dilution 25.0 μM), and the absorbance was recorded. Aliquots of a solution containing the receptor (25.0 μM), 5(6)-carboxyfluorescein (25.0 μM) and each guest (499 μM) in Tris buffer were then added to the cuvette and the absorbance was recorded after each addition. At a chosen wavelength of 5(6)-carboxyfluorescein absorptions, the change in absorbance was calculated relative to the first absorbance reading. These values were then plotted versus the concentration of the added guest for each aliquot. The binding isotherm from this raw data was curve fit using the 1:1 binding equation in Origin.⁶

2.5 References

- ¹ a) Schultz, C. *Bioorg. Med. Chem.* **2003**, *11*, 885-898. b) Aoki, S.; Kimura, E. *Rev. Mol. Biotech.* **2002**, *90*, 129-155
- ² a) Dixon, R. P.; Geib, S. J.; Hamilton, A. D. *J. Am. Chem. Soc.* **1992**, *114*, 365-366. b) Jubian, V.; Dixon, R. P.; Hamilton, A. D. *J. Am. Chem. Soc.* **1992**, *114*, 1120-1121. c) Jubian, V.; Veronese, A.; Dixon, R. P.; Hamilton, A. D. *Angew. Chem., Int. Ed. Engl.* **1995**, *34*, 1237-1239. d) Schneider, S. E.; O'Neil, S. N.; Anslyn, E. V. *J. Am. Chem. Soc.* **2000**, *122*, 542-543. e) McCleskey, S. C.; Griffin, M. J.; Schneider, S. E.; McDevitt, J. T. Anslyn, E. V. *J. Am. Chem. Soc.* **2003**, *125*, 1114-1115. f) Zhong, Z.; Anslyn, E. V. *Angew. Chem., Int. Ed.* **2003**, *26*, 3005-3008
- ³ a) Kimura, E.; Kodama, M.; Yatsunami, T. *J. Am. Chem. Soc.* **1982**, *104*, 3182-3187. b) Kimura, E.; Koike, T. *Chem. Commun.* **1998**, *15*, 1495-1599. c) Dietrich, B.; Guilhem, J.; Lehn, J.; Pascard, C.; Sonveaux, E. *Helv. Chim. Acta* **1984**, *67*, 91-104. d) Marecek, J. F; Fischer, P. A.; Burrows, C. J. *Tetrahedron Lett.* **1988**, *29*, 6231-6234. e) Bianchi, A.; Micheloni, M.; Paolett, P. *Coord. Chem. Rev.* **1991**,

- 110, 17-113. f) Aguilar, J. A.; Garcia-Espana, E.; Guerrero, J. A.; Luis, S. V.; Llinares, J. M.; Miraver, J. F.; Ramirez, J. A.; Soriano, C. *J. Chem. Soc., Chem. Commun.* **1995**, 2237-2239. g) Andres, A.; Bazzicalupi, C.; Bencini, A.; Bianchi, A. F.; Garcia-Espana, E.; Giorgi, C.; Nardi, N.; Paoletti, P.; Ramirez, J. A.; Baltancoli, B. *J. Chem. Soc., Perkin Trans. 2* **1994**, 2367-2373. h) Schneider, H.; Blatter, T.; Eliseev, A.; Rudiger, V.; Raevsky, O. A. *Pure Appl. Chem.* **1993**, *65*, 2329-2334. i) Andres, A.; Burguete, M. I.; Garcia-Espana, E.; Luis, S. V.; Miravet, J. F.; Soriano, C. *J. Chem. Soc., Perkin Trans. 2* **1993**, 749-755. j) Bencini, A.; Bianchi, A.; Giorgi, C.; Paoletti, P.; Valtancoli, B.; Fusi, V.; Garcia-Espana, E.; Llinares, J. M.; Ramirez, J. A. *Inorg. Chem.* **1996**, *35*, 1114-1120. k) Bazzicalupi, C.; Bencini, A.; Bianchi, A.; Fusi, V.; Giorgi, C.; Granchi, A.; Paoletti, P.; Valtancoli, B. *J. Chem. Soc., Perkin Trans. 2* **1997**, *4*, 775-781. l) Bazzicalupi, C.; Beconcini, A.; Bencini, A.; Fusi, V.; Giorgi, C.; Masotti, A.; Valtancoli, B. *J. Chem. Soc., Perkin Trans. 2* **1999**, *8*, 1675-1682. m) Menger, F. M.; Catlin, K. K. *Angew. Chem., Int. Ed. Engl.* **1995**, *34*, 2147-2150. n) Hartley, J. H.; James, T. D.; Ward, C. J. *J. Chem. Soc., Perkin Trans. 1* **2000**, 3155-3184. o) Powell, D.; Bowman-James, K. *Coord. Chem. Rev.* **2003**, *240*, 57-75. o) Chu, F.; Flatt, L. S.; Anslyn, E. V. *J. Am. Chem. Soc.* **1994**, *116*, 4194-4204. p) Flatt, L. S.; Lynch, V.; Anslyn, E. V. *Tetrahedron Lett.* **1992**, *33*, 2785-2788. q) Tohda, K.; Tange, M.; Odashima, K.; Umezawa, Y.; Furuta, H.; Sessler, J. L. *Anal. Chem.* **1992**, *64*, 960-964. r) Furuta, H.; Magda, D.; Sessler, J. L. *J. Am. Chem. Soc.* **1991**, *113*, 978-985
- ⁴ Das, G.; Onouchi, H.; Yashima, E.; Sakai, N.; Matile, S. *ChemBioChem.* **2002**, *3*, 1089-1096.
- ⁵ a) Kelly, T. R.; Kim, M. H. *J. Am. Chem. Soc.* **1994**, *116*, 7072-7080. b) Yeo, W.; Hong, J. *Tetrahedron Lett.* **1998**, *39*, 3769-3772. c) Gale, P. A. *Coord. Chem. Rev.* **2000**, *199*, 181-233
- ⁶ a) Tobey, S. L.; Anslyn, E. V. *Org. Lett.* **2003**, *5*, 2029-2031. b) Tobey, S. L.; Jones, B. D.; Anslyn, E. V. *J. Am. Chem. Soc.* **2003**, *125*, 4026-4027. c) Tobey, S. L.; Anslyn, E. V. *J. Am. Chem. Soc.* **2003**, *125*, 14807-14815
- ⁷ Bouzide, A.; Sauve, G. *Org. Lett.* **2002**, *4*, 2329-2332
- ⁸ Cabezon, B.; Cao, J.; Raymo, F. M.; Stoddart, J. F.; White, A. J. P.; William, D. J. *Chem. Eur. J.* **2000**, *6*, 2262-2273
- ⁹ Connors, K. A. *Binding Constants*, John Wiley and Sons, New York **1987**

Chapter 3: The Successful Application of Differential Receptors in the Recognition of Phosphorylated Peptides

3.1 Introduction

Effort to mimic nature's protein-based receptors especially for those with high molecular weights using small synthetic analogs is of great difficulty due to the complexity of three-dimensional protein structures, and the lack of knowledge for prediction of protein folding. Down-graded peptide recognitions are therefore more essential in chemical biology and drug discovery research for their abilities of providing fundamental information in close relation to complicated protein interactions.¹

One of the keys to selective recognition using synthetic hosts is the ingenious design of hydrogen bonding, hydrophobic and ionic interactions, as well as steric effects, between the host and guest molecules. Early work by Still used cyclic receptor structures developed for apolar solvents, and bound to di- and tripeptides in an impressively, albeit unpredictably, sequence- or stereoselective fashion.² Since then, the development of synthetic receptors for specific amino acid sequences under physiological conditions has been focused to be a challenging task for researchers in the field of molecular recognition. Although considerable progress has been achieved in designing artificial receptors for small biomolecules, including most amino acids, the task of sequence-specific amino acid recognition in peptides still poses a severe problem. For example, an

efficient host for oligopeptides must be able to distinguish the consecutive order of side chains.³

Chemical sensing of small peptides would be typically approached by the creation of highly selective receptors for each component to be detected within a complex mixture. However, it is difficult and synthetically prohibitive to design selective receptors for each of a potentially vast number of peptide targets. An alternative approach is to create devices that rely on a series of chemo- or biosensors, where analysis of complex mixtures arises from patterns produced by the combined response of all the sensors in the array.⁴ This “differential sensing” approach has been particularly successful for vapor-phase analysis.⁵ Patterns can also be created that are diagnostic for single analytes.⁶

Phosphorylated peptides and phosphoproteins, which regulate cellular functions, are examples of important and challenging target molecules in supramolecular chemistry because of their importance in biological and environmental settings.⁷ However, the large size of phosphate as an anion, and its high hydrophilicity, placed it at the bottom of Hofmeister selectivity (hydration energy) series: $\text{ClO}_4^- > \text{IO}_4^- > \text{CN}^- > \text{F}^- > \text{I}^- > \text{Cl}^- \sim \text{Br}^- \sim \text{OAc}^- > \text{NO}_3^- > \text{HCO}_3^{2-} > \text{SO}_4^{2-} > \text{H}_2\text{PO}_4^-$. As a result, phosphate is one of the most challenging of anionic targets. Thus, receptors providing multiple interactions have been designed to increase the bind affinity to phosphate and organophosphates. However, the overwhelming majority of these receptors utilized organic solvents as the detection media because they rely on hydrogen-bonding and electrostatic interactions for the recognition of analytes. Unfortunately, the strength of these interactions will decrease drastically in a highly polar media such as water, because of the competing solvation effect. Selective

anion sensing is likely to result mainly from selective anion binding, engineered by complementarity of host-guest charge and shape.⁸

The strategy in this chapter had been popularized for sensing builded on the notion of differential binding, a core receptor is designed containing one or more functional groups, to establish an affinity for a particular analyte class. Functional groups include basic or acidic moieties for ion-pairing, heteroatoms for metal coordination, and shape selective scaffolds. Proximally appended from the core are differential binding moieties, such as peptide chains, that can be readily varied between the receptors. In this type of system, receptors are designed to target particular classes of analytes, but not necessarily designed to be selective for any specific analyte. The array's selectivity is manifested from the collective response of the differential receptor ensemble to an analyte or mixtures of analytes. Introduction of an analyte to the array of differential receptors produces a unique "pattern" based upon the composite cross-reactive response. Chemometric methods make pattern identification facile by reduction of the response data.⁹ In combination with chemometric tools, a single differential receptor array can potentially discriminate multiple analytes without requiring the design of specific receptors.

The arising need of solution-based analysis using differential synthetic receptor arrays for environmental pollutants testing, on-line process monitoring, and medical diagnostics, requires the progress in fundamental analyses of simple analytes, to complex bioanalytes, and ultimately to complicated mixtures in natural media¹⁰

Parkinson's disease (PD) belongs to a group of conditions called motor system disorders, which are the result of the loss of dopamine-producing brain cells. Recent research has discovered that the protein Filamentous R-synuclein, in those disease brains is extensively phosphorylated at Ser129 (**Scheme 3.1**).¹¹ With the estimate protein in mind as a target, three tripeptides and their phosphorylated Serine analogs were particularly studied by using new developed a set of receptors bearing a metalloligand core (**Figure 3.1**), and make it to differential receptors by appending tripeptide arms. Unique patterns created by the analytes were identified and analyzed using multivariate analytical tools.¹²



Scheme 3.1 Sequences in protein Filamentous R-synuclein

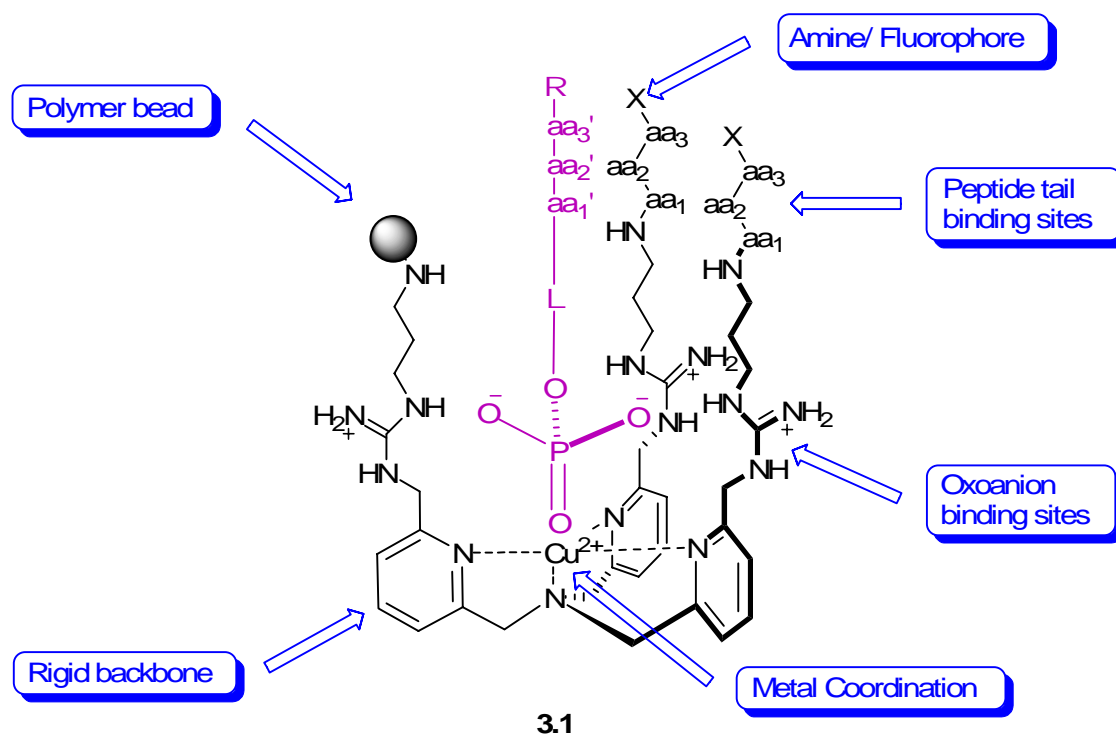


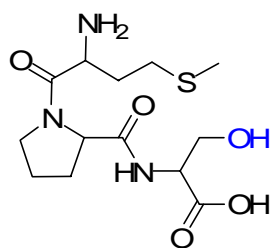
Figure 3.1 Metalloligand core

3.2 Results and discussions

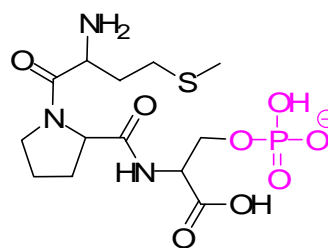
3.2.1 Peptide synthesis

To determine whether these receptors could differentiate between peptides and phosphorylated derivatives, the Filamentous R-synuclein protein sequence (described previously) was targeted, specifically in the region near Ser-129, to design peptides for this study.

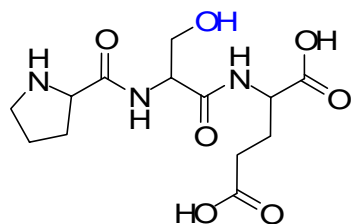
Truncated tripeptides (MPS, PSE and SEE) and derivatives in which serine in these peptides was phosphorylated (MPS(P), PS(P)E and S(P)EE), were synthesized on solid phase using 2-Cl Trityl chloride resin¹³ and TGR resin (**Figure 3.2**).¹⁴



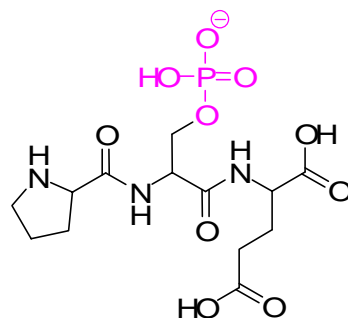
MPS
3.2



MPS(P)
3.3



PSE
3.4



PS(P)E
3.5

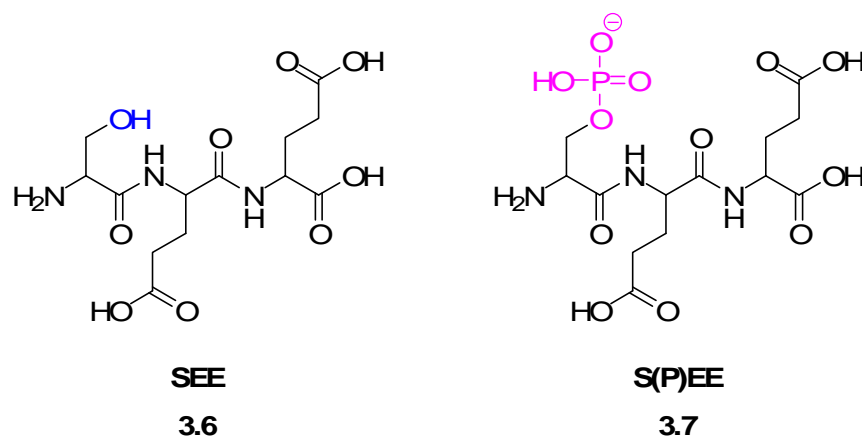
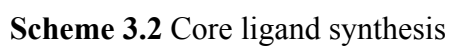


Figure 3.2 Selectively synthesized tri-peptides

3.2.2 Differential receptors' core ligand synthesis

The synthesis of core ligand started with previous reported compound **3.8**,¹⁵ mono-t-Boc protection of one of three primary amino groups (compound **3.9**) was afforded effectively by using boc-on (2-(Boc-oxyimino)-2-phenylacetonitrile).¹⁶ Fmoc and alloc protected thiourea compound **3.10** was then applied on generation of compound **3.11** with two Alloc protected guanidinium groups. Deprotection of t-Boc and addition of t-Boc and alloc protected thiourea compound **3.12** followed by another deprotection of t-Boc group would give us compound **3.13** as protected core ligand of differential receptors.



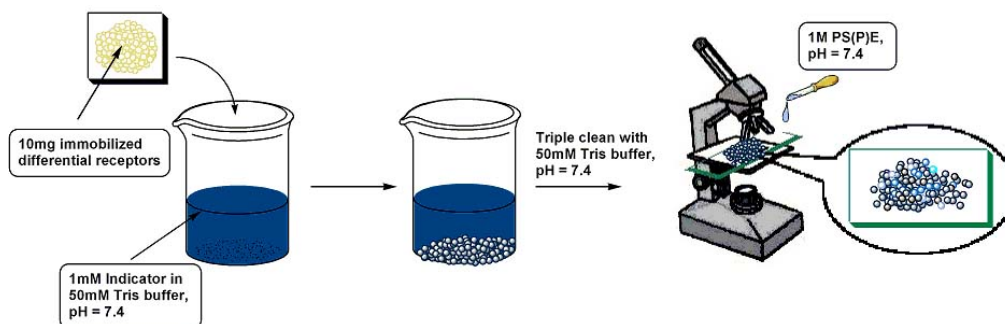
Differential receptors' screening for their affinities to targeted tripeptides is essential because with different amino acid combinations, it would be difficult to predict the desired group of receptors for these target molecules. Combinatorial solid phase

differential receptor synthesis,¹⁷ however, offers a facile way to obtain large varieties of receptors. Among these, a designed experiment screening process is able to provide clued receptors for further solution phase synthesis that will be applied in real recognition studies. Thus, Split-and-Pool synthesis technology was applied in obtaining differential receptors that are immobilized on NovaSyn TG resin, where 19 amino acids except for cysteine were chosen to build up the tripeptide arms on the top of ligand core.

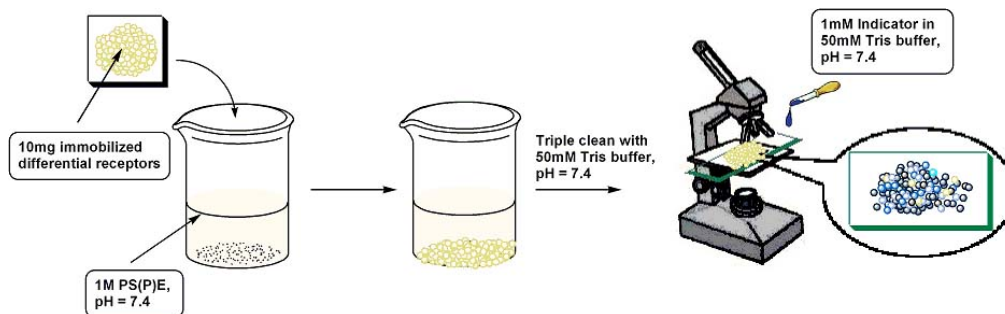
In the following screening step after the receptors are obtained, two methods were applied on arbitrary and practical receptor selections in order to collect optimized receptors.

PS(P)E and PSE couple were chosen here for the screening because serine was the middle amino acid in this tripeptide, which would generate the largest steric effect upon associating to the core ligand molecule among the three, even it was still a primary phosphate.¹⁸ As a result, consider the phosphate moiety only, the differential receptors screened using PS(P)E would also be able to bind to less steric MPS(P) and S(P)EE, on the hypothesis that the core ligand in these differential receptor system design would play an essential role in the recognition of phosphorylated tripeptides over those regular tripeptides.

Method 1:



Method 2:



Scheme 3.3 Screening methods

Method 1: Obtaining receptor resins initially having relatively strong interactions with the indicator. In this method, two pieces of information can be obtained: 1. whether the particular receptor has strong interaction with the indicator; 2: whether this particular resin has higher surface receptor concentration.

In this method, the immobilized receptor resins (10 mg) were soaked for twenty minutes in an indicator solution (1mM in Tris buffer (50 mM at pH=7.4)). After subsequently washing steps, 20 resins which displayed a significant degree of indicator

uptake were arbitrarily selected and placed under the microscope. PS(P)E (1 M, much higher in concentration in comparison to other components was to perform quick competition displacement reaction due to high resin surface concentration (1-5 M)) was also prepared in TRIS buffer (pH=7.4, 50mM). Three drops of peptide solution were placed on the glass plate. Within 10 minutes, ten lighter beads, which indicate stronger peptide competitions, were randomly selected out and characterized via Edman degradation.

Method 2: Obtaining receptor resins initially having relative strong interactions with the tripeptide. Theoretically, three pieces of information can be postulated: 1. this receptor has strong interaction with the tripeptide; 2. this resin has a low surface receptor concentration that is not able to uptake more tripeptide; 3. this complimentary method also excludes the possibility that on a particular resin, this arbitrarily chosen indicator exhibits much stronger interaction than the tripeptide, even though this receptor could be a good candidate for differentiation.

Immobilized receptors (10 mg) were soaked into PS(P)E solution (1M) in TRIS (pH=7.4, 50mM). After 20 minutes, the solution was removed and the beads were placed onto a glass plate. A few drops of 1mM indicator solution prepared in TRIS buffer (pH=7.4, 50mM) were washed and placed on to the glass plate and stood for ten minutes. Five light beads were randomly chosen for Edman degradation.

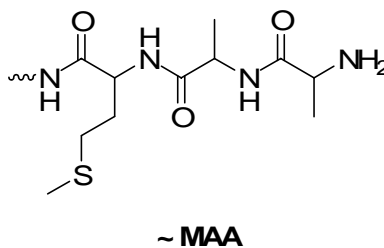
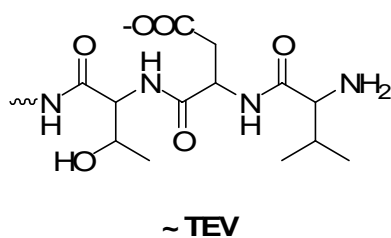
These fifteen immobilized receptors combined from two methods were performed by Edman Degradation followed by the mass spectrometry analysis. Fourteen out of fifteen receptors were successfully characterized and shown in **Table 3.1**, where the very

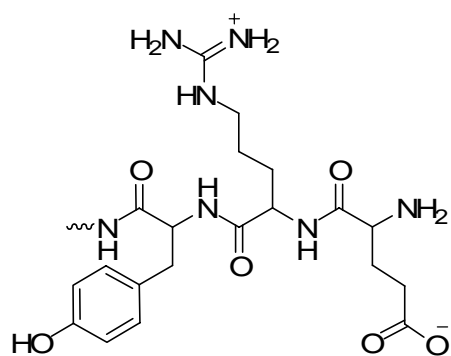
left amino acids were those that connected to the core ligand (compound **3.13**). The resolved sequences display several similarities which are detailed as follows (**Figure 3.3**):

1. Almost all of the sequences except (MAA) had at least one amino acid with a polar functional group. These groups would serve as hydrogen bonding donors and acceptors that facilitate the binding events; 2. Many sequences contained amino acids with non-polar side chains. These could be explained by a hydrophobic effect contributing in the guest molecule association. The nonpolar end groups generated an entropic favorable pocket that would further enhance binding.

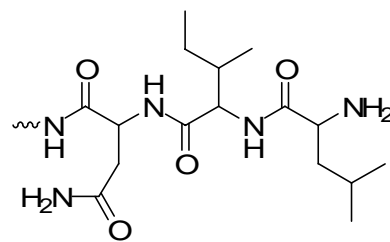
Table 3.1 Peptide sequences identified by Edman Degradation mass spectrometry

Identified tripeptides
~TEV, ~YVP, ~MAA, ~NIL, ~DFF, ~RLL, ~YRE, ~EDP, ~YDP, ~KDK, ~QTP, ~FDE, ~IRP, ~ESP

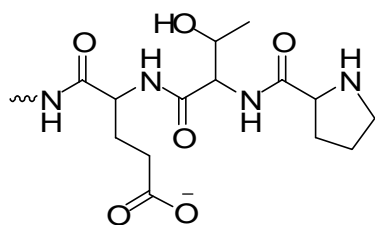




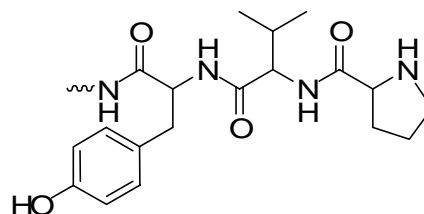
~ YRE



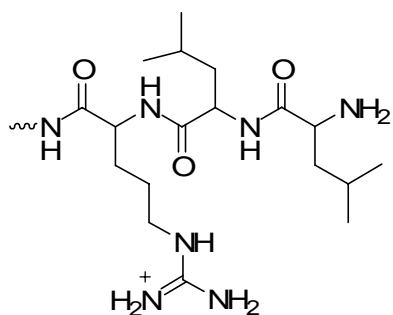
~ NIL



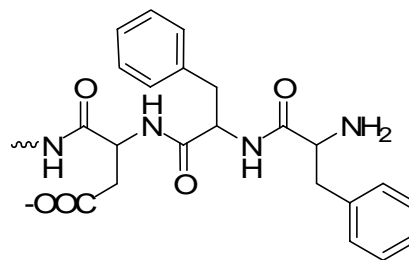
~ QTP



~ YVP



~ RLL



~ DFF

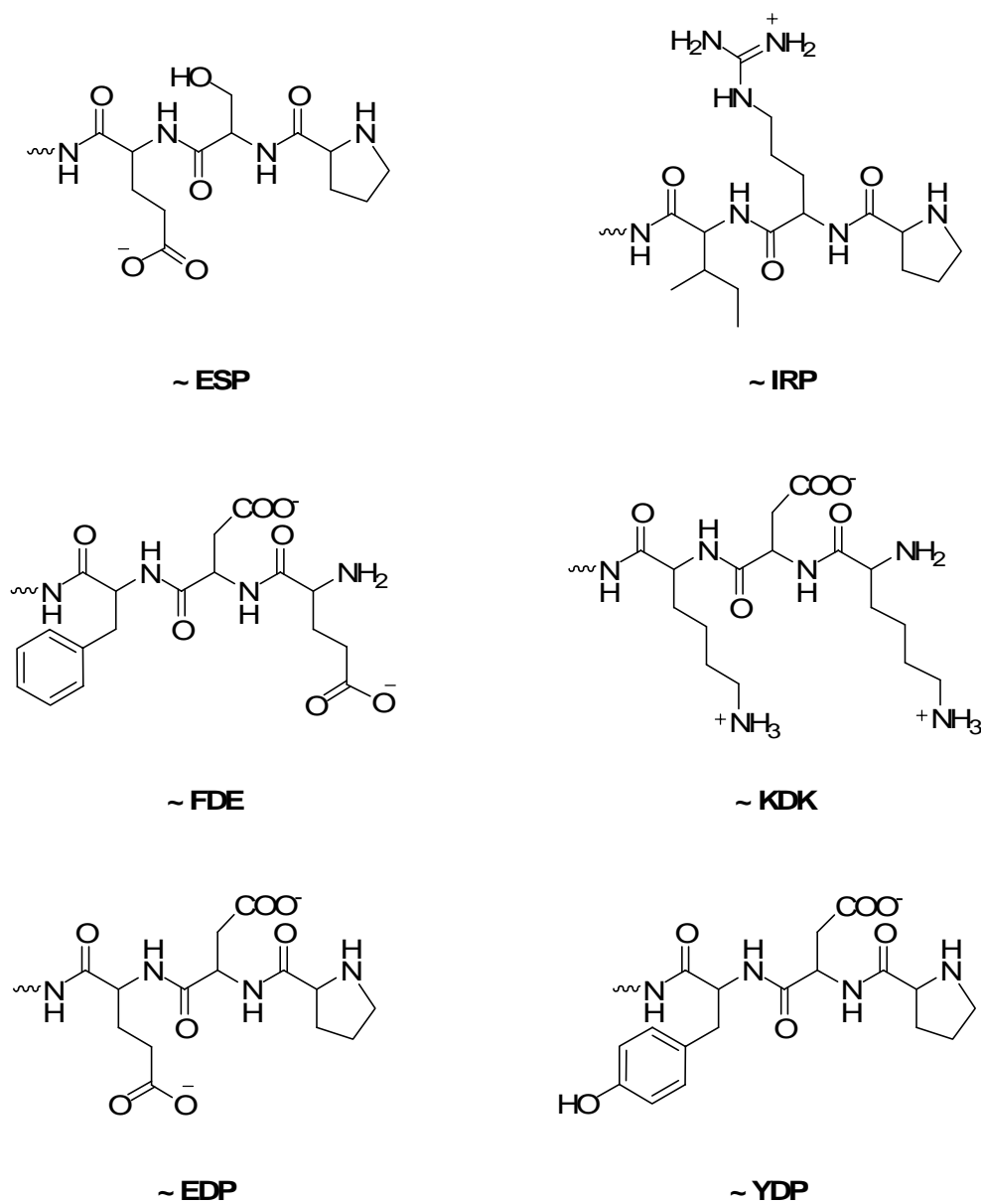


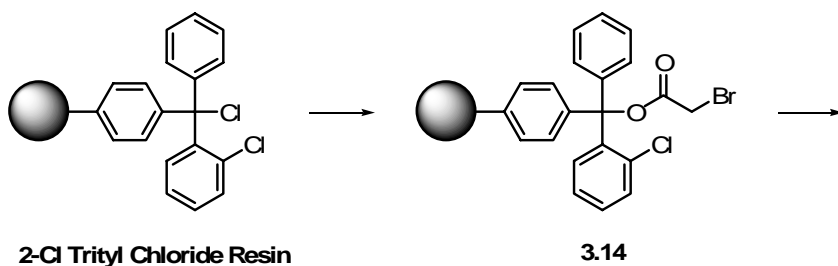
Figure 3.3 Mass spectrometry characterized tripeptides

Five tripeptides (TEV, RLL, YRE, KDK, YDP), representative of this set of receptors, were chosen to as the peptidic side chains of the differential receptors for the

solution-based assays taking the advantage of high-throughput, multifunctional microarray studies using 96-well plate reader.

3.2.4 Solution based differential receptors synthesis

The 2-Cl Trityl chloride resin was chosen for solution based receptor synthesis (**Scheme 3.4**). In order to connect the core ligand (compound **3.13**) to resin, the trityl resin had to be derivatized (compound **3.14**) using bromo-acetic acid.¹⁹ Potassium carbonate was used as base in the core ligand (compound **3.13**) substitution step to afford compound **3.15**. The Fmoc protection groups were then removed to free up terminal amino functionalities for further peptide additions (compound **3.16**). Three amino acids were then extended on the functionalized resin in a specific order to afford compound **3.17**. Deprotecting the Fmoc and Alloc groups²⁰ and followed by TFA cleavage, solution based differential receptor (compound **3.18**) was obtained after precipitating in ice-cold diethyl ether and lyophilization.





Scheme 3.4 Differential receptor synthesis

3.2.5 Metal and indicator screening

Metal and indicator screenings are also very important in this differential receptor system design, because their applications would provide a very efficient and economic pathway to increase the diversities of receptor combinations.

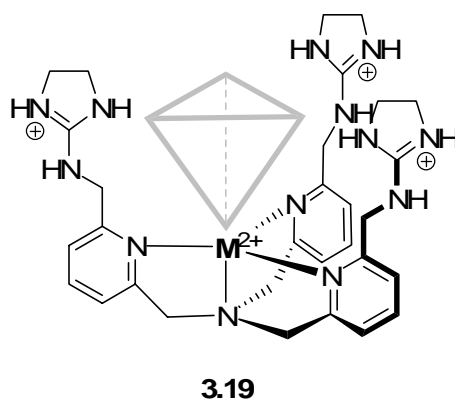


Figure 3.4 Model core ligand

For the purpose of simplicity and less expense, a model core ligand (**Figure 3.4**) was used,¹⁸ reported in a previous study, and phosphor-serine (**Ser(P)**) in screening various indicators and metals.

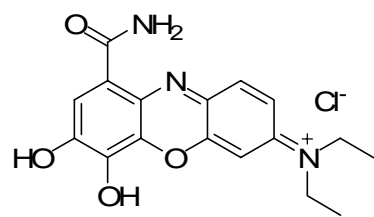
The criteria on choosing metals and indicators are:

1. Metal selection

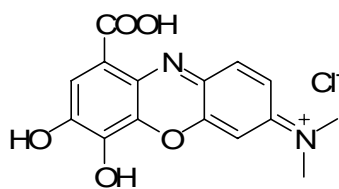
Based on the previous core ligand study,¹⁵ in which cupric ion was observed the strongest and most sturdy coordination center, the metal choice was spreaded out through the metals in the same series and groups: a. The metals should have potentials in forming dative bonds with nitrogen to build up a rigid backbone; b. The metals chosen from same series and groups could easily offer size, charge, coordination preference differentiations in pattern recognition. Cr^{3+} , Mn^{2+} , Fe^{2+} , Fe^{3+} , Co^{2+} , Ni^{2+} , Cu^{2+} , and Cd^{2+} are then selected that likely to have the similar but not exactly the same coordination activities. In order to achieve experimental comparability, only metal chloride salts are used in the study.

2. Indicator selection

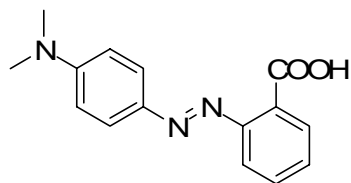
Since indicator displacement assay (IDA) technology was applied in this differential receptor system design, the choice of indicators requires moderate interaction between indicator and the receptor. Thus, the indicators with capable of nitrogen coordinations are excluded. Also, the choice of indicators will be avoided using functional groups that are similar as the targeted analytes, such as phosphate and arsenate moieties that will cause severe competitions in the recognitions. As result, methyl red, fluorescein, alizarin complexone, pyrocatechol violet, celestine blue, pyrogallol red, alizarin red S, mordant orange 1, gallocyanine are chosen due to their readily available in the lab (**Figure 3.5**).



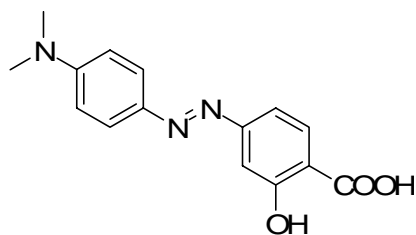
Celestine blue



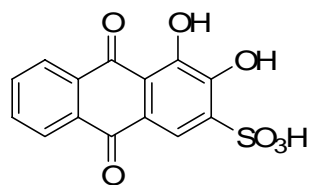
Galocyanine



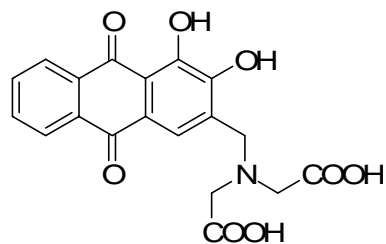
Methyl red



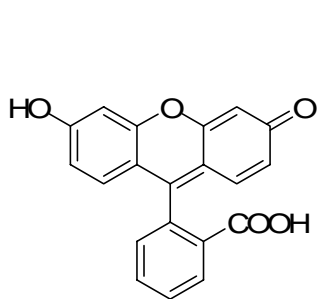
Mordant orange 1



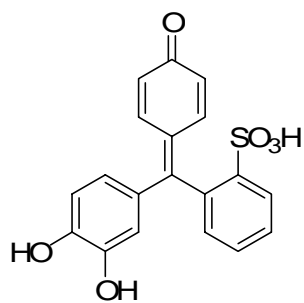
Alizarin red S



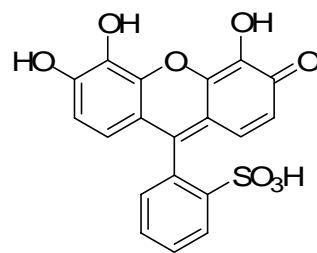
Alizarin complexone



Fluorescein



Pyrocatechol violet



Pyrogallol red

Figure 3.5 Indicators structures

Solutions of eight transition metals and nine indicators are prepared respectively in TRIS buffer (pH=7.4, 50mM): $[M^{n+}] = 0.2\text{mM}$, $[\text{In}] = 0.1\text{mM}$, $[\text{LG}_1] = 0.2\text{mM}$, $[\text{Ser(P)}] = 1.0\text{mM}$. Two 96 well plates were then set up exactly the same: 72 wells out of 96 were used, each well contained one of 72 (metal 8×indicator 9) combinations (50μl M^{n+} , 100μl In, and 50μl LG_1) (**Figure 3.6**).

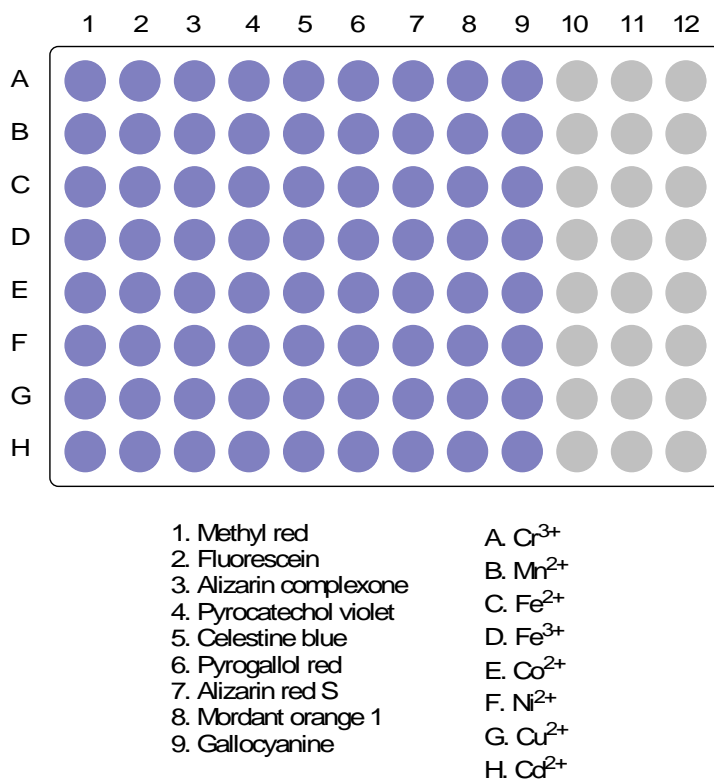
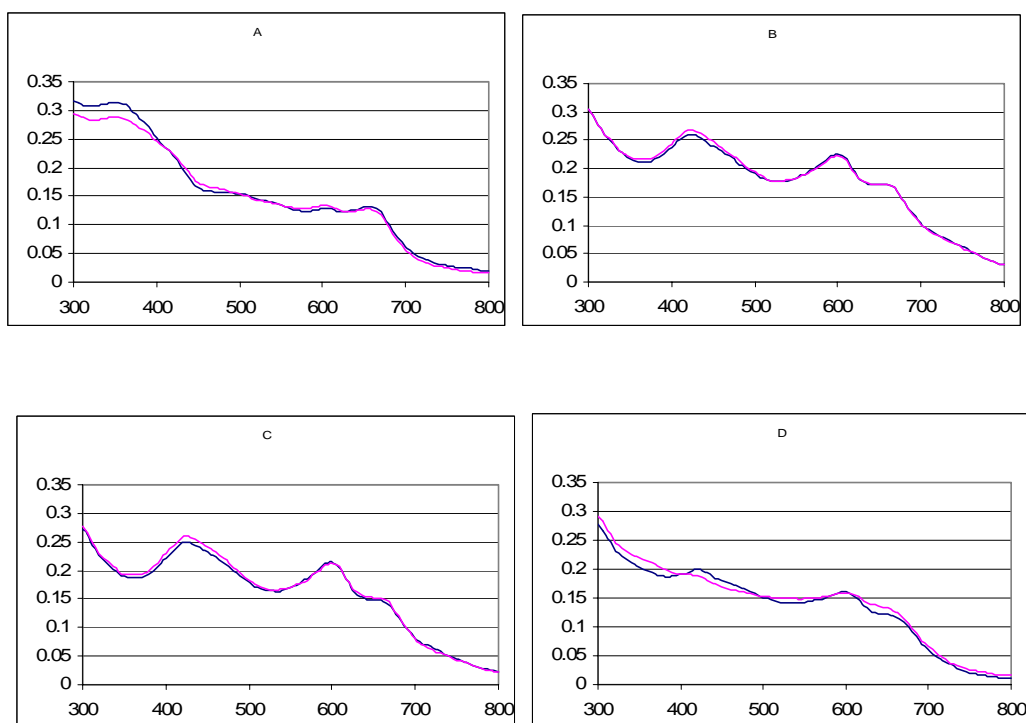


Figure 3.6 Metal and indicator screening preparation. Conditions: Total volume in each well is 300μl: Plate #1: $[M^{n+}] = [\text{In}] = [\mathbf{3.19}] = 0.03\text{mM}$, $[\text{Ser(P)}] = 0.3\text{mM}$; Plate #2: $[M^{n+}] = [\text{In}] = [\mathbf{3.19}] = 0.03\text{mM}$. $[\text{Tris}] = 50\text{ mM}$, pH = 7.4, 25 °C

In one of the plates, 100 μ l Ser(P) was added in each well; the other plate was added 100 μ l buffer instead to maintain the same metal, indicator and receptor concentration. UV-Vis absorbance was collected by 96-well plate reader and plotted through a range from 300 nm to 800 nm (**Figure 3.7, 3.8 and 3.9**). Two indicators (methyl red and mordant orange 1) and one metal were ruled out because they either precipitated in the experiment condition or observed little to no spectral modulation.



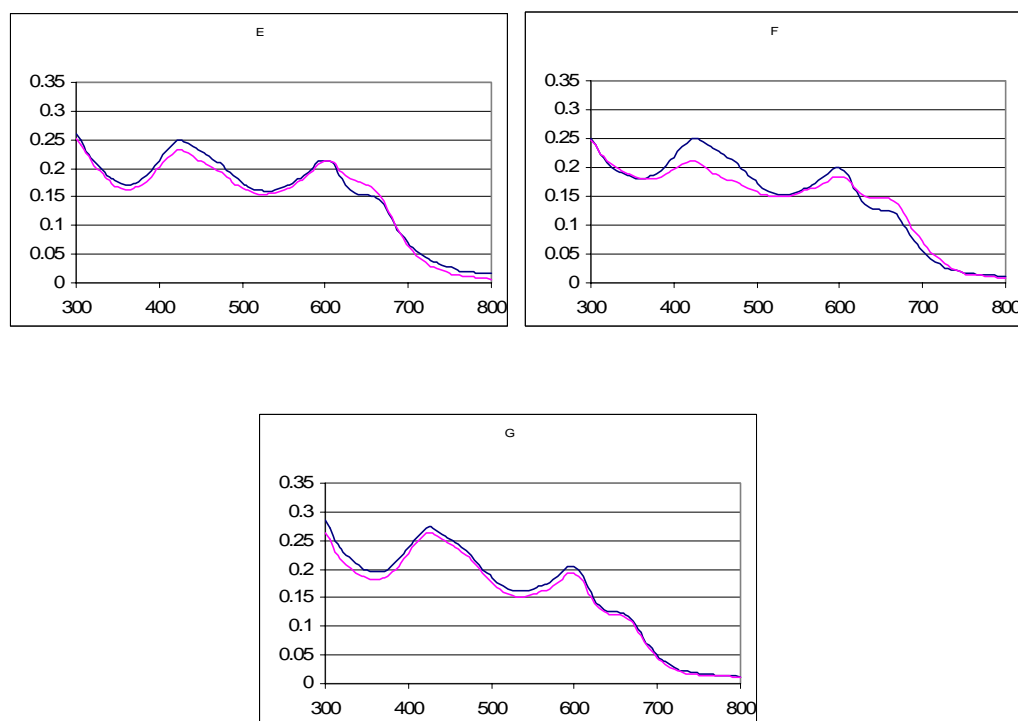
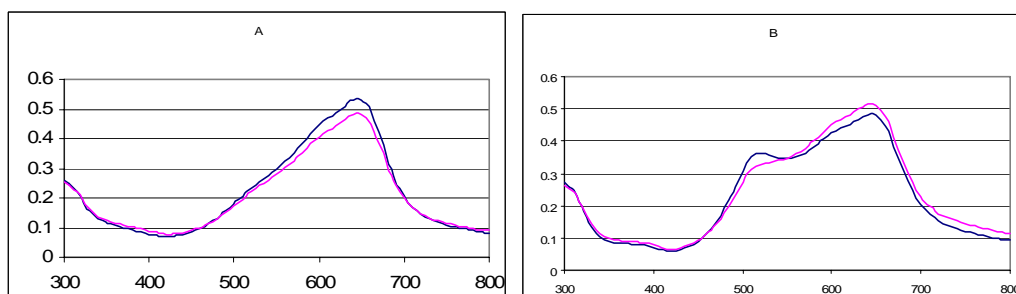


Figure 3.7 UV-Vis absorbances captured by 96-well plate reader in metals and pyrocatechol violet screening using Ser(P) vs. Blank. A. Cr^{3+} ; B. Mn^{2+} ; C. Fe^{2+} ; D. Fe^{3+} ; E. Co^{2+} ; F. Ni^{2+} ; G. Cu^{2+} . Conditions: Total volume in each well is 300 μl : Plate #1 (blue): $[\text{M}^{n+}] = [\text{pyrocatechol violet}] = [\mathbf{3.19}] = 0.03\text{mM}$, $[\text{Ser(P)}] = 0.3\text{mM}$; Plate #2 (pink): $[\text{M}^{n+}] = [\text{pyrocatechol violet}] = [\mathbf{3.19}] = 0.03\text{mM}$. $[\text{Tris}] = 50\text{ mM}$, Solvent: water, pH = 7.4, 25 $^{\circ}\text{C}$



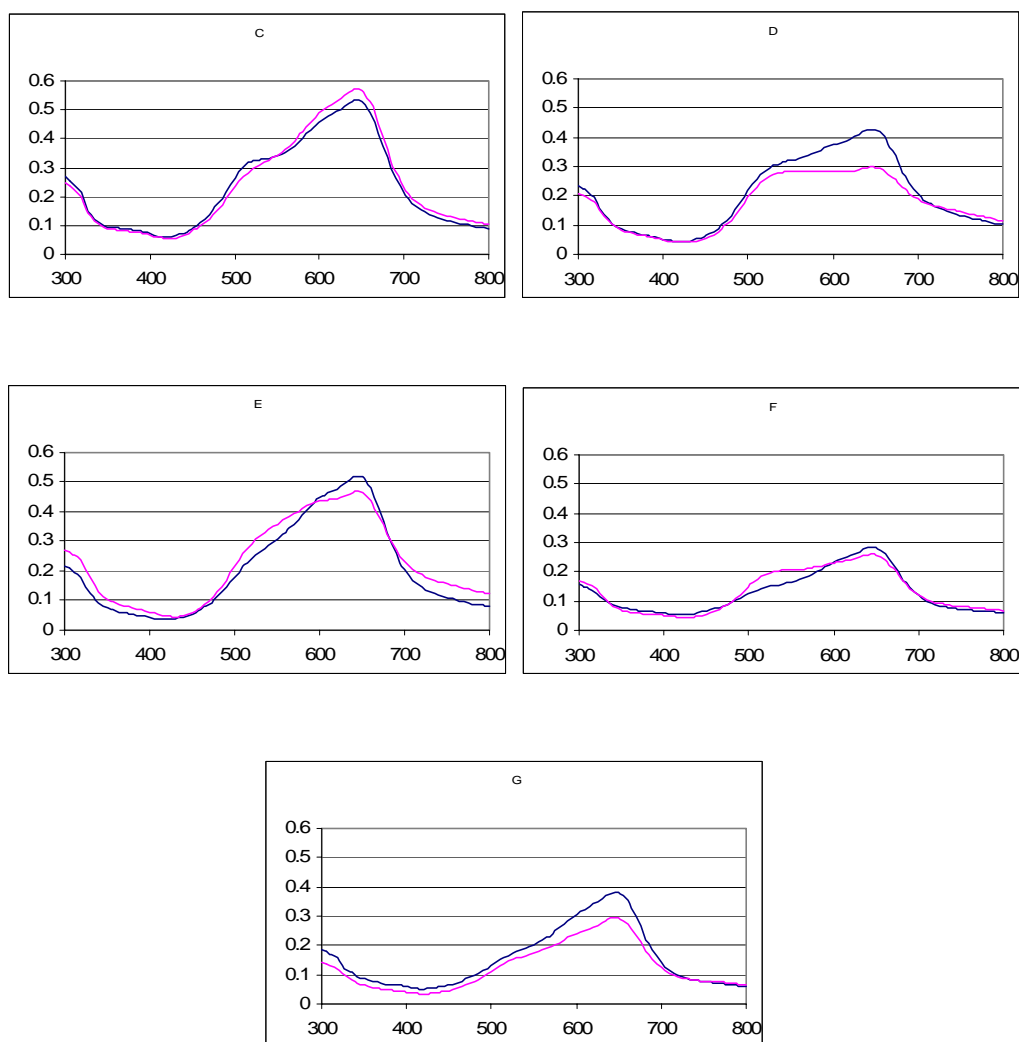


Figure 3.8 UV-Vis absorbances captured by 96-well plate reader in metals and celestine blue screening using Ser(P) vs. Blank. A. Cr^{3+} ; B. Mn^{2+} ; C. Fe^{2+} ; D. Fe^{3+} ; E. Co^{2+} ; F. Ni^{2+} ; G. Cu^{2+} . Conditions: Total volume in each well is 300 μl : Plate #1 (blue): $[\text{M}^{n+}] = [\text{Celestine blue}] = [3.19] = 0.03\text{mM}$, $[\text{Ser(P)}] = 0.3\text{mM}$; Plate #2 (pink): $[\text{M}^{n+}] = [\text{Celestine blue}] = [3.19] = 0.03\text{mM}$. $[\text{Tris}] = 50\text{mM}$, Solvent: water, pH = 7.4, 25 $^{\circ}\text{C}$.

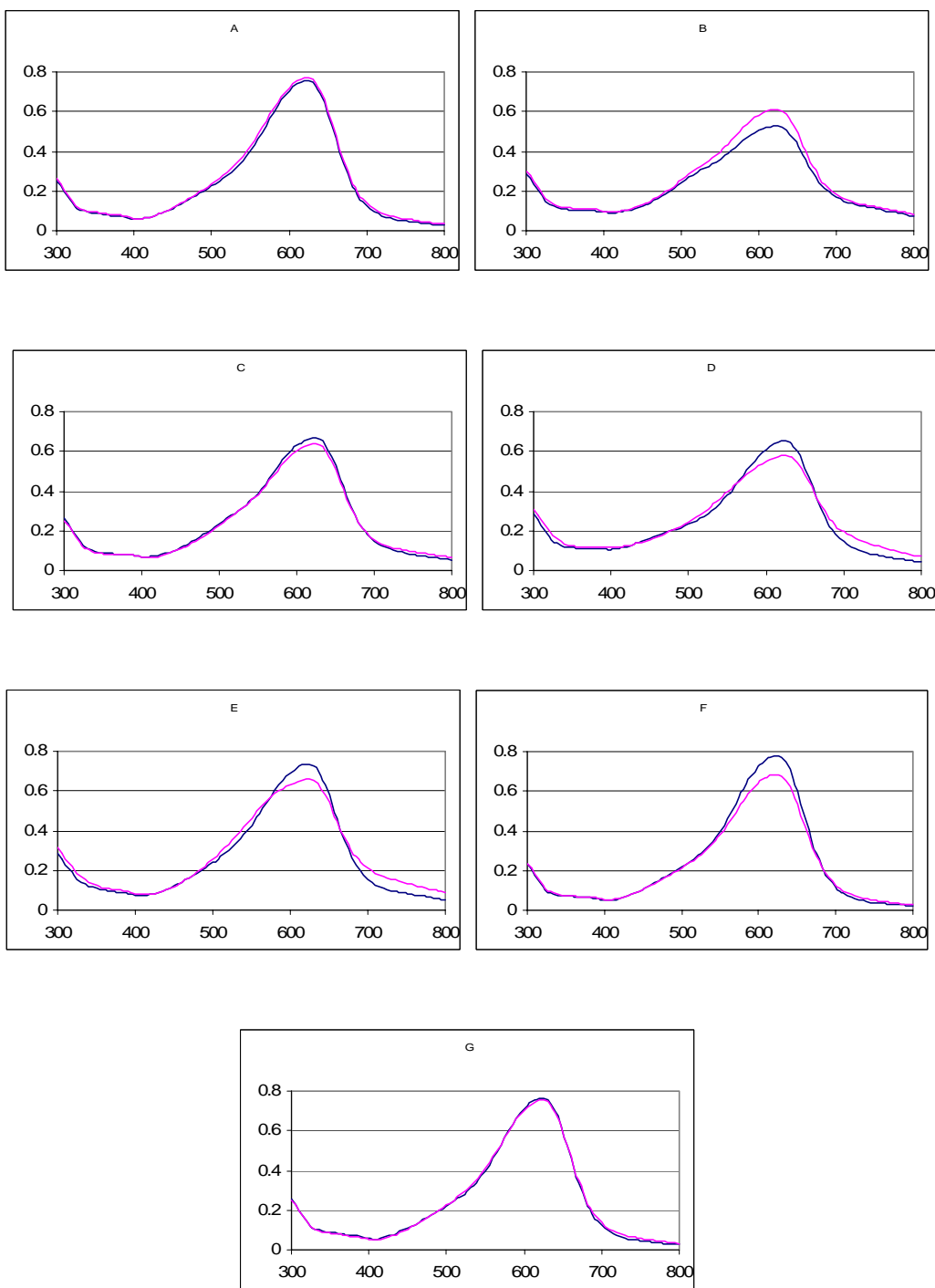


Figure 3.9 UV-Vis absorbances captured by 96-well plate reader in metals and gallocyanine screening using Ser(P) vs. Blank. A. Cr^{3+} ; B. Mn^{2+} ; C. Fe^{2+} ; D. Fe^{3+} ; E. Co^{2+} ; F. Ni^{2+} ; G. Cu^{2+} . Conditions: Total volume in each well is 300 μl : Plate #1 (blue): $[\text{M}^{n+}] = [\text{gallocyanine}] = [\mathbf{3.19}] = 0.03\text{mM}$, $[\text{Ser(P)}] = 0.3\text{mM}$; Plate #2 (pink): $[\text{M}^{n+}] = [\text{gallocyanine}] = [\mathbf{3.19}] = 0.03\text{mM}$. $[\text{Tris}] = 50\text{ mM}$, Solvent: water, pH = 7.4, 25 $^{\circ}\text{C}$.

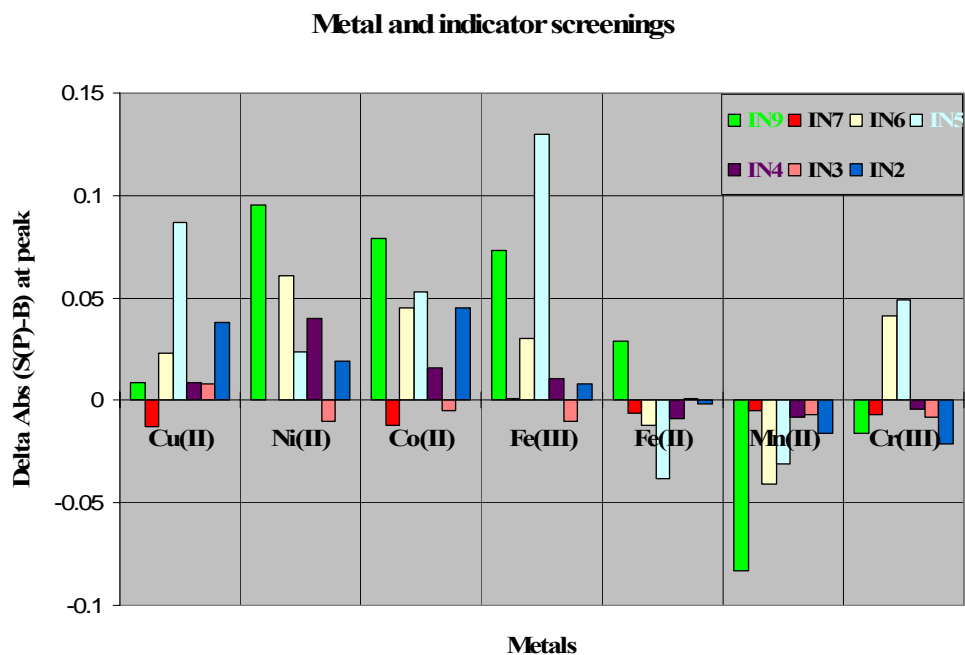


Figure 3.10 UV-Vis absorbance changes (Ser(P) vs. Blank) bar plots in metal and indicator screening. Conditions: Total volume in each well is 300 μl : Plate #1 (Ser(P)): $[\text{M}^{n+}] = [\text{In}] = [\mathbf{3.19}] = 0.03\text{mM}$, $[\text{Ser(P)}] = 0.3\text{mM}$; Plate #2 (Blank): $[\text{M}^{n+}] = [\text{In}] = [\mathbf{3.19}] = 0.03\text{mM}$. $[\text{Tris}] = 50\text{ mM}$, Solvent: water, pH = 7.4, 25 $^{\circ}\text{C}$.

The absorption differences between phosphor-serine and blank with different metals and indicators were plotted in Figure 3.10. By selecting the largest absorbance difference and/or visible color change upon addition of phosphor-serine over pure buffer solution, three metals (Co^{2+} , Ni^{2+} , Cu^{2+}) and two indicators (celestine blue, gallocyanine)

are chosen for array setup. Pyrocatechol violet was also chosen as the third indicator because in the previous study, higher affinity of this indicator to receptor **2.1** was observed when titrated with inorganic phosphate using indicator displacement technology.²¹ With more complicated receptor molecules and phosphates derived in this chapter, it will be more valueable if phosphorylated peptides can efficiently displace this indicator out from receptor pocket. Metals, which were observed negative absorbance changes, were eliminated because those changes were more likely from other complexation phenomina instead of displacing the indicator from the receptor pocket.

3.2.6 Linear discriminant analysis (LDA) studies

After a series of screening processes, peptide modified core ligand, metals and indicators (**Table 3.2**) are selected, combined and employed as differential receptors.

Table 3.2 Optimized differential receptor combinations

Criteria	Modified choices
LG	TEV (LG 1), RLL (LG 2), YRE (LG 3), YDP (LG 4), KDK (LG 5)
Indicator	Pyrocatechol Violet (In 4), Celestine Blue (In 5), Galocyanine (In 9)

M^{2+}	$Co^{2+}, Ni^{2+}, Cu^{2+}$
----------	-----------------------------

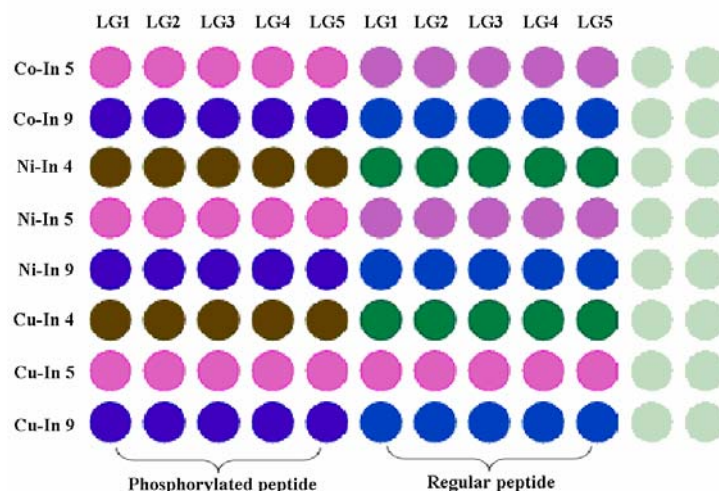
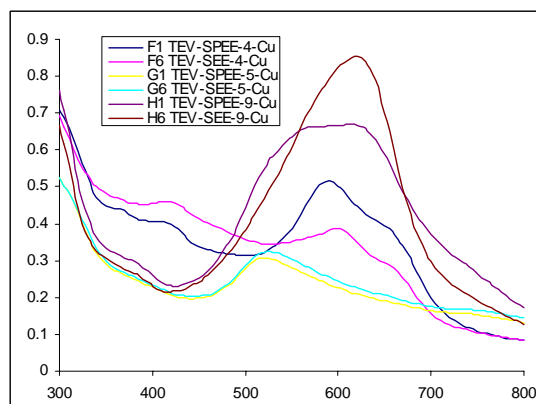
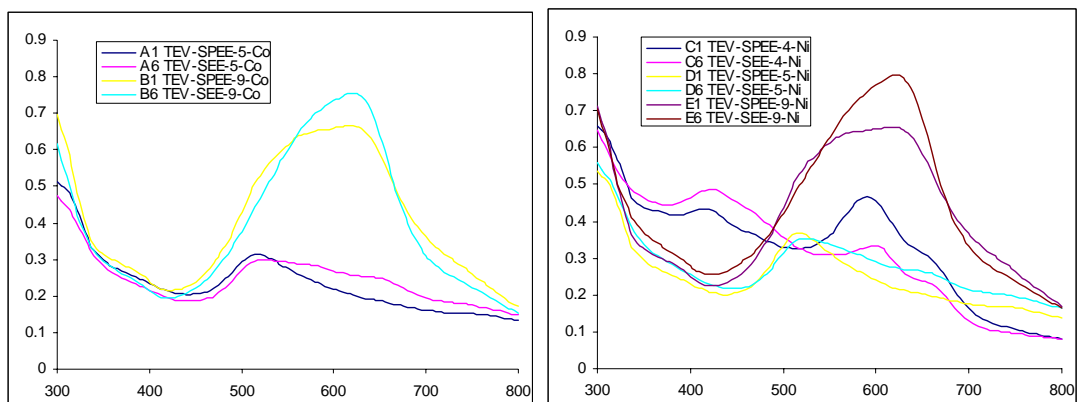
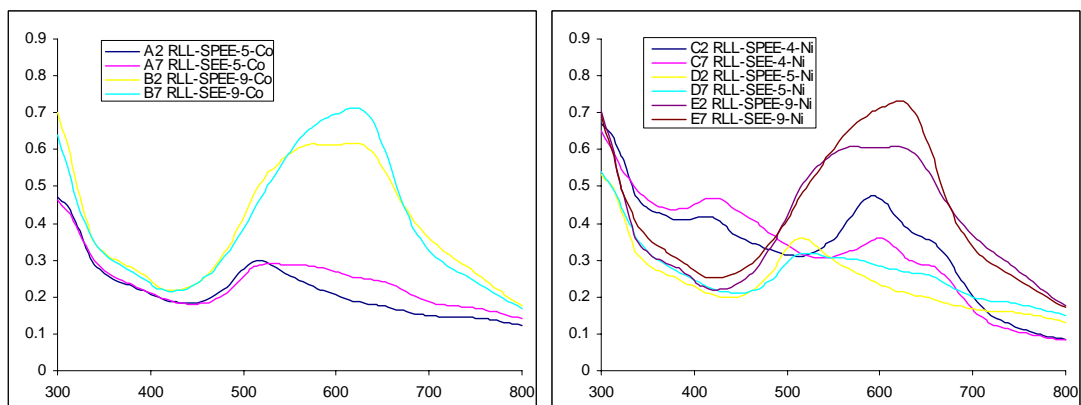


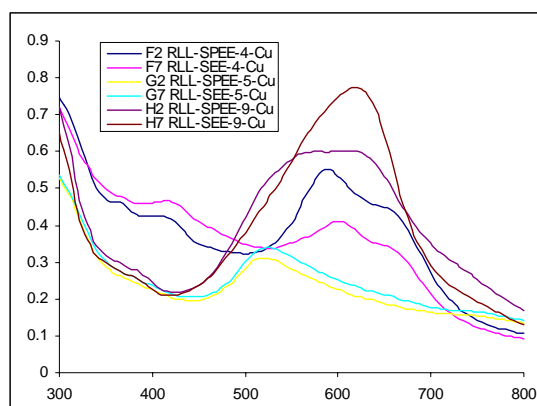
Figure 3.11 A typical simulated colorimetric observation in 96-well plate. Conditions: Total volume in each well is 300 μ l: $[M^{n+}] = [In] = [LG_n] = 0.03$ mM, $[peptides] = 0.3$ mM, $[Tris] = 50$ mM, Solvent: water, pH = 7.4, 25 $^{\circ}$ C.

A typical colorimetric observation in a 96-well plate is shown in **Figure 3.11**. Color change is clearly observed by naked-eye as well as 96-well plate reader. (**Figure 3.12**)

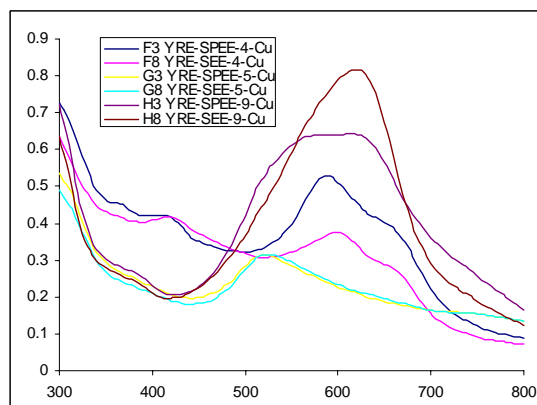
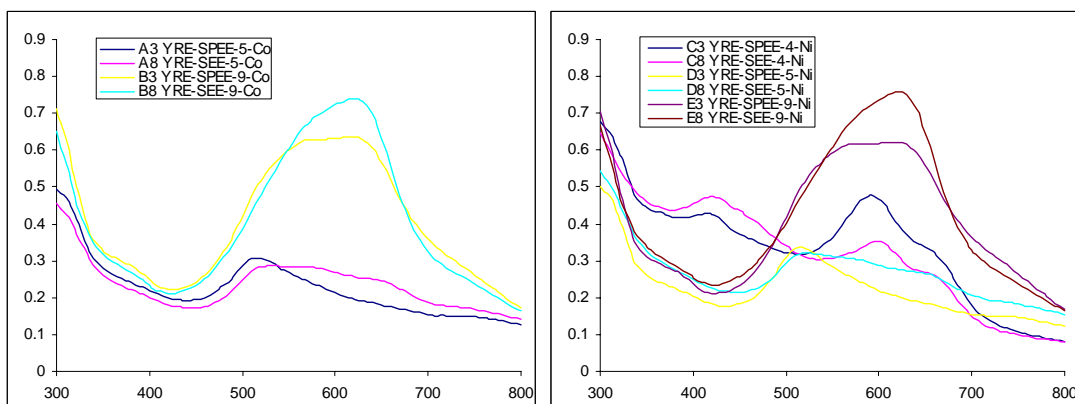


A. Receptor TEV

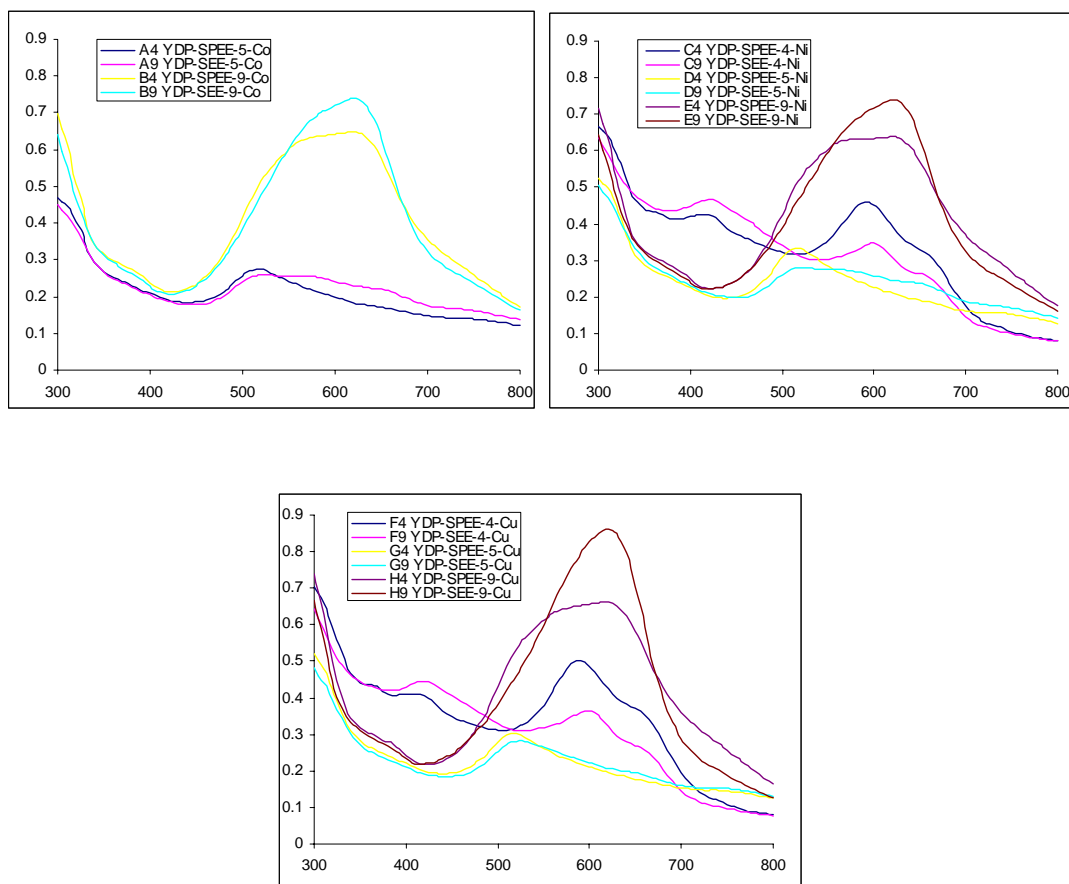




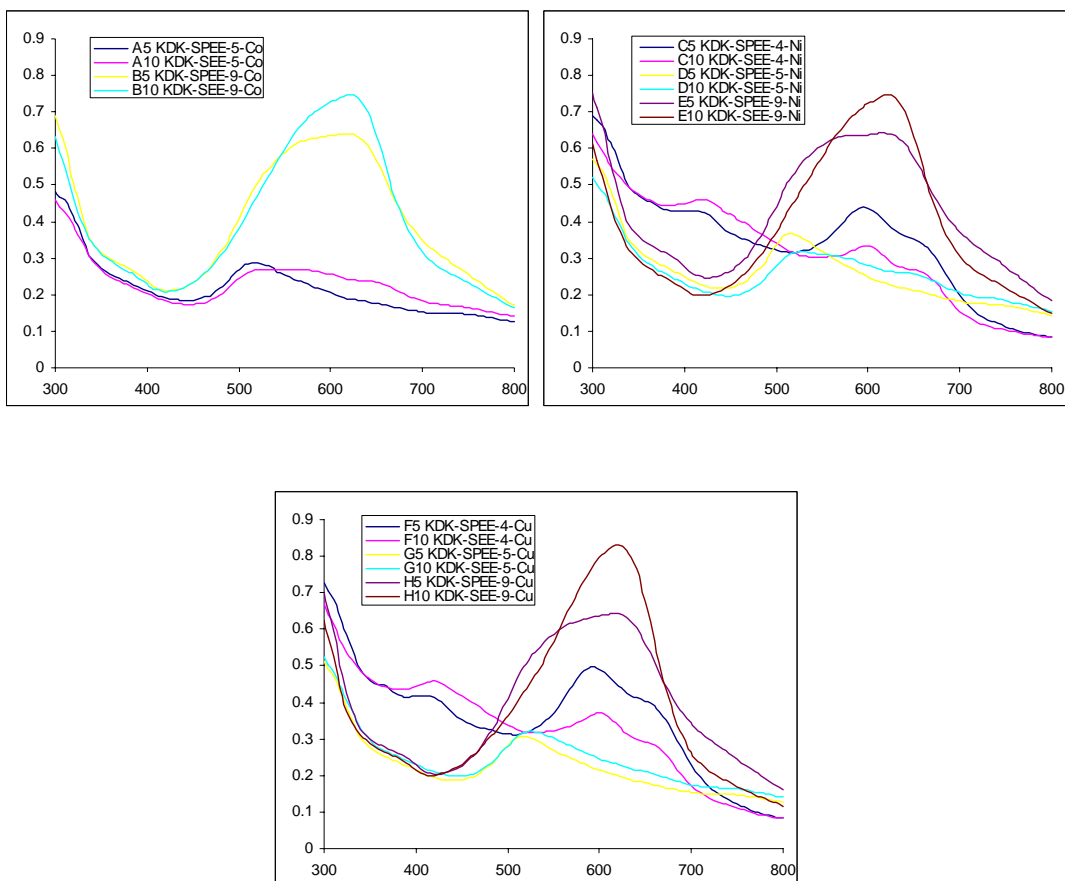
B. Receptor RLL



C. Receptor YRE

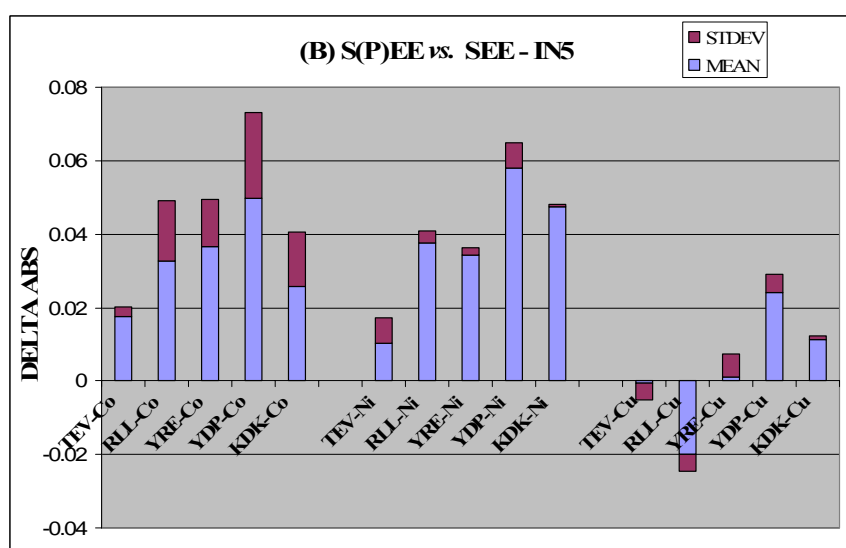
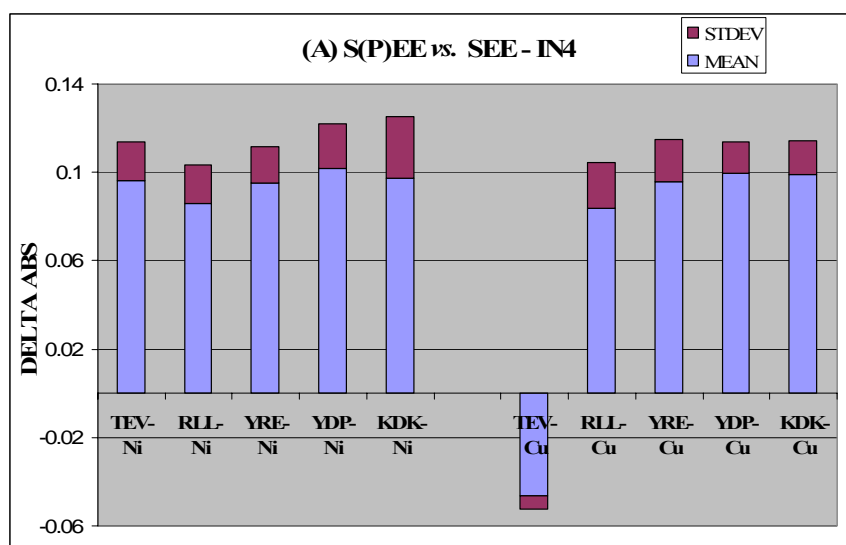


D. Receptor YDP



E. Receptor KDK

Figure 3.12 Example: UV-Vis spectra of S(P)EE/SEE couple with different metallated receptors: A. Receptor TEV (LG 1); B. Receptor RLL (LG 2); C. Receptor YRE (LG 3); D. Receptor YDP (LG 4); E. Receptor KDK (LG 5). Conditions: Total volume in each well is 300 μ l: $[M^{n+}] = [In] = [LG_n] = 0.03$ mM, [peptides] = 0.3mM, [Tris] = 50 mM, Solvent: water, pH = 7.4, 25 $^{\circ}$ C.



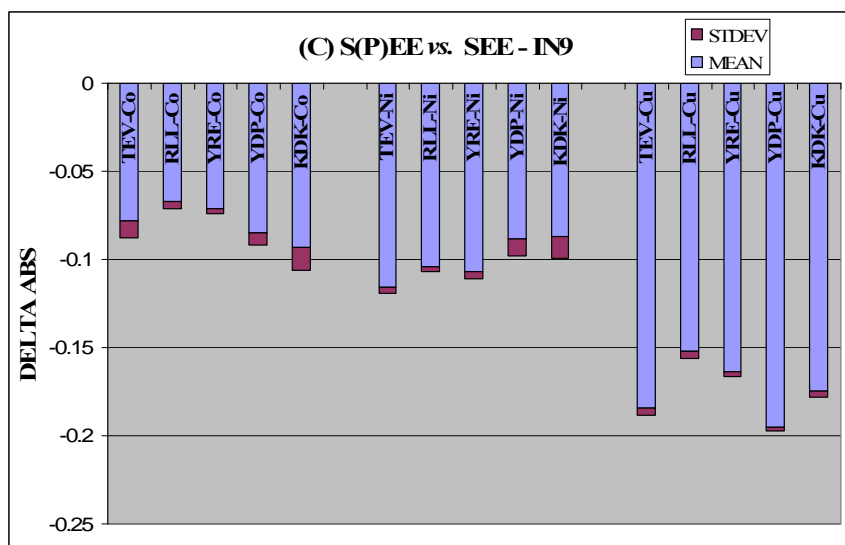
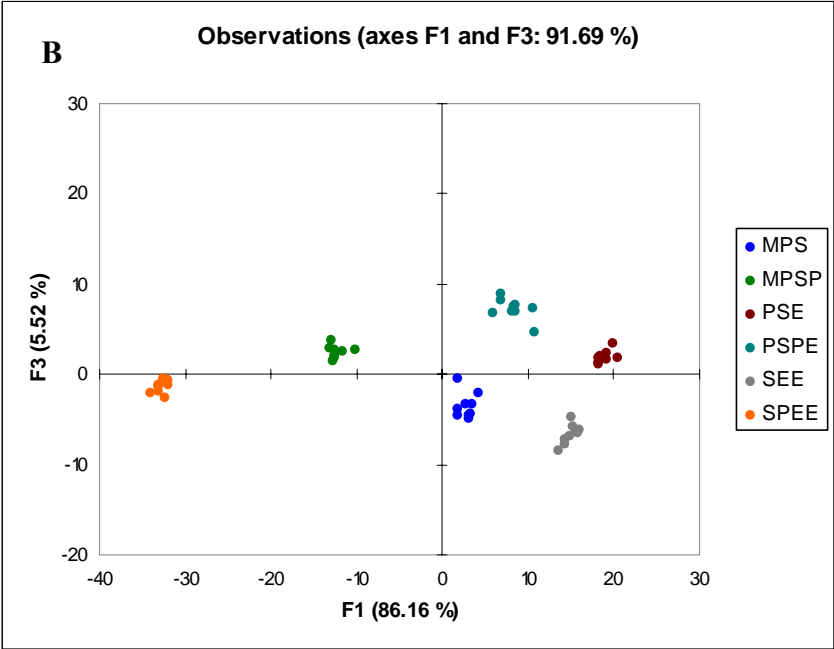
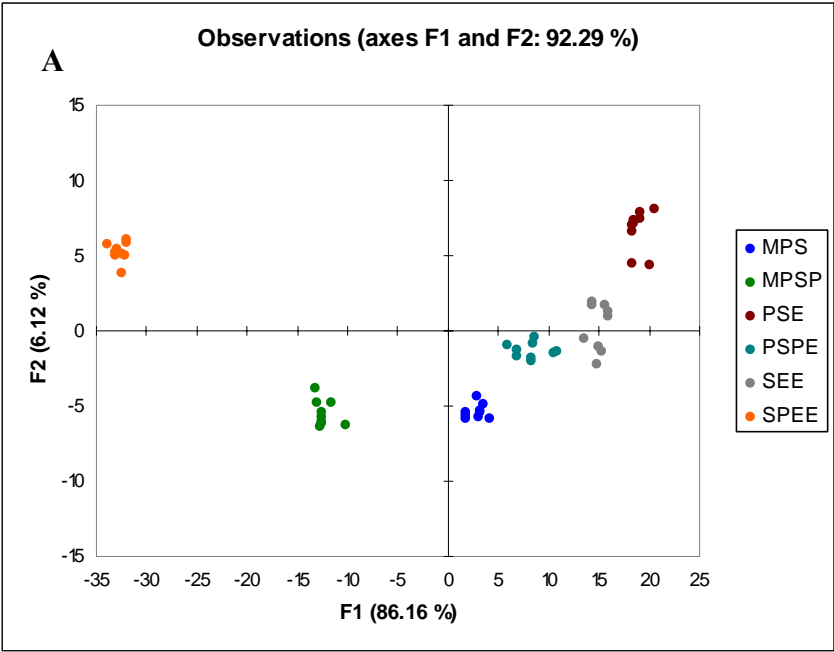


Figure 3.13 Example: UV-Vis absorbance changes of S(P)EE vs. SEE couple with different metallated receptors (totally 9 trials, the mean values (blue) and standard deviations (purple) are shown): A. Pyrocatechol Violet (In 4); B. celestine blue (In 5); C. galloxyanine (In 9). Conditions: Total volume in each well is 300 μ l: $[M^{n+}] = [In] = [LG_n] = 0.03$ mM, [peptides] = 0.3mM, [Tris] = 50 mM, Solvent: water, pH = 7.4, 25 $^{\circ}$ C.

Principle component analysis (PCA) and discriminant analysis (DA), on other hand, would be able to differentiate the subtle absorbances differences (**Figure 3.13**) by mathematic statistic calculations (**Figure 3.14**).



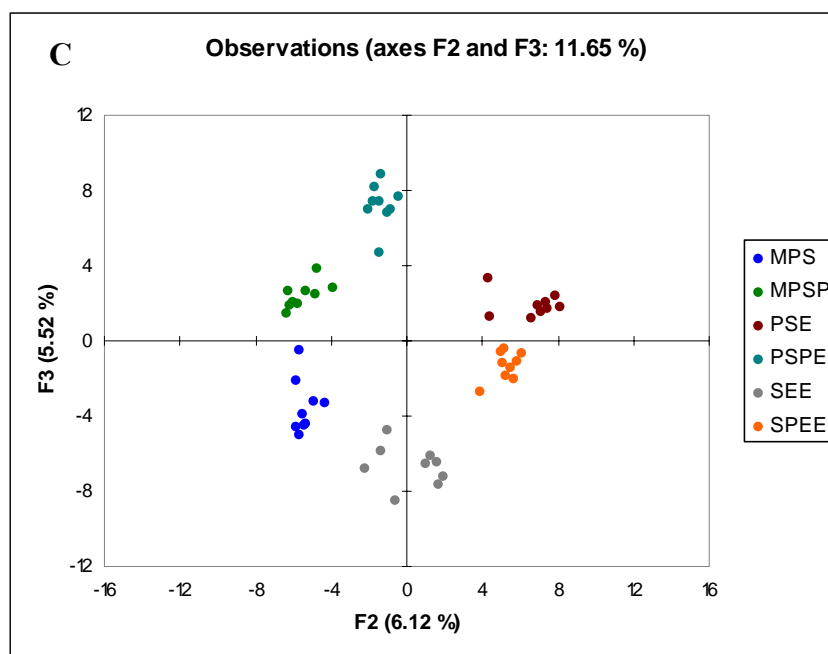


Figure 3.14 LDA analysis of six peptides. A. F1:F2; B. F1:F3; C. F2:F3

The spectra obtained in the final study were pre-processed in similar fashion to those obtained in the model study. That is, for each metal-receptor-indicator combination, spectra obtained in the presence of the phosphorylated and non-phosphorylated peptides were compared and the absorbance values of the peaks showing the greatest difference between these two peptides were then noted. Forward stepwise discriminant analysis²² was performed using XLSTAT²³ on this data matrix (absorbance values at peaks of interest) consisting of peptides (rows) and receptor-metal-indicator combinations (columns) and yielded 5 discriminant functions, linear composites of seventeen receptor-metal combinations. The maximum amount of the variance (99%) is captured by the first four functions. Scores plots of F2 vs. F1, F3 vs. F1 and F3 vs. F2 are shown in Figure X-

A, B, C. These plots feature excellent classification of all peptides: large spatial separation between peptides and clustering of the experimental replicates within each peptidic group. F1 discriminates PSE and PS(P)E, F2 discriminates MPS and MPS(P) and SEE and S(P)EE and F3 discriminates MPS and MPS(P) and SEE and S(P)EE.

The variables which were selected for the forward stepwise model on the basis of their F values²² and hence deemed to have the most discriminating power were determined to be all metal-receptor pairs in the presence of indicators 4 and 9. This is consistent with the fact that these metal-receptor-indicator combinations also accounted for the largest absorbance changes at the peaks of interest.

Validation of this forward discriminant model was carried out using 3 methods: the re-substitution method, the leave-one-out test and by randomly selecting five replicates from each peptidic group to create a discriminant model which was subsequently used to determine the identity of the four remaining experimental replicates from each peptidic group.²³ For the first two methods, 100% classification was obtained whereas for the last validation method, only one experimental replicate was misclassified. These high rates of classification attested to the soundness of the training set.

3.3 Conclusion

In this chapter, a new type of efficient differential receptors were synthesized and studied in combination with diverse indicators and metal ions. This group of differential

receptors could successfully recognize the phosphorylated peptides from their regular structures that were clarified by statistic LDA analysis.

3.4 Experimental section

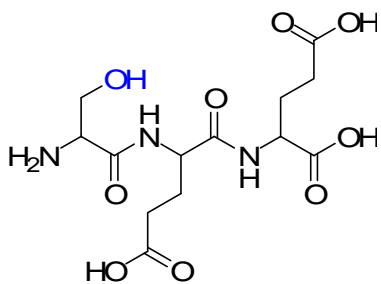
3.4.1 General considerations

The chemicals were obtained from Acros Organics, Aldrich, Alfa Aesar and NovaBiochem and were used without further purification unless otherwise noted. NovaSyn TG amino resin and 2-Cl trityl chloride resin were both purchased from NovaBiochem. A Varian Gemini 300 MHz and 400 MHz NMR were used to obtain ^1H and ^{13}C spectra. A Finnigan MAT-VSQ 700 spectrometer and DSQ spectrometer were used to obtain mass spectra. 96-well plate absorbance spectra were recorded at ambient temperature on a Bio-Teck Synergy HT multi-well plate spectrophotometer. A Costar 96-well flat bottom plate was used for all array experiments. All products were dried for at least 6 hours or lyophilized prior to spectral analysis.

3.4.2 Peptide synthesis

All the glasswares were flame dried and argon purged. Only dry solvent was used in solid phase synthesis. Fmoc-Ser(Bu^t)-OH, Fmoc-Pro-OH, Fmoc-Glu(OBu^t)-OH, and Fmoc-Met-OH, and 2- Chloro trityl chloride resin were employed in the synthesis.¹³

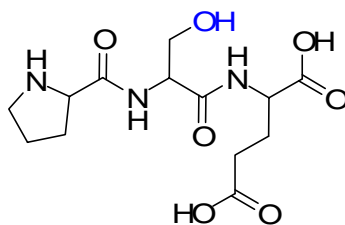
To an argon purged dry flask was charged 2- Chloro trityl chloride resin and dry DMF. The mixture was stood for an hour for adequate resin swelling. To another argon purged dry flask was charged one Fmoc-protected amino acid (2 eq), coupling reagents HOBT (2 eq.) and TBTU (2 eq.), N-methylmorpholine (4 eq.) and dry DMF (the amount was limited by adequate solubilities). The mixture was stirred at room temperature for 10 minutes. Color change was observed from white clear to yellow solution. The resin suspension was then added to a solid phase synthesis reactor. The DMF was removed. The amino acid solution was then added to above reactor. The mixture was stood for 30 minutes with occasionally swirling. The solution was then removed. The resin was triply washed with DMF, 17:2:1 (DCM: MeOH: diisopropylethyl amine) and DCM, and followed by next cycle of amino acid coupling using a different amino acid. After three cycles, the tripeptide was successfully coupled onto the resin. Cleavage step was then performed using a solution of 95:2.5: 2.5 TFA: H₂O: Triethylsilane. The dark red solution was collected and concentrated. The peptide was obtained through precipitation by using ice-cold diethyl ether followed by vacuum filtration (yield ~70%).



SEE

3.6

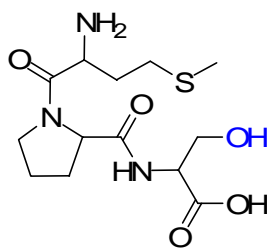
SEE ^1H NMR (CDCl_3 , 400 MHz) δ 4.41-4.48 (m), 3.83-3.98 (m), 2.39-2.45(m), 2.10-2.22 (m), 1.90-1.98(m) , 2.71(m), 2.31 (m), 2.03(m); CI-MS $\text{C}_{13}\text{H}_{21}\text{N}_3\text{O}$ (M+1) 364 (cal. 364);



PSE

3.4

PSE ^1H NMR (CDCl_3 , 400 MHz) δ 4.46-4.50 (m), 3.77-3.89(m), 3.45-3.51 (m), 3.31-4.44(m) , 2.12-2.45 (m), 2.00-2.07(m) , 1.88-1.97(m); CI-MS $\text{C}_{13}\text{H}_{21}\text{N}_3\text{O}_7$ (M+1) 332 (cal. 332);



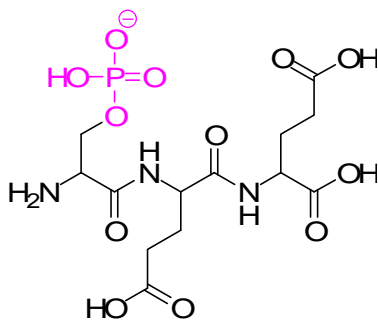
MPS

3.2

MPS ^1H NMR (CDCl_3 , 400 MHz) δ 4.60 (m), 4.46(m), 4.38 (m), 3.91(m) , 3.84 (m), 3.72(m) , 2.69(m), 1.99-2.40(m); CI-MS $\text{C}_{13}\text{H}_{23}\text{N}_3\text{O}_5\text{S}$ (M+1) 334 (cal. 334).

3.4.3 Phosphopeptide synthesis

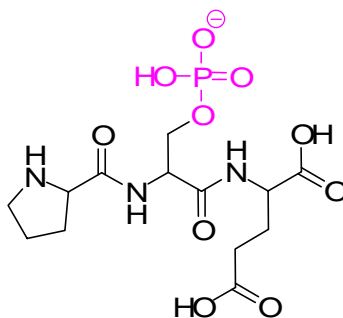
All the glasswares were flame dried and argon purged. Only dry solvent was used in solid phase synthesis. Fmoc-Ser(PO(OBzl)OH)-OH, Fmoc-Pro-OH, Fmoc-Glu(OBu^t)-OH, and Fmoc-Met-OH, were coupled to TGR resin.¹⁴ The synthesis of phosphorylated tripeptides were performed using the same solid phase synthesis technology (yield ~20-30%).



S(P)EE

3.7

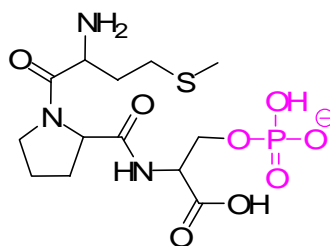
S(P)EE ^1H NMR (CDCl_3 , 400 MHz) δ 4.43 (m), 4.33(m), 4.26 (m), 2.44(m) , 2.14 (m), 2.00(m); CI-MS $\text{C}_{13}\text{H}_{22}\text{N}_3\text{O}_{12}\text{P}$ (M-1) 442 (cal. 442);



PS(P)E

3.5

PS(P)E ^1H NMR (CDCl_3 , 400 MHz) δ 4.66 (m), 4.37-4.44(m), 4.20 (m), 3.31-3.45(m) , 2.38-2.49 (m), 2.15(m) , 2.06(m), 1.94 (m); CI-MS $\text{C}_{13}\text{H}_{22}\text{N}_3\text{O}_{10}\text{P}$ (M-1) 410 (cal. 410);

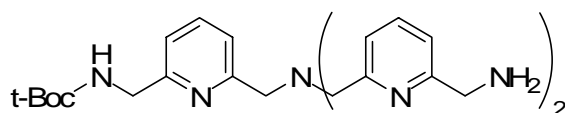


MPS(P)

3.3

MPS(P) ^1H NMR (CDCl_3 , 400 MHz) δ 4.65 (m), 4.53(m), 4.47 (m), 4.40(m) , 4.23 (m), 3.73(m) , 2.71(m), 2.31 (m), 2.03(m); CI-MS $\text{C}_{13}\text{H}_{24}\text{N}_3\text{O}_8\text{PS}$ (M-1) 412 (cal. 412).

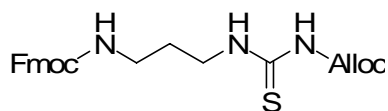
3.4.4 Differential receptor core ligand synthesis



3.9

Compound **3.9**: Triamino compound **3.8** (0.24g) was dissolved in 1ml dry DCM. Dry TEA (0.09ml) was added in the solution. The system was purged with argon, and then cooled to 0 °C for 15 mins. At this temperature, 1ml DCM solution of Boc-on (0.15g) was added to the reaction mixture dropwise under argon protection. The mixture was then slowly warmed up to room temperature, and stirred for another 16 hours. Compound **3.9** was obtained 0.15g, 49%, yellow oil with gradient flash column chromatography (DCM+5-50% ammonia saturated MeOH). ^1H NMR (CDCl_3 , 300 MHz)

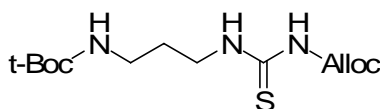
δ 7.52 (t, J = 7.5 Hz, 3H), 7.37(d, J = 7.2 Hz, 3H), 7.023(d, J = 7.5 Hz, 3H), 4.30 (d, J = 5.1 Hz, 2H), 3.83 (s, 4H), 3.77 (s, 4H), 3.75 (s, 2H), 2.02 (b, 4H), 1.35 (s, 9H); ^{13}C NMR (CDCl_3 , 75 MHz) δ 160.85, 158.73, 136.94, 136.73, 120.86, 120.53, 119.57, 119.21, 79.07, 59.95, 59.76, 47.38, 45.44, 28.21; HR-ESI-MS m/z $\text{C}_{26}\text{H}_{36}\text{N}_7\text{O}_2$ ($\text{M}+\text{H}$) $^+$ 478.2939 (cal. 478.2930).



3.10

Compound **3.10**: 1,3-diamino propane (31ml) was dissolved in 100ml DCM, and stirred at room temperature. $(\text{Boc})_2\text{O}$ (26.11g) in 800 ml DCM was added to the reaction mixture dropwise. The mixture was stirred at room temperature overnight. Clear solution turned to white cloudy. The mixture was concentrated and the white precipitate and most of 1, 3-diamino propane were washed with water (3 times). The organic phase was put onto flash silica column and separated using hexane and ethyl acetate. The mono-(*t*-Boc) protected diamine was obtained at 15g, 75%. Mono-*t*Boc protected diamino propane (11g) was added in a mixture of 200 DCM and 200ml saturated NaHCO_3 . Fmoc-Cl (17g) was then added to the reaction mixture as a solid portion. The mixture was stirred at room temperature overnight. The water layer was then removed, and the organic layer was washed with water 3 times. The organic layer was concentrated and purified with flash column chromatography. Fmoc and *t*-Boc protected diamine was afforded at 25.2g, 100%. The *t*-Boc group was removed by TFA. The mono-Fmoc protected diamino

propane was obtained by recrystallization in 1:1 Hexane: Ethyl acetate, 18.63g, 94%. The mono-Fmoc protected diamino propane (6.6g) and 4.6 ml diisopropylethyl amine were dissolved in 110 ml DCM. Alloc protected isothiocyanate in 30 ml was then added to the mixture solution dropwise. The reaction mixture was stirred at room temperature overnight, solvent was removed, and precipitated from 1:1 Hexane: Ethyl acetate, 5.8g, 82%, white solid. ^1H NMR (CDCl_3 , 400 MHz) δ 9.81 (s, 1H), 8.33 (s, 1H), 7.75 (d, J = 7.6 Hz, 2H), 7.59 (d, J = 7.6 Hz, 2H), 7.37 (t, J = 7.2 Hz, 2H), 7.29 (d, J = 7.2 Hz, 2H), 5.84 (m, 1H), 5.30 (m, 3H), 4.61 (d, J = 5.2 Hz, 2H), 4.40 (d, J = 6.8 Hz, 2H), 4.19 (t, J = 6.4 Hz, 1H), 3.73 (d, J = 6.0 Hz, 2H), 3.25 (d, J = 6.0 Hz, 2H), 1.82 (t, J = 6.0 Hz, 2H); ^{13}C NMR (CDCl_3 , 100 MHz) δ 179.40, 152.27, 143.85, 141.22, 130.77, 127.59, 126.96, 125.03, 119.88, 119.41, 66.91, 66.60, 47.17, 42.35, 37.70, 28.93; HR-CI-MS m/z $\text{C}_{23}\text{H}_{26}\text{N}_3\text{O}_4\text{S}$ ($\text{M}+\text{H}$) $^+$ 440.1659 (cal. 440.1644).



3.12

Compound **3.12**: The synthesis was performed similar to the synthesis of compound **3.11** with a yield of 86%, yellow crystals. ^1H NMR (CDCl_3 , 400 MHz) δ 9.75 (s, 1H), 8.55 (s, 1H), 5.84 (m, 1H), 5.33 (m, 2H), 4.93 (s, 1H), 4.60 (d, J = 5.6 Hz, 2H), 3.67 (m, 2H), 3.13 (d, J = 6.4 Hz, 2H), 1.77 (m, 2H), 1.38 (s, 9H); ^{13}C NMR (CDCl_3 , 100 MHz) δ 179.34, 156.07, 152.36, 130.81, 119.28, 79.16, 66.79, 42.55, 37.38, 28.99, 28.28; HR-CI-MS m/z $\text{C}_{13}\text{H}_{24}\text{N}_3\text{O}_4\text{S}$ ($\text{M}+\text{H}$) $^+$ 318.1472 (cal. 318.1488).

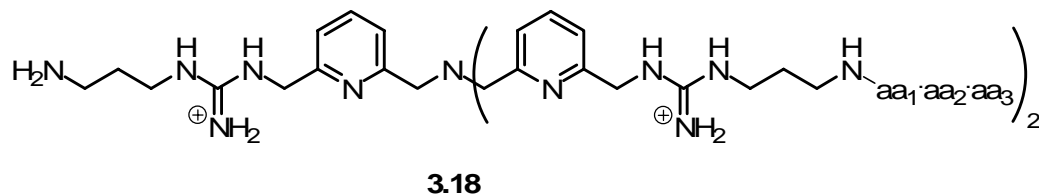
Compound **3.13**: Compound **3.11** (0.7g) was dissolved in 20 ml dry DCM and protected with argon. Diisopropylethyl amine (0.15 ml), compound **3.12** (0.19g) and EDCI (0.21g) were added to the reaction solution in order. The reaction mixture was stirred at room temperature overnight, purified with flash column chromatography and followed by deprotection using TFA. Compound **3.13** was obtained at 0.73g, 99%, yellow oil. ^1H NMR (CDCl_3 , 400 MHz) δ 7.72 (d, J = 7.2 Hz, 4H), 7.53 (d, J = 7.2 Hz, 4H), 7.35 (t, J = 6.8 Hz, 4H), 7.26 (t, J = 6.8 Hz, 4H), 7.21 (d, J = 7.6 Hz, 3H), 7.14 (d, J = 7.2 Hz, 3H), 5.91 (m, 3H), 5.22-5.31 (m), 4.59 (d, J = 6.0 Hz, 6H), 4.15-4.34 (m), 1.34 (s, 9H); ^{13}C NMR(CDCl_3 , 100 MHz) δ 161.33, 160.80, 160.29, 159.7, 143.46, 141.15, 129.76, 127.79, 127.07, 124.90, 121.05, 119.89, 117.24, 113.42, 109.60, 54.84, 46.84, 42.78, 30.69, 18.10, 16.73, 11.98; HR-FAB-MS m/z Boc protected Compound **3.13**: $\text{C}_{80}\text{H}_{95}\text{N}_{16}\text{O}_{12}$ ($\text{M}+\text{H}$) $^+$ 1471.7329 (cal. 1471.7315); ESI-MS m/z Compound **3.13**: $\text{C}_{75}\text{H}_{86}\text{N}_{16}\text{O}_{10}$ ($\text{M}+\text{H}$) $^+$ 1371 (cal. 1371).

3.4.5 Differential receptor synthesis

The differential receptors were built up onto two types of polymer resins (NovaSyn TG amino resin and 2-Cl Trityl chloride resin) for screening and solution based studies respectively.

NovaSyn TG amino resin (1g) was first soaked in dry DMF for one-hour preswelling. Bromoacetic acid (1.05g), HOBT (0.55g), DIC (0.6 ml) and NMM (2 ml) were dissolved in minimum amount of dry DMF, and stirred for 10min before placing to

preswelled resin. The mixture was gently stirred for 3 hours, and then the resin was washed out with 3 times DMF, MeOH, DCM for the generation of core ligand amino reacting sites. TNBS showed a negative testing result, meaning the amino groups on the resin were effectively covered by bromoacetic acid. The core ligand compound **3.13** (2.6g, 2eq) and K₂CO₃ (1.2g, 10eq) were mixed in dry DMF and stirred for 20 min before putting onto the derivatized resin. The resin mixture was then gently stirred for 18 hours, followed by triply washing using DMF, MeOH, and DCM. The resin was further doubly washed by DMF before 20% piperidine in DMF deprotecting of Fmoc groups. After washed with DMF, MeOH, and DCM, TNBS offered a positive result on resin, meaning the amino groups were generated. Combinatorial split-and-pool^{17a} synthesis was then applied to obtain the tripeptide arms.^{17b,c} An TNBS test was performed in each step to monitor the completion of reaction. In the last step the alloc protecting groups were removed by Me₂NH·BH₃ (6eq) and Pd(PPh₃)₄ (10 mol%) twice in DCM.²⁰



Solid phase synthesis on 2-Cl trityl chloride resin was similar to the reaction performing on NovaSyn TG amino resin. Only that the differential receptors immobilized on resin was able to be cleaved by TFA. HPLC-ESI-MS LG-TEV: C₆₃H₁₀₂N₂₂O₁₄ (M+2TFA+2H⁺)²⁺ 811 (cal. 811); ESI-MS LG-YDP: C₇₁H₉₈N₂₂O₁₄ (M+2TFA+2H⁺)²⁺ 856 (cal. 856); ESI-MS LG-YRE: C₇₅H₁₁₂N₂₈O₁₄ (M+3TFA+3H⁺)³⁺ 657 (cal. 657); ESI-

MS LG-KDK: $C_{67}H_{114}N_{26}O_{12}$ (M+2TFA+2H⁺)²⁺ 852 (cal. 852); ESI-MS LG-RLL: $C_{71}H_{124}N_{28}O_8$ (M+3TFA+3H⁺)³⁺ 614 (cal. 614).

3.5 References

- ¹ (a) Collins, B. E.; Anslyn, E. V. *Chem. Eur. J.* **2007**, *13*, 4700-4708; (b) Heitman, L. M.; Taylor, A. B.; Hart, P. J.; Urbach, A. R. *J. Am. Chem. Soc.* **2006**, *128*, 12574-12581. (c) Chang, K. -H; Liao, J. -H, Chen, C. -T.; Mehta, B. K.; Chao, P. -T.; Fang, J.-M. *J. Org. Chem.* **2005**, *70*, 2026-2032. (d) Wehner, M.; Janssen, D.; Schäfer, G.; Schrader, T. *Eur. J. Org. Chem.* **2006**, 138-153. (e) Kubo, M.; Nashimoto, E.; Tokiyo, T.; Morisaki, Y.; Kodama, M.; Hioki, H. *Tetrahedron. Lett.* **2006**, *47*, 1921-1931. (f) Niv, M. Y.; Weinstein, H. A. *J. Am. Chem. Soc.* **2005**, *127*, 14072-14079. (g) Tong, A. H. Y.; Drees, B.; Nardelli, G.; Bader, G. D.; Brannetti, B.; Castagnoli, L.; Evangelista, M.; Ferracuti, S.; Nelson, B.; Paoluzi, S.; Quondam, M.; Zucconi, A.; Hogue, C. W. V.; Fields, S.; Boone, C.; Cesareni, G. *Science* **2002**, *295*, 321-324. (h) Stites, W. E. *Chem. Rev.* **1997**, *97*, 1233-1250.
- ² (a) Still, W. C. *Acc. Chem. Res.* **1996**, *29*, 155-163. (b) Yoon, S. S.; Still, W. C. *J. Am. Chem. Soc.* **1993**, *115*, 823. (c) Chen, C. -T.; Wagner, H.; Still, W. C. *Science* **1998**, *279*, 851-853. (d) Famulok, M.; Jeong, K. -S.; Deslongchamps, G.; Rebek Jr. *J. Angew. Chem. Int. Ed. Engl.* **1991**, *103*, 880-882
- ³ (a) Imai, H.; Munakata, H.; Uemori, Y.; Sakura, N. *Inorg. Chem.* **2004**, *43*, 1211-1213. (b) Sun, S.; Abul Fazal, M.; Roy, B. C.; Mallik, S. *Org. Lett.* **2000**, *2*, 911-914. (c) Tashiro, S.; Tominaga, M.; Kawano, M.; Therrien, B.; Ozeki, T.; Fujita, M. *J. Am. Chem. Soc.* **2005**, *127*, 4546-4547; (d) Davies, M.; Bonnat, M.; Guillier, F.; Kilburn, J. D.; Bradley, M. *J. Org. Chem.* **1998**, *63*, 8696-8703.
- ⁴ (a) Hayashi, K.; Yamanaka, M.; Toko, K.; Yamafuji, K. *Sens. Actuators B* **1990**, *2*, 205-213. (b) Albert, K.; Lewis, N.; Schauer, C.; Sotzing, G.; Stitzel, S.; Vaid, T.; Walt, D. *Chem. Rev.* **2000**, *100*, 2595-2626.; (c) Jurs, P. C.; Bakken, G. A.; McClelland, H. E. *Chem. Rev.* **2000**, *100*, 2649-2678.; (d) Kodadek, T. *Chem. Biol.* **2001**, *8*, 105-115.; (e) Rakow, N. A.; Suslick, K. S. *Nature* **2000**, *406*, 710-713.

- ⁵ (a) Lonergan, M.; Severin, E.; Dolemand, B.; Beaber, S.; Grubbs, R.; Lewis, N. *Chem. Mater.* **1996**, *8*, 2298-2312. (b) Pearce, T.; Gardner, J.; Friel, S.; Barlett, P.; Blair, N. *Analyst* **1993**, *118*, 371-377.
- ⁶ (a) Drew, S.; Janzen, D.; Mann, K. *Anal. Chem.* **2002**, *74*, 2547-2555. (b) Rakow, N.; Suslick, K. *Nature* **2000**, *406*, 710-712. (c) Mayr, T.; Liebsch, G.; Klimant, I.; Wolfbeis, O. S. *Analyst* **2002**, *127*, 203-208. (c) Mayr, T.; Igel, C.; Liebsch, G.; Klimant, I.; Wolfbeis, O. S. *Anal. Chem.* **2003**, *75*, 4389-4397. (d) Zhang, Z.; Suslick, K. S. *J. Am. Chem. Soc.* **2005**, *127*, 11548-11549. (e) Stojanovic, M. N.; Green, E. G.; Semova, S.; Nikic, D. B.; Landry, D. W. *J. Am. Chem. Soc.* **2003**, *125*, 6085-6089.
- ⁷ (a) Ojida, A.; Park, S.; Mito-oka, Y.; Hamachia, I. *Tetrahedron Lett.* **2002**, *43*, 6193-6195. (b) Ojida, A.; Inoue, M.; Mito-oka, Y.; Tsutsumi, H.; Sada, K.; Hamachi, I. *J. Am. Chem. Soc.* **2006**, *128*, 2052-2058. (c) Ojida, A.; Miyahara, Y.; Kohira, T.; Hamachi, I. *Biopolymers (Pept. Sci.)* **2004**, *76*, 177-184. (d) Ojida, A.; Hamachi, I. *Bull. Chem. Soc. Jpn.* **2006**, *79*, 1. (e) Ojida, A.; Kohira, T.; Hamachi, I. *Chem. Lett.* **2004**, *33*, 8. (f) Ojida, A.; Mito-oka, Y.; Inoue, M.; Sada, K.; Hamachi, I. *J. Am. Chem. Soc.* **2002**, *124*, 6256-6258. (g) Ojida, A.; Inoue, M.; Mito-oka, Y.; Hamachi, I. *J. Am. Chem. Soc.* **2003**, *125*, 10184-10185. (h) Ojida, A.; Mito-oka, Y.; Sada, K.; Hamachi, I. *J. Am. Chem. Soc.* **2004**, *126*, 2454-2463. (i) Ojida, A.; Honda, K.; Shinmi, D.; Kiyonaka, S.; Mori, Y.; Hamachi, I. *J. Am. Chem. Soc.* **2006**, *128*, 10452-10459. (j) Anai, T.; Nakata, E.; Koshi, Y.; Ojida, A.; Hamachi, I. *J. Am. Chem. Soc.*, **2007**, *129*, 6232-6239. (k) Martýnez-Manez, R.; Sancenon, F. *Chem. Rev.* **2003**, *103*, 4419-4476; (l) Snowden, T. S.; Anslyn, E. V. *Curr. Opin. Chem. Biol.* **1999**, *3*, 740-746. (m) Seo, J. S.; Sung, N.; Hynes, R. C.; Chin, J. *Inorg. Chem.*, **1996**, *35*, 7472-7473; (n) Han, M. S.; Kim, D. H. *Angew. Chem. Int. Ed. Engl.* **2001**, *41*, 3809-3811; (o) Bianchi, A.; Micheloni, M.; Paolett, P. *Coord. Chem. Rev.* **1991**, *110*, 17-113; (p) Powell, D.; Bowman-James, K.; *Coord. Chem. Rev.* **2003**, *240*, 57-75.
- ⁸ (a) Antonisse, M. M. G.; Reinhoudt, D. N. *Chem. Commun.*, **1998**, *4*, 443-448. (b) Tobey, S. L.; Jones, B. D.; Anslyn, E. V. *J. Am. Chem. Soc.*, **2003**, *125*, 4026-4027. (c) Beer, P. D.; Gale, P. A. *Angew. Chem. Int. Ed.* **2001**, *40*, 486-516. (d) Verboom, W.; Rudkevich, D. M.; Reinhoudt, D. N. *Pure&Appl. Chem.*, **1994**, *66*, 679-686; (e) Starnes, S. D.; Arungundram, S.; Saunders, C. H. *Tetrahedron Lett.* **2002**, *43*, 7785-7788; (f) Lee, D. H.; Lee, H. Y.; Lee, K. H.; Hong, J. *Chem. Commun.*, **2001**, *13*, 1188-1189; (g) Xie, H.; Yi, S.; Wu, S.; *J. Chem. Soc., Perkin Trans. 2*, **1999**, *12*, 2751-2754; (h) Best, M. D.; Anslyn, E. V. *Eur. J. Chem.* **2003**, *9*, 51-57. (i) Chu, F.; Flatt, L. S.; Anslyn, E. V. *J. Am. Chem. Soc.* **1994**, *116*, 4194-4204; (j) Furuta, H.; Magda, D.; Sessler, J. L. *J. Am. Chem. Soc.* **1991**, *113*, 978-985; (k) Chin, J.; Banaszczyk, M. *J. Am. Chem. Soc.* **1989**, *111*, 4103-4105; (m) Dale, T.; Rebek, Jr. J. *J. Am. Chem. Soc.* **2006**, *128*, 4500-4501.

- ⁹ Jurs, P. C.; Bakken, G. A.; McClelland, H. E. *Chem. Rev.* **2000**, *100*, 2649-2678
- ¹⁰ (a) Buryak, A.; Severin, K. *J. Am. Chem. Soc.* **2005**, *127*, 3700-3701. (b) Baldini, L.; Wilson, A. J.; Hong, J.; Hamilton, A. D. *J. Am. Chem. Soc.* **2004**, *126*, 5656-5657. (c) Rangin, M.; Basu, A. *J. Am. Chem. Soc.* **2004**, *126*, 5038-5039. (d) Wright, A. T.; Griffin, M. J.; Zhong, Z.; McCleskey, S. C.; Anslyn, E. V.; McDevitt, J. T. *Angew. Chem., Int. Ed.* **2005**, *44*, 6375-6378.
- ¹¹ (a) Nonaka, T.; Iwatsubo, T.; Hasegawa, M. *Biochem.* **2005**, *44*, 361-368 (b) Fujiwara, H.; Hasegawa, M.; Dohmae, N.; Kawashima, A.; Masliah, E.; Goldberg, M. S.; Shen, J.; Takio, K.; Iwatsubo, T. *Nature Cell Bio.* **2002**, *4*, 160-164
- ¹² Rencher, A. C.; Bloomfield, P.; Cressie, N. A. C.; Fisher, N. I.; Johnstone, I. M.; Kadane, J. B.; Ryan, L. M.; Scott, D. W.; Silverman, B. W.; Smith, A. F. M.; Teugels, J. T. *Methods of Multivariate Analysis*; Eds. Wiley-Interscience: New York, **2002**, 270-298, 156-247
- ¹³ Bernhardt, A.; Drewello, M.; Schutkowski, M. *J. Peptide Res.* **1997**, *50*, 143-152
- ¹⁴ (a) Perich, J. W. *Lett. Pept. Sci.* **1996**, 127-132; (b) Perich, J. W. *Int. J. Pept. Res. Therap.* **1998**, 49-55; (c) Perich, J. W.; Ede, N. J.; Eagle, S.; Bray, A. M. *Int. J. Pept. Res. Therap.* **1999**, 91-97
- ¹⁵ (a) Zhang, T.; Anslyn, E. V. *Tetrahedron* **2004**, *60*, 11117-11124; (b) Tobey, S. L.; Anslyn, E. V. *Org. Lett.* **2003**, *5*, 2029-2031
- ¹⁶ Malabarba, A.; Ciabatti, R.; Kettenring, J. Scotti, R.; Candiani, G.; Pallanza, R.; Berti, M.; Goldstein, B. P. *J. Med. Chem.* **1992**, *35*, 4054-4060
- ¹⁷ (a) Kapoor, T.; Andreotti, A. H.; Schreiber, S. L. *J. Am. Chem. Soc.* **1998**, *120*, 23-29. (b) Bayer, E. *Angew. Chem. Int. Ed. Engl.* **1991**, *30*, 113-129; (c) Gowravaram, M.; Gallop, M. *Tetrahedron Lett.* **1997**, *38*, 6973-6976
- ¹⁸ Zhang, T.; Anslyn, E. V. *Tetrahedron* **2004**, *60*, 11117-11124
- ¹⁹ Zuckermann, R. N.; Kerr, J. M.; Kent, S. R. H.; Moos, W. H. *J. Am. Chem. Soc.* **1992**, *114*, 10646-10647
- ²⁰ (a) Gomez-Martinez, P.; Dessolin, M.; Guibe, F.; Alvericio, F. *J. Chem. Soc. Perkin Trans. 1*, **1999**, 2871-2874; (b) Varshavsky, S. J.; Kiseleva, N. V. US Patent **1973**, C07F 9/50, #1338741
- ²¹ Tobey, S. L. *Thesis (Ph. D.)--University of Texas at Austin*, **2003**.

²² Rencher , A. C.; Bloomfield, P.; Cressie, N. A. C.; Fisher, N. I.; Johnstone, I. M.; Kadane, J. B.; Ryan, L. M.; Scott, D. W.; Silverman, B. W.; Smith, A. F. M.; Teugels J. T. *Methods of Multivariate Analysis*, Eds. Wiley-Interscience: New York, **2002**, 270-298, 156-247

²³ This program is available from www.xlstat.com

Chapter 4: A Colorimetric Boronic Acid - Based Sensing Ensemble for Carboxy and Phospho Sugars, and Its Application in Monitoring of Glucose Oxidase Activity in Blood Serum

4.1 Introduction

A cadmium-centered tris-boronic acid receptor was synthesized, and its binding properties toward various anionic sugars were determined. This receptor shows high affinity for different anionic sugars, especially gluconic acid, which has an association constant near 10^7 M^{-1} at neutral pH. Furthermore, using an indicator-displacement assay a color change was observed upon addition of anionic sugars. This colorimetric test was used as a facile screening technique to qualitatively analyze guest affinities.

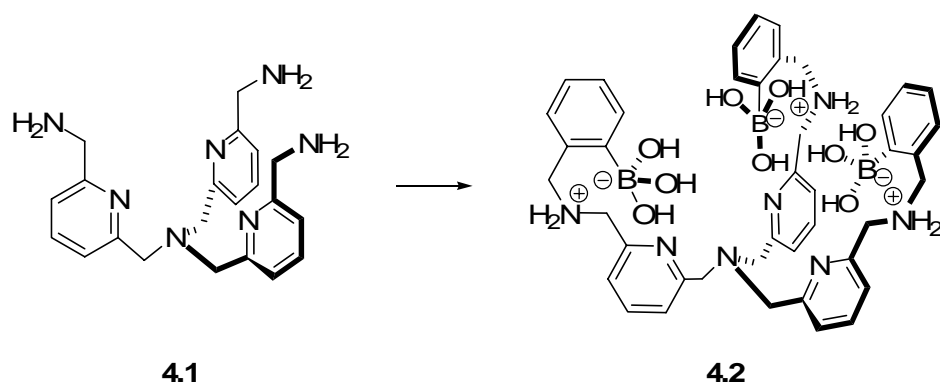
The design of artificial receptors that have high selectivity/affinity and can compete with those in natural systems is an attractive area of research.¹ Sugar recognition, especially in aqueous solution at neutral pH, has been a particular focus because of its potential applications in the development of therapeutic agents, chemosensors, and glycomics tools.²

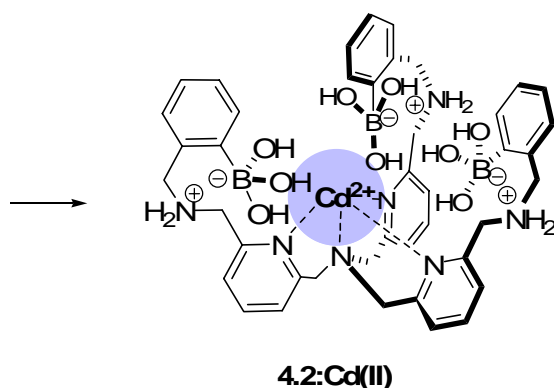
The boronic acid functional group is known to form reversible covalent linkages with diols, α -hydroxy acids, and some α -amino acids, thereby making it a common recognition moiety used in sugar-sensing systems.³ The vast majority of current detection methods rely on fluorescence modulations that occur upon addition of carbohydrates. Yet, the previously described receptors often show relatively low binding affinities in aqueous solution at neutral pH.

Transition metal ions provide coordination modes for anionic molecules. The use of transition metal ions offers the dual possibility of preorganizing a receptor by metal ligation, and enhancing the binding properties for anionic guest molecules.⁴ Many receptors have been designed to exploit these dual properties,⁵ but metallo-boronic acid receptors are rare.⁶ In this chapter a C_{3v} -symmetric tris-boronic acid receptor, **4.2**:Cd(II) was reported, that binds various carboxy and phospho sugars with high affinity in protic media at neutral pH.

4.2 Results and discussions

Compound **4.2** was synthesized via reductive amination with tris-amino compound **4.1**,⁷ 2-formylbenzene boronic acid, and NaBH₄ in dry MeOH with added molecular sieves⁸ (**Scheme 4.1**).





Scheme 4.1 Synthesis of boronic acid receptor **4.2: Cd(II)**

The ligand strength of compound **4.2** was tested with several metal ions chosen based upon their sizes and nitrogen coordination abilities. Neither zinc nor lanthanide ions were found to have significant affinity for **4.2** via analysis of UV-Vis absorbance changes. However, Cu(II) promoted UV-Vis absorbance shifts upon titration with **4.2**, but the stoichiometry of binding was found to be 2:1 metal:ligand. This finding is in contrast to those previously reported for a guanidinium-based receptor for phosphate.⁹ With this previous receptor, Zn(II) and Cu(II) were found to bind with a 1:1 stoichiometry. As an explanation for this difference, recent studies from Anslyn group were showed this α -aminomethyl boronic acids exist predominately in the zwitterionic form,¹⁰ as indicated in the manner in **4.2**. In this form, free-based N-atoms of the aminomethyl groups are available to coordinate with metals, and hence with Cu(II) these nitrogens are proposed to be involved in binding along with the pyridines, creating higher order stoichiometries.

In contrast, Cd(II) bound receptor **4.2** with a 1:1 stoichiometry, which was similar to its reported binding properties with tris(2-pyridylmethyl)amine(TPA) and the associated crystal structure.¹¹ Due to the larger size of Cd(II), the cavity created upon ligation with TPA is more open than with Cu(II), and this steric effect may alter the binding stoichiometry. However, it is also well-known that softer metals such as Cd(II) have weaker coordination properties to nitrogen ligands than do harder metals such as Cu(II).reference This lower affinity may also be part of the reason for the different stoichiometries found, because the Cd(II) would not gain as much binding energy upon increased nitrogen ligation as would Cu(II), thus allowing the zwitterionic form of the α -aminomethyl boronic acid ligand to persist. Hence, cadmium was chosen as the metal center.

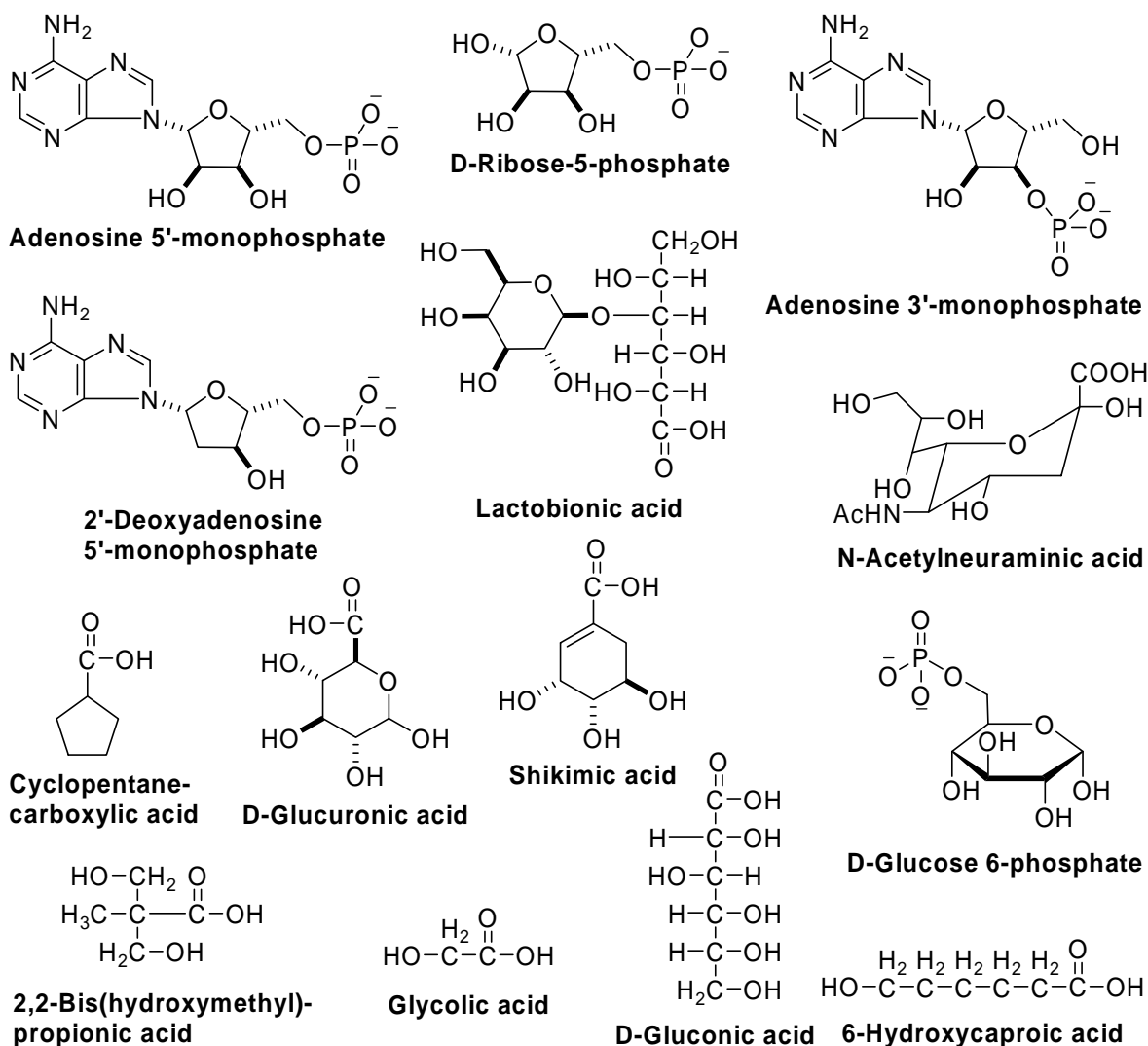


Figure 4.1 Anionic sugars

Various carboxy- and phosphor- sugars in aqueous solution were examined as guests (**Figure 4.1**). A protocol for screening the guests prior to full thermodynamic analyses was developed. Indicator-displacement assays were applied to screen the binding affinities of **4.2**:Cd(II) to various sugar moieties at neutral pH (~7.4).

Pyrocatechol violet (PV) was chosen as the indicator, because its displacement from the receptor creates a color change in the UV-vis spectra. The experiments were carried out in 3:1 MeOH/water mixture due to the low water solubility of compound **4.2**:Cd(II).

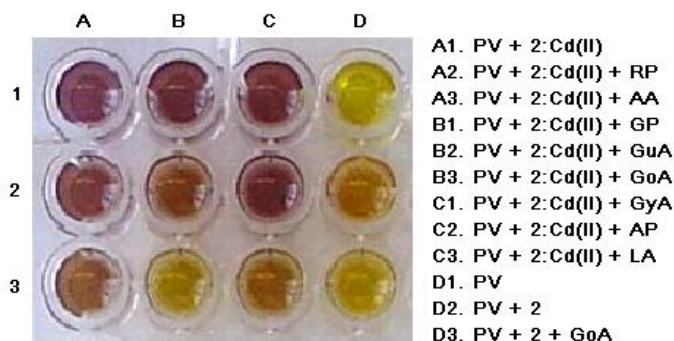


Figure 4.2 Sugar screening. Conditions: Total volume: 300 μ l; [**4.2**:Cd(II)] = [PV] = 0.1 mM; [Sugars] = 0.5 mM; [HEPES] = 10 mM; Solent: MeOH: Water = 3:1 (v:v); pH = 7.4; 25 $^{\circ}$ C.

As shown in **Figure 4.2** of this paper (columns A-D), in each well, **4.2**:Cd(II), PV, and one of the guests were placed at 0.1, 0.1, and 0.5 mM, respectively, in \sim 10 mM HEPES buffer. The pure PV gives a yellow solution (D1), whereas **4.2**:Cd(II) + PV is purple (A1). Upon addition of the different guest molecules, PV is partially displaced from the receptor molecules, and hence the color of the solutions changes to different extents from purple to yellow dependent upon the strength of the associations. By examining **Figure 4.2**, it is clear that glucuronic acid and lactobionic acid give intermediate colors, whereas gluconic acid exhibits a close to that of free PV. This

qualitative colorimetric analysis suggests gluconic acid has the strongest affinity for the receptor.

A typical UV-vis titration for quantitative analysis is shown in **Figure 4.3**. A clear isosbestic point exists in the overlaid spectra. The titration results were readily fit by 1:1 isotherms¹² (**Figure 4.4**), and the association constants of sugars to the receptors were calculated: $K_{4.2:\text{Cd(II)}:\text{PV}} = 3.18 \times 10^5 \text{ M}^{-1}$ and $K_{4.2:\text{PV}} = 2.54 \times 10^3 \text{ M}^{-1}$ (**Table 4.1**).

Table 4.1 Association Constants Determined for the Binding of Anionic Sugars in MeOH/ H₂O (v/v 3/1).

Sugars	log K _a
glucose 6-phosphate (GP)	-
glycolic acid (GyA)	3.76 ^a
adenosine 5'-monophosphate (AP)	3.95 ^a
ribose 5-phosphate (RP)	4.76 ^a
N-acetylneuraminic acid (AA)	4.77 ^a
glucuronic acid (GuA)	5.34 ^a
lactobionic acid (LA)	5.44 ^a
gluconic acid (GoA)	6.75 ^a ; 4.32 ^b

a. Association constants to **4.2**:Cd(II). b. Association constants to **4.2**.

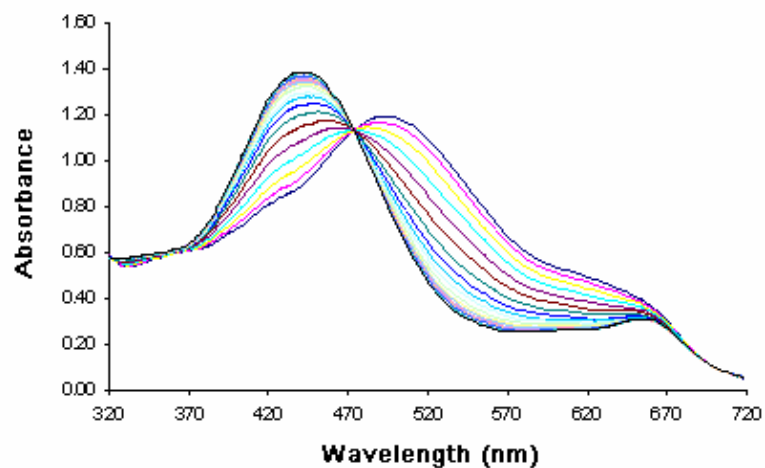


Figure 4.3 Typical UV-Vis binding curves obtained upon titration of anionic sugars into 4.2: Cd(II)-indicator solution. Titration conditions: 3/1 Methanol/Water; HEPES buffer 50 mM, pH = 7.4; Indicator: Pyrocatechol Violet; [4.2: Cd(II)] = [PV] = 0.1 mM; 25 °C.

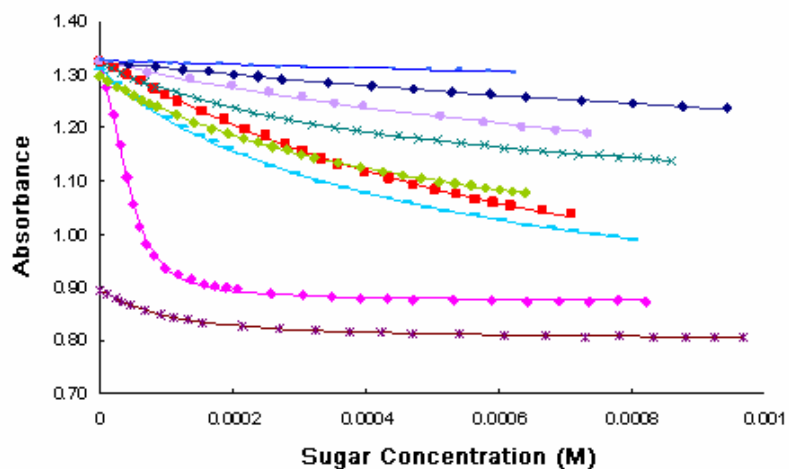


Figure 4.4 Relative absorbance of **4.2**:Cd(II)-indicator system upon addition of anionic sugars, modulated at 500 nm: —■— Glucose 6-Phosphate; —◆— Glycolic acid; —●— Adenosine 5'-monophosphate; —×— Glucuronic acid; —■— Ribose 5-phosphate; —◆— Lactobionic acid; —■— N-Acetylneuraminic acid; —◆— Gluconic acid (**4.2**:Cd(II)); —*— Gluconic acid (**4.2**).

On the basis of the analysis of **Figure 4.3** and the 96-well screening studies, it is clear that **4.2**:Cd(II) displays selectivity in its binding among the anionic sugars, likely due to arrangement of the boronic acid groups. Among the phosphor- sugars, only ribose 5-phosphate and adenosine 5'-monophosphate were found to have relatively strong binding. The lack of a 2'-hydroxyl group on a primary phosphate (2'-deoxyadenosine 5'-phosphate) or a secondary phosphate (adenosine 3'-phosphate) or even a one carbon extension in the ring (glucose 6-phosphate) dramatically decreased binding. Second, among carboxy sugars, a carboxylate group with an α - and/or β -hydroxyl group was found to have large affinity for the host. Other guests such as shikimic acid, cyclopentanecarboxylic acid, 6-hydroxycaproic acid, and 2,2-bis(hydroxymethyl)-propionic acid did not give observable spectral changes, even with large excesses of guest. Third, linear carboxy sugars were found to have stronger binding by 2 orders of magnitude relative to that of cyclic sugars. One interesting comparison was that of the binding affinity of **4.2** with and without metal coordination. In the gluconic acid titration experiment, both association constants ($\log K_a$) were determined: 6.75 with and 4.32 without the metal center, respectively. Obviously, the reversible covalent bond formation between boronic acid groups and sugars played a significant role in the recognition process. However, the cadmium metal center not only preorganized the C_{3v} ligand core

molecule, but likely also coordinated to the guest, which further enhanced the receptor affinity for the carboxy and phospho sugars.

4.3 Application: Monitoring Glucose Oxidase Activity in Blood Serum

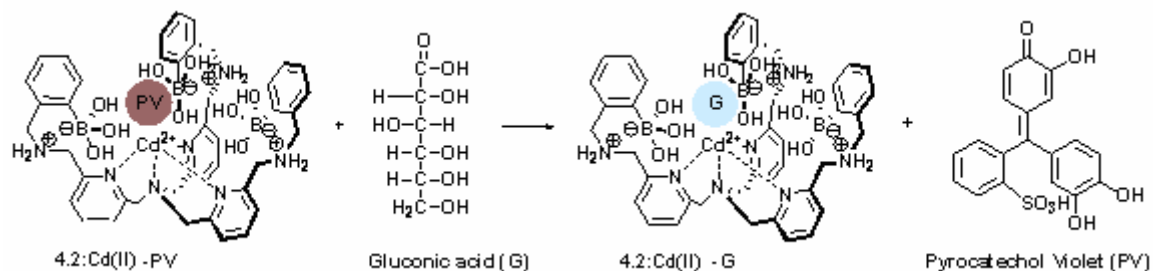
Using a boronic acid based receptor that was previously found to have high affinity for gluconic acid, a colorimetric indicator-displacement assay (IDA) was created that can report the concentration of the product of glucose oxidase (GOx) catalyzed glucose oxidation. The color change obtained directly reflects the concentration of glucose. This sensing ensemble was then successfully applied to determine the glucose concentration in human serum, where offers a facile, colorimetric, sensitive, and accurate glucose test.

Glucose sensing continues to be an active area of research because of the increasing number of individuals diagnosed with diabetes.¹³ The traditional commercial glucose test is electrochemical, involving an amperometric electrode that monitors glucose concentration by a change in current flow caused by the glucose oxidase (GOx) catalyzed production of hydrogen peroxide, or sometimes by the consumption of oxygen.¹⁴ In this method, the generated hydrogen peroxide is oxidized under a constant working potential, and the extent of oxidation corresponds to the glucose concentration. However, the electrode needs careful calibration because other oxidizable components may interfere at the working potential. Acid-sensitive polymers have alternatively been used.¹⁵ In this method, GOx generates gluconic acid which lowers the pH and causes

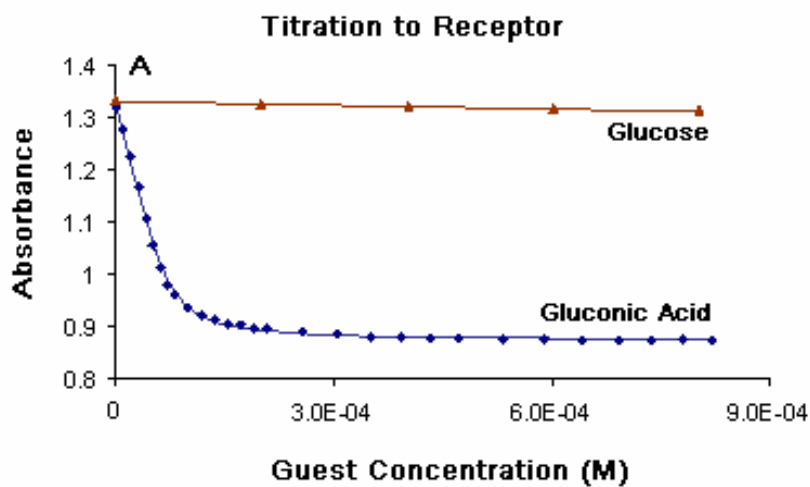
shrinking of the polymer. A vibrational frequency change correlates to the glucose concentration. The detection process is reversible, but the sensitivity dramatically decreases with increasing ionic strength. Optical methods have also been reported, along with their potential applicability *in vivo* for noninvasive detecting and high sensitivity.¹⁶ Asher has reported a crystalline colloidal array embedded polyacrylamine hydrogel that responds to low concentrations of glucose by a Bragg diffraction change from greenish blue to red.¹⁷ Further, the Shear group applies horseradish peroxidase to uptake the GOx product H_2O_2 , and the generated O_2 is trapped by 4-aminoantipyrine and 4-hydroxybenzoic acid to generate quinoneimine, a bright red dye. Via the absorbance change, the concentration of glucose can be determined in various drinks.¹⁸ In order to extend the use of indicator IDAs, which have been successfully applied in various media using sensitive colorimetric dyes, to the detection of glucose *in vitro*.

Earlier in this chapter a metalated boronic acid-based receptor (**4.2**:Cd(II)) was described that demonstrated excellent selectivity and high affinity to gluconic acid with a binding stoichiometry of 1:1 and a K_a of $5.6 \times 10^6 \text{ M}^{-1}$.¹⁹ A colorimetric response to gluconic acid was created using an IDA in 3:1 (v/v) MeOH/ H_2O at neutral pH. Pyrocatechol violet was chosen as the indicator (**Scheme 4.2**), and a 1:1 (molar ratio) of **4.2**:Cd(II)/PV solution was prepared, giving a purplish red color. Because of gluconic acid's stronger association to receptor **4.2**:Cd(II), PV was displaced from the receptor pocket upon introduction of the gluconic acid, resulting in the yellowish green of the free indicator. A large spectral response is found for gluconic acid, demonstrating an ability of monitoring this product of from GOx oxidation reaction. As shown in **Figure 4.5**, little to

no displacement of the indicator occurs upon the addition of glucose. This control experiment demonstrates that the detection of gluconic acid was efficient even in the presence of glucose or other sugars.



Scheme 4.2 IDA Application in Gluconic Acid Association



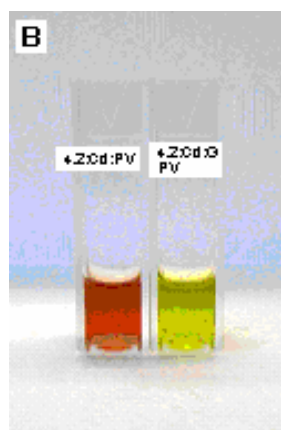
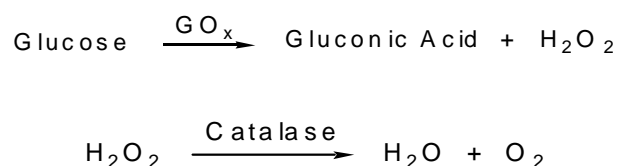


Figure 4.5 (A) UV-Vis titration results, where $[4.2:\text{Cd}(\text{II})] = 0.13 \text{ mM}$ and $[\text{PV}] = 0.13 \text{ mM}$ in MeOH- H_2O 3:1 (v/v). (B) Example pictures: Addition of gluconic acid to receptor $4.2:\text{Cd}(\text{II})$ causes a displacement of PV from $4.2:\text{Cd}(\text{II})$, resulting in a large color change. $[4.2:\text{Cd}(\text{II})] = 0.13 \text{ mM}$, $[\text{PV}] = 0.13 \text{ mM}$, and $[\text{G}] = 0.13 \text{ mM}$, all in MeOH- H_2O 3:1 (v/v).

Using this IDA, and the fact that gluconic acid was the only product generated with GOx, the determination of gluconic acid concentrations in blood was explored. Because the reaction generates hydrogen peroxide, the enzyme catalase was applied to sequester the H_2O_2 (**Scheme 4.3**). The H_2O_2 was sequestered because boronic acid-based receptors have previously been shown to react with H_2O_2 .²⁰



Scheme 4.3 Enzyme Catalyzed Glucose Oxidation

To optimize the reaction conditions, several variables were examined: the [GOx] (**Figure 4.12**), [catalase] (**Figure 4.13**), pH (**Figure 4.14**), and reaction time. The optimization led us to prepare a series of aqueous solutions (5 mL) at pH ~ 7 as standards, each of which contained (the volumes should be in parantheses after the item) 30 μL of GOx (1 mg/mL), 200 μL of catalase (1 mg/mL), 50 mM Tris buffer, and 0-140 μL of a glucose solution (50.23 mM), resulting in glucose concentration between 0 and 1.41 mM. This concentration range was targeted because the procedure ultimately used with blood involves a dilution (see below).

The oxidation commences upon the addition of different amounts of glucose to the 5 mL aliquot containing GOx and catalase. Aliquots of 250 μL of this solution were removed from the reaction and mixed with a 750 μL MeOH solution containing receptor **1** (0.13 mM) and an indicator (pyrocatechol violet, 0.13 mM). The solutions were analyzed by UV-vis spectroscopy, and the absorbance was correlated to gluconic acid concentrations, giving a calibration curve (**Figure 4.6**). This curve was then used to analyze glucose concentrations in crude blood samples.

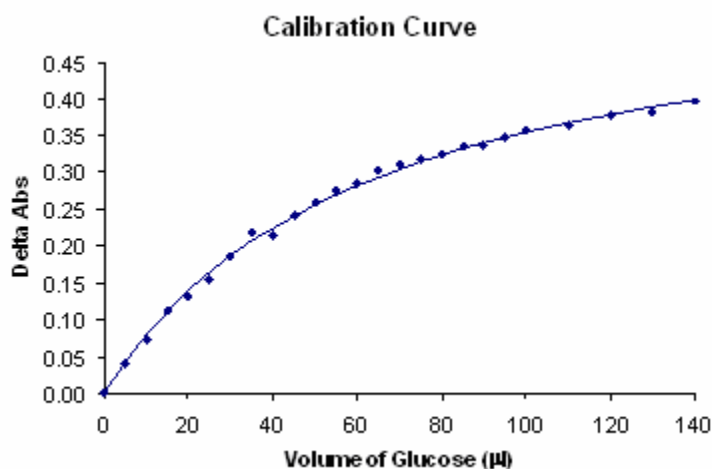


Figure 4.6 Glucose calibration curves. Titration conditions: 3/1 Methanol/Water; HEPES buffer 50 mM, pH = 7.4; Indicator: Pyrocatechol Violet; [4.2:Cd(II)] = [PV] = 0.1 mM; [Glucose] = 50.34 mM, 25 °C.

Human serum (glucose 110 mg/dL, Sigma-Aldrich) was analyzed. Using the enzyme and buffer solutions described above, the human serum was directly applied in varying amounts (50, 100, 150, 200, 250, 300 μ L). A series of concentrations were employed because patients with diabetes routinely withdraw varying volumes that are not necessarily controlled. The sample treatment procedure was the same as that in the calibration experiment. The absorbance was recorded and converted to glucose concentration using the calibration curve (mg/mL) (**Figure 4.6**). For each addition of serum, the glucose concentration was determined. In each analysis, the concentration (110 mg) quoted by Sigma-Aldrich with an average $\pm 7\%$ error: [glucose] = 110 ± 8 mg/dL (**Figure 4.7**). Hence, this colorimetric methodology is accurate in determining glucose concentration in human blood at a variety of different blood volumes.

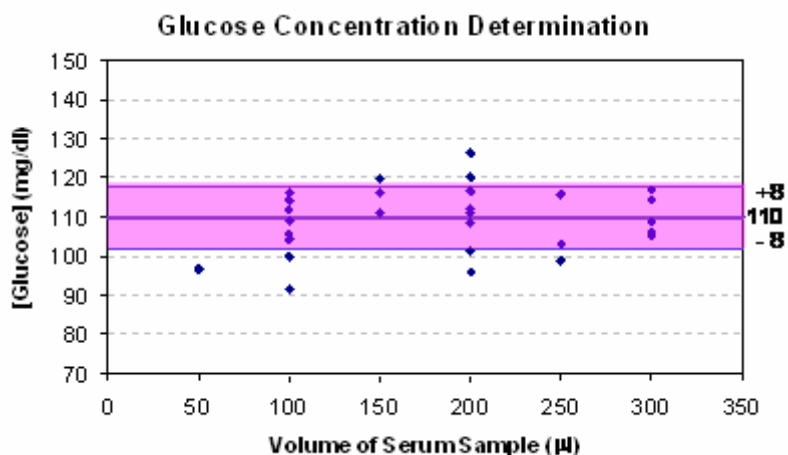


Figure 4.7 Glucose concentration determinations in human serum (110 ± 8 mg/dL). All samples were glucose (110 mg/dL), and several tests were performed for different volumes of the serum. Each test was within 7% of the correct glucose value.

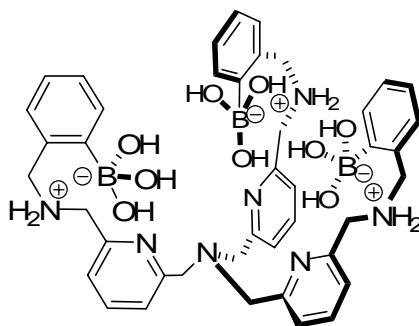
4.4 Conclusion

In conclusion, a rigid cadmium-centered tris-boronic acid-based receptor was synthesized and its binding properties toward various carboxy- and phosphor- sugars were screened with a quick 96-well plate analysis. This preorganized and functionalized receptor displays high affinities toward specific carboxy and phospho sugars in protic media at neutral pH. A particularly large affinity was found for gluconic acid, which has an association constant on the order of 10^7 M^{-1} . Using this receptor, a colorimetric IDA that can report the concentration of the product of GOx catalyzed glucose oxidation was created. The color change obtained directly reflects the concentration of glucose. This sensing ensemble was then successfully applied to determine the glucose concentration in

human serum, where it offers a facile, colorimetric, sensitive, and accurate glucose analysis.

4.5 Experimental section

4.5.1 Synthesis



4.2

Compound **4.2**: 2-formylbenzene boronic acid (0.26g, 1.73mmol) was added to a solution of **4.1** (0.18g, 0.49mmol) in dry MeOH over 3Å molecular sieves. The mixture was stirred under argon at room temperature for 12 h. NaBH₄ (0.14g, 3.75mmol) was then added to the reaction mixture, and stirred for another 4 h. The reaction mixture was filtered through celite, the filtrate was collected, the solvent was removed, and a cream solid was collected. The solid was redissolved in water and the white precipitate was removed. The yellow solution was collected and lyophilized. The cream solid obtained was further purified with a flash alumina column using CH₂Cl₂/MeOH. Compound **4.2** was obtained (0.06g, 16%): m.p. 185 °C Decompose; ¹H NMR (400MHz, CD₃OD): δ =

7.684 (t, 3H, J = 0.02), 7.564 (d, 3H, J = 0.02), 7.466 (d, 3H, J = 0.018), 7.303 (d, 3H, J = 0.018), 7.204 (p, 6H, J = 0.015), 7.035 (d, 3H, J = 0.017), 4.090 (s, 6H), 3.952 (s, 12H); ^{13}C NMR (100MHz, CD_3OD): δ = 160.115, 155.227, 142.372, 139.103, 131.473, 128.449, 127.769, 124.110, 123.751, 123.033, 60.800, 55.202, 52.613, 49.855; CI MS: $\text{C}_{45}\text{H}_{49}\text{B}_3\text{N}_7\text{O}_3^+$ (M+1): calcd: 768, obsd: 768 (dehydrated methoxy form).

4.5.2 UV-Vis titration determination of the ratio of **4.2**: Cd^{2+} :

Stock solutions of **4.2** ($[\text{4.2}] = 0.040$ mM) and **4.2** + $\text{Cd}(\text{NO}_3)_2$ ($[\text{4.2}] = 0.040$ mM, $[\text{Cd}(\text{NO}_3)_2] = 0.81$ mM) were prepared in 3:1 MeOH:H₂O buffered with HEPES (~10mM) at pH = 7.4. An aliquot of 750 μl **4.2** was placed in a cuvette, and intervals of 5 μl **4.2** + $\text{Cd}(\text{NO}_3)_2$ was added gradually into the same cuvette. UV-Vis absorbance modulations were recorded and plotted at 264 nm, which gave clear 1:1 binding of **4.2** to Cd(II) (**Figure 4.8**).

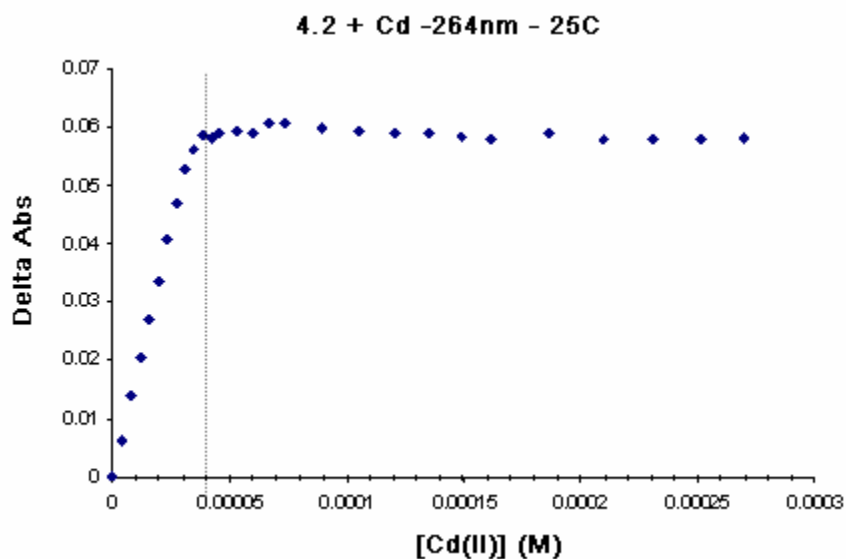
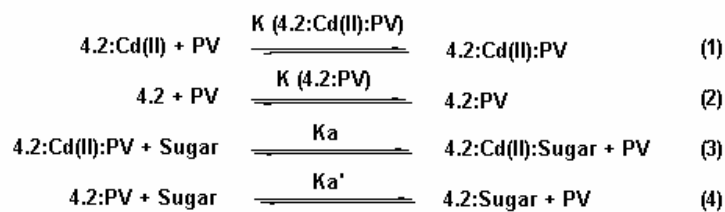


Figure 4.8 UV-Vis titration determination on Cd^{2+} association. Conditions: $[\mathbf{4.2}] = 0.040$ mM, 750 μl ; $[\text{Cd}(\text{NO}_3)_2] = 0.81$ mM; 3:1 MeOH:H₂O; HEPES (~ 10 mM) at pH = 7.4; 25 °C.

4.5.3 Determinations of association constant of a 1:1 binding isotherm:

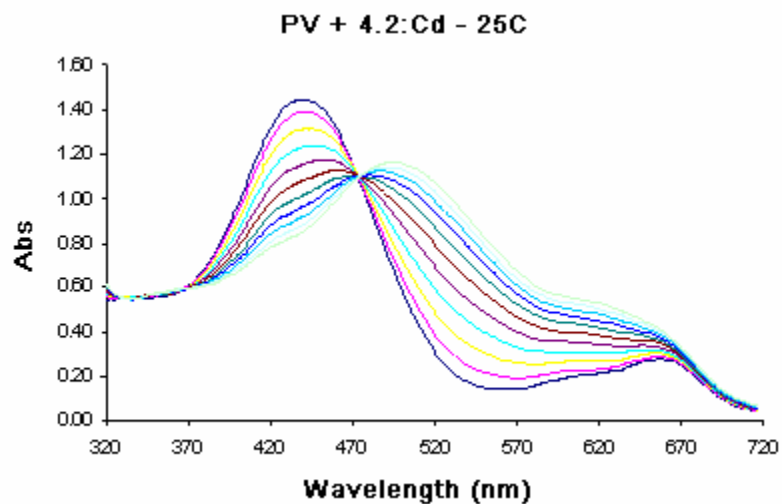
The exchange association constants are calculated via a computational mathematical method with predeterminations of $K_{\mathbf{4.2}:\text{Cd}:\text{PV}}$ and $K_{\mathbf{4.2}:\text{PV}}$.



Scheme 4.4 Equations in determinations of association constants

4.5.3.1 Determination of $K_{4.2:\text{Cd}:\text{PV}}$ and $K_{4.2:\text{PV}}$:

Stock solutions {PV} ($[\text{PV}] = 0.10 \text{ mM}$) and {4.2:Cd(II) + PV} ($[\text{PV}] = 0.10 \text{ mM}$, $[\text{4.2:Cd(II)}] = 2.00 \text{ mM}$) were prepared in 3:1 MeOH:H₂O buffered with HEPES (~10mM) at pH = 7.4. An aliquot of 750 μl {PV} was placed in a cuvette, and an interval of 5 μl {4.2:Cd(II) + PV} was added gradually into the same cuvette. Spectral modulations were recorded and plotted at 500 nm, which gave clear 1:1 binding of PV to 4.2:Cd(II) (**Figure 4.9**). The association constant of $K_{4.2:\text{Cd}:\text{PV}}$ was calculated at $K_{4.2:\text{Cd(II)}:\text{PV}} = 3.18 \times 10^5 \text{ M}^{-1}$.



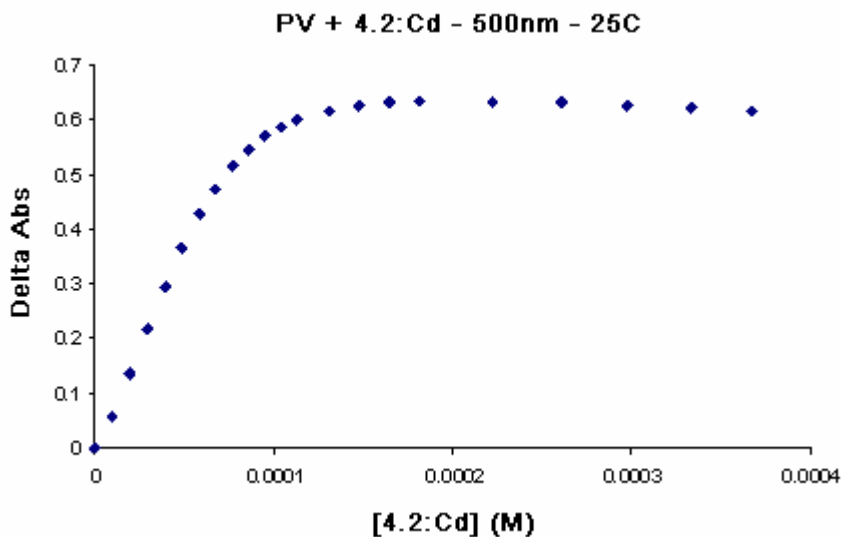


Figure 4.9 UV-Vis titration on association constant determination of **4.2**:Cd(II) to PV. Conditions: [PV] = 0.1 mM; [4.2: Cd(II)] = 2.00 mM, 5 μ L aliquots; 3:1 MeOH:H₂O; HEPES (~10mM) at pH = 7.4; 25 °C.

The $K_{4.2:PV}$ was determined using the same methodology, $K_{4.2:PV} = 2.54 \times 10^3 \text{ M}^{-1}$.

4.5.3.2 Determination of K_a and K_a' :

Stock solutions {4.2: Cd(II) + PV} ([PV] = [4.2: Cd(II)] = 0.10 mM) and {4.2: Cd(II) + PV + Sugar} ([PV] = [4.2: Cd(II)] = 0.10 mM, [Sugar] ~ 2.00 mM) were prepared in 3:1 MeOH:H₂O buffered with HEPES (~10mM) at pH = 7.4. An aliquot of 750 μ L {4.2: Cd(II) + PV} was placed in a cuvette, and an interval of 5 μ L {4.2: Cd(II) +

PV + Sugar} was added gradually into the same cuvette. Spectral modulations were recorded and plotted at 500 nm (**Figure 4.10**).

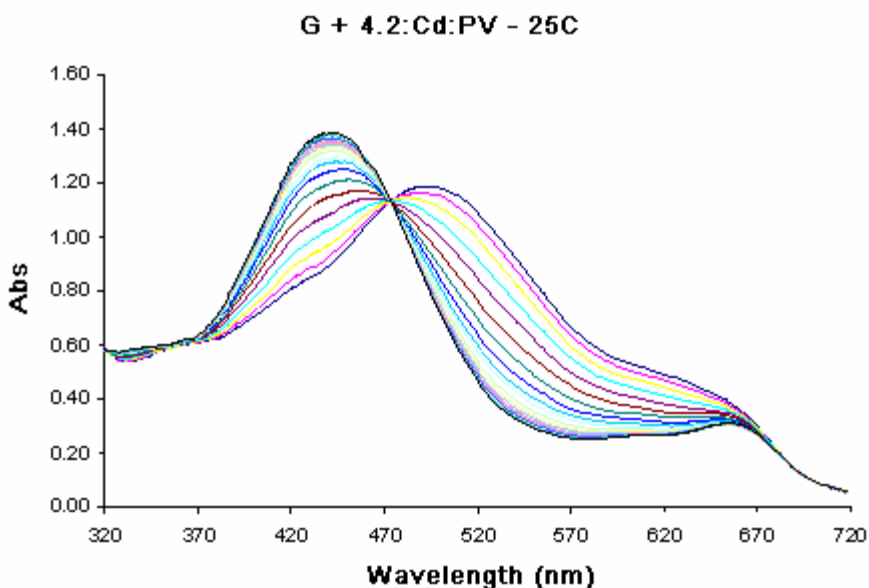
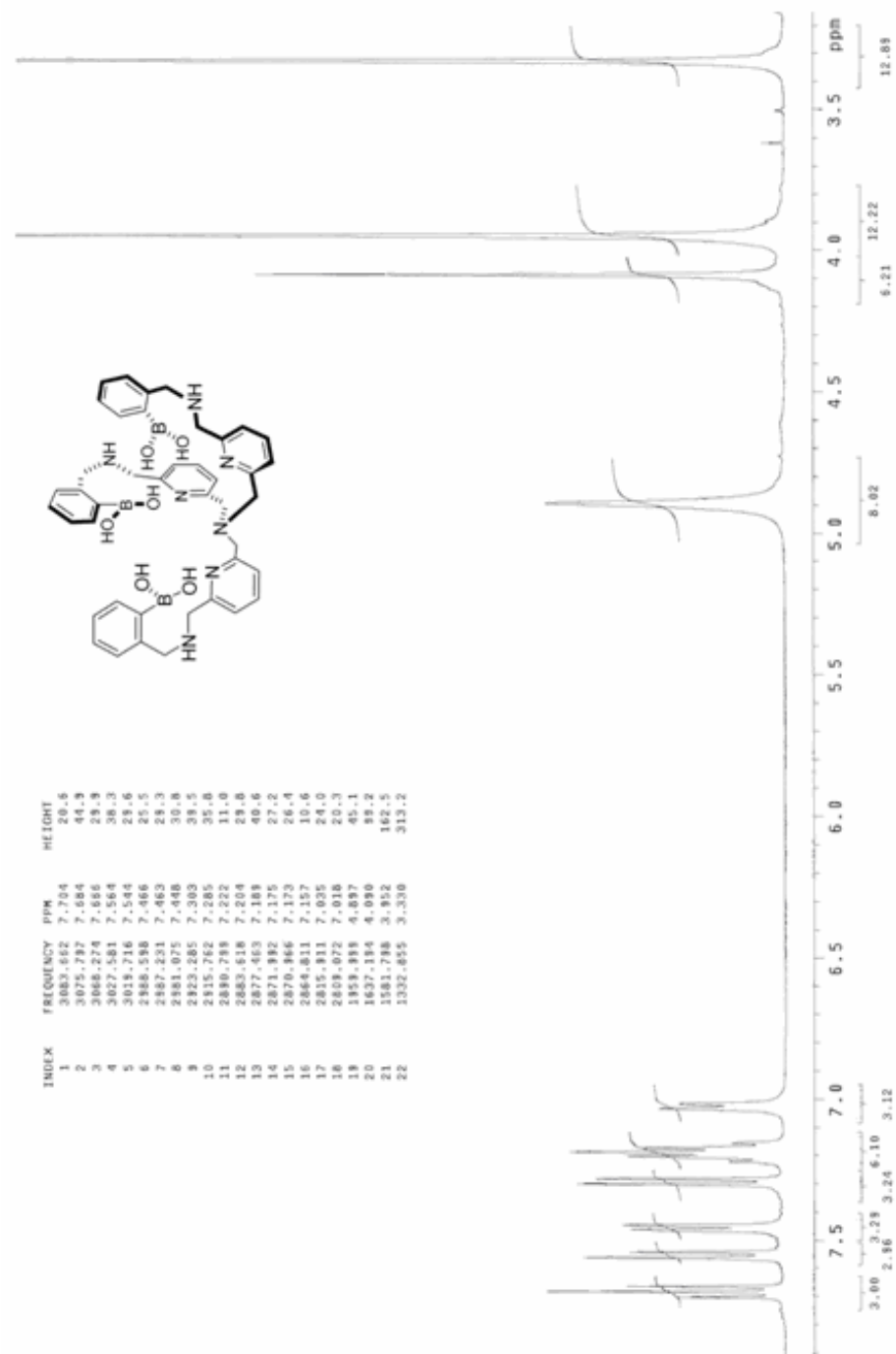


Figure 4.10 UV-Vis titration determination of **4.2**:Cd(II): PV to Sugar. UV-Vis titration on association constant determination of **4.2**:Cd(II) to PV. Conditions: [PV] = [4.2:Cd(II)] = 0.1 mM; [Sugar] = 2.00 mM, 5 μ L aliquots; 3:1 MeOH:H₂O; HEPES (~10mM) at pH = 7.4; 25 °C.

The titration of **4.2**:Cd(II) to PV showed a clear 1:1 binding, and the titration of sugar to {**4.2**:Cd(II) + PV} showed a clear isosbestic point, meaning the complexation didn't change through out the titration process. Thus, it was concluded that the sugar binds to **4.2**:Cd(II) in a 1:1 stoichiometry. Since the high association constant was determined for the binding of **4.2**:Cd(II) to PV, the sugars tested would compete with PV to associate with **4.2**:Cd(II). Unless the interaction is super strong, the competition would make the absorbance change less significant.

4.5.4 ^1H NMR and ^{13}C NMR spectra for 4.2 (Figure 4.11):



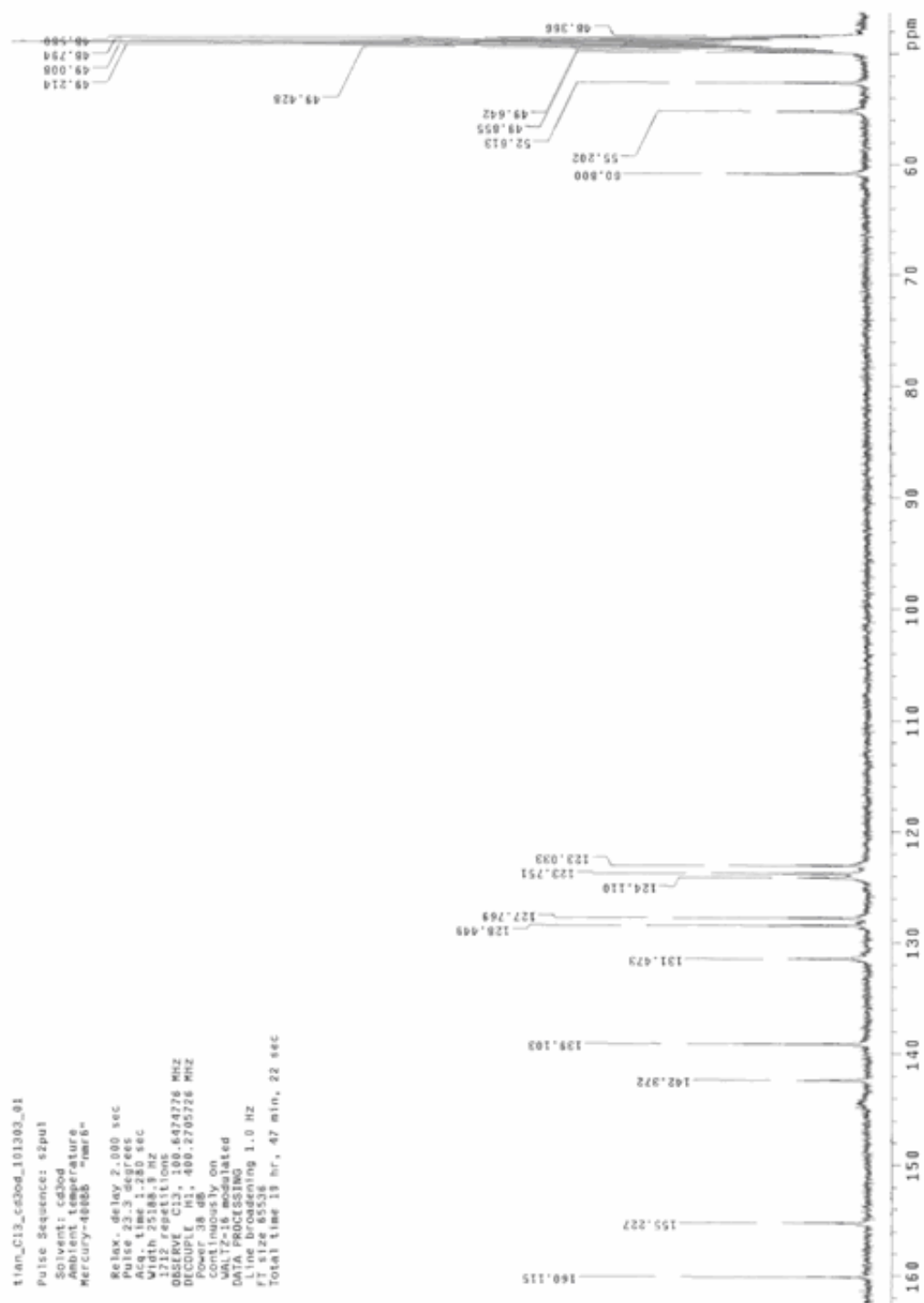


Figure 4.11 ^1H NMR and ^{13}C NMR spectra for 4.2.

4.5.5 Stock solution preparation:

Tris buffer **1**: 50mM in H₂O, pH ~ 7.

Tris buffer **2**: 50mM in MeOH, pH ~ 7.

Receptor concentration: 0.13 mM in Tris buffer **2**.

PV concentration: 0.13 mM in Tris buffer **2**.

Glucose Oxidase (GOx) concentration: 10 mg/ml in Tris buffer **1**.

Catalase concentration: 10 mg/ml in Tris buffer **1**.

Glucose: 50 mM in Tris buffer **1**.

4.5.6 Concentration effect of glucose oxidase (GOx):

With constant concentrations of other components, glucose oxidase was varied within a range of 5 µl to 50 µl. 30 µl was chosen for a relatively rapid and inexpensive reactions. (**Figure 4.12**)

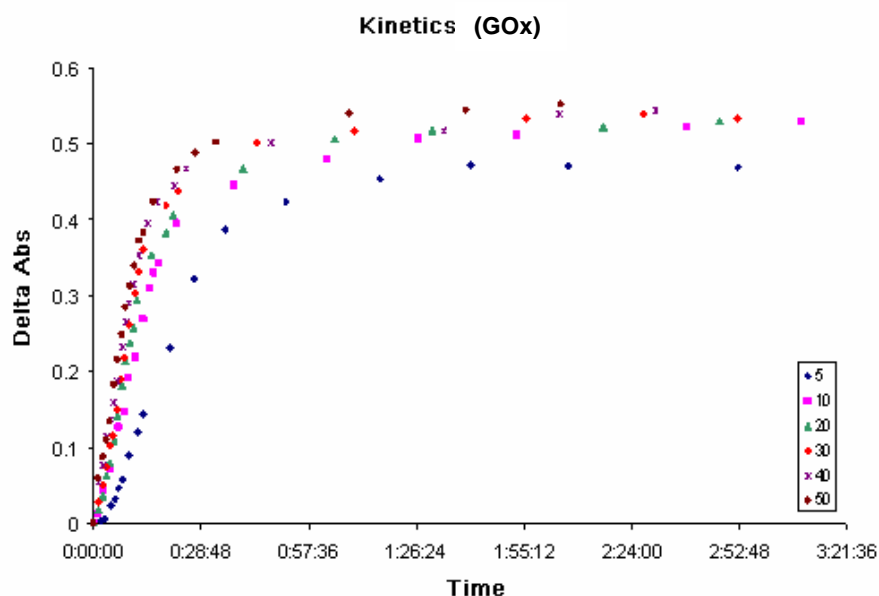


Figure 4.12 Effect of glucose oxidase concentration. Conditions: Glucose 200 μ l, Catalase 200 μ l, Total volume: 5ml; 250 μ l aliquot was used to observe UV absorbance modulations. [PV] = [4.2: Cd(II)] = 0.13 mM; [Sugar] = 50.00 mM; [catalase] = 10 mg/ml; [GO_x] = 10 mg/ml; 3:1 MeOH:H₂O; TRIS (~50mM) at pH = 7.4; 25 °C.

4.5.7 Concentration effect of catalase:

With constant concentrations of other components, catalase was varied in a range of 0 μ l to 400 μ l. 200 μ l was chosen for a relatively rapid and inexpensive reaction. Even though the reaction seemed to occur without catalase, catalase was still used to sequester H₂O₂ generated in the oxidation reaction to avoid possible degradation of the boronic acid-based receptor and deactivation of GOx (**Figure 4.13**).

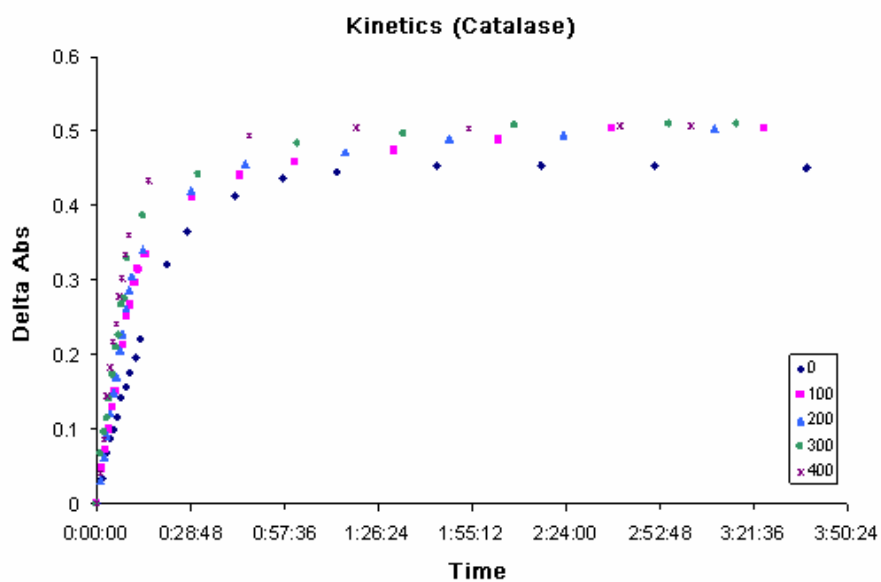


Figure 4.13 Effect of catalase concentration. Condition: GOx 30 μ l, Glucose 200 μ l, Total volume: 5ml; 250 μ l aliquot was used to observe UV modulation. [PV] = [4.2: Cd(II)] = 0.13 mM; [Sugar] = 50.00 mM; [catalase] = 10 mg/ml; [GO_x] = 10 mg/ml; 3:1 MeOH:H₂O; TRIS (~50mM) at pH = 7.4; 25 °C.

4.5.8 pH effect:

The generation of gluconic acid can affect the pH value, but it was effectively controlled by relatively high buffer concentrations (**Figure 4.14**).

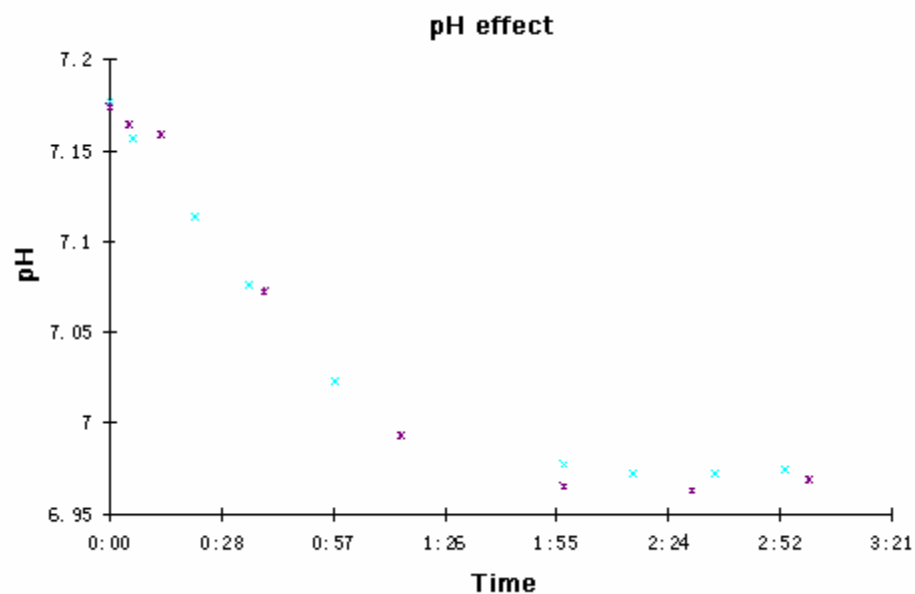


Figure 4.14 Effect of pH (2 trials at the same conditions). Condition: GOx 30 μ l, Glucose 200 μ l, Total volume: 5ml; 250 μ l aliquot was used to observe UV modulation. [PV] = [4.2: Cd(II)] = 0.13 mM; [glucose] = 50.00 mM; [catalase] = 10 mg/ml; [GO_x] = 10 mg/ml; 3:1 MeOH:H₂O; TRIS (~50mM) at pH = 7.4; 25 °C.

4.5.9 Glucose interaction to receptor system:

Glucose had no observable effective association to the receptor molecule (**Figure 4.15**).

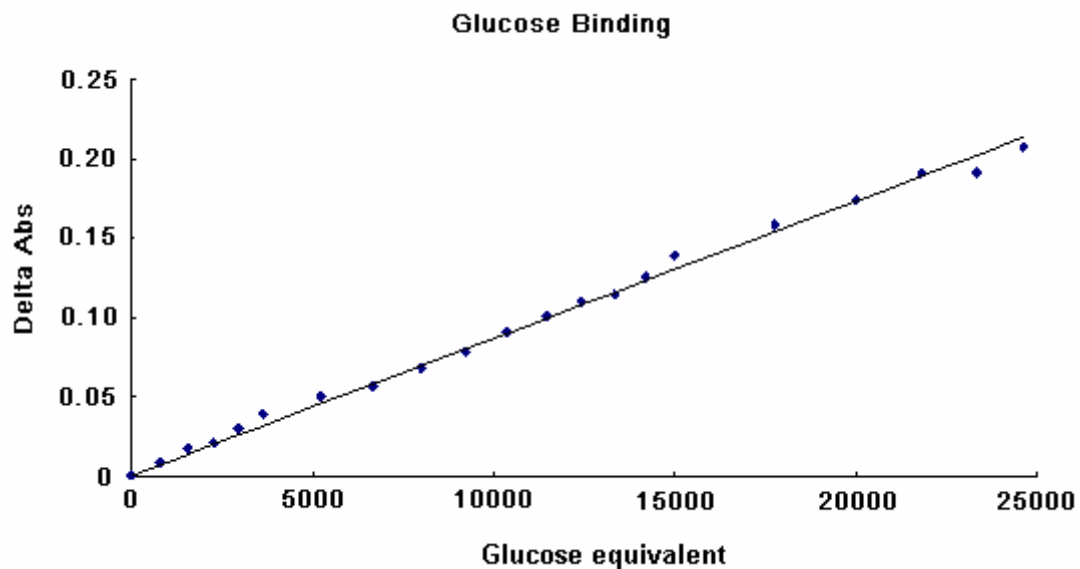
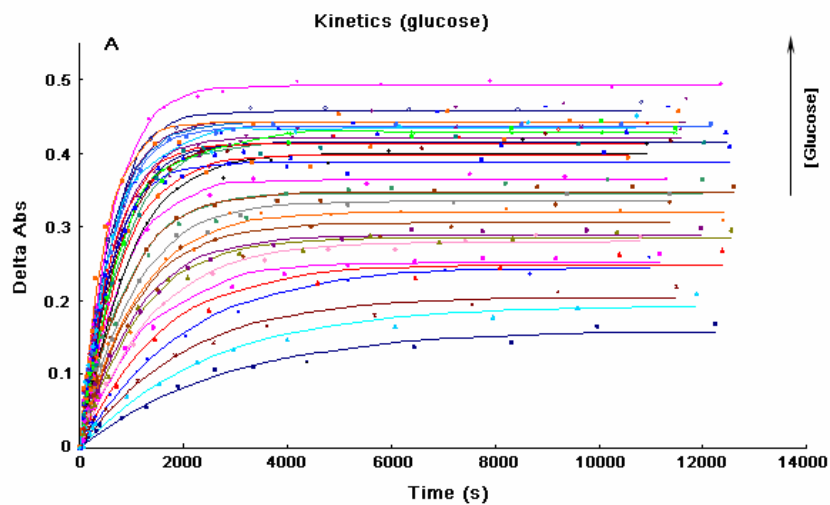


Figure 4.15 Effect of glucose concentration. Conditions: [PV] = [4.2:Cd(II)] = 0.13 mM; [glucose] = 100 mM, 5 μ l aliquots; 3:1 MeOH:H₂O; TRIS (~50mM) at pH = 7.4; 25 °C.

4.5.10 Kinetics studies confirmed enzyme reactions at setup conditions:



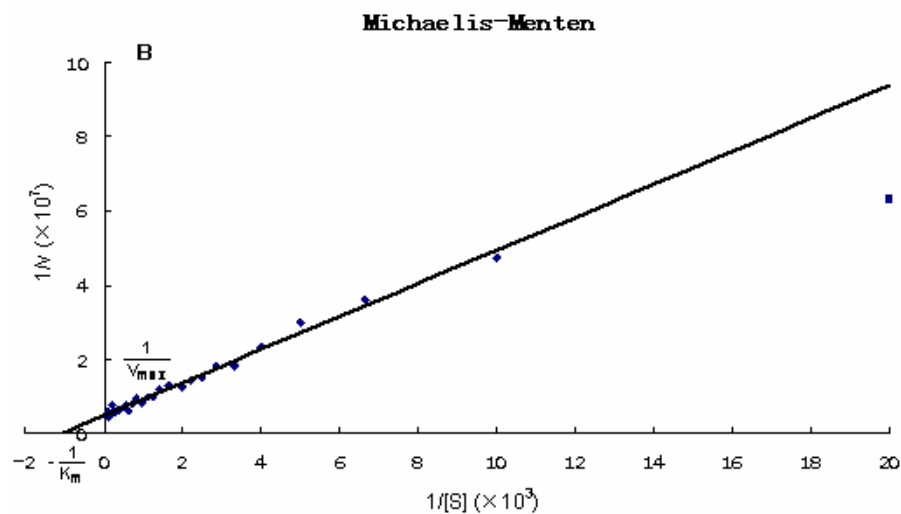


Figure 4.16 Kinetic studies showed enzyme catalyzed ability of glucose oxidation by GO_x. Condition: GO_x 30 µl, Catalase 200 µl, Total volume: 5ml; 250 µl glucose aliquot was used to observe spectral modulation. A) UV-Vis titrations at different glucose concentrations. B) Michaelis-Menten curve. [P_V] = [4.2: Cd(II)] = 0.13 mM; [glucose] = 50.00 mM; [catalase] = 10 mg/ml; [GO_x] = 10 mg/ml; 3:1 MeOH:H₂O; TRIS (~50mM) at pH = 7.4; 25 °C.

4.6 References

- ¹ (a) James, T. D.; Shinkai, S. *Top. Curr. Chem.* **2002**, 218, 159-200. (b) Striegler, S. *Curr. Org. Chem.* **2003**, 7, 81-102
- ² (a) Cao, H.; Heagy, M. D. J. *Fluoresc.* **2004**, 14, 569-584. (b) Schmuck, C.; Schwegmann, M. *Org. Lett.* **2005**, 7, 3517-3520. (c) Lirvinchuk, S.; Sorde, N.; Matile, S. *J. Am. Chem. Soc.* **2005**, 127, 9316-9317. (d) Mazik, M.; Cavga, H.; Jones, P. G. *J. Am. Chem. Soc.* **2005**, 127, 9045-9052. (e) Davis, A. P.; Wareham, R. S. *Angew. Chem., Int. Ed. Engl.* **1999**, 38, 2979-2996. (f) Cho, H.; Kim, H.; Lee, K. H.; Hong, J. *Bull. Korean Chem. Soc.* **2004**, 25, 1714-1716. (g) Shinkai, S.; Takeuchi, M. *Biosens. Bioelectron.* **2004**, 20, 1250-1259

- ³ (a) Zhu, L.; Anslyn, E. V. *J. Am. Chem. Soc.* **2004**, *126*, 3676-3677. (b) Matsumoto, A.; Yoshida, R.; Kataoka, K. *Biomacromolecules* **2004**, *5*, 1038-1045. (c) Sakamoto, S.; Kudo, K. *Pept. Sci.* **2004**, *Y*, 369-370. d. Zhao, J.; Fyles, T. M.; James, T. D. *Angew. Chem., Int. Ed.* **2004**, *43*, 3461-3464. (e) Yang, W.; Yan, J.; Fang, H.; Wang, B. *Chem. Commun.* **2003**, 792-793. f. Badugu, R.; Lakowicz, J. R.; Geddes, C. D. *Bioorg. Med. Chem.* **2005**, *13*, 113-119. (g) Zhao, J.; Davidson, M. G.; Mahon, M. F.; Kociok-Kohn, G.; James, T. D. *J. Am. Chem. Soc.* **2004**, *126*, 16179-16186. (h) Wang, J.; Jin, S.; Wang, B. *Tetrahedron Lett.* **2005**, *46*, 7003-7006. (i) Zhao, J.; James, T. D. *J. Mater. Chem.* **2005**, *15*, 2896-2901. (j) Yuasa, H.; Miyagawa, N.; Nakatani, M.; Izumi, M.; Hashimoto, H. *Org. Biomol. Chem.* **2004**, *2*, 3548-3556. (k) Badugu, R.; Lakowicz, J. R.; Geddes, C. D. *Talanta* **2005**, *65*, 762-768. (l) Gao, X.; Zhang, Y.; Wang, B. *Tetrahedron* **2005**, *61*, 9111-9117
- ⁴ Bowman-James, K. *Acc. Chem. Res.* **2005**, *38*, 671-678
- ⁵ (a) Gale, P. A. *Coord. Chem. Rev.* **2003**, *240*, 191-221. (b) Beer, P. D. *Acc. Chem. Res.* **1998**, *31*, 71-80
- ⁶ Arnold, F. H.; Guan, Z.; Chen, C. *PCT Int. Appl.* WO 9705489 A1 19970213 CAN 126:209292 AN **1997**:231065, 1997
- ⁷ Zhang, T.; Anslyn, E. V. *Tetrahedron* **2004**, *60*, 11117-11124
- ⁸ Wiskur, S. L.; Lavigne, J. J.; Metzger, A.; Tobey, S. L.; Lynch, V.; Anslyn, E. V. *Chem. Eur. J.* **2004**, *10*, 3792-3804
- ⁹ (a) Tobey, S. L.; Anslyn, E. V. *J. Am. Chem. Soc.* **2003**, *125*, 10963-10970; (b) Tobey, S. L.; Anslyn, E. V. *J. Am. Chem. Soc.* **2003**, *125*, 14807-14815
- ¹⁰ Zhu, L.; Anslyn, E. V. *J. Am. Chem. Soc.* **2006**, *128*, 1222-1232
- ¹¹ (a) Allen, C. S.; Chuang, C.; Cornebise, M.; Canary, J. W. *Inorg. Chim.* **1995**, *239*, 29-37. (b) Bebout, D. C.; Stokes, S. W.; Butcher, R. *J. Inorg. Chem.* **1999**, *38*, 1126-1133
- ¹² Zhu, L.; Zhong, Z.; Anslyn, E. V. *J. Am. Chem. Soc.* **2005**, *127*, 4260-4269
- ¹³ (a) Pickup, J.; McCartney, L.; Rolinski, O.; Birth, D. *BMJ* **1999**, *319*, 1-4. (b) Fang, H.; Kaur, G.; Wang, B. *J. Fluoresc.* **2004**, *14*, 481-489. (c) Koschinsky, T.; Heinemann, L. *Diabetes Metab. Res. Rev.* **2001**, *17*, 113-123. (d) Moschou, E. A.; Sharma, B. V.; Deo, S. K.; Daunert, S. *J. Fluorescence* **2004**, *14*, 535-547. (e) Ramamoorthy, R.; Dutta, P. K.; Akbar, S. A. *J. Mater. Sci.* **2003**, *38*, 4271-4282. (f) Wang, J. *Sens. Update* **2002**, *10*, 107-119

- ¹⁴ (a) Pereira, C. M.; Oliveira, J. M.; Silva, R. M.; Silva, F. *Anal. Chem.* **2004**, *76*, 5547-5551. (b) Heller, A. *Annu. Rev. Biomed. Eng.* **1999**, *01*, 153-175. (c) Wu, J.; Qu, Y. *Anal. Bioanal. Chem.* **2006**, *385*, 1330-1335. (d) Gao, Z.; Xie, F.; Shariff, M.; Arshad, M.; Ying, J. Y. *Sens. Actuators, B* **2005**, *B111-B112*, 339-346. (e) Lawrence, N. S.; Deo, R. P.; Wang, J. *Anal. Chem.* **2004**, *76*, 3735-3739. (f) Li, J.; Chia, L. S.; Goh, N. K.; Tan, S. N.; Ge, H. *Sens. Actuators, B* **1997**, *B40*, 135-141. (g) Granot, E.; Basnar, B.; Cheglakov, Z.; Katz, E.; Willner, I. *Electroanalysis* **2006**, *18*, 26-34. (h) Wolfbeis, O. S.; Oehme, I.; Papkovskaya, N.; Klimant, I. *Biosens. Bioelectron.* **2000**, *15*, 69-76
- ¹⁵ Cai, Q.; Zeng, K.; Ruan, C.; Desai, T. A.; Grimes, C. A. *Anal. Chem.* **2004**, *76*, 4038-4043
- ¹⁶ (a) Pickup, J. C.; Hussain, F.; Evans, N. D.; Rolinski, O. J.; Birch, D. J. S. *Biosens. Bioelectron.* **2005**, *20*, 2555-2565. (b) Yoon, J.; Czarnik, A. W. *J. Am. Chem. Soc.* **1992**, *114*, 5874-5875. (c) Antwerp, V.; Peter, W.; Mastrototaro, J. J. *PCT Int. Appl.*, **1997**, *58*, WO 9719188. (d) James, T. D.; Shinkai, S. *Top. Curr. Chem.* **2002**, *218*, 159-200. (e) DiCeswere, N.; Pinto, M. R.; Schanze, K. S.; Lakowicz, J. R. *Langmuir* **2002**, *18*, 7785-7787. (f) Ye, K.; Schultz, J. S. *Anal. Chem.* **2003**, *75*, 3451-3459. (g) Shiomi, Y.; Miwako, S.; Tsukagoshi, K.; Shinkai, S. *J. Chem. Soc., Perkin Trans. 1* **1993**, 2111-2117. (h) Zhang, L.; Small, G. W. *Anal. Chem.* **2002**, *74*, 4097-4108. (i) Berger, A. J.; Koo, T.; Itzkan, I.; Korwitz, G.; Feld, M. S. *Appl. Opt.* **1999**, *38*, 2916-2926. (j) Shafer-Pektuer, K. E.; Haynes, C. L.; Glucksberg, M. R.; Van Duyne, R. P. *J. Am. Chem. Soc.* **2003**, *125*, 588-593. (k) Luebbers, D. W.; Opitz, N. *Sens. Actuators* **1983**, *4*, 641-654. (l) Fang, H.; Kaur, G.; Wang, B. *J. Fluoresc.* **2004**, *14*, 481-489. (m) Pringsheim, E.; Terpetschig, E.; Piletsky, S. A.; Wolfbeis, O. S. *Adv. Mater.* **1999**, *11*, 865-868. (n) Thoniyot, P.; Cappuccio, F. E.; Gamsey, S.; Corders, D. B.; Wessling, R. A.; Singgaram, B. *Diabetes Technol. Therapeutics* **2006**, *8*, 279-287
- ¹⁷ Asher, S. A.; Alexeev, V. L.; Goponenko, A. L.; Sharma, A. C.; Lednev, I. K.; Wilcox, C. S.; Finegold, D. N. *J. Am. Chem. Soc.* **2003**, *125*, 3322-3329
- ¹⁸ Curey, T. E.; Salazar, M. A.; Oliveira, P.; Javier, J.; Dennwas, J.; Rao, P.; Shear, J. S. *Anal. Biochem.* **2002**, *303*, 42-48
- ¹⁹ Zhang, T.; Anslyn, E. V. *Org. Lett.* **2006**, *8*, 1649-1652
- ²⁰ Wu, S.; Waugh, W.; Stella, V. J. *J. Pharm. Sci.* **2000**, *89*, 758-765

Vita

Tianzhi Zhang was born in Changchun, Jilin, P. R. China on August 11, 1973, the daughter of Siyuan Zhang and Xiangyu Song. Prior to moving to Austin, Texas for graduate school she was a graduate student in University of California at Riverside. Tianzhi had her undergraduate studies at Jilin University in Changchun, Jilin, P. R. China. She completed her B.S. in chemistry in July 1996 with honors.

In August 2002, Tianzhi entered the University of Texas at Austin chemistry graduate program.

Permanent address: 3176 Gongnong Ave, 69-1-302, Chaoyang District, Changchun, Jilin, P. R. China, 130021

This dissertation was typed by Tianzhi Zhang.